Annett Kühn (Ed.)

THERMALLY DRIVEN HEAT PUMPS FOR HEATING AND COOLING

Annett Kühn (Ed.)

Thermally driven heat pumps for heating and cooling

Thermally driven heat pumps for heating and cooling

Annett Kühn (Ed.)

Universitätsverlag der TU Berlin

Bibliographic information published by the Deutsche Nationalbibliothek
The Deutsche Nationalbibliothek lists this publication in the Deutsche Nationalbibliografie; detailed bibliographic data are available in the Internet at http://dnb.dnb.de.

Annett Kühn
Senior researcher
Technische Universität Berlin
Institute of Energy Engineering
Chair of Energy Conversion Technology (Prof. Dr.-Ing. Felix Ziegler)

Universitätsverlag der TU Berlin 2013
http://www.univerlag.tu-berlin.de

Fasanenstr. 88 (im VOLKSWAGEN-Haus), 10623 Berlin
Tel.: +49 (0)30 314 76131 / Fax: -76133
E-Mail: publikationen@ub.tu-berlin.de

Layout: Annett Kühn, Berlin, Germany
Cover photographs: Gas absorption heat pump installation © Gust/Berliner NetzwerkE
Public swimming pool Stadtbad Mitte © Berliner Bäder-Betriebe

ISBN (online) 978-3-7983-2596-8

Online published on the Digital Repository of the Technische Universität Berlin:
URL http://opus4.kobv.de/opus4-tuberlin/frontdoor/index/index/docId/3945
URN urn:nbn:de:kobv:83-opus4-39458
http://nbn-resolving.de/urn:nbn:de:kobv:83-opus4-39458

PREFACE

The International Energy Agency (IEA) reports that 46% of global energy demand is devoted to heating and cooling. Two thirds of this demand is met by fossil fuels, either via electricity generation or direct combustion. Both the heating and cooling energy demands are expected to grow rapidly in the coming decades. In order to achieve the global goal of CO_2 emission reduction, energy efficiency must be strongly improved. Thermally driven heat pumps, due to their efficient energy use and their adoption of environmentally benign refrigerants with no Global Warming Potential (GWP), are able to contribute to reduce the environmental impact of heating and cooling.

Worldwide interest in thermally driven heat pumps and cooling machines is continually increasing. This book, a result of Annex 34 “Thermally Driven Heat Pumps for Heating and Cooling” of the International Energy Agency’s Heat Pump Programme (HPP), aims to improve the understanding of this environmentally friendly technology by providing information on both the fundamentals and the recent developments. With cooperation from experts from about twenty institutions and more than ten countries, it has been made possible to address a large number of topics in this wide field. Therefore a thank you is in order to all contributing participants for their work and willingness to share results.

The target audience for this book includes planners, scientists, students and anyone who would like an overview of the technology. Individual papers contributed by the research institutes and companies are arranged in the following chapters: “Thermally driven heat pumps for heating”, “Thermally driven heat pumps for cooling”, and, as useful heat and cold can also be supplied simultaneously or seasonally consecutively, “Thermally driven heat pumps for heating and cooling”. A final chapter discusses “Research on working pairs and apparatus technology”. The intentions of this book are to encourage the reader to pursue the approaches, to overcome remaining hurdles and lastly to apply the technology in practice.

Annett Kühn, Editor
Peter Schossig, Operating Agent of Annex 34

October, 2013
Berlin, Germany

INTRODUCTION

Annett Kühn, Technische Universität Berlin, Institute of Energy Engineering, KT 2, Marchstraße 18, D-10587 Berlin, Germany, annett.kuehn@tu-berlin.de

Today, most heat pumps for heating and cooling are mechanically driven. However, the principles of sorption heat pumping have already been discovered in the second half of the 18th century. William Cullen (1756) experimented with diethyl ether and produced small quantities of ice by vacuum generation. Gerald Nairne used sulfuric acid to absorb water in 1777. By a combination of these principles, John Leslie in 1810 first created artificial ice (Vallance 1824). The adsorption phenomenon was discovered by Michael Faraday (1823) while studying the liquefaction of gases. He used an experimental set-up in which ammonia was adsorbed by silver chloride and calcium chloride. It was not until 1850 when Edmond Carré constructed the first commercial discontinuously working ice-maker with water and sulfuric acid. It was used in coffee-houses in Paris. In 1878, Franz von Windhausen built the first continuously working absorption refrigerator. Shortly later, the first large absorption machines were being manufactured for ice making and process cooling in the chemical and petroleum industries. The availability of cheap electricity then promoted the introduction of electrically driven compression heat pumps, which nearly stopped the dissemination of absorption heat pumps. They only regained popularity to a significant extent in periods of high electricity rates.

Absorption refrigeration machines became a highly developed technology between 1920 and 1940 when also most of the theoretical fundamentals were laid down, largely driven by Edmund Altenkirch. The German company Borsig constructed single and two stage machines with an average cooling capacity of 35 to 60 kW. The biggest plant had a refrigeration capacity of around 4 MW at an evaporator temperature of -20°C and a condenser temperature of 30°C. It was steam driven (Stephan 1983). In 1923, the Swedish company AB Arctic begun to manufacture a diffusion absorption refrigerator based on the patents of Baltzar von Platen and Carl Munters. Electrolux acquired the company and patent two years later and introduced the world’s first absorption refrigerator for domestic use. Also in this period so-called intermittent 'dry' absorption machines, i.e. adsorption machines, were fabricated, for example, by the German companies Humboldt and Siemens-Schuckert. The latter company fabricated air-cooled machines operated with ammonia and calcium chloride as a working pair (Stephan 1983).

The first large water/LiBr chiller for air conditioning was marketed by the US company Carrier in 1945. Today, such absorption cooling technology is considered to be mature. The market for large absorption chillers (up to 30 MW) is concentrated in China, Japan, and South Korea. They are mainly manufactured in those countries (e.g. by Broad, Shuangliang, Sanyo, Yazaki, Hitachi, Kawasaki, Mitsubishi, Ebara, LG, and Century). A few absorption chillers are manufactured in the United States (e.g. by Carrier, Trane, and York/Johnson Controls) and India (e.g. by Thermax). The major growth area is still considered to be the Asia-Pacific region, led by China, India and South Korea (JARN 2011). Up to now, gas-fired absorption chillers have been used for economic reasons in areas with high electrical loads in summer. Currently, numbers of waste heat driven and combined cold/heat/power (tri-generation) installations are increasing worldwide. Energy strategies of governments also play an increasing role.

Large ammonia/water machines are produced in smaller quantities and are often tailor-made. They are mainly used for low temperature industrial applications. Ammonia/water absorption refrigerators were common in the household market up to the 1940s. Featuring a

thermally driven solution pump, they are still produced in relatively large quantities for the recreational vehicle market and the camping sector. Another market is hotel room refrigerators due to their silent operation.

Adsorption cycles for refrigeration were first used in the early 1900s. Plank and Kuprianoff (1960) reported on manufactured machines using ammonia/CaCl and methanol/activated carbon. Hulse (1929) reported on a sulfur dioxide/silica gel machine for the air-conditioning of rail freight cars in the United States. Critoph (2012), in his historical review, reports on a domestic activated carbon/methanol refrigerator called 'Eskimo' and sold in the 1930s by the Norwegian Amundsen Refrigerator Company. He also reports on research activities in the US in the 1980s and the manufacturing of several solar adsorption refrigerators in the 1990s. Nishiyodo and Mayekawa/Mycom, two Japanese companies, produced the first adsorption chillers operating with the working pair water/silica gel in the late 1980s. To date, Mayekawa is the only known manufacturer of medium scale adsorption chillers after Nishiyodo stopped the production a few years ago.

In the last decade, several small scale absorption and adsorption chillers (8 to 50 kW cooling capacity) for solar cooling or the use in tri-generation systems have been developed, mainly in Europe where academic R&D has always been relatively strong in this field. Companies currently in active production include Yazaki, EAW Energieanlagenbau, Thermax, Pink, and AGO (absorption) and Sortech and Invensor (adsorption).

Altenkirch (1914) and Nesselmann (1934) published the first papers on the use of absorption processes for heat pumps and heat transformers. They gave a comprehensive overview of the theory of heat transformation for single-stage and different possibilities of multi-stage applications. For some decades, there was only the Italian company Robur who sold gas fired ammonia/water absorption heat pumps of 35 kW heating output. Since 2010, the German company Vaillant provides a gas fired water/zeolite adsorption heat pump for domestic use. It is an air/water unit combined with a solar collector which serves to raise the air temperature level.

REFERENCES

Altenkirch E. 1914. *Zeitschrift für die gesamte Kälte-Industrie*, Vol. 21, 7-13, Gesellschaft für Kältewesen GmbH, Berlin, Germany.

Critoph R.E. 2012. "Solid sorption cycles: A short history", *International Journal of Refrigeration*, Vol. 35 (3), 490–493.

Cullen W. 1756. "Of the Cold Produced by Evaporating Fluids and of Some Other Means of Producing Cold", *Essays and Observations, Physical and Literary*. Read before a society in Edinburgh, and published by them, Vol. II, printed for John Balfour, Edinburgh, UK.

Faraday M. 1823. "On the condensation of several gases into liquids", *Philosophical Transactions of the Royal Society of London*, Vol. 113, 189-198.

Hulse G.E. 1929. "Freight car refrigeration by an adsorption system employing silica gel", *Refrigeration Engineering*, Vol. 17.

Japan Air Conditioning, *Heating & Refrigeration News*, www.ejarn.com, July, 2011.

Nesselmann K. 1934. *Zeitschrift für die gesamte Kälte-Industrie*, Vol. 41, 73-79, Gesellschaft für Kältewesen GmbH, Berlin, Germany.

Plank R., J. Kuprianoff 1960. Die Kleinkältemaschine. 2. Aufl., Springer-Verlag, Berlin, Göttingen, Heidelberg, Germany.

Stephan K. 1983. “History of absorption heat pumps and working pair developments in Europe”, *International Journal of Refrigeration*, Vol. 6, Issue 3, 160–166.

Vallance J. 1824. “Vallance’s improved method of freezing water”, *London Journal of Arts and Sciences*, 251-253.

CYCLE BASICS OF THERMALLY DRIVEN HEAT PUMPS

Annett Kühn, Felix Ziegler, Technische Universität Berlin, Institute of Energy Engineering, KT 2, Marchstraße 18, D-10587 Berlin, Germany, annett.kuehn@tu-berlin.de

1 FUNDAMENTALS

Thermally driven heat pumps (TDHP) work at three temperature levels. Driving heat Q_2 is supplied at a high temperature level. Useful cold (cooling operation) or low temperature heat (heating operation) Q_0 is supplied at a low temperature level. The sum of the heat supplied is released at a medium temperature level. Q_1 is the useful heat in heating operation. In cooling operation, it is usually released to the environment. However, medium and low temperature heat can also be used simultaneously for heating and cooling purposes.

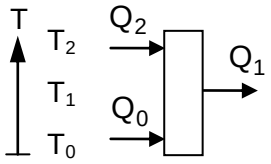

Figure 1: Temperature levels of thermally driven heat pumps for heating and cooling

In principle, all closed cycle TDHP types can be operated in heating and cooling mode. However, when we talk about thermally driven heat pumps, we usually refer to absorption or adsorption heat pumps. Having the highest process efficiencies (coefficient of performance, COP) they are far more widespread than TDHP processes like steam jet, double organic Rankine (ORC), thermoacoustic, thermoelectric, Stirling, Vuilleumier, Pulse tube, or Gifford-McMahon processes. These cycles are mainly discussed for applications with additional specific requirements such as, for example, very low useful temperatures. There are also combined (compression-sorption hybrid cycles, see Ziegler 1991) or successive heat and mechanically driven processes like Rankine and vapor compression.

The efficiency of TDHPs is defined by

$$COP_c = \frac{\dot{Q}_0}{\dot{Q}_2} \text{ for cooling operation,} \quad (1)$$

$$COP_h = \frac{\dot{Q}_1}{\dot{Q}_2} = 1 + COP_c \text{ for heating operation and} \quad (2)$$

$$COP_{h+c} = \frac{\dot{Q}_1 + \dot{Q}_0}{\dot{Q}_2} = 1 + 2 \cdot COP_c \text{ for combined heating and cooling operation.} \quad (3)$$

However, it is better to use COP_c or COP_h only, even for the combined operation, in order not to confuse the thermodynamic meaning.

The electrical energy input of TDHPs often is negligibly small. Otherwise, a second number, the electrical COP (COP_{el}), can be used in order to distinguish it from the thermal COP (COP_{th}).

2 ABSORPTION HEAT PUMPS

Just as in the conventional compression heat pump process, in the absorption heat pump process useful heat is produced by condensation of a refrigerant. Prior to that, in the evaporator (E) the refrigerant is evaporated at a lower pressure using a low temperature heat source (see Figure 2). However, in the absorption heat pump process the refrigerant vapor is not compressed by a mechanically driven compressor to overcome the pressure difference but is instead pumped in a liquid state. The electrical energy input required is very small due to the considerably lower specific volume of liquid compared to vapor refrigerant.

For suction of the vapor refrigerant of the evaporator a suitable liquid, the absorbent, is used. During the absorption process in the absorber (A) heat is generated and has to be released. It is used for heating purposes as the condensation heat. Therefore, the ratio of useful heat Q_1 to the heat from the low temperature heat source Q_0 is larger than in compression heat pumps. To liquefy the refrigerant at the evaporation pressure, but at a higher temperature, the effect of boiling point elevation due to the addition of a second liquid to the refrigerant is used.

During the absorption process, the absorbent is diluted and, therefore, has to be regenerated to maintain its absorption capability. To this end, the diluted solution is pumped to the higher pressure level into the desorber (D) where heat is supplied to boil off the refrigerant. The vapor refrigerant is condensed in the condenser (C) and throttled to the evaporator pressure, and the refrigerant cycle can start again. The concentrated solution is also throttled and flows back to the absorber where it can absorb the vapor refrigerant anew. Another heat exchanger, the so-called solution heat exchanger (SHX), is added into the solution circuit to increase the efficiency of the process by means of internal heat exchange.

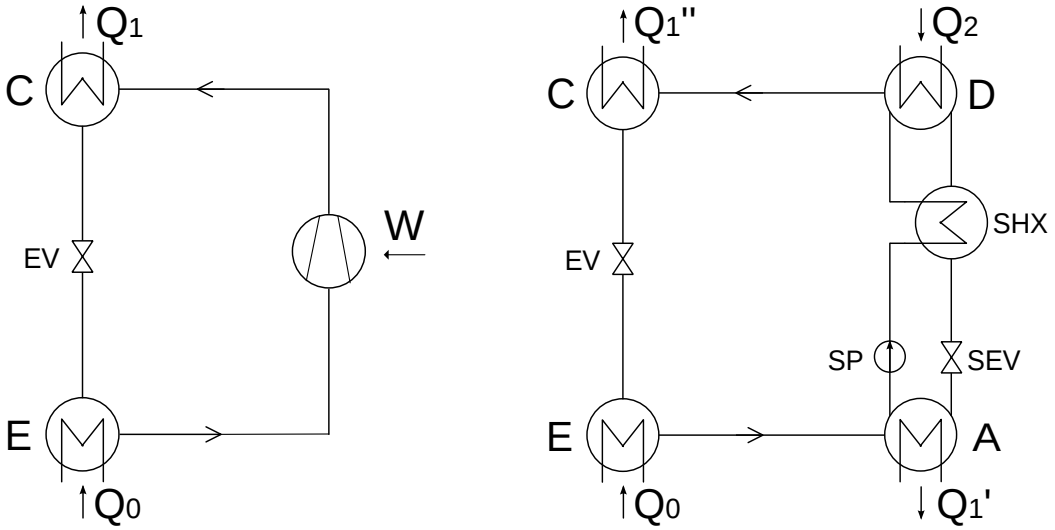

Figure 2: Compression (left) and absorption (right) heat pump cycle

The absorption heat pump cycle is usually displayed in a vapor pressure diagram (Figure 3) where due to the ln p/-1/T scaling the boiling curves are almost straight lines. In this diagram, the two pressure and the three temperature levels can be recognized easily. x_w and x_s are the absorbent mass fractions of the weak (diluted) and the strong (concentrated) solution. Their difference is called concentration difference Δx. The absorbent mass fraction is defined as the ratio of absorbent mass to the total mass of solution. Ideally, the volatility of the absorbent is small as compared to that of the refrigerant. In this case, the absorbent mass fraction of the refrigerant x_R is 0, i.e. there is no absorbent in the refrigerant cycle between

condenser and evaporator. Otherwise, a rectification is needed. Another characteristic number is the solution circulation ratio (pump rate) f defined as

$$f = \frac{\dot{m}_W}{\dot{m}_R} = \frac{x_S}{\Delta x} \quad . \tag{4}$$

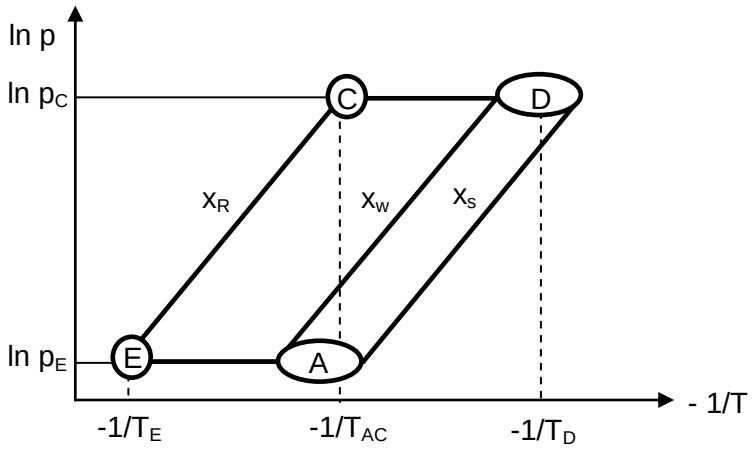

Figure 3: Absorption heat pump cycle in the ln p/-1/T diagram

The basic cycle described so far is the single effect cycle. The reversible COP,

$$COP_{rev,c} = \frac{r}{r+l} \tag{5}$$

$$COP_{rev,h} = 1 + \frac{r}{r+l} \tag{6}$$

of a single effect cooling cycle is always below 1 and that of a single effect heat pump cycle always below 2 as long as the specific heat of solution l is in the order of 10% of the heat of evaporation r. This is the case for all working pairs known to date.

To achieve higher cycle efficiencies, to decrease the required driving temperature level, or to achieve high temperature glides of the driving heat medium, several modifications of this cycle have been developed, namely multi effect or multi lift cycles (e.g. Ziegler et al. 1993). The term "effect" is used especially for cooling applications to describe how often the heating unit supplied is used to achieve a regeneration effect and thus a useful cooling effect. The term "lift" is used to describe the multiple by which the temperature lift between the heat sink and the heat source is higher than the temperature thrust between the driving heat and the heat sink. This is equivalent to the number of heating units supplied per useful cooling unit. Multi effect cycles are used to increase the efficiency (coefficient of performance, COP). Multi lift cycles make it possible to drive the process at low temperatures (e.g. low temperature waste heat). In this case, a reduction of the COP is accepted.

Figure 4 presents a schematic of a double effect absorption cycle in the vapor pressure diagram. A COP_c of 1.0 to 1.3 can be achieved due to an internal heat exchange. Triple or quadruple effect cycles are also possible if high temperature driving heat is available and limiting factors like corrosion problems can be solved.

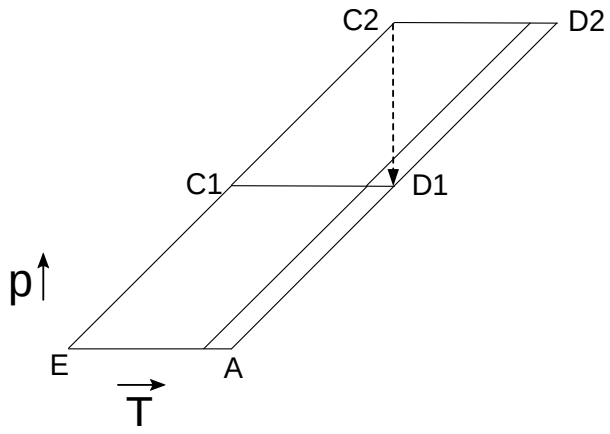

Figure 4: Double effect absorption heat pump cycle in the ln p/-1/T diagram

The double effect principle is also possible with an internal heat transfer when the temperature glide in the absorber and desorber overlaps (high concentration difference between strong and weak solution). In this case, the heat of absorption is used to partly regenerate the solution in the desorber (generator). This principle is called generator-absorber heat exchange (GAX) (Altenkirch 1913/1914, Scharfe et al. 1986).

In Figure 5, a typical double lift cycle is represented. Cooling COPs of up to 0.4 are achieved.

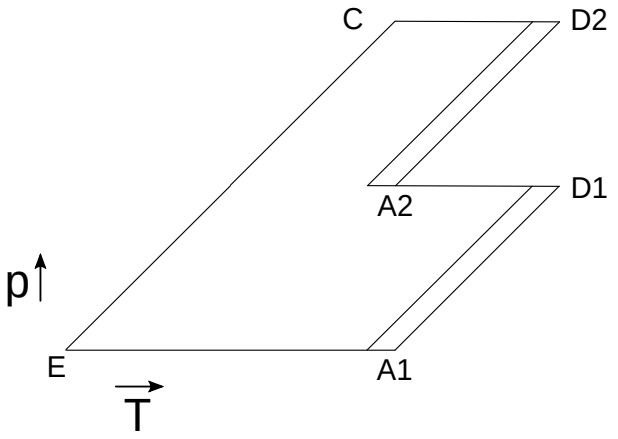

Figure 5: Double lift absorption heat pump cycle in the ln p/-1/T diagram

Although many working pairs for absorption heat pumps and cooling machines have been suggested over the last half century, only two prevail: water/LiBr and ammonia/water.

Water has a high latent heat, is chemically stable, non-toxic, environmentally-neutral, and economical. A drawback, however, is the low vapor pressure which requires a vacuum-tight construction of the vessels. The application is limited by the freezing temperature of 0°C. However, a depression of the freezing point is possible by adding substances like salts (Kojima 2003, Richter 2007, Kühn 2008). Aqueous LiBr solution has a negligible vapor pressure, a low viscosity and is non-toxic. The formation of crystals at high absorbent concentration is unfavorable (see crystallization line in Figure 6) and limits the possible temperature lift, i.e. the difference between low and medium temperature level. Nevertheless, the working pair water/LiBr permits the highest energetic and economic efficiency using simple, well-engineered, and relatively compact systems.

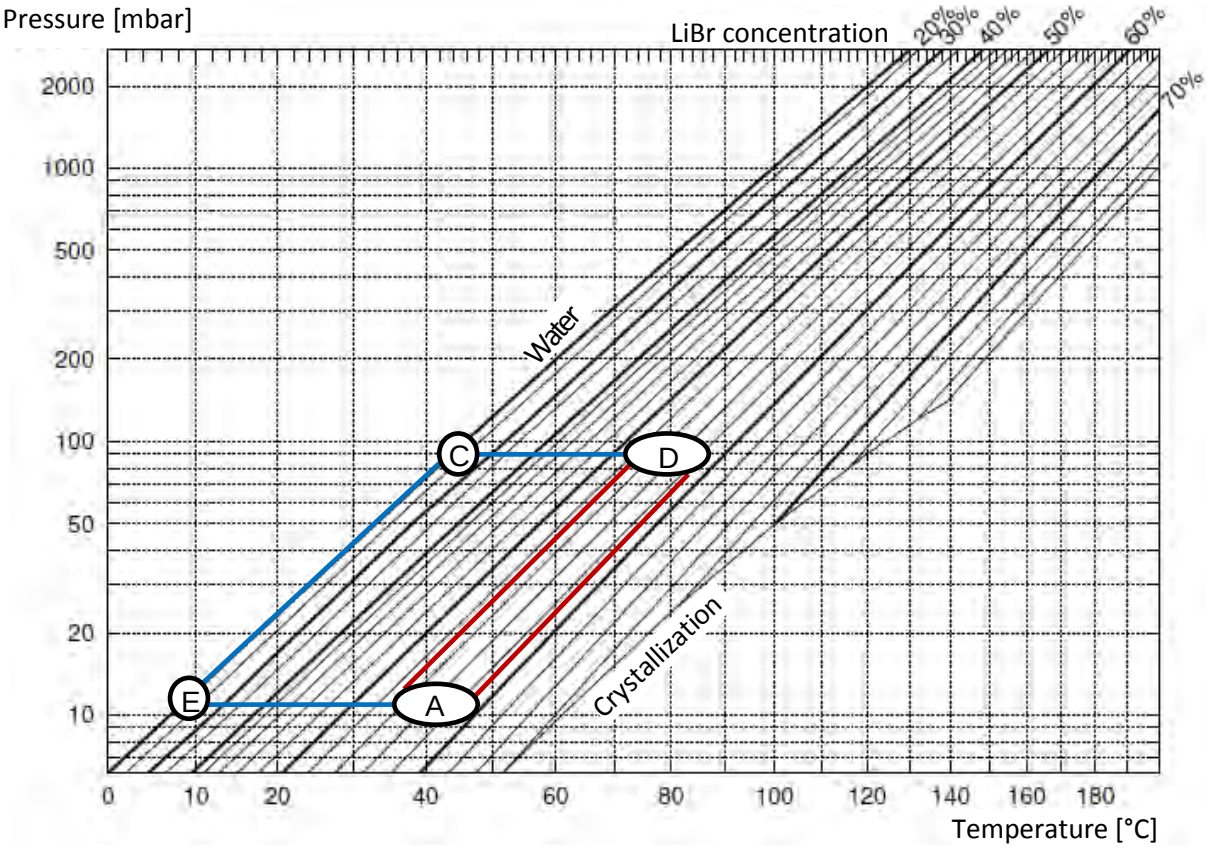

Figure 6: Absorption heat pump cycle plotted over the vapor pressure lines of water/LiBr (Feuerecker 1994)

Ammonia, in contrast, is toxic, and is flammable and explosive in air for some concentrations. Depending on the charge, special safety precautions are necessary. The vapor pressure is high (see Figure 7). Therefore, pressure vessels are needed, and the solution pump requires more energy. Water has a significant vapor pressure as compared to ammonia and, consequently, for high temperature lift a rectification or a liquid bleed is required which reduces the process efficiency. One advantage of ammonia/water is that the solution does not crystallize. Ammonia/water permits the generation of very low refrigeration temperatures down to -40°C and the use of high heating supply (heat pump mode) or cooling water temperatures (cooling mode) if the driving temperature is high enough. Ammonia/water systems are slightly more complex, not as efficient as water/LiBr systems and need more auxiliary power. However, as opposed to water/LiBr heat pumps, it is possible to use compact and cost efficient plate heat exchangers instead of tube bundles.

In recent years, new working pairs based on ionic liquids as absorbents have been investigated (Radspieler and Schweigler 2011, Schneider et al. 2011). Ionic liquids are considered to have a high potential to overcome the weaknesses of the prevalent pairs.

A modification of the absorption heat pump process described so far is the diffusion absorption heat pump process developed by the Swedes Platen and Munters as early as 1922. The idea is to introduce an auxiliary inert gas (e.g. helium) which is able to compensate the refrigerant partial pressure difference between condenser and evaporator and desorber and absorber, respectively. The result is a unique total pressure in the whole machine. In Figure 8, the third cycle, the thermosyphon driven auxiliary gas circulation, can be seen. The big advantage of this technology is that a simple bubble pump with no moving parts is able to circulate the NH_3/water solution. This principle has been used a millionfold for absorber refrigerators in the hotel or camping business.

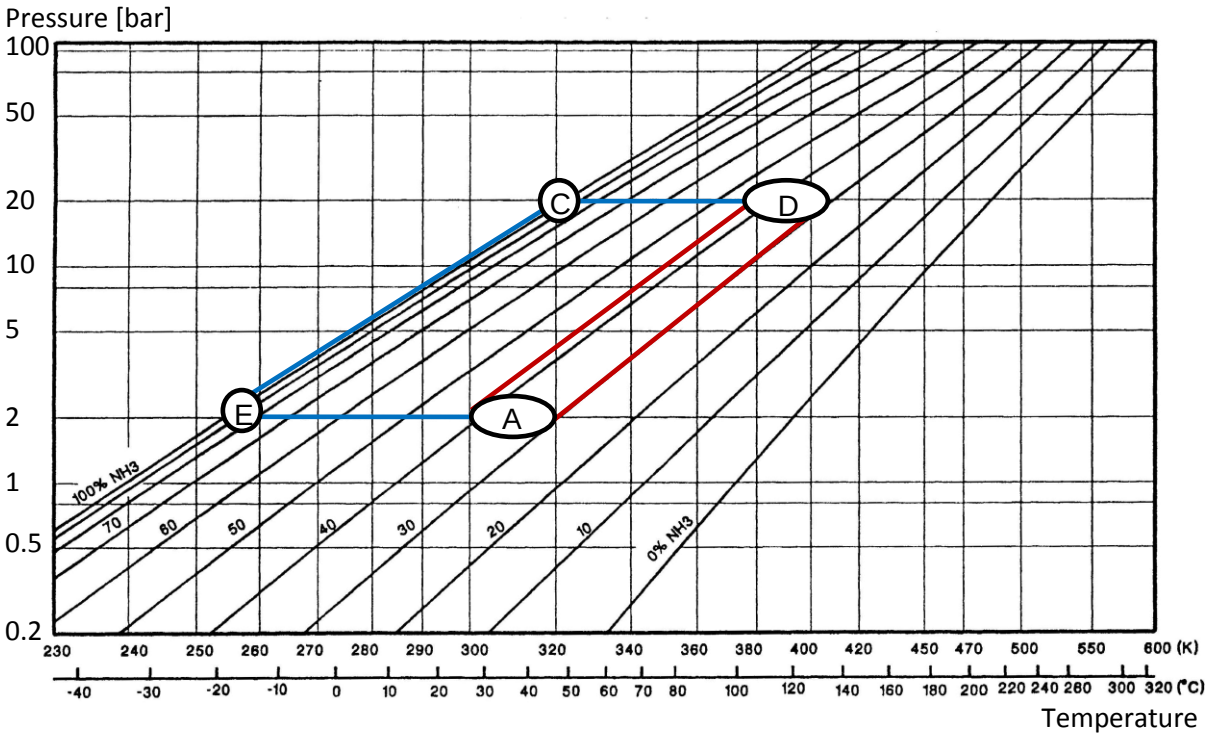

Figure 7: Absorption heat pump cycle plotted over the vapor pressure lines of NH_3/water (Ziegler and Trepp 1984)

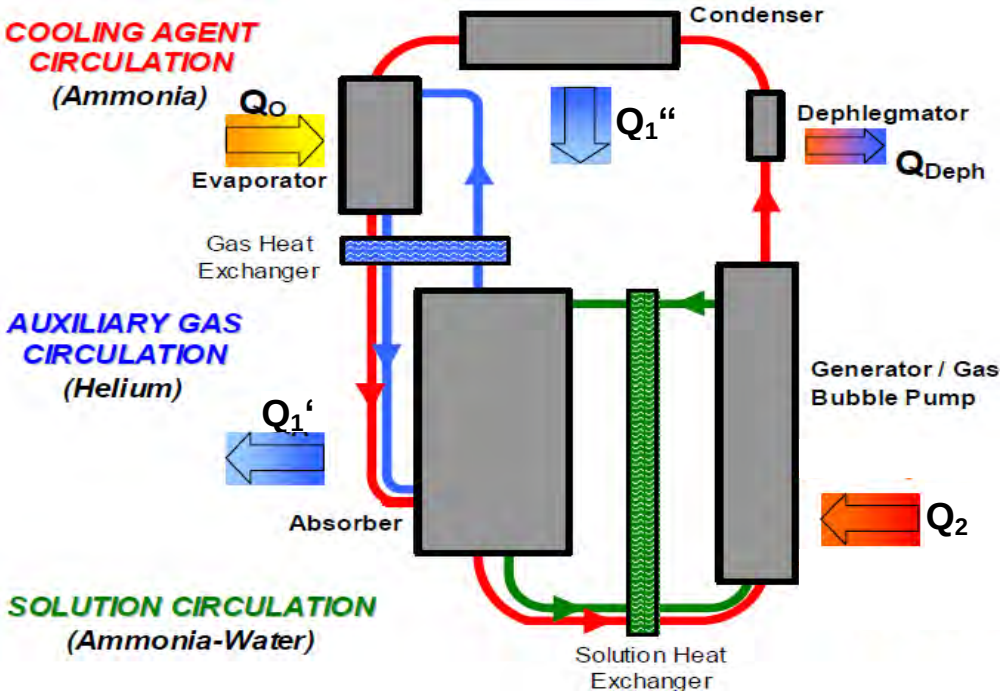

Figure 8: Functional principle of a diffusion absorption heat pump (Jakob and Eicker 2002)

3 ADSORPTION HEAT PUMPS

Unlike absorption where the refrigerant is absorbed in a liquid sorbent, in the case of adsorption the refrigerant is adsorbed in the pores of a solid sorbent. The adsorption heat pumping cycle is thermodynamically similar to the absorption cycle. It consists of the same main heat exchangers: evaporator, condenser, and a heat exchanger for adsorption and desorption. Unlike the absorption process where the liquid absorbent is pumped between absorber and desorber, adsorption is a discontinuously working process as the solid adsorbent cannot easily be moved from one vessel to the other. Adsorption and desorption can occur successively in the same vessel. However, to ensure a reasonably continuous useful heating or cooling effect, two so-called reactors are usually used and operated in counter-phase. Figure 9 shows a typical construction of an adsorption heat pump.

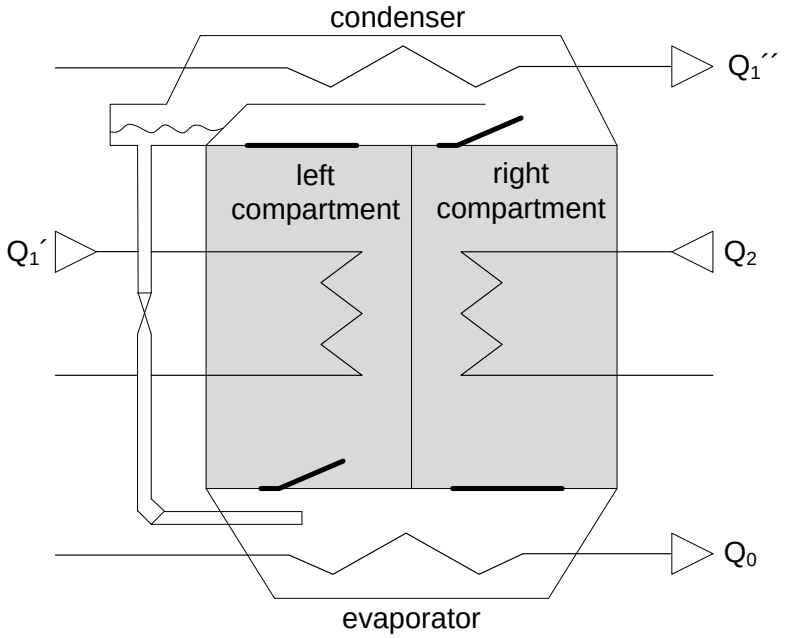

Figure 9: Typical adsorption heat pump design (on the basis of Henning 2004a)

In Figure 10, a typical adsorption process is explained. In phase 1, the refrigerant evaporates and is taken up by the adsorbent in the right compartment. The adsorption heat has to be removed by an external heat carrier and is used for heating purposes (heat pump mode) or rejected to the environment (cooling mode). Simultaneously, in the left compartment the adsorbent regeneration takes place. Heat is supplied to desorb the refrigerant. The refrigerant vapor flows to the condenser where it is condensed, and then throttled and returned to the evaporator like in the conventional compression or absorption process. Usually, flaps ensure an autonomous connection or disconnection of adsorber/desorber and evaporator/condenser. In phase 3, the same processes occur with the difference that adsorption takes place in the left and desorption in the right compartment.

When changing the phases there is a short period without cold/heat production followed by a peak in the heat/cold production. Over time, adsorption capability decreases. Cycling time is therefore a more important control parameter compared to the pump rate in absorption heat pumps. While short cycles tend to provide higher useful heating or cooling power density, process efficiency is mostly higher with longer cycle times. It is possible to have either fixed or variable cycle times, depending on a defined minimum useful heat or cold delivered.

In order to reduce the decrease in efficiency due to the lack of a solution heat exchanger, there are several concepts for heat recovery of adsorbent, heat exchanger, and vessels

when shifting the phase. In commercial applications, both compartments are usually connected thermally (heat recovery) or directly (mass recovery) during the switching phases 2 and 4. Nevertheless, internal heat recovery is not as effective as it is for absorption heat pumps, resulting in lower process efficiencies.

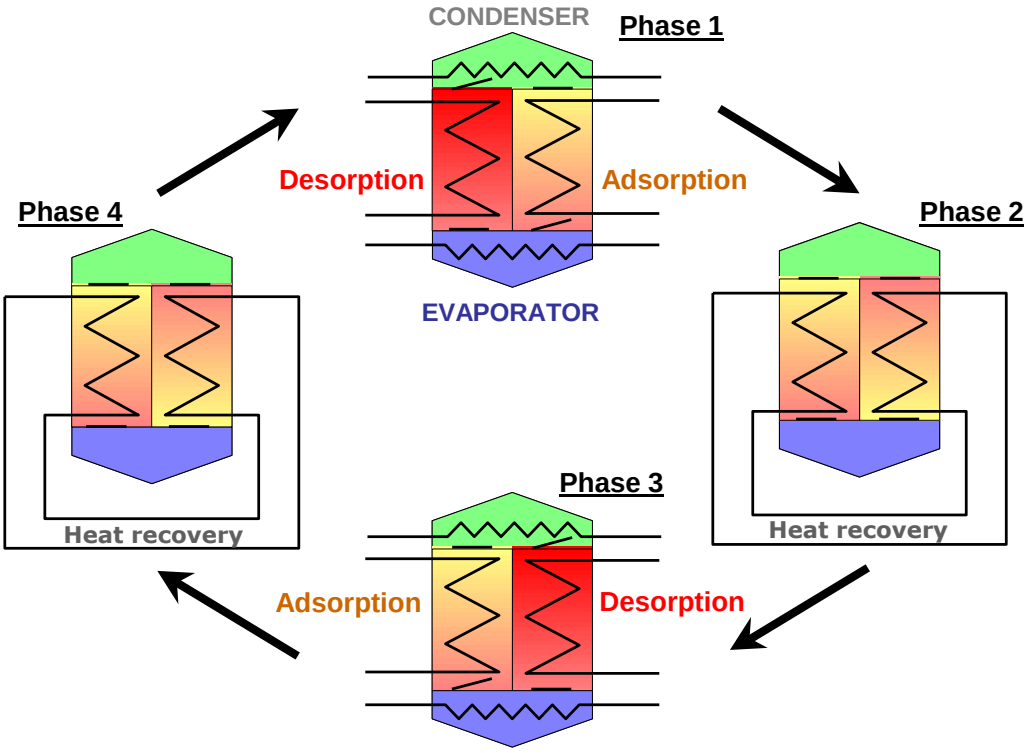

Figure 10: Adsorption cycle with heat recovery (on the basis of Henning 2004b)

In order to increase the performance of the machines, some more sophisticated configurations have been developed, such as thermal wave (Shelton et al. 1989, see Figure 11) or multi-bed (e.g. Saha et al. 2003). As for absorption heat pumps, cycles have been adapted for lower driving temperatures (e.g. Saha et al. 2003).

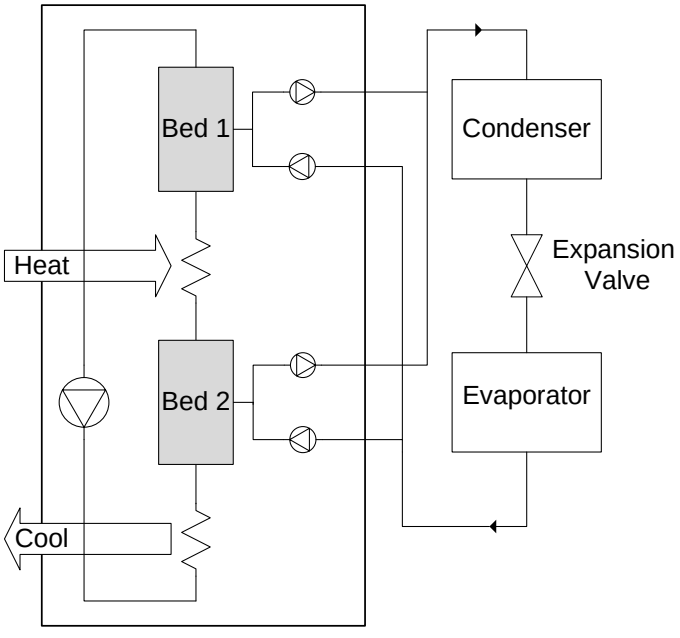

Figure 11: Thermal wave adsorption heat pump (Critoph 1999)

A suitable adsorbent is a porous, solid material with a high internal surface. The most common adsorption heat pump working pairs are water/silica gel, water/zeolite, ammonia/ activated carbon and methanol/activated carbon.

It is standard, like for the absorption heat pump process, to represent the adsorption process in a ln p/-1/T diagram. Figures 12 and 13 show the diagrams of water/silica gel Grace 125 and water/zeolite Z13X, two typical examples.

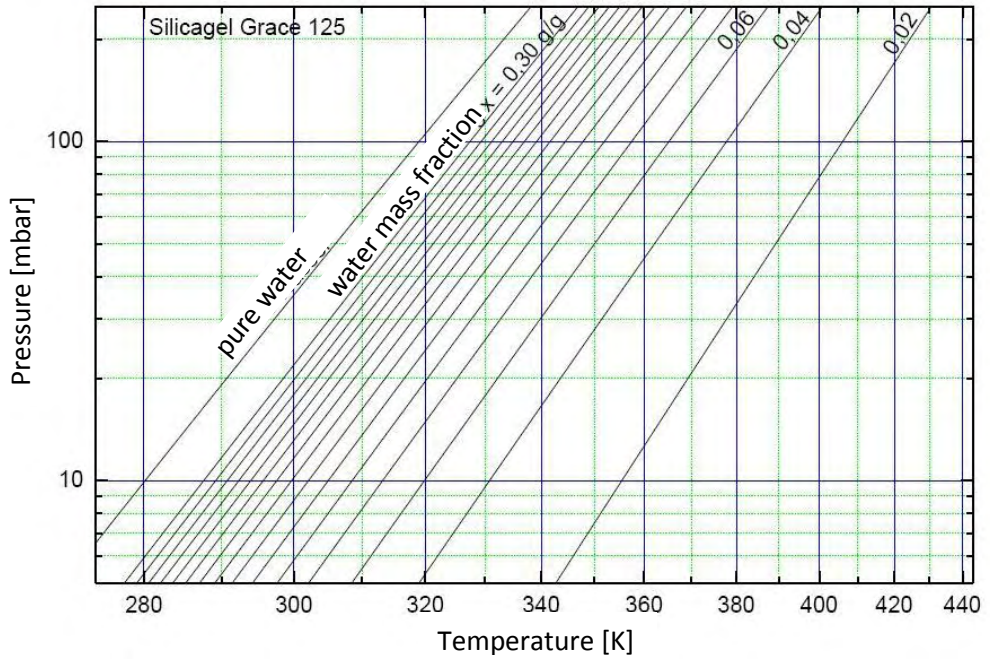

Figure 12: ln p/-1/T diagram of silica gel Grace 125 (Jahnke 2008 on the basis of Nuñez 2001)

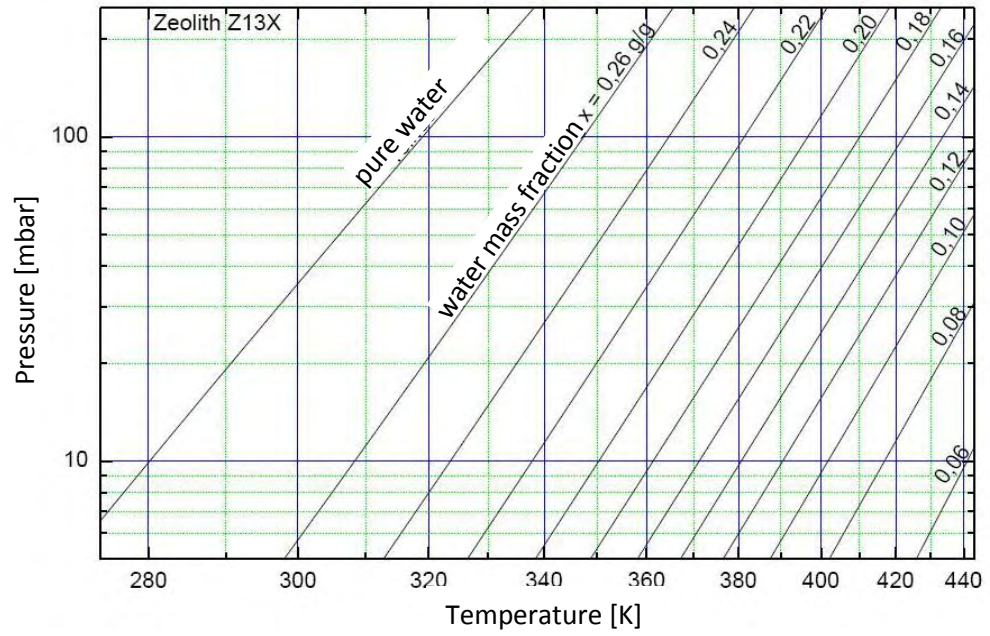

Figure 13: ln p/-1/T diagram of zeolite Z13X (Jahnke 2008 on the basis of Nuñez 2001)

Isosteres describe all boiling states with the same mass fraction x (vapor pressure/boiling curves). High refrigerant uptake in certain temperature ranges can be realized where isosteres are narrow. From a comparison of Figures 12 and 13, it can be concluded that

silica gel Grace 125 is more suitable for low temperature lifts and low driving temperatures while zeolite Z13X fits for higher temperature lifts and higher driving temperatures. Today, like in the case of ionic liquids for absorption heat pumps, adsorbents are expected to be tailor-made by the manufacturers in accordance to the user requirements (e.g. suitable for low driving temperatures or suitable for high temperature lifts).

4 COMPARISON

Water/LiBr absorption heat pumps offer the highest thermal efficiencies. Water/LiBr chillers have been produced and operated in large numbers and a wide power range for many decades. Nevertheless, the temperature lift is limited by the potential crystallization of the sorbent. Ammonia/water absorption heat pumps can be operated with environmental heat sources below zero degrees (e.g. air or ground collectors) or employed for refrigeration. Market available ammonia/water heat pumps supply domestic hot water up to 70°C. The drawback is the high upper pressure level and the high energy consumption of the circulation pump that requires special design. Adsorption heat pumps are not limited in the temperature lift by these constraints. However, their efficiency is generally lower. The discontinuously working process involves fluctuating outlet temperatures of the hydraulic circuits.

It is very often said that adsorption chillers need lower driving temperatures than absorption chillers. Ziegler and Lamp derived as early as 1996 by physical means that for identical boundary conditions and vanishing concentration difference between strong and weak solution or loaded and unloaded adsorbent the theoretical minimum driving temperature is almost the same for absorption and adsorption systems which were used frequently at that time. For real but fixed pump rates absorption heat pumps require even lower driving temperatures than adsorption heat pumps. Kühn et al. (2005) presented a small scale water/LiBr absorption chiller with 55°C minimum driving hot water temperature (50% part load) with nearly no efficiency drop compared to the design point.

Adsorption heat pumps operate without moving components like pumps. The opening and closing of the flaps is self-regulating or controlled by valves. In terms of power density, no clear statement for the preference of absorption or adsorption can be given yet. It seems today that adsorption units of around 10 kW can be very compact, but for higher capacity, absorption systems are supposed to be more compact and more efficient.

Adsorption machines are less affected by motion, but absorption heat pumps can also be applied successfully in the automotive or shipping sector as reported by Safarik et al. (2011). Motion can even be used to increase the heat and mass transfer (e.g. Gilchrist 2002).

Academic research activities, today, focus more on adsorption heat pumps as there is still potential of process optimization in order to increase the performance. Absorption cooling machines are technically mature, although the use as a heat pump could certainly be intensified. One major next step for both absorption and adsorption heat pumps is the increase of power density and reduction of manufacturing costs. In future, moreover, it could be crucial whether the tailor-making of absorbents or adsorbents leads to better results.

5 SYSTEMS

To be operated, the sorption heat pump has to be connected to a high temperature heat source, a low temperature heat source, and a medium temperature heat sink. Possible system configurations are presented in Figures 14 (heat pump mode) and 15 (cooling mode).

The reject heat in heat pump operation is used to provide room heating or domestic warm water with a temperature level of typically 20 to 70°C. As for compression heat pumps the low temperature heat source is usually an environmental heat source: air (directly used or indirectly, e.g. preheated by a solar collector) and different ground sources are available. Sewage water is an interesting alternative. The big advantage over compression heat pumps is that the low temperature heat source needed for the same heating duty is only about half the size. Driving heat is provided most commonly by an internal gas burner but can also be provided by other heat sources as e.g. district or waste heat.

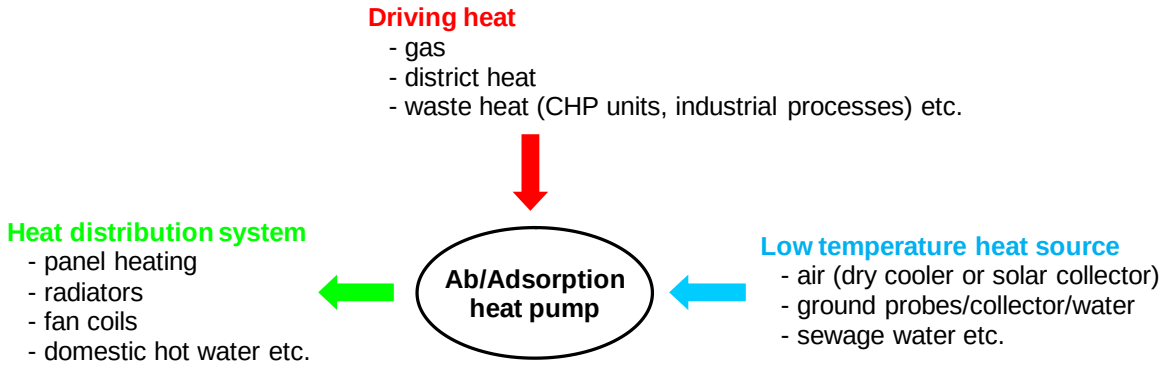

Figure 14: Ab/Adsorption heat pump system

For chillers and refrigeration systems the low temperature heat source is the cold distribution system. The low temperature level provided by sorption cooling machines ranges from -40°C for refrigeration purposes or industrial processes to 6 to 18°C for air-conditioning (chilled water). Condensation and absorption heat are usually rejected to the ambient air directly or via a cooling water circuit (dry cooler, wet or hybrid cooling tower) or to the ground (ground probes, ground collector, ground water). The cooling water temperature range is mainly between 23 and 40°C but may also be higher. Driving heat is preferably provided by solar or waste heat (e.g. from combined heat and power units or plants). For reasons of energy efficiency, the use of fossil fuels to drive a sorption chiller should be avoided (Ziegler 2009). The driving heat level required depends on the temperature lift. A high temperature lift requires a high driving temperature. Temperatures from typical driving heat sources range from around 55°C (solar cooling) up to 95°C (district heat). Higher driving temperatures, e.g. from industrial processes or concentrating solar collectors above 120°C allow for the use of advanced cycles, e.g. double-effect.

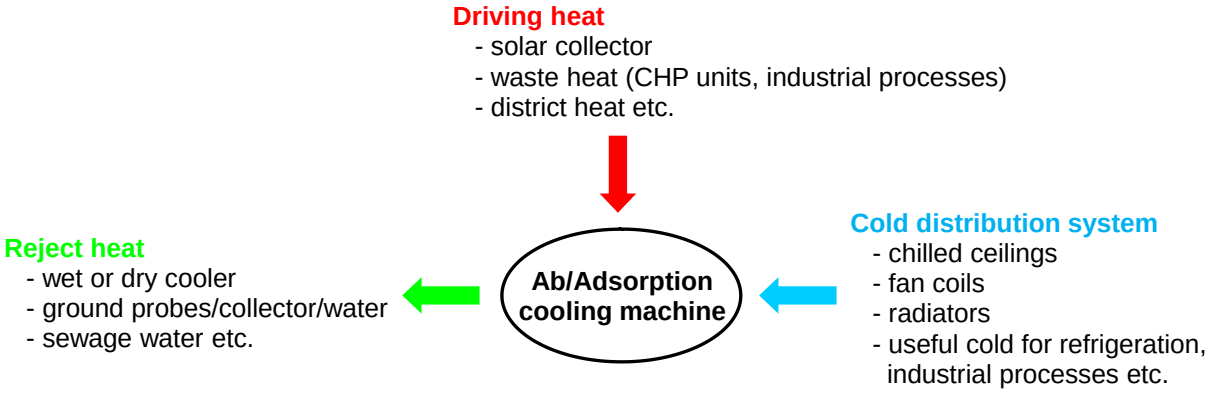

Figure 15: Ab/Adsorption cooling system

It is easy to see that the heat pump can be used for heating in winter and cooling in summer when heat sink and low temperature heat source are interchanged. The heat pump can also

be used for simultaneous heating and cooling, e.g. if in heating period server rooms have to be cooled. In this case, efficiency is the highest. However, in most cases cooling and heating demands do not occur at the same time.

6 REFERENCES

Altenkirch E. 1913/1914. Reversible Absorptionsmaschinen, Zeitschrift für die gesamte Kälte-Industrie (1) 1913 pp. 1-9, (6) 1913 pp. 114-119, (8) 1913 pp. 150-161, (1) 1914 pp. 7-14, (2) 1914 pp. 21-24.

Critoph R.E. 1999. "Forced convection adsorption cycle with packed bed heat regeneration", *Int. J. of Refrigeration*, 22, pp. 38-46.

Feuerecker G. 1994. "Entropieanalyse für Wärmepumpensysteme: Methoden und Stoffdaten", Dissertation, Technische Universität München, Germany.

Gilchrist K., R. Lorton, J.R. Green 2002. "Process intensification applied to an aqueous LiBr rotating absorption chiller with dry heat rejection", *Appl. Therm. Eng.*, 22, pp. 847-854.

Henning H.-M. (Ed.) 2004a. Solar-Assisted Air-Conditioning in Buildings, Springer-Verlag Wien, Austria.

Henning H.-M. 2004b. Klimatisieren mit Sonne und Wärme, BINE Themeninfo I/04, Fachinformationszentrum Karlsruhe, Germany.

Jahnke A. 2008. Konzeption, Aufbau und Funktionsüberprüfung eines Teststandes zur experimentellen Charakterisierung von Adsorberwärmeübertragern, Diplomarbeit, Technische Universität Berlin, Germany.

Jakob U., U. Eicker 2002. "Solar cooling with diffusion absorption principle", *Proc. of the 7th World Renewable Energy Congress*, Köln, Germany.

Kojima M., T. Fujita, T. Irie, N. Inoue, T. Matsubara 2003. "Development of Water-LiBr Absorption Machine Operating Below Zero Degrees", *Proc. of the Int. Congress of Refrigeration*, Washington, D.C., USA.

Kühn A., T. Meyer, F. Ziegler 2008. "Operational results of a 10 kW absorption chiller in heat pump mode", *Proc. of the 9th IEA Heat Pump Conference*, Zürich, Switzerland.

Nunez T. 2001. Charakterisierung und Bewertung von Adsorbentien für Wärmetrans-formationsanwendungen. Dissertation, Albert-Ludwigs-Universität Freiburg, Germany, http://www.freidok.uni-freiburg.de/volltexte/335/pdf/DissertationNunez.pdf.

Radspieler M., C. Schweigler 2011. "Experimental investigation of ionic liquid EMIM EtSO4 as solvent in a single-effect cycle with adiabatic absorption and desorption", *Proc. of the Int. Sorption Heat Pump Conf.*, April 6-8, Padua, Italy.

Richter L., M. Kuhn, M. Safarik 2007. "Kälteerzeugung unter 0°C mit einer Wasser/ Lithiumbromid-Resorptionskältemaschine", *Tagungsband der DKV-Tagung, November 21-23*, Hannover, Germany.

Safarik M., L. Richter, G. Weidner, Y. Wild, P. Albring 2011. "Application of absorption chillers on vessels", *Proc. of the Int. Sorption Heat Pump Conf., April 6-8*, Padua, Italy.

Saha B.B., S. Koyama, T. Kashiwagi, A. Akisawa, K.C. Ng, H.T. Chua 2003. “Waste heat driven dual-mode, multi-stage, multi-bed regenerative adsorption system”, *Int. J. of Refrigeration*, 26, pp. 749–757.

Scharfe J., F. Ziegler, R. Radermacher 1986. “Analysis of advantages and limitations of absorber-generator heat exchange“, *Int. J. of Refrigeration*, 9, pp. 326–333.

Schneider M.-C., R. Schneider, O. Zehnacker, O. Buchin, F. Cudok, A. Kühn, T. Meyer, F. Ziegler, M. Seiler 2011. “Ionic Liquids: New high-performance working fluids for absorption chillers and heat pumps”, *Proc. of the Int. Sorption Heat Pump Conf., April 6-8*, Padua, Italy.

Shelton S.V., W.J. Wepfer, D.J. Miles 1989. “Square wave analysis of the solid-vapour adsorption heat pump”, *J. Heat Recov. Syst. CHP*, 9 (3), pp. 233-247.

Ziegler B., C. Trepp 1984. “Equation of state for ammonia-water mixtures”, *Int. J. of Refrigeration*, Vol. 7 (2), pp. 101–106.

Ziegler F. 1991. Kompressions-Absorptions-Wärmepumpen, Forschungsberichte des Deutschen Kälte- und Klimatechnischen Vereins Nr. 34, DKV, Stuttgart, Germany.

Ziegler F. 2009. “Sorption heat pumping technologies: Comparisons and Challenges“,*Int. J. of Refrigeration*, 32, pp. 566-576.

Ziegler F., R. Kahn, F. Summerer, G. Alefeld 1993. “Multi-effect absorption chillers”, *Int. J. of Refrigeration*, Vol. 16 (5), 301.

GAS-DRIVEN SORPTION HEAT PUMPS; A POTENTIAL TREND-SETTING HEATING TECHNOLOGY

Dr. Belal Dawoud, Viessmann Werke Allendorf GmbH, Viessmann Street 1, D-35107 Allendorf/Eder, Germany, DrDaw@Viessmann.com

This paper was published in the IEA Heat Pump Centre Newsletter Volume 29 - No. 1/2011 (www.heatpumpcentre.org).

Abstract: Increased efforts to reduce CO_2 emissions and continuous increases in fossil energy prices have led to stronger legislation concerning energy utilisation efficiency in the domestic heating sector. Accordingly, German gas utilities and the key European manufacturers of gas heating appliances have teamed up to form what is known as the "Gas Heat Pump Initiative" to introduce new heating technologies, which are capable of achieving an incremental improvement of gas utilisation efficiency compared to that delivered by gas condensing technology. This article provides a brief introduction to these innovative heating appliances and a presentation of the gas heat pump initiative.

Key Words: Gas heating, Sorption heat pumps, Zeolite-Water, Ammonia-Water, Initiative gas heat pumps

1 INTRODUCTION

According to the "EE-Wärmegesetz, 2008" (the Renewable Energy Heating Law) for increasing the share of renewable energy in household heating applications in Germany, a significant part of the heating demand shall be covered by renewable energy resources or shall be reduced by carrying out relevant building's modernisation efforts. This means that more efficient and environmentally friendly gas heating appliances will have a significant market share compared with conventional technologies.

The spread of natural gas on the market was based, among other factors, on developments of low-pollution burners and later energy-efficient low-temperature boilers. The role of natural gas as a modern and ecologically compatible energy source was substantially extended by the introduction of gas condensing boiler technology in the 1990s. The heating market has subsequently become the largest consumption sector for natural gas. Since 2005, and particularly in the new buildings sector, the growth of the gas heating market has been clearly reduced, with a decline in service connection density from 80% to now less than 60%. In addition, expansion of the gas supply networks has reached the limits of economic feasibility.

The gas industry therefore needs to respond to customers' increased environmental awareness and demands for autonomous solutions with innovative and modern heating technologies utilising renewable energy. Along with the established condensing boilers plus solar energy solutions, gas heat pumps, in particular, enable end users to meet the market's political demands for high-efficiency heating systems in conjunction with renewable energy utilisation.

In addition, sorption heat pumps have attracted considerable attention due to their lower environmental impact than that of conventional vapour compression heat pumps using

HCFCs and HFCs, since sorption systems make use of natural refrigerants (ammonia and water), which have zero global warming potential. For these reasons, German gas utilities and the key European manufacturers of gas heating appliances established the Gas Heat Pump Initiative (www.igwp.de) in 2008 as a concerted action to carry out laboratory and field tests, prepare the market and work out the required standards framework for the introduction of gas heat pump-based heating appliances. This article presents a brief introduction to the sorption heat pump technologies involved, as well as to the Gas Heat Pump Initiative (IGWP) and its activities.

2 WORKING PRINCIPLES OF THE GAS-DRIVEN SORPTION HEAT PUMP HEATING PROCESSES

Heat pumps can in general be classified by the following technical principles:

- Vapour compression heat pumps (electrically-driven or gas-motor-driven heat pumps). In this type, the heat pump process is delivered solely by mechanical energy.
- Sorption heat pumps (absorption or adsorption heat pumps), in which heat is the main driving energy.

Common to both heat pump processes is that the liquid refrigerant leaving the condenser after transferring its heat of condensation to the heating system passes through an expansion valve in order to reduce its pressure, and therefore its temperature, below the temperature of the ambient heat source before entering the evaporator. In the evaporator, the expanded refrigerant vaporises as it picks up its heat of evaporation from the ambient heat source (air, ground, groundwater or solar collectors).

In a vapour compression heat pump, the gaseous refrigerant leaving the evaporator is induced by a mechanical compressor, where its pressure, and therefore temperature, is increased before entering the condenser to be liquefied again.

The duty of the mechanical compressor is tackled differently in a sorption heat pump, where heat becomes the main driving energy (thermal compression). There are several ways of realising what is known as the “thermal compressor” in a sorption heat pump. The main idea remains, however, to apply a sorbent for the refrigerant in the thermal compression process. If the sorbent remains in the solid state (silica gel, zeolite or active carbon are typical adsorbents for water, methanol or ammonia as refrigerants), we talk about an adsorption heat pump. Absorption heat pumps utilise liquid sorbents (LiBr-H_2O solution or diluted NH_3-H2O solutions for water or ammonia as refrigerants).

Figure 1 shows a simplified schematic of the gas-driven absorption heat pump process. The right-hand side of the diagram shows the components of the thermal compressor. Refrigerant vapour is first absorbed into the liquid sorbent after being expanded in the solution expansion valve, to form a refrigerant-rich solution. Both the heat of condensation of the refrigerant vapour and the binding energy of the refrigerant into the absorbent (the latent heat of absorption) are then transferred to the heating water in the form of useful heat. The pressure of the enriched solution is then raised to the condenser pressure by a solution pump, which requires only about 1 % of the mechanical energy required to raise the pressure of the refrigerant vapour in a mechanical compressor (mechanical work required for compression is proportional to the specific volume of the medium). The high-pressure enriched solution enters the generator, which is directly fired by natural gas. From here, refrigerant vapour at high pressure and temperature flow into the condenser, while the weakened refrigerant solution flows back to the absorber after being expanded to the absorber or evaporator pressure to absorb more refrigerant coming out of the evaporator. This is a simplified explanation: in fact, the real absorption heat pump process employs more units for internal heat recovery and therefore for further improvement of gas utilisation efficiency. The first

gas-driven heat pump technology in the IGWP framework utilises ammonia-water as a working pair and is available in a heating power range of 40 kW (Dummer 2010). This type of heat pump technology can be used to cover the nominal heating demand or to cover the base load if integrated with a condensing boiler for peak loads.

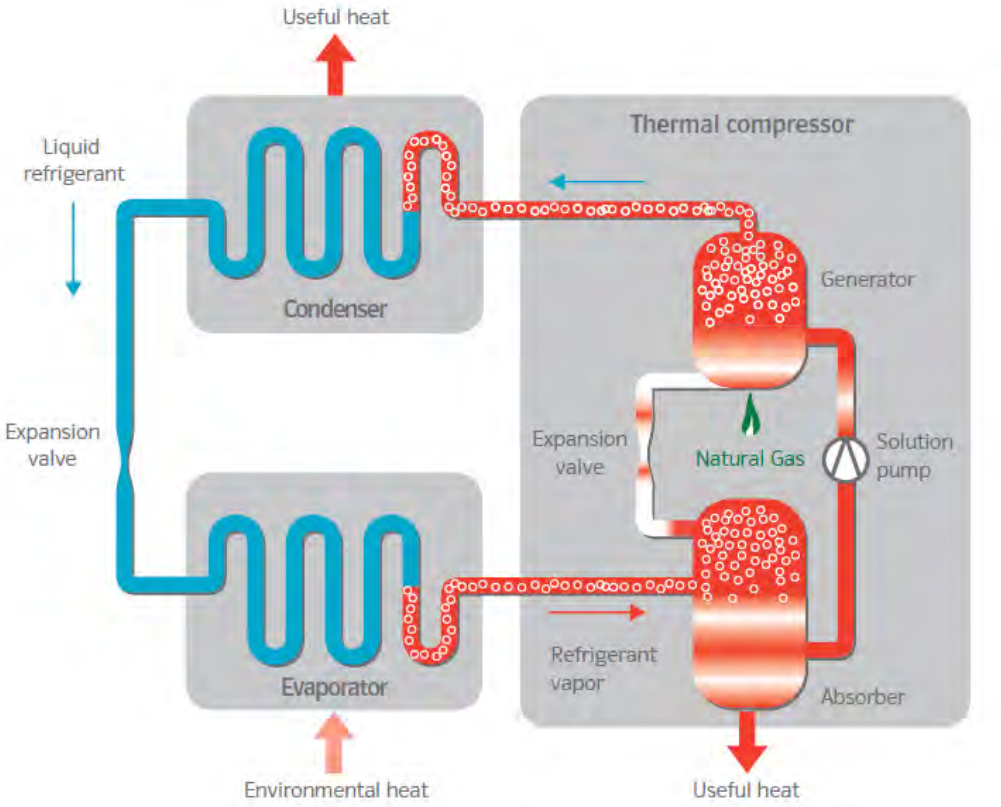

Figure 1: Schematic of the single-stage absorption heat pump process

The second type of gas-driven heat pump technology in the IGWP framework is shown in Figure 2. It is a hybrid heating appliance, comprising a gas condensing boiler to drive an intermittent adsorption heat pump module and to meet the peak load if the required heat demand exceeds the rated heat pump heating capacity (Lang and Marx 2010). This Vaillant zeolite heat pump module is referred to as a two- heat exchanger module, as it incorporates two heat exchangers. The top heat exchanger functions either as a desorber or an adsorber, while the lower heat exchanger works respectively as a condenser or evaporator. This technology utilises zeolite (as an adsorbent) in the form of loose pellets between the fins of a finned-tube adsorber heat exchanger, with water as a refrigerant. One important feature of this technology is the utilisation of solar collectors as an ambient heat source. Figure 2 left side depicts the heating appliance in the desorption phase, during which zeolite is heated up by a hot water loop connecting the adsorber heat exchanger with the gas burner heat exchanger. The water vapour from the zeolite pellets condenses on the lower heat exchanger (working as a condenser), delivering useful heat to the heating water through the lower plate heat exchanger. After reaching a certain desorption end temperature, the burner is switched off and the adsorber heat is transferred to the house heating system through the plate heat exchanger just below the zeolite module, resulting in reducing the temperature of the zeolite. The cold and dried zeolite then adsorbs water vapour from the condenser, progressively reducing its temperature until it is lower than the temperature of the brine flowing out of the solar collector panel. From then on, the lower heat exchanger works as an evaporator, feeding ambient heat into the process (Figure 2, right side).

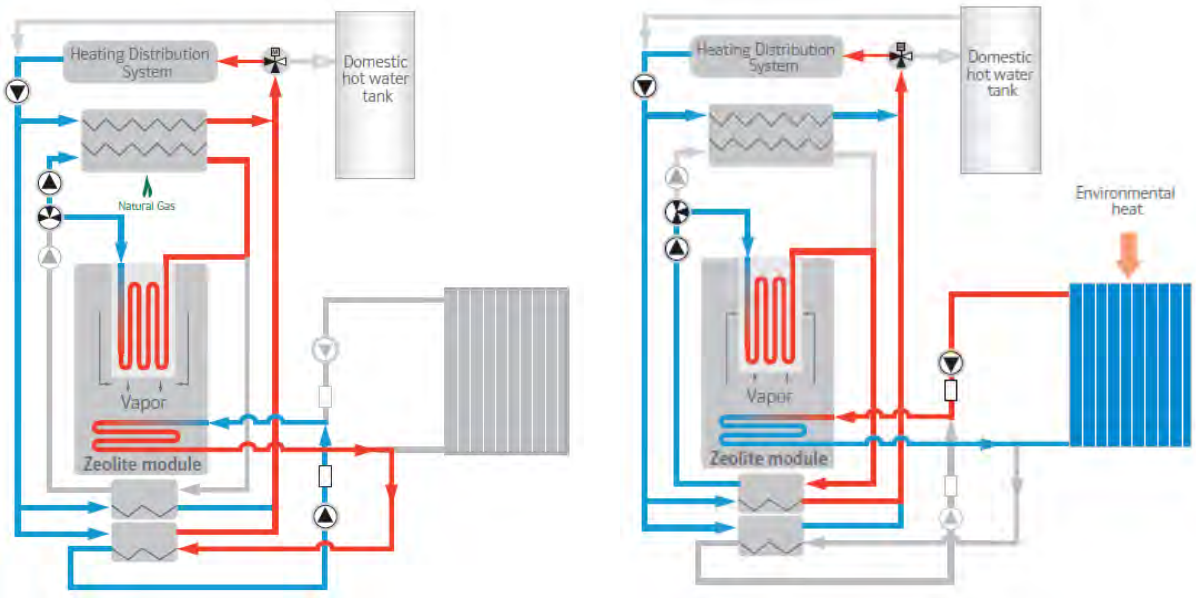

Figure 2: Vaillant gas-driven heat pump during the desorption phase (left) and the adsorption phase (right)

The third heating appliance based on a gas-driven heat pump process is from Viessmann and is shown in Figure 3.

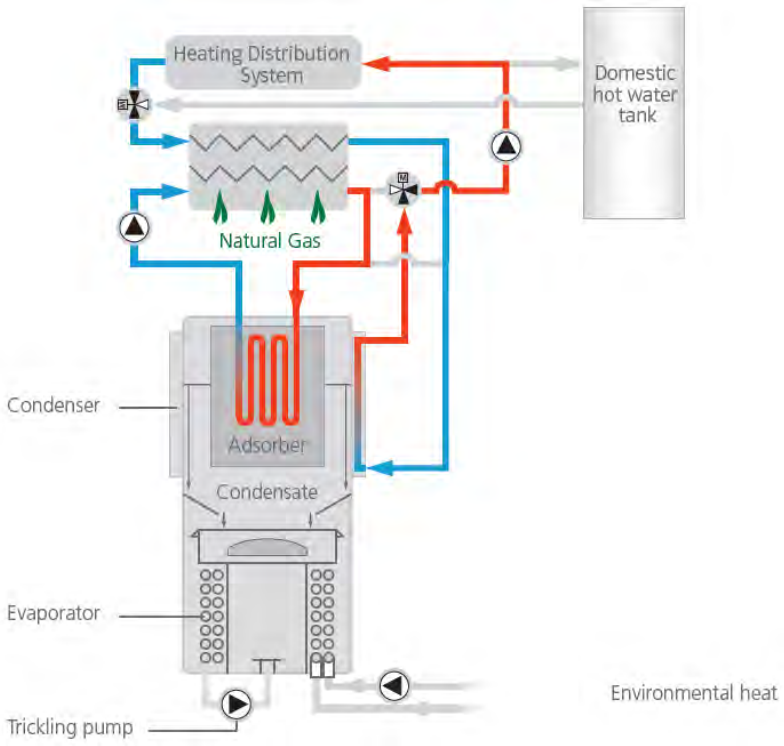

Figure 3.a: Viessmann compact heating appliance based on a gas-driven intermittent heat pump during the desorption phase

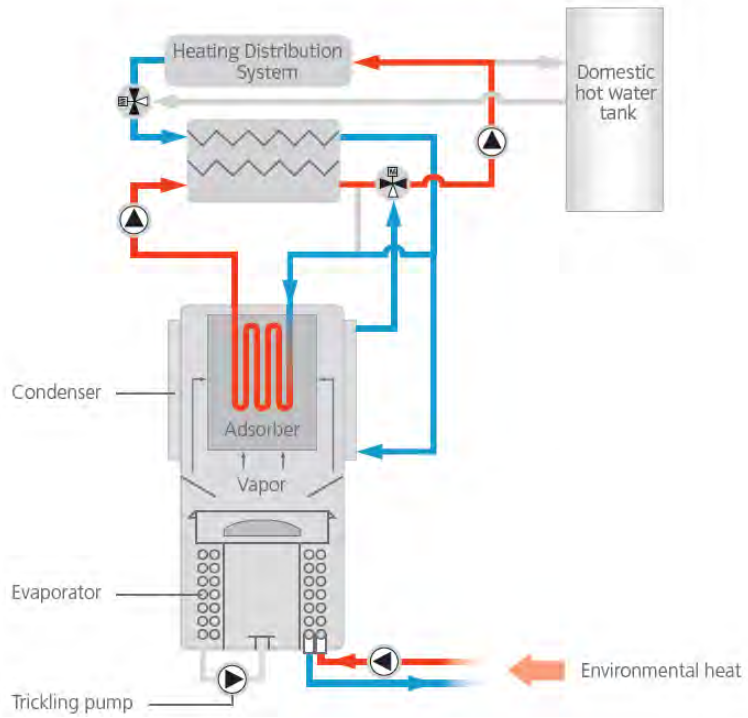

Figure 3.b: Viessmann compact heating appliance based on a gas-driven intermittent heat pump during the adsorption phase

This is again a hybrid system comprising an intermittent heat pump module with a condensing boiler driving the heat pump process, assisting the heat pump in the mixed-operation mode, and working alone as a peak boiler in the direct heating mode (Dawoud et al. 2010a). The main differences between Viessmann and Vaillant technologies can be summarized as follows:

1) The Viessmann heat pump module comprises three heat exchangers; namely, adsorber-desorber, condenser, and evaporator, thus eliminating the internal heat losses from heating up and cooling down the same heat exchanger working periodically as an evaporator or condenser (Dawoud and Stricker 2008).
2) There is always a direct heat transfer between the heating water and either condenser or adsorber (Dawoud and Stricker 2008).
3) Zeolite is utilised in form of consolidated layers over the fins of the adsorber heat exchanger (Dawoud et al. 2010b).
4) The evaporator is constructed as a falling film evaporator (Dawoud et al. 2009).

For a vapour compression heat pump with a rated heating capacity of 8 kW, 2 kW of electrical energy and 6 kW of ambient energy are required to deliver a seasonal performance factor (SPF) of 4. With an assumed average power station efficiency of 38.5%, this SPF equals 1.54 based on primary energy consumption. With a gas-driven heat pump, the 8 kW are delivered from 5.2 kW of gas and 2.8 kW of ambient heat, to give a primary energy SPF of 1.54. This means that the ambient heat utilised by a gas-driven heat pump is less than 50% of that utilised by a vapour compression heat pump of the same heating capacity and same primary energy SPF. This gives a cost benefit concerning the ambient heat source in favour of gas-driven sorption heat pumps.

3 THE GAS HEAT PUMPS INITIATIVE (IGWP)

The IGWP was founded in February 2008 by the German gas utility companies EnBW, E.ON Ruhrgas, ESB, EWE, GASAG, MVV, RWE and VNG, together with key European appliance manufacturers Bosch Thermotechnik, Robur, Vaillant and Viessmann. The know-how of all these member companies is brought together to promote the market maturity of the previously described heating appliances. Appliance development remains with each manufacturer, but marketing and lobbying work is done cooperatively. So far, twelve gas heat pump heating appliances have been successfully tested in the E.ON Ruhrgas laboratory, and three more units are planned for tests this year. These units have been subjected to a comprehensive test program to ensure their durability and to evaluate their gas utilisation efficiencies under laboratory and real conditions. In addition, 39 units from the different manufacturers have been installed and are being field-tested by the gas utility customers, distributed over the entire country. A further 27 units are planned for installation before the beginning of the 2011-2012 winter season. The laboratory and field test results obtained so far confirm the high efficiency and durability of all the tested appliances. However, a good deal of development and optimisation work is still needed in connection with thorough investigation of the field test results, leading to more efficient control and hydraulics and better gas utilisation efficiencies in the field.

In parallel with this work, market analyses and an IGWP-sponsored marketing campaign have been started. Technical seminars and training programs for the installation sector have also been started. A guideline for evaluating the seasonal performance factor of gas-driven sorption heat pumps has also been worked out (VDI-4650-2), and is now being considered as a basis for the corresponding DIN and EN standards.

A study has been carried out to estimate the potential of gas-driven sorption heat pumps compared with different heating technologies (Oschatz and Kleemann 2010). Figure 4 illustrates the differences in primary energy consumption, CO_2 reduction, and the share of renewable energy for an existing German house having 150 m^2 floor area as delivered by seven different heating methods.

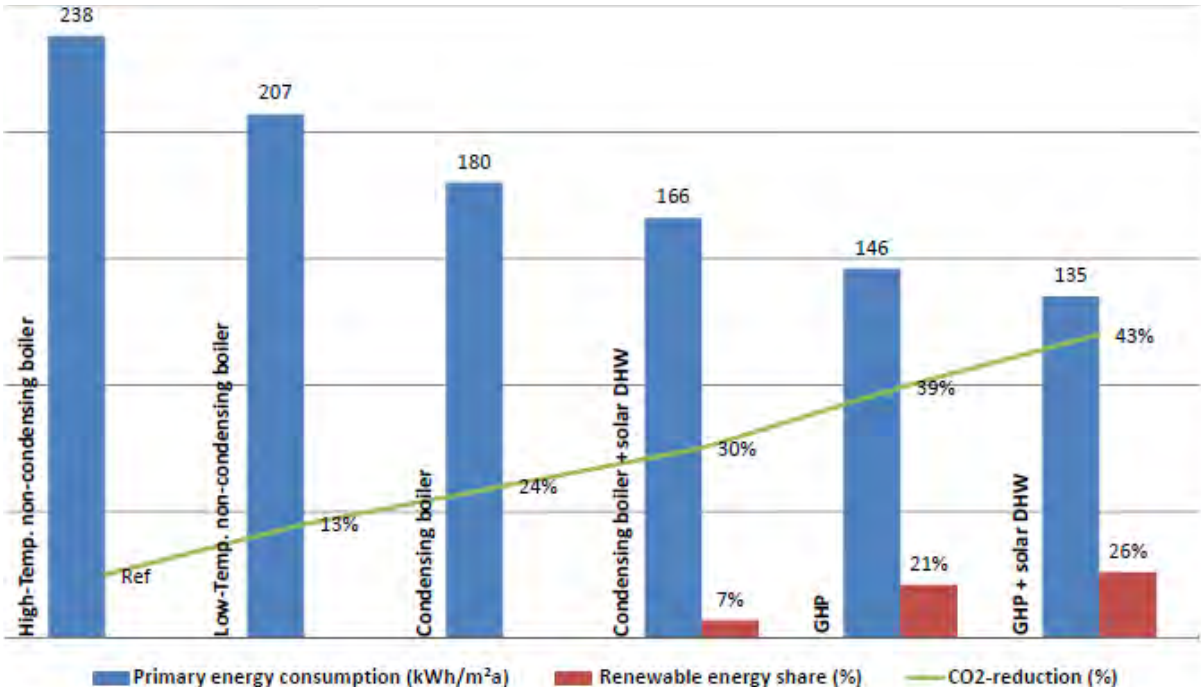

Figure 4: Potential of gas-driven sorption heat pumps for a typical 150 m^2 existing house in Germany (Oschatz and Kleemann 2010)

Compared with high-temperature non-condensing technology, which is the main heating technology in existing houses in Germany, the GHP technology offers 39% reduction in primary energy consumption, and therefore also in CO_2 emissions, and, at the same time, delivering 21% of the heating from renewable energy. Coupling solar energy for domestic hot water with a GHP results in 25% less primary energy consumption and CO_2 emissions, and utilises 26% renewable energy share compared with state-of-the-art gas-condensing boilers. This emphasises the need to promote GHPs as a possible trend-setting heating technology in the household sector.

As a result of the previous concerted actions within the framework of the IGWP, Robur could launch its E3 gas absorption heat pump model (Dummer 2010) at the ISH Fair 2009 in Frankfurt. In addition, Vaillant launched its zeolite heating appliance (Lang and Marx 2010) in April 2010. In addition, Viessmann is planning to launch its zeolite compact heating appliance in 2012.

4 CONCLUSIONS

The German gas utilities and the key European manufacturers of gas heating appliances have established an outstanding platform to support and stimulate the market introduction of a new heating technology based on small-scale gas-driven sorption heat pumps. The “Initiative Gas Heat Pump” was established in February 2008 and has since then comprehensively tested twelve heating appliances of this type in the E.ON Ruhrgas laboratory for durability and gas utilisation efficiency. In addition, 39 heating appliances have been installed in the field at customers of the German gas utilities. A further 27 units are planned for installation this year. Both laboratory and field test results have proved the durability of the new heating appliances and their clear efficiency enhancement over condensing boiler technology allowing at least compliance with the German Renewable Energy Act, 2008. An independent study of the potential of the new heating appliances in existing houses in Germany found that around 39% primary energy savings could be achieved compared with high-temperature non-condensing heating systems, which represent the state of the art of heating in existing houses, together with utilising a renewable energy share of 21%. Compared with condensing boilers, the GHP with solar collectors for domestic hot water production has the potential to save 25% of primary energy and deliver 26% from renewable energy. This indicates the need to promote the GHP as a possible trend-setting heating technology in the household sector.

5 REFERENCES

Dummer, H. 2010. Innovation – Gas-Absorptionswärmepumpe, Die VDI-Fachkonferenz „Wärmepumpen; Umweltwärme effizient nutzen“, 8. und 9. Juni 2010, Stuttgart, pp. 119-127.

Lang, R. and U. Marx 2010. Zeolith-Gas-Wärmepumpe mit Einbindung von Solarwärme, Die VDI-Fachkonferenz „Wärmepumpen; Umweltwärme effizient nutzen“, 8. und 9. Juni 2010, Stuttgart, pp. 129-136.

Dawoud, B., S. Chmielewski, P. Höfle, and A. Bornmann 2010a. Das Viessmann Zeolith-Kompaktgerät – Eine gasbetriebene Wärmepumpe, Die VDI-Fachkonferenz „Wärmepumpen; Umweltwärme effizient nutzen“, 8. und 9. Juni 2010, Stuttgart, pp. 111-117.

Dawoud, B. and M. Stricker 2008. A hydraulic concept of an intermittent adsorption heat pump; EP 1 985 948 A1.

Dawoud, B., J. Sauer, S. Chmielewsli, H. Van Heyden, and H. Klaschinsky 2010b. Adsorber Element and Method for Producing an Adsorber Element, WO 2010/040355 A2.

Dawoud, B., A. Bornmann, and S. Lohmöller 2009. A construction and working process of an intermittent sorption heat pump with a falling film / spray evaporator; DE 10 2008 006 420 B3.

Oschatz, B. and M. Kleemann 2010. Potenzial der Gaswärmepumpentechnologie - Abschlussbericht, www.igwp.de.

RESULTS FROM FIELD TRIAL WITH GAS HEAT PUMP ZEOTHERM BY VAILLANT

Dipl. Ing. Johann Wienen, Dipl. Ing. Marcel Neubert, Dr. Rainer Lang, Dipl. Ing. Hendrik Tiemeier, Vaillant GmbH, Berghauser Str. 40, D-42859 Remscheid, Germany
johann.wienen@vaillant.de

Abstract: In 2012 Vaillant launched their second generation of gas heat pump "zeoTHERM" to the European market. Since 2009 several zeoTHERM gas heat pump systems have been operating and analyzed as part of a field trial organized by Germany's "IGWP" (initiative for gas heat pumps in Germany). This report shows the results of the field trial as well as the relevant solar simulations. The total system efficiency was proven to be 35% higher than a "state of the art" heating systems with a wall hung condensing gas boiler. The Vaillant zeoTHERM heat pump system was also proven to be extremely reliable and robust. Since 2010 zeoTHERM has been manufactured in series production and has been freely available in the trade.

Key Words: gas heat pump, zeolite, solar collector, field trial

1 RESULTS FROM THE FIELD TRIAL CARRIED OUT WITH GAS HEAT PUMP ZEOTHERM BY VAILLANT

Within the scope of the "Initiative für Gaswärmepumpen" (IGWP - Initiative for Gas Heat Pumps), a field trial was conducted over 29 sites in different geographical locations across Germany. The spread of the installations has given clear and conceded results of the zeoTHERM heat pump in different environmental situations and heating systems. The zeoTHERM unit is an adsorption heat pump working with the material system zeolite (sorbent) and water (coolant).

2 ZEOLITE

Zeolite is a porous ceramic material produced synthetically. Via the composition and the porous structure it is possible to widely adjust the adsorption properties of a zeolite molecule. The zeolite used at Vaillant is highly hygroscopic.

For many decades zeolite has been used in gas separation / gas cleaning in the form of molecular filters. Since the beginning of the eighties, zeolite has replaced polyphosphates in domestic detergents, they are also used for the eco-friendly softening of water. The working agents of zeolite and water are non-toxic, non-combustible and completely ecological.

3 FUNCTIONAL PRINCIPLE OF THE GAS HEAT PUMP ZEOTHERM

The sorption process runs in two major phases: First, during desorption the water vapour is expelled from the zeolite. The heat transfer medium water is heated up to about 110°C by means of a gas condensing heat cell and flows through the adsorber/desorber. The thus produced hot vapor spreads inside the module, cools down at the bottom part of the module

and condenses. The condensation energy that is released in this process phase is then discharged as useful heat.

At the end of the desorption phase the heat supply to the adsorber/desorber is interrupted; as a consequence the pressure and the temperature in the module decrease. As soon as the temperature of the evaporator/condenser falls below the temperature level of the environmental heat source, the adsorption phase starts. Now, "cold" ambient energy is transferred to the evaporator. The coolant in the bottom part of the module evaporates, the cold vapour moves upwards and is adsorbed by the zeolite. The adsorption heat released in this process is then discharged and used as useful heat too.

The evaporation of the coolant at low temperature is realised with environmental heat produced by commercially available solar panels. Considering that this installation requires an environmental output of up to 2 kW for an installation size of 10 to 15 kW, flat plate collectors of 4 sqm are sufficient to cover the heat demand.

4 STRUCTURE

At a net weight of 160 kg, the unit has a width of about 80 cm, depth of 70 cm and height of 170 cm. For ease of installation the unit can be split up for mounting and installation. The heat cell in the upper part contains the complete burner and the primary heat exchanger. All these components are Vaillant standard parts which are familiar to the installer.

The zeolite module and the appliance hydraulics are located in the lower part of the appliance (zeolite unit). This module contains the zeolite and does not require any maintenance. The extent of maintenance work for the zeoTHERM appliance is similar to the common Vaillant gas-fired condensing boilers.

It is recommended to install the zeoTHERM in a matched system (see Figure 1) with bivalent solar storage tank for domestic hot water (d.h.w.) preparation, solar station and solar thermal collectors (flat or tubular). However it can also be integrated in an existing solar thermal system.

Figure1: Complete zeoTHERM system

Thanks to choosing solar energy as environmental heat source the simultaneous operation of direct solar hot water preparation and adsorption is possible.

Due to the compact design of the collectors and the flexible solar mounting systems for both on- and in-roof installations, the zeoTHERM is easy installable and suitable for applications in both new build and retro fit.

5 FIELD TRIAL

For the IGWP field trial, 29 units were installed all over Germany (see Figures 2 and 3) and extensively surveyed and measured.

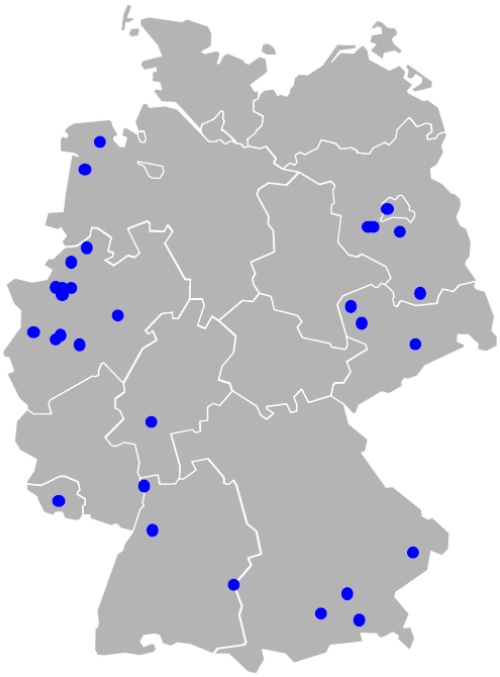

Figure 2: 29 field trial appliances and 4 laboratory appliances of the zeoTHERM (Vaillant) in Germany

Figure 3: Field trial in Odenthal (Remscheid)

The 29 sites monitored as part of this trial confirmed that the zeoTHERM system is 35% more efficient when compared to a condensing gas boiler connected to an under floor heating system. The considered efficiency is defined as usable energy in relation to the gas consumption (see Figure 4).

In locations with high levels of solar radiation the performance of the zeoTHERM heatpump system greatly improves. When installed in high efficient properties with low heating loads even higher levels of efficiency can be expected. The high efficiencies at low heating loads

are caused by covering the heat demand by mere heat pump operation. Increasing heating loads involve increasing part of direct heating mode which reduces the efficiency.

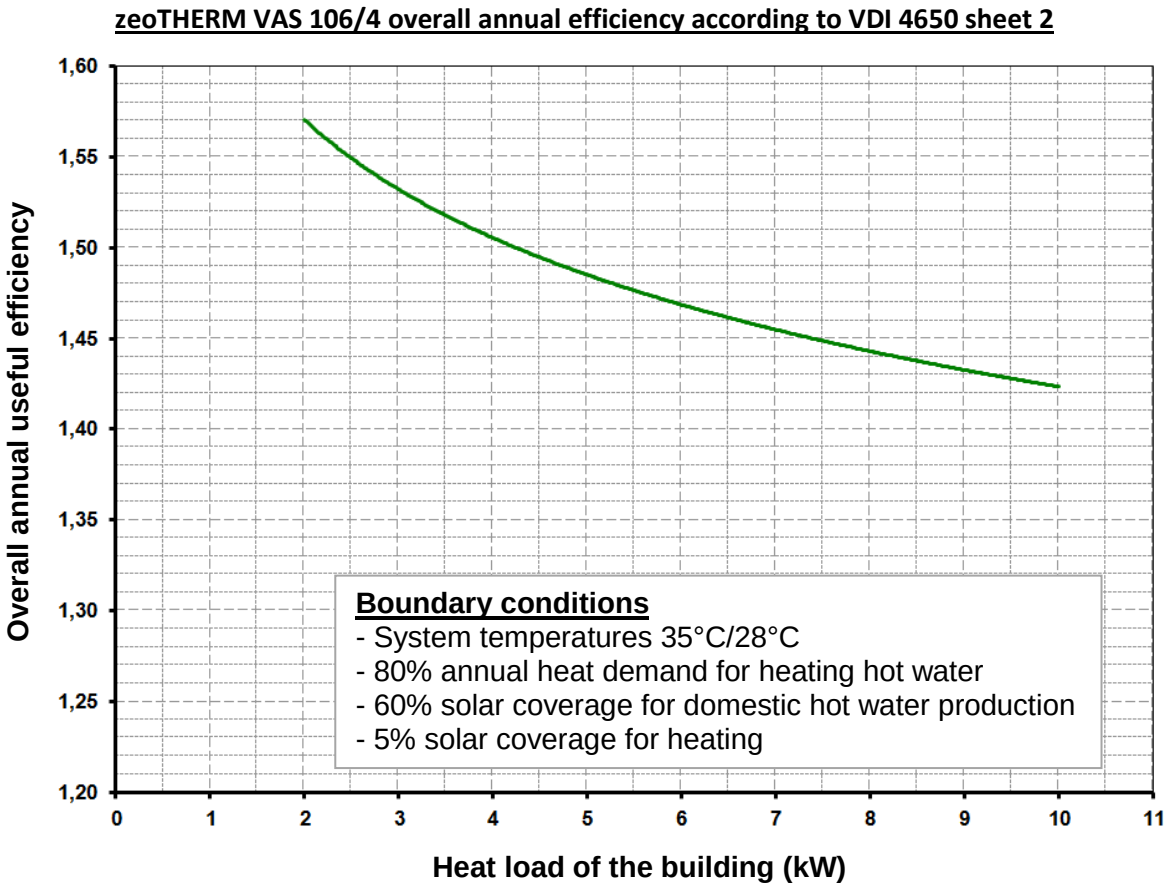

Figure 4: Annual efficiency according to the VDI 4650 sheet 2

From 2011, the zeoTHERM units have been equipped with an integrated solar direct heating function. This allows the zeoTHERM heat pump to link to solar thermal systems, directly transferring solar energy to both domestic hot water and direct solar heating. In this type of system, the zeoTHERM heatpump can make use of the solar energy across the massive temperature range of 3°C to 130°C (see Figure 5).

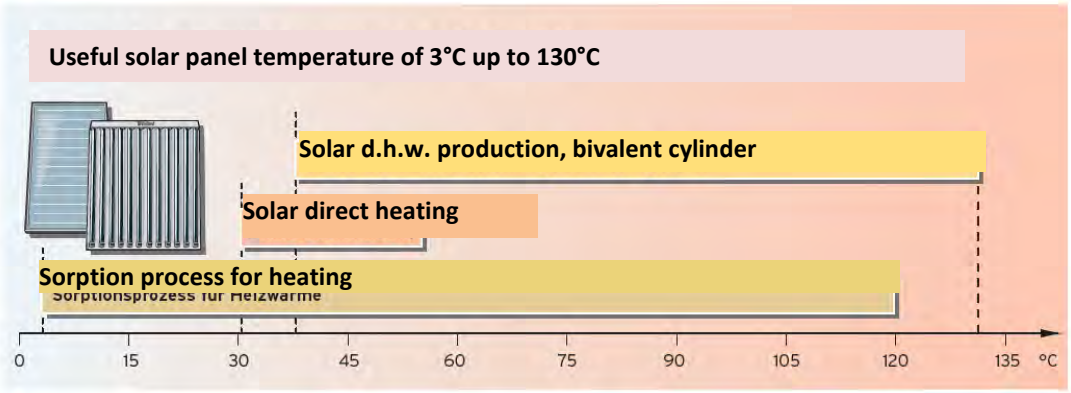

Figure 5: Useful solar collector temperature

6 SOLAR DIRECT HEATING

The zeoTHERM system can transfer solar energy into the system without the need for buffer storage. As a result of this the system operates without any buffer losses and it is possible to realize direct solar heating with only 7 sqm flat plate collector surface.

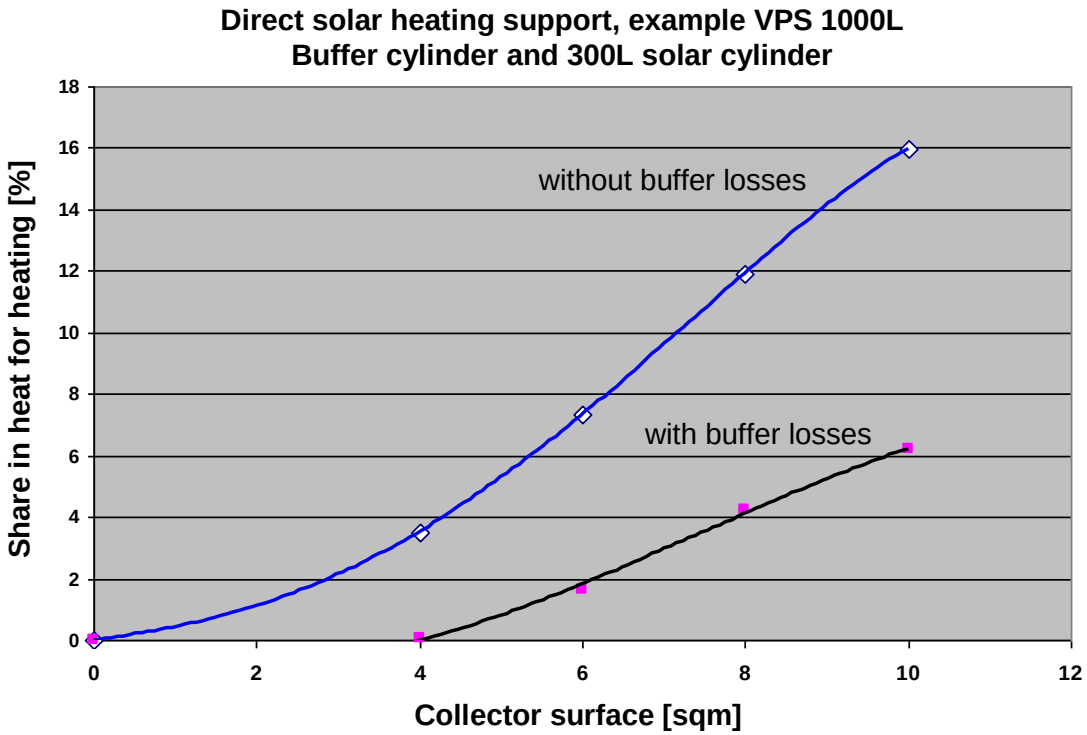

Figure 6: Simulation results [Vaillant]

In Figure 7, we present the time-wise fractions of the condensing DHO (Direct Heating Operation) (incl. production of d.h.w.), of heat pump operation HP and of solar direct heating SDH for the period 20th to 24th October 2011 found with 10 field test appliances positioned all over Germany.

On the average, SDH (solar direct heating) covered the heat demand for 24% of the heating time. The ambient air temperature for monitored period was from 3-10°C with slightly cloudy skies. Even in the winter months January to March 2012, SDH could be recorded during a time slice of 10% on the average. Thus, thanks to SDH, the system efficiency increased by about 10%.

The results from a simulation as well show a solar fraction for heating of 11% and of 60% for d.h.w. production for the installation recommended by Vaillant: equipped with a solar cylinder 300 L for a 3 - 4 person household and an aperture surface of 7.05 sqm. These results prove that the system has been matched such that the production of domestic hot water is not impaired by solar direct heating function. With a higher demand in hot water, such a cannibalization, often discussed among experts, could easily be compensated by an additional solar panel.

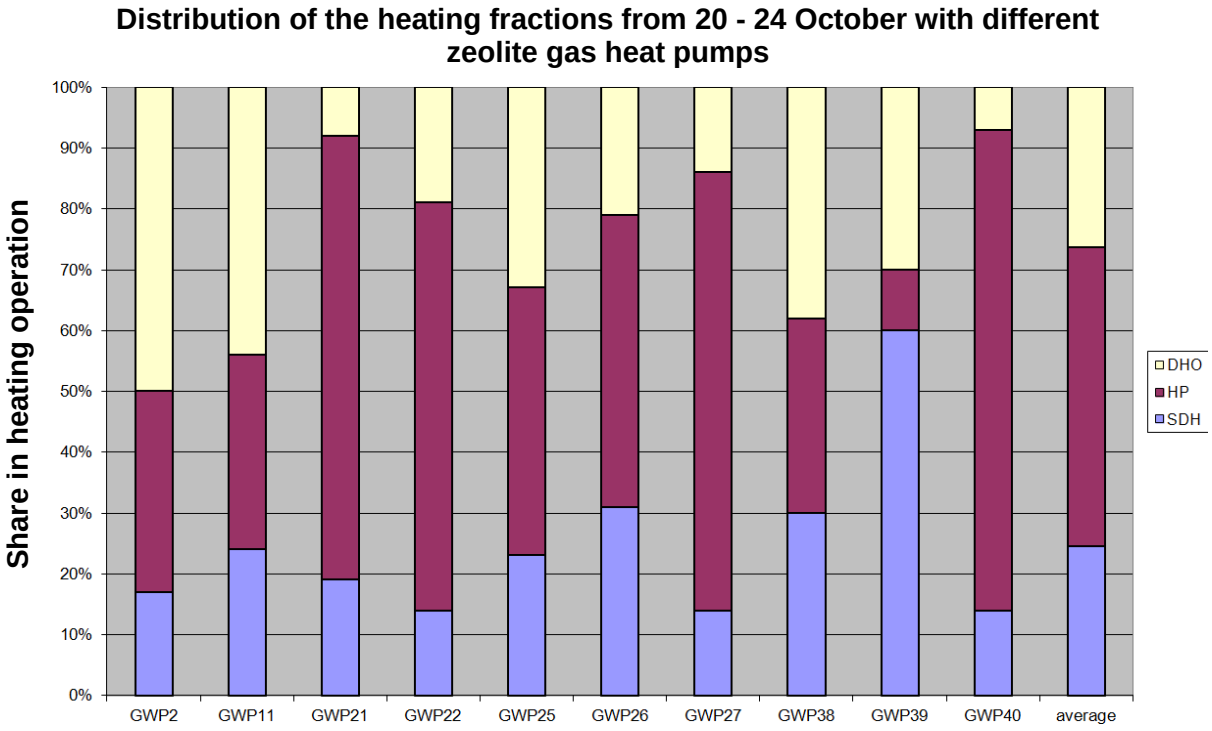

Figure 7: Time-wise fractions of different heating operations

7 PANEL TYPE

As part of this field trial we also compared the differences between the flat plate and evacuated tube solar systems. For these analyses, 4 installations were equipped with evacuated tube collectors (3 x 6 sqm, 1 x 5 sqm). When comparing the systems (Figures 8 and 9), you can see that the evacuated tube collector provides significantly higher temperatures, especially in diffused sun light. Thus, the system equipped with the evacuated tubes offers an average temperature increase of 12.5°C compared to the ambient temperature and with diffused sun light while the flat plate collector installed in the vicinity only supplied an increase of 5°C. With strong solar radiation the temperature ranges are similar.

Simulation confirmed the aforesaid results according to which the evacuated tube collector supplies temperatures that are about 5.3 K higher on the annual average than the flat plate collector temperatures. These higher source temperatures support the operation of installations with higher heating temperatures (55°C/45°C, radiators). Therefore, it is recommended to equip such systems with evacuated tube collectors.

As described in VDI4650 sheet 2, the average temperature difference between the collector temperature and the ambient temperature is determined by

$$T_{koll,in} - T_U = \Delta T_R \cdot \left[1 - e^{-\left(\frac{A}{A_R}\right)} \right] \qquad (1)$$

whereby

A aperture surface of the collector in m^2

ΔT_R reference temperature difference

A_R reference collector surface

with the parameters for flat plate collectors given in Table 1. For the evacuated tube collectors, derived from simulation and field tests, the results are also given in Table 1.

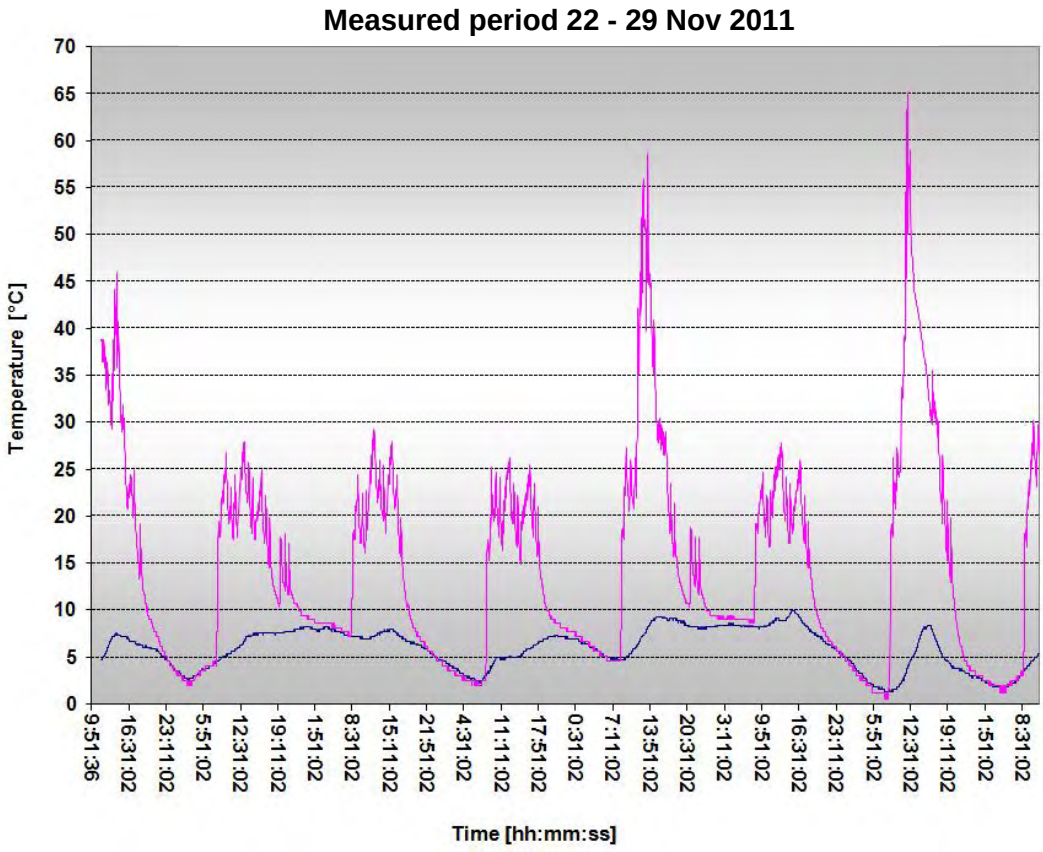

Figure 8: Tube collector (pink) temperature and ambient (blue) temperature

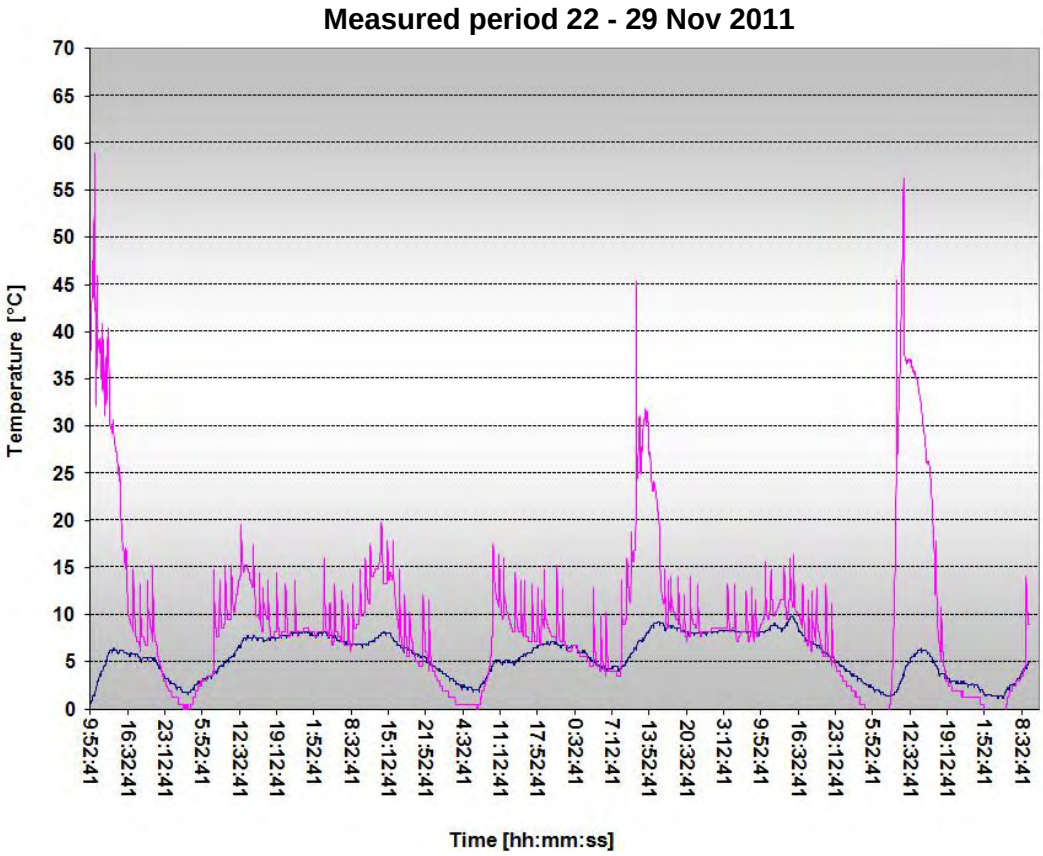

Figure 9: Flat plate collector (pink) temperature and ambient (blue) temperature

Table 1: Parameters ΔT_R and A_R

Collector type	ΔT_R	A_R
	[K]	[m^2]
Flat plate collector	8.2	6.9
Evacuated tube collector	16	6.9

The difference between collector temperature and ambient temperature for flat plate and evacuated tube collectors is shown in Figure 10 depending on the collector aperture surface.

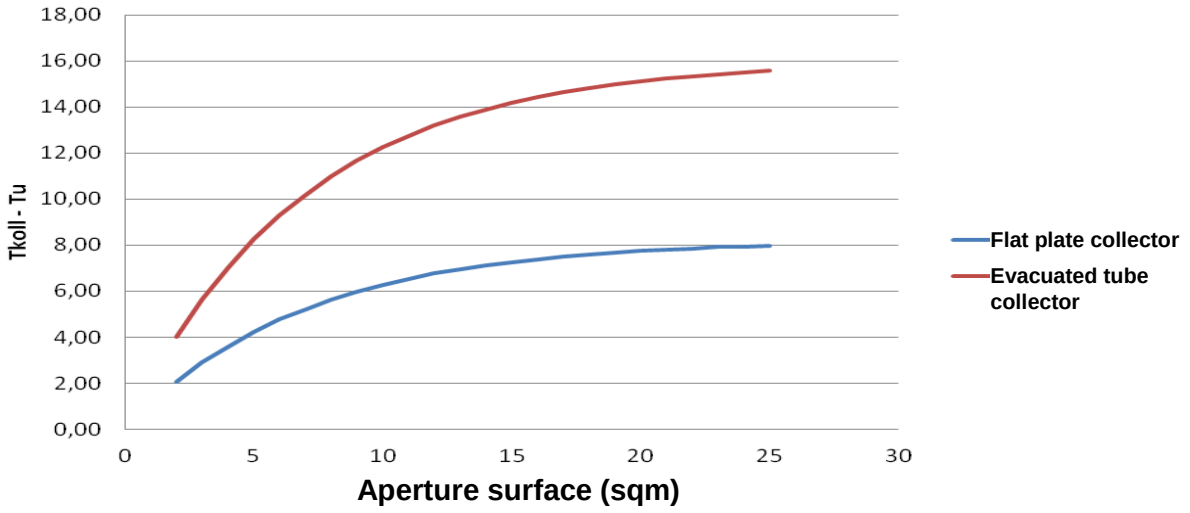

Figure 10: Difference between collector and ambient temperature with different collector types

The solar coverage has a similar characteristic curve. Here, the influence of the aperture surface increases with the square.

Thus, the following relation results for the solar coverage from simulations:

$$\eta_{sol,Hz} = \frac{\Delta\eta_R}{Qn} \cdot \left[1 - e^{-\left(\frac{A^2}{A_R{}^2}\right)}\right] \qquad (2)$$

whereby

A aperture surface of the collector in m^2

$\Delta\eta_R$ reference fraction

$A_R{}^2$ square of the reference collector surface

Qn appliance output.

The parameters are given in Table 2 and the coverage for solar direct heating with evacuated tube collectors and flat plate collectors combined with a gas heat pump unit of 10 kW in Figure 11.

Table 2: Parameters $\Delta\eta_R$ and A_R^2

Collector type	$\Delta\eta_R$	A_R^2
	[kW]	[m^4]
Flat plate collector	2.3	80
Evacuated tube collector	2.3	65

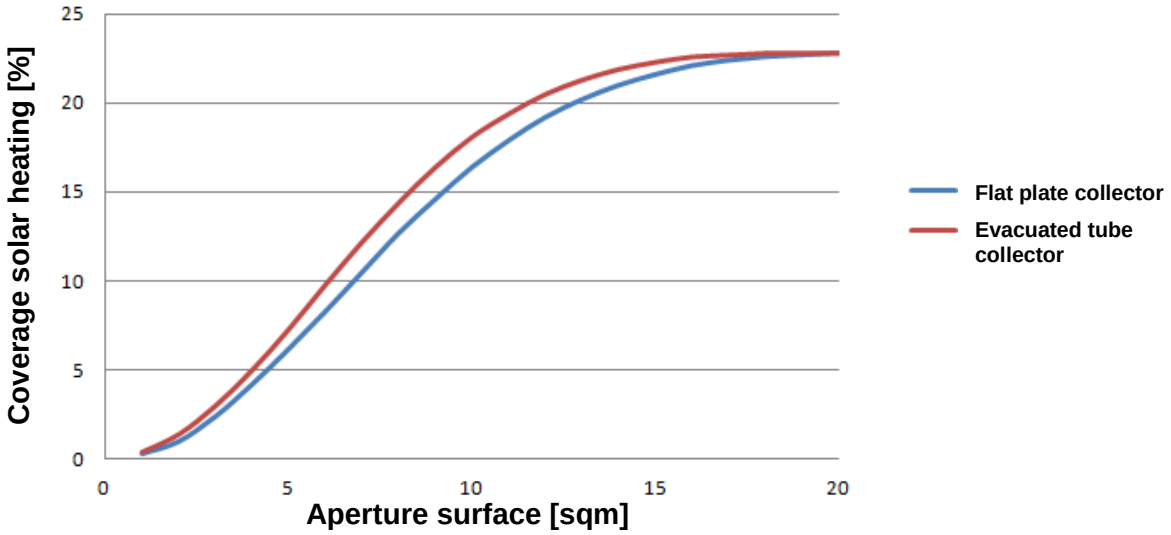

Figure 11: Solar heating coverage

8 COMPARISON OF CONSUMPTION

A comparison of consumption in case of changing from a condensing underfloor heating system to the zeoTHERM system without solar direct heating proved a reduction of about 30% in gas consumption. This is in compliance with the previously given results.

Yet, for a radiator system “Non-condensing boiler with solar d.h.w. production" changed to a zeoTHERM system (aperture surface of 5 sqm) the gas consumption was reduced by 30% compared to the previous year.

A third system of GASAG showed 19% savings in case of a change from a condensing underfloor heating system to a zeoTHERM system without solar direct heating.

8.1 Comparison of theory (VDI 4650 sheet 2) and practice

When comparing the annual useful efficiencies of the field trial systems with the expected useful efficiencies according to VDI 4650 sheet 2 for a heating system 35°C/28°C, we state a difference below 10% despite not yet ideal conditions for many field trial systems (see Figure 12). The aforesaid results elaborated by Gas und Wärmeinstitut (Essen) prove that the VDI guideline properly describes the zeolite system.

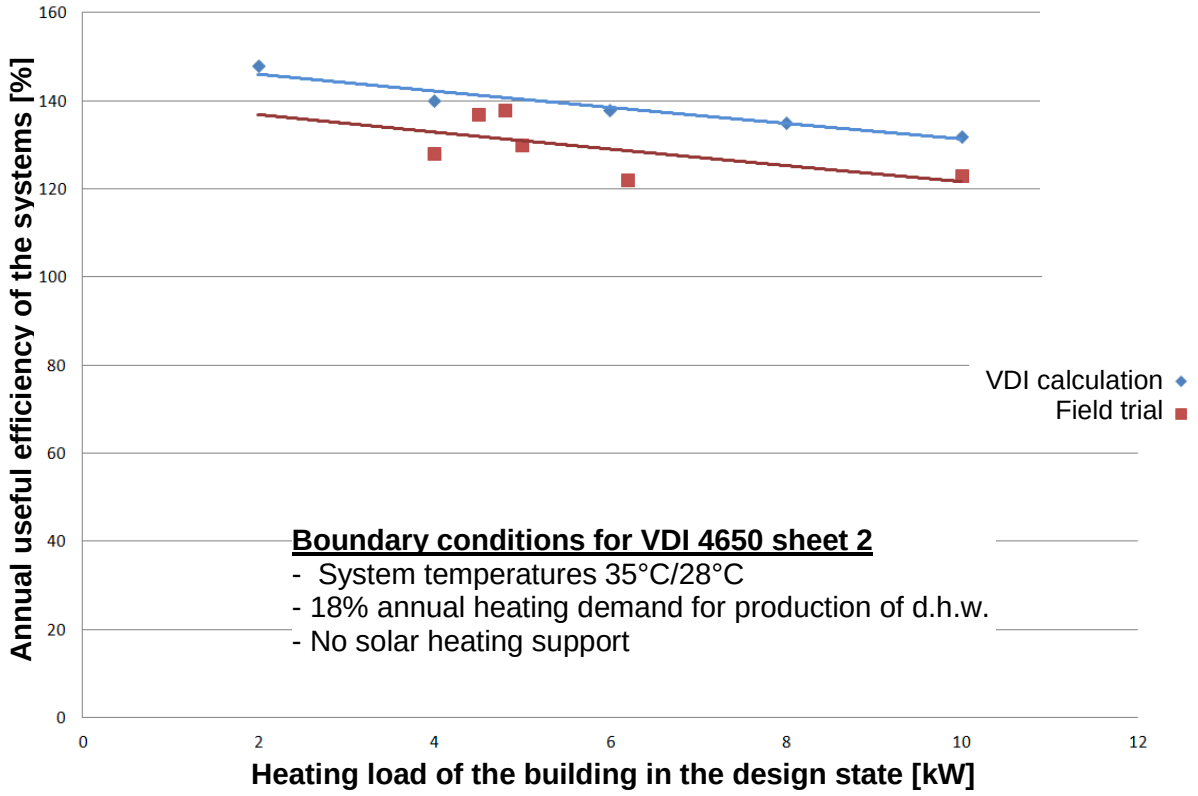

Figure 12: Comparison of field trial data (w/o solar heating support) and of the expected values (VDI 4650 sheet 2, w/o solar heating support) [Source GWI Essen]

8.2 Comparison zeoTHERM system with a condensing boiler with solar heating support

An additional simulation compares the zeolite system to a system equipped with a condensing unit with solar heating support. To achieve the same system efficiencies as with a zeolite system, the condensing system must be equipped with a 1400 L buffer cylinder and a collector aperture surface of about 25 sqm. Thus, it would be possible to replace a condensing boiler system (with a collector surface of 25 sqm) by a zeolite system offering a collector surface of only 7 sqm. The collector surface relation would be 1:3.5.

9 SUMMARY

We can state here that the Vaillant zeolite heat pumps are able to provide an increase in efficiency of about 35% compared to a condensing boiler system. Here, the following parameters turn out to be positive

- low heat demand
- low heating temperatures
- high solar radiation on the collectors
- evacuated tube collectors for higher heating temperatures
- the d.h.w. cylinder must not be bigger than required for the hot water demand.

In the field the systems proved to be extremely reliable and robust. Costumer expectations were completely met and in some cases exceeded. Sheet 2 of VDI 4650 describes the Vaillant zeolite system with proper accuracy. In view of the efficiency increase with the reduction of the heat demand, insulating the building after the installation of the unit still makes sense. This would not result in overdimensioning of the unit as only the heat pump fraction would increase.

DEVELOPMENT OF A DOMESTIC ADSORPTION GAS-FIRED HEAT PUMP

Prof R.E. Critoph MEI, Dr S.J. Metcalf, School of Engineering, University of Warwick, Coventry CV4 7AL, UK, R.E.Critoph@warwick.ac.uk

Abstract: A gas-fired heat pump system intended to replace conventional condensing boilers is under development. The machine uses four sorption generators with heat recovery between all beds plus mass recovery and has a nominal heat output of 7 kW. Predicted annual average heating COP (Heat output / gas energy input based on gross calorific value) is 1.35 in a UK application with low temperature radiators. The system is described together with the simulation model, the test facilities and procedures.

Key Words: gas heat pump, adsorption, four bed cycle, activated carbon, ammonia

1 PROJECT BACKGROUND

Previous work at the University of Warwick has concentrated on the use of carbon-ammonia adsorption systems. The rationale for ammonia is fairly straightforward. We would like to develop gas heat pump systems for domestic use in the UK and elsewhere in the EU with the maximum possible market. This implies that they should be air source machines that are capable of replacing condensing boilers in retrofit applications. Approximately one million condensing boilers are installed each year in the UK as replacements for old irreparable systems. Whilst ground and water sources are desirable, air is a ubiquitous source and is the lowest capital cost option. If air is the heat source and the heat pump is to provide a significant proportion of the load it is necessary to evaporate at less than 0°C for much of the time, thereby ruling out water as a refrigerant, despite its excellent latent heat and other desirable characteristics. Methanol or ethanol are feasible regarding evaporating pressure but not sufficiently stable at higher temperatures if we want to take advantage of the higher COP offered by high driving temperatures. Ammonia is stable to temperatures of at least 200°C and so is selected despite the increased demands of system safety compared to other refrigerants.

A number of novel cycles have been investigated at Warwick in the past, including the Convective Thermal Wave (Critoph 1999), fixed bed or moving bed modular systems (Critoph 2005, Critoph 2001), and finally a 4-bed isothermal cycle with heat and mass recovery (Metcalf 2009).

The work described here, based on the 4-bed isothermal cycle has been carried out by the University of Warwick as part of a project called CALEBRE (Consumer Appealing Low Energy Technology for Building Retrofit) funded by EPSRC and EON and is the subject of further development by Sorption Energy Ltd, a university spin-out company. The concept is an affordable air source sorption heat pump that can replace a conventional gas-fired boiler and reduce gas consumption by over one third.

1.1 Choice of Cycle

There are a large number of possible cycles, ranging from Shelton's original thermal wave (Shelton 1986), through variations proposed by Critoph (1999) to isothermal beds with heat recovery (Meunier 1985). Metcalf (2009) carried out modelling to determine the advantages of various cycle types in an objective way. Specifically, he compared a 2-bed cycle with heat and mass transfer between beds, a 4-bed cycle with 3 stages of regenerative heating/cooling between beds and a modular thermal wave cycle from Critoph (2005). These results are shown in Figure 1. Each line for a system shows the best combination of COP and Specific Heating Power (SHP in Watts per unit mass of adsorbent) that can be obtained when using the optimum cycle time. The conditions used were 200°C input from the gas heat exchanger, 40°C condensing and adsorber inlet water, 5°C evaporating temperature.

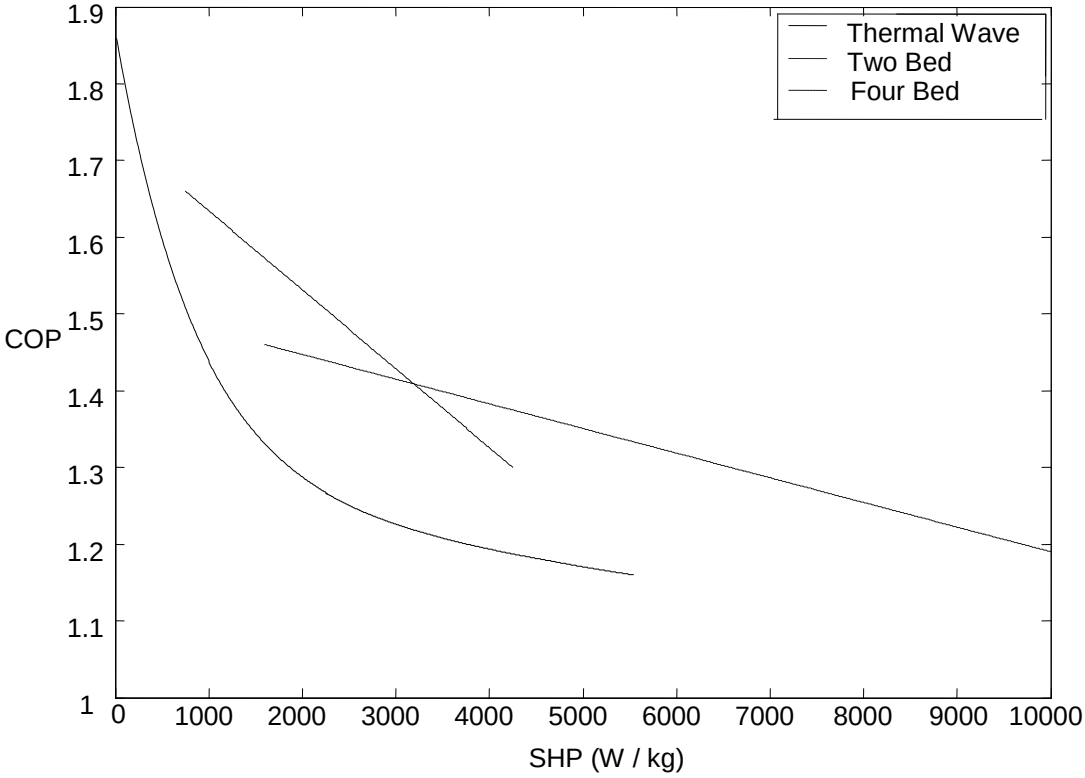

Figure 1: Cycle comparison in a heat pump application.

It can be seen that whilst the thermal wave can deliver very high heating COP's it has a correspondingly very low SHP which would imply a very large and costly machine (per unit of heating power). At the other extreme a simple two bed system with heat recovery and mass recovery between beds has much higher SHP's although lower COP's.

This leads to consideration of a four bed cycle. The four bed performance envelope is superior to that of the thermal wave for COP's less than 1.66 (SHP about 750 W/kg) and gives way to the two bed system for COP's less than 1.4 (SHP about 3200 W/kg). It was decided not to look at even larger numbers of beds since the mechanical complexity of valves and pumps would be excessive.

Similar comparisons can be made for different operating conditions but the conclusion made was that a four bed cycle was most suitable for a domestic heat pump system. It requires complex valves and extra pumps but in the range of interest the COP is about 25% higher than that of a two bed design.

1.2 Description of four bed cycle

The operation of a four bed system is described in more detail in Figure 2. The six parts of the figure show progress through half the cycle. In the first part (a) Bed 1 has reached the maximum temperature. Mass recovery is carried out by opening a valve to Bed 4, resulting in further desorption from 1 and adsorption in 4. In (b) to (c) high temperature heat recovery is carried out between 1 and 2 and low temperature heat recovery between 3 and 4. From (c) to (d) high temperature (driving) heat goes to Bed 2, heat is rejected from Bed 3 and medium temperature heat recovery occurs between Beds 1 and 4. In (d) mass recovery is carried out between 2 and 3. In (e) to (f) high temperature heat recovery is carried out between 2 and 4 and low temperature heat recovery between 1 and 3. Finally in (f) high temperature (driving) heat goes to Bed 4, heat is rejected from Bed 1 and medium temperature heat recovery occurs between Beds 2 and 3. This is half the cycle in which Bed 1 has gone from maximum to minimum temperature and Bed 4 has gone from minimum to maximum temperature. The second half continues in similar fashion to complete the cycle. Such an arrangement demands five pumps: one each for the source and sink and three for heat recovery. Obviously their electricity consumption must be minimised but in principle the pumping power can be very low.

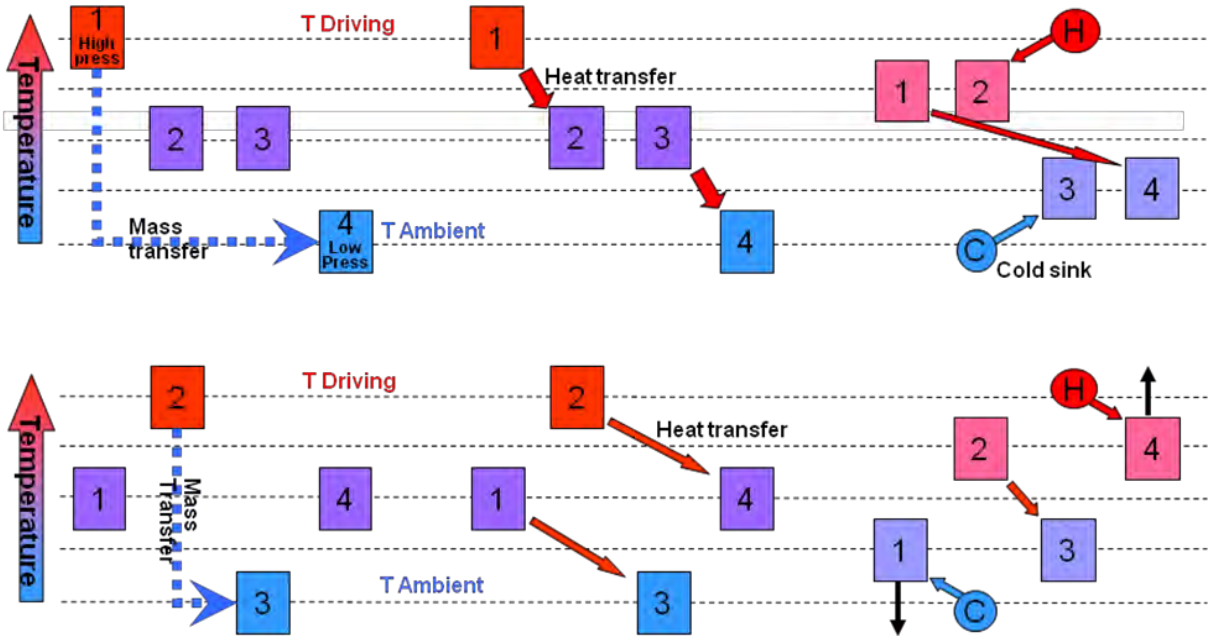

Figure 2: Processes in a four bed cycle.

2 MODELLING AND DESIGN

2.1 Modelling

A simulation model of a four bed system has been validated by Metcalf (2009) and used to generate the predicted performance data of Figure 3.

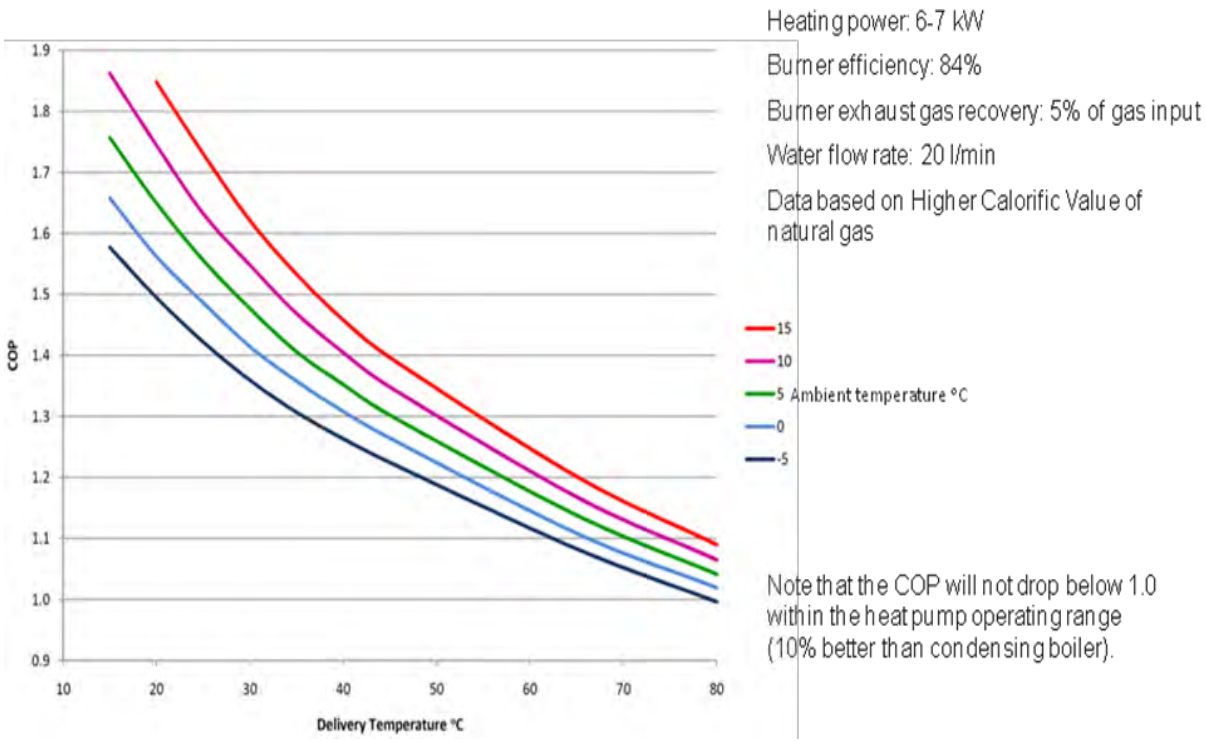

Figure 3: Predicted COP.

The machine was designed around a specification for a typical UK house that had been retrofitted with good insulation to the point that the heat pump needed to deliver 7 kW of heat. Assuming the UK climate and heat delivery at 50°C to low temperature radiators the calculated mean annual COP based on the higher calorific value of gas burnt would be 1.35. Running costs (2010 UK prices) comparative to an electric heat pump and a condensing boiler are given in Figure 4 and CO_2 emissions in Figure 5.

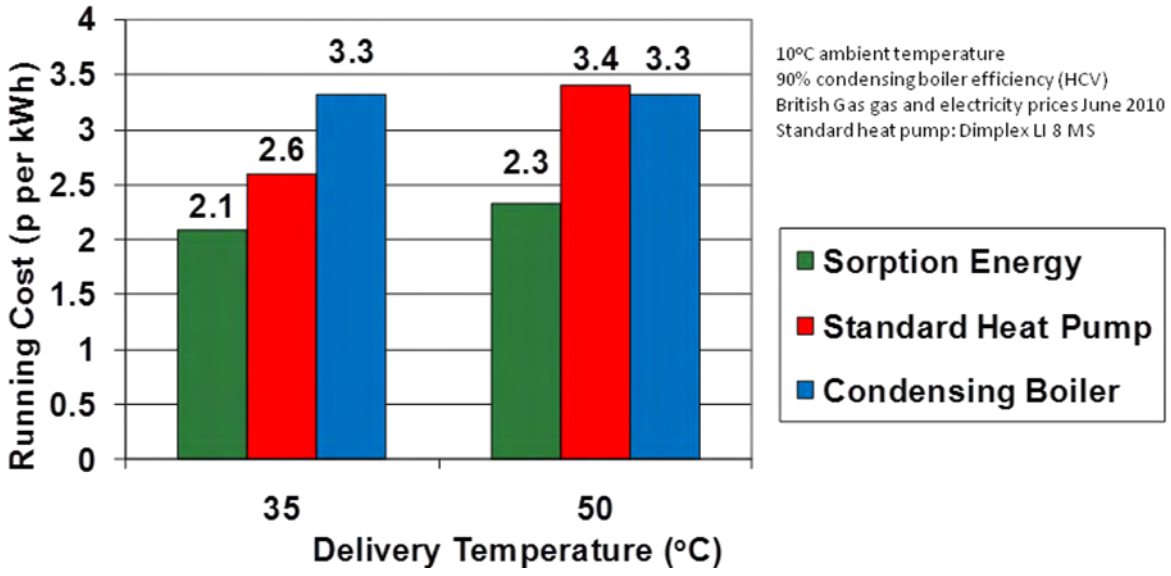

Figure 4: Comparison of Heating Costs (UK)

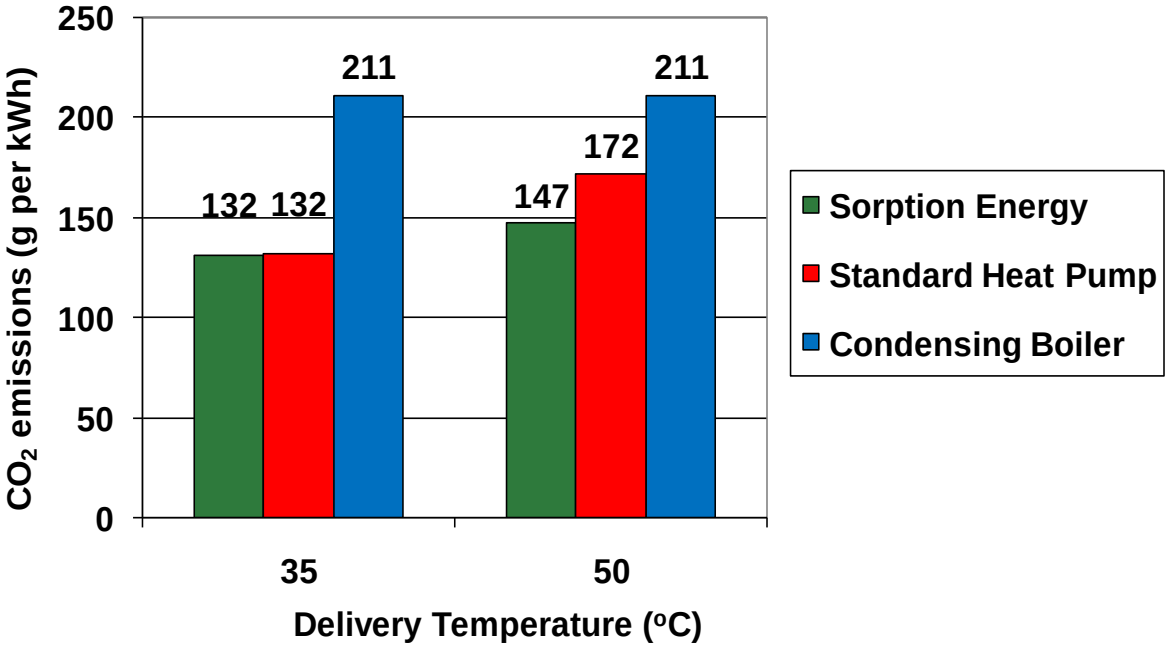

Figure 5: Comparison of CO_2 emissions (UK)

2.2 Component design

Previous sorption generators (Critoph et al. 2009) have used plate shim designs but theoretical modelling suggests that a shell and micro-tube construction could have less thermal mass and equivalent heat transfer. The core of such a heat exchanger is shown in Figure 6 and fully assembled in Figure 7.

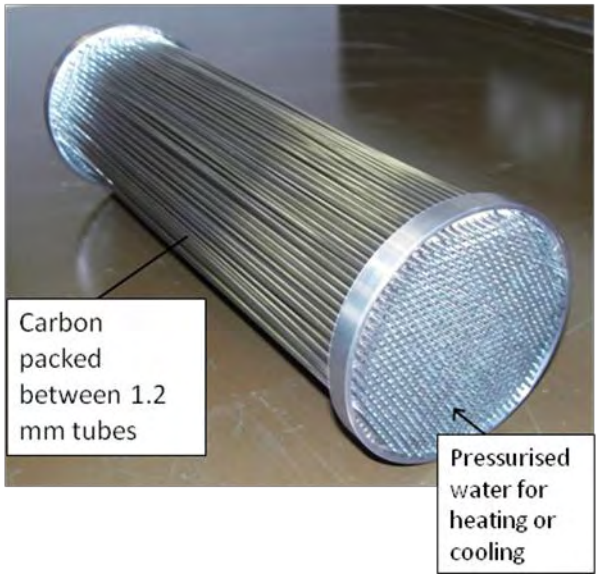

Figure 6: Generator core.

Figure 7: Complete generator.

The four generators form a sub-assembly as shown in the drawing of Figure 8. The module consists of the generators, ammonia check valves that connect to the evaporator and condenser and the mass recovery solenoid valves.

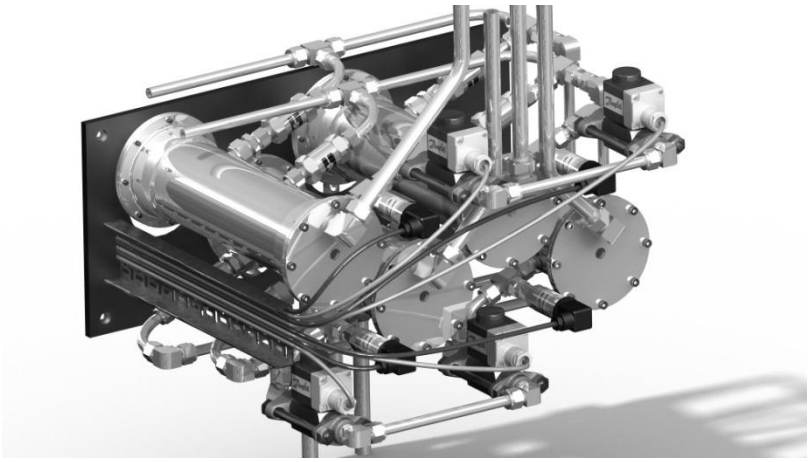

Figure 8: Generator module in Solidworks™.

Figure 9 shows the complete unit but without insulation. It is designed as a single unit to be installed outside the house with water, gas and electrical connections being made through the wall.

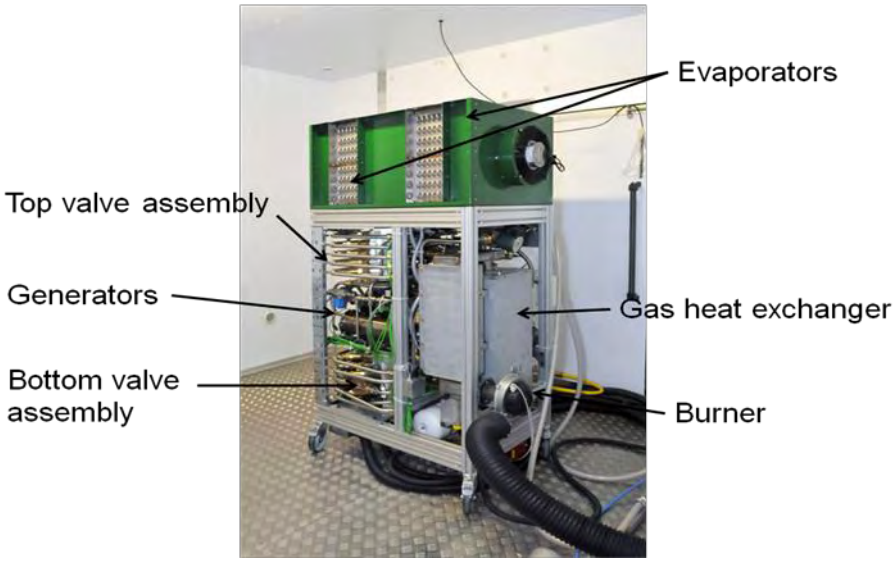

Figure 9: Prototype heat pump.

The gas burner and heat exchanger have been developed especially for this project and can modulate from 3 to 11 kW heat output at 170°C with a gross efficiency exceeding 80%. The unit has been tested outside the heat pump and performs well. It delivers pressurised water supplied to any of the four beds via the water valve assemblies. The water valve assemblies were very complex. Each was the equivalent of a 4-pole 5-way switch. They had 8 positions during a complete cycle and individual poppet valves were actuated by push rods driven by a cam shaft. This was intended to be a comparatively risk free design but not suitable for production.

3 DEVELOPMENT

The prototype was first tested in May 2011. Whilst the machine functioned as a heat pump and delivered hot water at up to 60°C internal leakage in the water valve assemblies meant that performance was unacceptably low and further testing would not be beneficial until the

water valves were re-designed. After two iterations of development bespoke ceramic disc valves in a polymeric shell were manufactured and successfully tested. The new valve bodies were only 75 mm in diameter and 120 mm long and had negligible leakage of water and heat loss.

New system tests in April 2012 revealed a different challenge, related to generator heat transfer. The overall thermal resistance between the water in the generators and the bulk of the carbon was approximately twice the predicted figure which was based on measured data from a previous design (Critoph et al. 2009). The output power of the machine (at a given COP) is roughly inversely proportional to the thermal resistance and so a solution is needed to achieve a realistic power output sufficient for domestic heating.

Two approaches are being followed in parallel. The first (short term) approach is to build and install larger generators with the same basic design (150 mm nominal diameter and 400 mm long). Given the same thermal resistance they should achieve the required 7 kW output. The objective is to demonstrate the concept to potential manufacturers/investors and validate the system computer models. It is hoped that this work will be completed early in 2013. The second activity is to investigate the heat transfer problems in much greater detail and find cost effective solutions that allow the use of the smaller generators. The work being undertaken includes a range of conductivity measurements on adsorbents to reveal the diverse effects of particle size distribution, bulk density, particle shape and wall geometry on the overall thermal resistance.

4 ACKNOWLEDGEMENTS

The project has been funded by EPSRC / EON project EP/G00387/1 and by the EPSRC Follow on Fund project EP/G00387/1. Instrumentation and test chambers are made available by the AWM / ERDF Birmingham Science City project.

5 REFERENCES

Critoph R.E. 1999. “Forced convection adsorption cycle with packed bed heat regeneration”, *Int. J. of Refrigeration*, 22(1), pp. 38-46, ISSN:0140-7007.

Critoph R.E. 2001. “Simulation of a continuous multiple-bed regenerative adsorption cycle”, *Int. J. of Refrigeration*, 24(5), pp. 428-437, ISSN:0140-7007.

Critoph R.E. 2005. “Modular regenerative adsorption cycles with fixed beds applied to trigeneration", *J. Process Mech. Eng*, 219 Part E, pp. 197-204, ISSN:09544089.

Critoph R.E., Z. Tamainot-Telto, S.J. Metcalf 2009. “Novel compact sorption generators for car air conditioning”, *Int. J. Refrigeration*, 32(4), pp. 727-733.

Metcalf S.J. 2009. “Compact, Efficient Carbon-Ammonia Adsorption Heat Pump”, PhD thesis, University of Warwick.

Meunier F. 1985. “Second law analysis of a solid adsorption heat pump operating on reversible cascaded cycles: application to the zeolite water pair”, *Heat recovery systems and CHP*, 5, pp. 133-141.

Shelton S.V. 1986. United States patent No. 4,610,148, Solid adsorbent heat pump system.

THEORETICAL STUDY OF THERMALLY DRIVEN HEAT PUMPS BASED ON DOUBLE ORGANIC RANKINE CYCLE: WORKING FLUID COMPARISON AND OFF-DESIGN SIMULATION

Jonathan Demierre, Daniel Favrat, Industrial Energy Systems Laboratory (LENI)
Ecole Polytechnique Fédérale de Lausanne (EPFL), 1015 Lausanne, Switzerland
jonathan.demierre@a3.epfl.ch

This paper was published in the proceedings of the 10th International Heat Pump Conference 2011 (www.heatpumpcentre.org/en/hppactivities/ieaheatpumpconference).

Abstract: This study deals with a type of thermally driven heat pumps that consists of a reverse Rankine heat pump cycle, the compressor of which is driven by the turbine of a supercritical Organic Rankine Cycle (ORC). The application is residential heating (domestic hot water and floor heating) of small buildings requiring a cumulated thermal power of approximately 40 kW. An approach that enables the comparison of performance that can be expected with different working fluids is presented. It appears that R134a, R1234yf, R227ea and R236fa are among the best candidates. An off-design simulation tool of such thermally driven heat pumps has been implemented that includes both turbine and compressor off-design models. This thermally driven heat pump model has been used to predict the performance of an existing experimental prototype about to be tested.

Key Words: thermally driven heat pumps, ORC, off-design, radial turbine, oil-free

1 INTRODUCTION

Nowadays environmental and global warming concerns, increasing costs, potential shortage of fossil fuels and the need for a more efficiency conversion of biofuels stimulate the development of equipment for a more rational use of energy. One of the solutions is the improvement of the energy conversion for heating and cooling in particular. Concerning heating, the main alternatives are linked to using heat pumps, which enable a use of renewable energy from the environment.

The present heat pump market is dominated by two main categories of heat pumping systems: the electrically driven compression heat pumps, which are the most widely used, and the thermally driven heat pumps. The thermally driven heat pumps are usually realized with absorption cycles. These cycles are based on two pressure and three temperature levels, the driving exergy power being the heat exergy provided at the highest temperature level to the generator (Borel and Favrat 2010). Note that to the category of thermally driven heat pumps we can also add systems made of a compression heat pump, the compressor of which is directly or indirectly driven by a heat engine, usually an internal combustion engine.

The system studied in this work is a thermally driven hermetic heat pump that consists of a compression heat pump and an organic Rankine cycle (ORC) in which the turbine is directly driving the compressor. The condenser is common to both cycles (see Figure 1). The vapor generation of the Rankine cycle is pictured as a supercritical process, but it could equally be subcritical. However the preliminary results (Demierre and Favrat 2008) show that it is particularly interesting to have a supercritical evaporation. As the compression heat pump cycle is a reversed organic Rankine cycle, this system is called here an ORC-ORC heat

pump. Like absorption heat pumps, ORC-ORC systems have the advantage of being able to operate with a variety of fuels or heat sources like wood pellets, natural gas, solar heat, geothermal heat or waste heat. An earlier concept of gas driven ORC-ORC heat pump using the same working fluid in both cycles and a dynamic compressor and turbine rotating on refrigerant vapour bearings was proposed by Strong (Strong 1980), but difficulties were encountered which could have been caused by the lack of appropriate materials. Moreover, an additional point that penalized such a system was the problematic of the CFC refrigerants, which were, at the time, among the best candidates for high temperature cycles. Progress in materials, bearing knowledge and new ozone depletion free refrigerants having a reasonably high temperature chemical stability and/or acceptance, allow the reconsideration of this approach. The recent demonstration of one concept of miniature high speed (about 210 krpm) centrifugal compressor directly driven by an electric motor rotating on refrigerant gas bearings (Schiffmann and Favrat 2009) opens the way to such devices with or without electric motor.

The concept studied in this work is a low power system (for small buildings) with a single-stage radial compressor and a single-stage radial inflow turbine. The compressor and turbine are directly coupled on the same shaft rotating on refrigerant vapor gas bearings. This gives the system the advantage of being oil-free, fully hermetic and with low maintenance costs. Because of the characteristics of dynamic compressors and turbines a low density fluid is preferred and refrigerant HFC-134a has been selected at this stage. It is chemically stable at relatively high temperatures (at least up to 200°C), particularly in an oil-free environment.

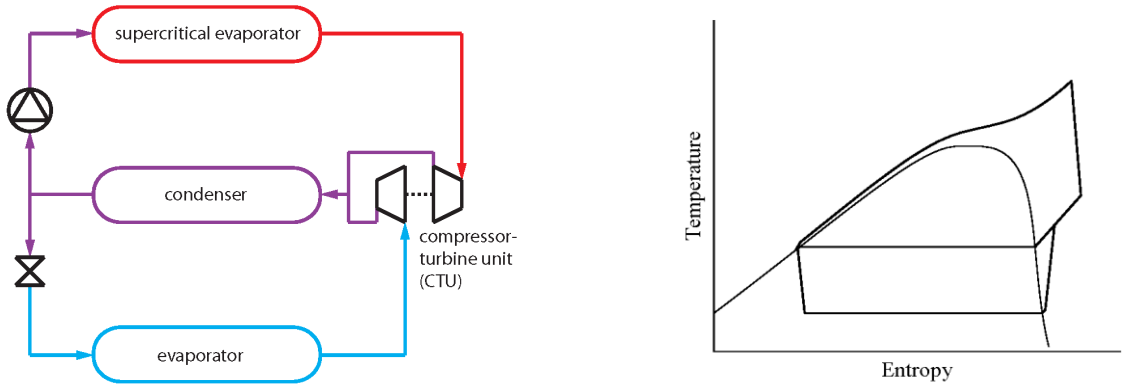

Figure 1: Schematic flowsheet and T-s diagram of a simple ORC-ORC heat pump unit

2 WORKING FLUID COMPARISON

2.1 Approach

In previous developments, a tool has been developed to evaluate the potential of ORC-ORC systems for residential heating applications (Demierre and Favrat 2008). The approach used to evaluate the performances of ORC-ORC systems is summarized in Figure 2.

The first step of the computation process is the calculation of the cycles (the thermodynamic properties at all points and the mass flows in the Rankine cycle and the heat pump). The thermodynamic properties of the refrigerant are calculated with *REFPROP* (Lemmon et al. 2010).

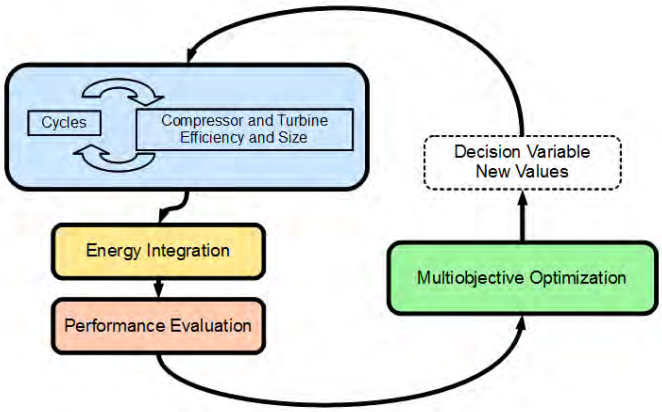

Figure 2: Diagram of the ORC-ORC design and optimization tool

A polynomial approximation of the correlation of (Rohlik 1968) is used to model the turbine isentropic efficiency η_T. This relation gives the maximum efficiency that can be achieved for a fixed turbine specific speed n_{sT}:

$$n_{sT} = \frac{\omega \dot{V}_T^{1/2}}{\Delta h_{0sT}^{3/4}} \quad (1)$$

with $\dot{V}_T$: the volumetric flow at the turbine outlet
ω : the angular velocity
Δh_{0sT} : the isentropic enthalpy difference between the inlet and outlet of the turbine

The compressor isentropic efficiency η_C is modelled using a similar method. A correlation adapted from (Balje 1981) by (Whitfield and Baines 1990) that relates the maximum efficiency to the compressor specific speed n_{sC} is approximated. The compressor specific speed is defined by

$$n_{sC} = \frac{\omega \dot{V}_C^{1/2}}{\Delta h_{0sC}^{3/4}} \quad (2)$$

with $\dot{V}_C$: the volumetric flow at the compressor inlet
ω : the angular velocity
Δh_{0sC} : the isentropic enthalpy difference between the outlet and inlet of the compressor

The optimal turbine and compressor wheel diameters, respectively D_{2T} and D_{2C}, can be roughly estimated using the relations:

$$n_{sT}\, d_{sT} = 2 \qquad \text{where } d_{sT} = \frac{D_{2T}\, \Delta h_{0sT}^{1/4}}{\dot{V}_T^{1/2}} \qquad \text{for the turbine} \quad (3)$$

$$n_{sC}\, d_{sC} = 3 \qquad \text{where } d_{sC} = \frac{D_{2C}\, \Delta h_{0s\,C}{}^{1/4}}{\dot{V}_C{}^{1/2}} \qquad \text{for the compressor} \qquad (4)$$

Those relations approximate the lines of best efficiency of the n_s - d_s diagrams from (Balje 1981).

Once the cycles have been determined, the mass flows of the heat sources and the heat sinks (hot domestic water and heating water) have to be optimally set, which is the energy integration step. The energy integration of the system is made using an in-house software tool based on the pinch analysis method. The mass flows of the heat sources and the heat sinks are calculated by solving a problem of operating cost minimization. The stream costs are set in order that the operating cost is minimal when the COP is maximal. The heat service cost is set negative, the hot source (the fumes) cost is set positive and the cost of the cold source (the glycol water) is equal to 0 as it is considered as a free resource. The ratio between the heat service cost and the hot source cost is set in order that the hot source power is increased only if the heat service power increases faster. In other words, this avoids using the fumes to only heat directly the water.

The performance of the system is characterized by the overall coefficient of performance (COP) that is defined as the ratio of the heat rate supplied and the power consumed by the system that is not free of charge:

$$COP = \frac{\dot{Q}_W^-}{\dot{Q}_{fumes}^+ + \dfrac{\dot{E}_p^+}{0.56}} \qquad (5)$$

where $\dot{Q}_W^-$ is the heat rate supplied (hot water and heating), $\dot{Q}_{fumes}^+$ is the heat provided by the fumes resulting from the combustion of natural gas (assumed to be 100% methane) and $\dot{E}_p^+$ is the electrical power consumed by the ORC-ORC pump (which is the only electrical power consumed by the ORC-ORC). $\dot{E}_p^+$ is divided by 0.56 to take into account for the efficiency of a modern combined cycle power plant that produces this electrical power from the same fuel, in order to define a COP which is strictly based on the conversion of the fuel (here, methane) into heat.

An in-house multiobjective optimization tool, MOO (Molyneaux et al. 2010), based on an evolutionary algorithm is used to find optimal sets of design parameters, that are the temperature and pressure levels of the cycles and the rotational speed of the compressor-turbine unit (CTU). This optimization is done with the COP maximization as the first objective and the rotational speed of the CTU as the second objective. The CTU rotational speed is chosen as the second objective, because for low power compressor and turbine the optimal rotational speed becomes critically high. The coupling of the different software programs is performed thanks to an in-house energy system optimization platform, OSMOSE (Marechal et al. 2004).

2.2 Results

A study was made on a system using R134a as working fluid (Demierre and Favrat 2008). The hot heat source consists of the fumes coming from a stoechiometric combustion of methane that can be cooled down to 4°C and the cold heat source is the brine of a ground source that cools down from 4°C to 1°C. The heating services are the production of domestic hot water (from 10°C to 60°C) and heating water for floor heating (from 30°C to 35°C). The

total power of the heating services is about 40 kW with a distribution of 80% for the heating system of the building and 20% for domestic hot water, which is typical for the winter season.

A similar study has been made for different working fluids that are commonly used or expected to be good candidates for heat pump, refrigeration or ORC applications. Two-objective optimizations with the COP and the CTU rotational speed as objectives are made and the resulting Pareto curves are shown in Figure 3. The Pareto curve (or Pareto front) of a two-objective optimization can be plotted in a 2-D graph with the two objectives on the respective axis. The Pareto front divides the solution domain into two sub-domains: the sub-domain of unfeasible solutions and the sub-domain of sub-optimal solutions. For a solution located on the Pareto curve, it is not possible to find another solution that improves both objectives. Each point of the Pareto front is an optimal solution. The optimization algorithm does not eliminate systematically all the points that are not near the Pareto front. Nevertheless, those points are clearly not optimal solutions and as such can be ignored. It can be seen that R410A (orange points) is not a good candidate because the maximum COP is about 2.16 and the CTU rotational speed N for this value of COP is excessive. A large number of refrigerants show more or less the same results with a maximum COP between 2.2 and 2.4 for a rotational speed between 200 krpm and 250 krpm. However, in this group of fluids, R134a (green points), R1234yf (red points) and Isobutan (dark blue points) are the best candidates, as their curve is shifted to the right compared to the others. At this stage, the best candidates seem to be R227ea (dark purple points) with a COP of 2.36 at about 163 krpm, R236fa (dark green points) with a COP of 2.40 at about 160 krpm and R245fa (brown points) with a COP of 2.45 at about 142 krpm.

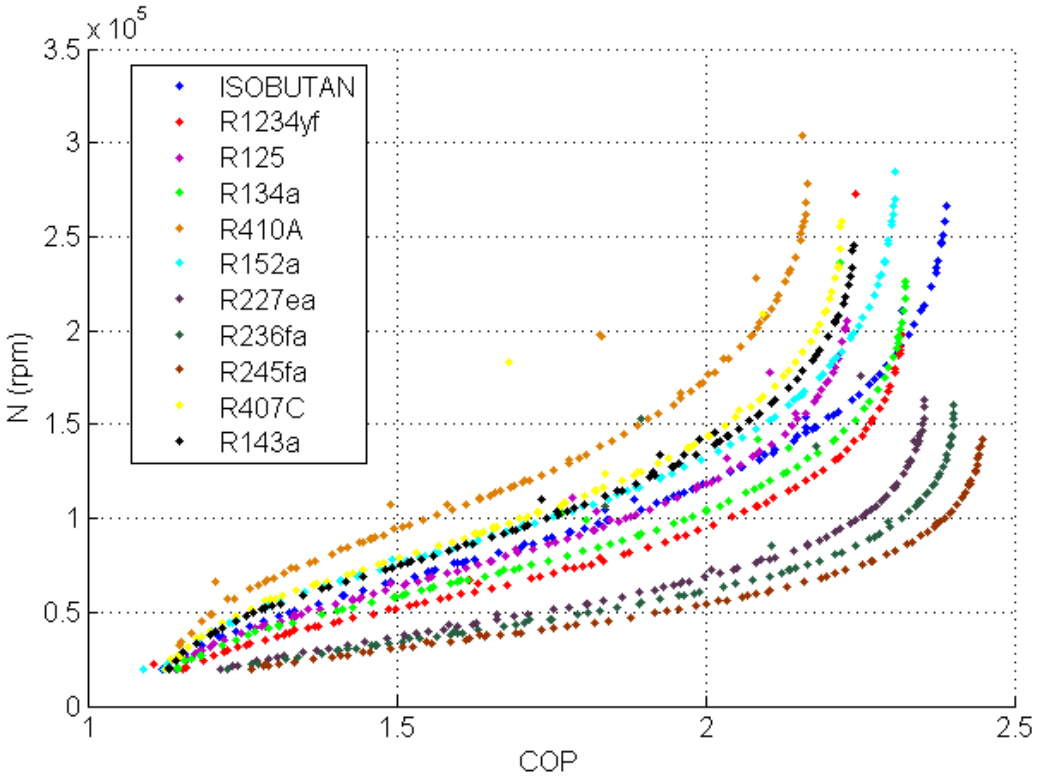

Figure 3: Pareto curves resulting from optimizations with maximization of the COP as first objective and minimization of the CTU rotational speed as second objective for different working fluids

R134a, R1234yf, R227ea, R236fa and R245fa are compared in Table 1 by looking at several key parameters. Even if Isobutan enables to reach a high COP, it is eliminated because of its flammability. It has to be noted that the evaporation pressure (which corresponds to a temperature of about 0°C) of the heat pump cycle for R245fa is below the atmospheric

pressure. This is an important disadvantage, since the working fluid could be contaminated with ambient air, if the system happens not to be totally hermetic. The compressor and turbine wheel diameters are in the range 20 mm to 45 mm, which is not problematic regarding the machining with today's technology. A reason that can explain why R227ea, R236fa and R245fa are better is the shaft losses that are lower with a lower rotational speed. It can be seen in Table 1 that the shaft losses are 53% lower with R227ea, 63% lower with R236fa and 77% lower with R245fa than with R134a. With R236fa and R245fa, a turbine pressure ratio of respectively 13.1 and 18.6 are obtained, which cannot realistically be achieved with a one stage radial machine. It has to be mentioned that this approach of modeling the compressor and turbine efficiencies as functions of the specific speed does not take into account the effect of the pressure ratio. In reality, the compressor and turbine efficiency are negatively affected by too high pressure ratios and thus, the COP for R236fa and R245fa should be lower than the predicted value with this approach.

Table 1: Comparison of the design parameter values for different working fluids

		R134a	R1234yf	R227ea	R236fa	R245fa
N	(krpm)	226	198	163	160	142
COP	(-)	2.33	2.32	2.36	2.40	2.45
Compressor wheel diameter	(mm)	21	21	23	26	33
Turbine wheel diameter	(mm)	21	22	23	27	34
HP evaporation pressure	(bar)	2.9	3.2	2.0	1.1	0.53
Condensing pressure	(bar)	9.1	9.1	6.3	3.9	2.2
ORC evaporation pressure	(bar)	77	70	62	51	41
Compressor pressure ratio	(-)	3.1	2.8	3.2	3.5	4.2
Turbine pressure ratio	(-)	8.5	7.7	9.8	13.1	18.6
Shaft losses	(W)	115	91	54	42	27

At this stage, the best candidates seem to be R134a, R1234yf, R227ea and R236fa. R245fa is eliminated for this application because its pressure at the heat pump evaporation is below the atmospheric pressure. It has to be mentioned that some of the tested working fluids exhibit a slope of the saturation curve that is positive at the saturated vapor side in a T-s diagram, which implies that a sufficient superheating before the compressor is required in order to avoid crossing the saturation line during compression. This is of course taken into account in this analysis.

3 OFF-DESIGN MODELING

The aim of the off-design modeling is to predict the system performance for a given compressor-turbine unit geometry. In this work, the other parts of the system (heat exchangers, pump, expansion valve and pipes) are not modeled in detail, which means that the inputs and outputs of each component are simply set by the user or calculated using the equations of conservation of mass and energy. The CTU model must allow the prediction of the efficiency and the capacities of the compressor and turbine that are required to calculate the thermodynamic cycles. The modeling approach that is used for the compressor and the turbine is the mean line or one-dimensional modeling. This consists of predicting the performance of the turbomachine by calculating the flow properties along the mean stream line of the channels. The implementation of the compressor and shaft loss models was a part of a previous PhD thesis (Schiffmann 2008) and so, modeling details on those elements are not presented in this paper. The radial turbine model is described in the following subsection.

3.1 Radial Turbine Model

The approach that is used to model the turbine is the one described by Baines in (Moustapha et al. 2003). The flow properties are calculated at the inlet and exit of each element of the

turbine along the mid-streamline. Figure 4 shows the layout of a radial inflow turbine and the locations that are considered to calculate the flow. Each element of the turbine is calculated one after the other in the direction of the flow. The model does not include the modeling of the volute. It is assumed that the flow velocity is low in this element and thus, the losses can be neglected.

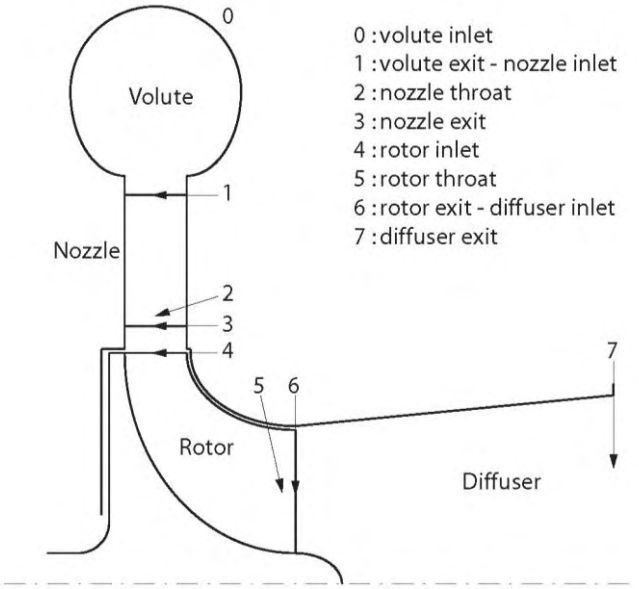

Figure 4: Radial turbine layout and locations that are considered for the mean line model

Nozzle

The nozzle throat is usually the first location at which the flow chokes and therefore, the nozzle throat area is an important parameter to set the turbine flow capacity. In order to calculate the flow properties at this location, the loss that occurs between nozzle inlet and throat is expressed using a static enthalpy loss coefficient:

$$\xi = \frac{h_2 - h_{2s}}{\frac{1}{2}C_2^2} \tag{6}$$

where C_2 is the absolute flow velocity at the nozzle throat. To estimate this loss coefficient, a modified expression of the correlation of Rodgers proposed by Baines (Baines 2006) is used:

$$\xi = \frac{0.05}{Re^{0.2}}\left(\frac{\tan^2\alpha_{b3}}{s_{noz}/c_{noz}} + \frac{o_{noz}}{b_3}\right) \tag{7}$$

where α_{b3} is the blade exit angle, s_{noz} is the blade spacing at exit, c_{noz} is the blade chord length, o_{noz} is the throat opening and b_3 is the blade exit high. The same procedure is used to calculate the loss from the nozzle inlet to the rotor inlet. The flow deviation at the nozzle exit is modelled by calculating the exit flow angle α_3 with the cosine rule expressed with the passage areas and the aerodynamic blockage coefficients:

$$\alpha_3 = \arccos\left(\frac{A_{th,noz}\ 1-B_{th,noz}}{A_3\ 1-B_3}\right) \tag{8}$$

where $A_{th,noz}$ is the nozzle throat area, A_3 is the annulus exit area, and $B_{th,noz}$ and B_3 are the blockage coefficients respectively at throat and exit. If the nozzle is not choked, the flow angle at rotor inlet is assumed to be equal to the flow angle at nozzle exit. If the nozzle is choked, supersonic expansion can occur in the nozzle-rotor interspace which turns the flow in the meridional direction.

Rotor

The internal losses in the rotor are modelled by a sum of four contributions: the incidence loss, the passage loss, the tip clearance loss and the trailing edge loss.

The incidence loss is related to the work that is needed to turn the flow in the required direction when entering into the rotor. The expression proposed by (Wasserbauer and Glassman 1975) is implemented in the model:

$$\Delta h_{inc} = \frac{1}{2} W_4^2 \sin^2 \left(\beta_4 - \beta_4, opt \right) \tag{9}$$

where W_4 is the relative flow velocity at rotor inlet, β_4 is the relative flow angle at rotor inlet and $\beta_{4,opt}$ is the optimal incidence angle which is usually between -20° and -40° (Moustapha et al. 2003).

The passage losses include the loss due to secondary flows and the loss due to friction on the walls. The correlation that is implemented in the model is a simple model based on the mean kinetic energy of the working fluid. The expression that is used was proposed by (Wasserbauer and Glassman 1975):

$$\Delta h_{pass} = \frac{1}{2} K_{pass} \left(W_4^2 \cos^2 \left(\beta_4 - \beta_{4,opt} \right) + W_6^2 \right) \qquad \text{with} \quad K_{pass} = 0.3 \tag{10}$$

where K_{pass} is a coefficient that has to be determined with experimental data and W_6 is the relative flow velocity at turbine outlet.

The tip clearance loss is due to the leakage of the flow in the gap between rotor tip and shroud. The expression that is implemented is the one given by Baines in (Moustapha et al. 2003):

$$\Delta h_{cl} = \frac{U_4^3 N_b}{8\pi} \left(K_x \varepsilon_x C_x + K_r \varepsilon_r C_r + K_{xr} \sqrt{\varepsilon_x \varepsilon_r C_x C_r} \right) \tag{11}$$

$$\text{with} \quad C_x = \frac{1 - r_{6t} / r_4}{C_{m4} b_4} \qquad \text{and} \quad C_r = \left(\frac{r_{6t}}{r_4} \right) \frac{l_{rot} - b_4}{C_{m6} r_{6rms} b_6}$$

where U_4 is the rotor tip velocity, N_b is the blade number, ε_x and ε_r are respectively the axial and radial clearances, r_{6t} is the tip radius at the exit, r_4 is the radius at the inlet, b_4 is the inlet blade height, C_{m4} and C_{m6} are the meridional component of the absolute velocity respectively at inlet and exit, l_{rot} is the axial length of the rotor, b_6 is the exit blade height and r_{6rms} is the mean radius at exit. K_x, K_r and K_{xr} are empirical coefficients and values of respectively 0.4, 0.75 and -0.3 are recommended from test data.

This trailing edge loss is due to the flow separation at the blade trailing edge that creates a region of lower pressure just behind the blade. To evaluate this loss, a simple correlation recommended by Baines (Baines 2006) that is based on axial turbine test data is used:

$$\Delta h_{TE} = \frac{1}{2} C_6^2 K_{TE} \frac{t_{TE}}{o_{rot}} \qquad \text{with} \qquad K_{TE} = 0.2 \tag{12}$$

where K_{TE} is an empirical coefficient, C_6 is the absolute flow velocity at the exit, t_{TE} is the blade trailing edge thickness and o_{rot} is the throat opening.

The exit flow angle deviation is calculated in the same way as for the nozzle (Eq. 8) using the cosine rule. If the rotor throat is choked, a supersonic expansion can occur at the trailing edge that turns the flow in the axial direction. An additional external loss related to the rotor, the windage loss, is taken into account in the modeling. This loss is due to the friction in the gap between the rotor back face and the back plate. This loss acts as a loss of power on the turbine shaft.

Diffuser

The aim of the diffuser is to enable the recovery of a part of the kinetic energy of the flow that leaves the rotor. In this model, it is assumed that the angular momentum is constant, which is expressed by:

$$rC_\theta = \text{cte} \tag{13}$$

where C_θ is the tangential component of the flow absolute velocity. The implemented loss model is due to Japikse (Moustapha et al. 2003) who gives a correlation for the diffuser efficiency defined as the ratio of the real and ideal pressure recovery coefficients, respectively C_p and C_{pi}:

$$\eta_{dif} = \frac{C_p}{C_{pi}} = \frac{P_7 - P_6 \ / \ P_{06} - P_6}{P_{7s} - P_6 \ / \ P_{06} - P_6} \tag{14}$$

The correlation proposed by Japikse is based on the examination of a large database and is expressed by the product of the different contributions:

$$\eta_{dif} = \eta_{AR} \eta_\alpha \eta_B \tag{15}$$

with

$\eta_{AR} = 0.72 + 3.0\exp\left(-0.9 - 1.5 \ A_7 / A_6\right)$ area ratio effect

$\eta_\alpha = 1.1 - 0.0001\alpha_6^{1.9}$ swirl effect

$\eta_B = 1.22 + 0.08\ln B_6$ aerodynamic blockage effect

where A_6 and A_7 are the passage areas of respectively the inlet and the exit of the diffuser, α_6 is the absolute flow angle at inlet and B_6 is the aerodynamic blockage coefficient at inlet.

3.2 Comparison of Turbine Mean Line Model and CFD

Comparison between mean line model and CFD performance prediction was made for the turbine that was developed for the ORC-ORC prototype. The CFD computations were made using a commercial software, AxCent (Concepts NREC 2010). Results have been compared for several operating conditions and with R134a as working fluid. It appears that the overall performances predicted by the mean line model are very close to the ones calculated with the CFD simulation. Figure 5 shows a comparison of the efficiency and of the power predicted by both methods for an inlet stagnation pressure of 50 bar and an inlet stagnation temperature of 160°C.

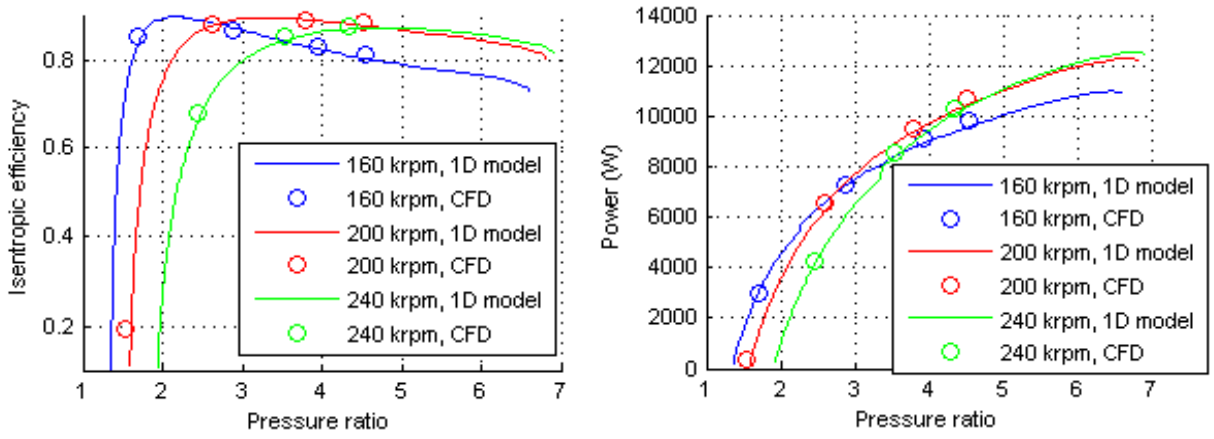

Figure 5: Comparison of the mean line (1D) model and the CFD on the predicted isentropic efficiency and power (inlet stagnation pressure is 50 bar and inlet stagnation temperature is 160°C)

3.3 ORC-ORC Off-design Prediction Example

The inputs to calculate an operating point of the CTU are the inlet stagnation temperature and pressure of the compressor, the mass flow in the compressor, the rotational speed and the inlet stagnation temperature of the turbine. First, the compressor is calculated which sets the power that it requires and the exit stagnation pressure, and thus, the condensing temperature of the cycles. Then, the power losses of the shaft are calculated. With the calculation of those two components, the power that has to be delivered by the turbine is set. Finally, the turbine is calculated in order to reach the required power and exit stagnation pressure. This is done by iterating on the inlet stagnation pressure and either on the mass flow or on the supersonic deviation at nozzle exit or at rotor exit depending on the choke locations. Once, the CTU is calculated, it is possible to determine the thermodynamic state of each point of the cycles.

Figure 6 shows the predicted map of the experimental ORC-ORC prototype but with a turbine nozzle throat area that is the half of the existing ones. It is calculated for a heat pump evaporation temperature of 0°C and a turbine inlet stagnation temperature of 120°C. The map of Figure 6 plots the condensing temperature that can be reached as a function of the COP. The COP calculated here does not integrate the heat sources and the heat sinks like in the previous section. It is simply the ratio of the heat rejected by the condenser and the heat supplied to the evaporator of the ORC plus the power given to the pump. The interesting part of this map is the left side where the temperature increase becomes useful for residential heating applications. The different lines are the iso-velocity curves. They are limited on the left side by compressor surge and on the right side by compressor choke. As it was shown in the previous section (see Figure 3), the rotational speeds required by R1234yf, R236fa and R227ea are lower than required by R134a for the same temperature lift. R1234yf and R236fa

allow to target the same temperature lifts for similar rotational speeds. R227ea has the lowest rotational speeds. The maximum temperature lift is about 35°C, which is just enough for an application with brine source cooled from 4°C to 1°C. The COP values are much lower than the values shown in Figure 3, because here the parameters of the system and the compressor and turbine geometry are not optimized.

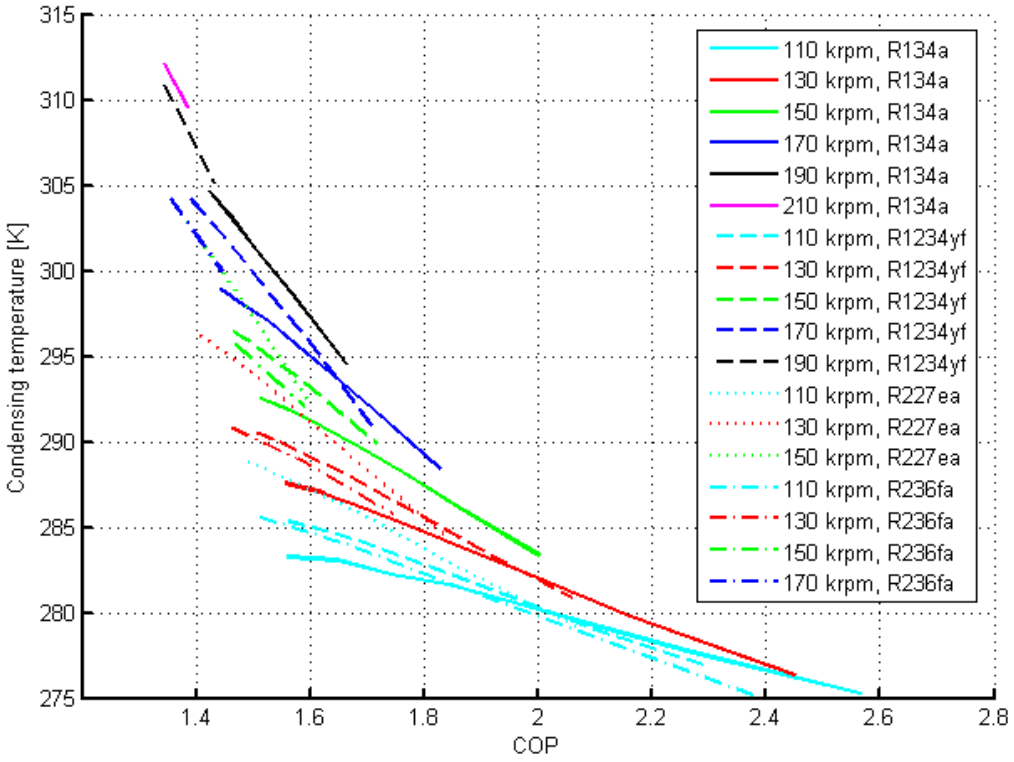

Figure 6: Predicted map of the ORC-ORC experimental prototype for different working fluids (heat pump evaporation temperature is 0°C and turbine inlet stagnation temperature is 120°C)

4 CONCLUSION

An approach to compare the potential of different refrigerants as working fluids for an ORC-ORC thermally driven heat pump has been described. A comparison is presented for an application of residential heating (about 40 kW). This comparison is made on the maximum COP that can be achieved and the minimum rotational speed that is required. Rotational speed is a key parameters for the feasibility of the system, as for small turbomachines the operating speed is critically high. It appears that the best candidates are R134a (COP = 2.33 @ 226 krpm), R1234yf (COP = 2.32 @ 198 krpm), R227ea (COP = 2.36 @ 163 krpm) and R236fa (COP = 2.40 @ 160 krpm).

An off-design radial turbine model is presented. It appears that performance predictions are very close to the ones predicted by CFD analysis. This model, together with previously developed models of the compressor and the shaft loss, enables to simulate off-design operation of ORC-ORC heat pumps. Performance evaluations of the existing experimental prototype have been performed for the four refrigerants mentioned above thanks to this off-design model. From the simulation results, it can be inferred that the existing compressor is capable of reaching the required temperature lift (about 35°C).

First tests of the experimental ORC-ORC prototype were performed at rotational speeds up to 140 krpm. Several technical difficulties were encountered and solved. The next step will be the test of the prototype at rotational speeds up to 200 krpm.

5 ACKNOWLEDGMENTS

The authors would like to thank the *Swiss Federal Office of Energy (OFEN)* for its financial support and *Fischer Engineering Solutions AG* in Herzogenbuchsee (BE, Switzerland) to have supplied the gas bearings and to have assembled and balanced the compressor-turbine unit.

6 REFERENCES

Baines N.C. 2006. Radial Turbines (course notes), Concepts ETI, Inc., White River Junction, USA.

Balje O.E. 1981. Turbomachines: A Guide to Design, Selection and Theory, John Wiley & Sons, New York, USA.

Borel L., D. Favrat 2010. Thermodynamics and energy systems analysis, EPFL Press, Lausanne, Switzerland.

Concepts NREC. 2010. AGILE Engineering Design System, http://www.conceptsnrec.com.

Demierre J., D. Favrat 2008. “Low power ORC-ORC systems for heat pump applications”, *Proc. of the 9th Int. IEA Heat Pump Conf.*, Zürich, Switzerland.

Lemmon E.W., M.L. Huber, M.O. McLinden 2010. REFPROP - NIST Standard Reference Database 23, Version 9.0, National Institute of Standards and Technology, USA.

Marechal F., et al. 2004. “Thermo-economic modeling and optimization of fuel cell systems”, Fuel Cells: From Fundamentals to Systems.

Molyneaux A., G. Leyland, D. Favrat 2010. “Environomic multi-objective optimisation of a district heating network considering centralized and decentralized heat pumps,” *Energy*, 35(2):751–758.

Moustapha H., M.F. Zelesky, N.C. Baines, D. Japikse 2003. Axial and Radial Turbines, Concepts NREC, White River Junction, USA.

Rohlik H.E. 1968. “Analytical determination of radial inflow turbine design geometry for maximum efficiency”, NASA TN D-4384.

Schiffmann J. 2008. “Integrated design, optimization and experimental investigation of a direct driven turbocompressor for domestic heat pumps”, Ph.D. Thesis, Ecole Polytechnique Fédérale de Lausanne, Switzerland.

Schiffmann J., D. Favrat 2009. “Experimental investigation of a direct driven radial compressor for domestic heat pumps”, *Int. J. of Refrigeration*, 32(8):1918–1928.

Strong D.T.G. 1980. “Development of a directly fired domestic heat pump”, Ph.D. Thesis, University of Oxford, UK.

Wasserbauer C.A., A.J. Glassman 1975. “FORTRAN program for predicting the off-design performance of radial inflow turbines”, NASA TN-8063.

Whitfield A., N.C. Baines 1990. Design of Radial Turbomachines, Longman Scientific & Technical, Harlow, UK.

HYBRID HEAT PUMP FOR WASTE HEAT RECOVERY IN NORWEGIAN FOOD INDUSTRY

Stein Rune Nordtvedt, Institute for Energy Technology, Instituttveien 18, N-2027 Kjeller
Bjarne R. Horntvedt, Hybrid Energy AS, Ole Deviks vei 4, N-0666 Oslo
Jan Eikefjord, John Johansen, Nortura AS, Rudshøgda, Norway
Stein.Nordtvedt@ife.no

This paper was published in the proceedings of the 10th International Heat Pump Conference 2011 (www.heatpumpcentre.org/en/hppactivities/ieaheatpumpconference).

Abstract: Traditional food companies usually have facilities for the production of refrigeration and steam. Typically, these facilities run independently of each other even if they are a part of the energy system in the companies. There are only a handful of companies that need steam and in most cases hot water up to 80-100°C is sufficient. Institute for Energy Technology has done research on energy recovery in an industrial context, and especially within the food industry since 1995. This has resulted in a hybrid heat pump (compression / absorption heat pump) using a mixture of ammonia and water as working fluid. The hybrid heat pump has the capability to deliver hot water up to 100°C, recovering waste heat at approx 50°C. This paper presents operational experiences with a specific hybrid heat pumps installation at a Norwegian slaughterhouse. The hybrid heat pump recovers heat from the refrigeration system and produce hot water at 90°C.

Key Words: industrial heat pumps, waste heat recovery, ammonia-water mixture

1 INTRODUCTION

Traditional food companies usually have facilities for the production of refrigeration and steam. Typically, these facilities run independently of each other even if they are a part of the energy system in the companies. There are only a handful of companies that need steam and in most cases hot water up to 80-100°C is sufficient.

Institute for Energy Technology has done research on energy recovery in an industrial context, and especially within the food industry since 1995. This has resulted in a hybrid heat pump (compression/absorption heat pump) using a mixture of ammonia and water as working fluid (Nordtvedt 2005). The hybrid heat pump has the capability to deliver hot water up to 100°C, recovering waste heat at approx 50°C. A pilot plant of the hybrid heat pump was installed in a Norwegian dairy in 2000 and after successful operation over several years the company Hybrid Energy AS was founded in 2004. The hybrid heat pump installation that will be described here is the first commercial hybrid heat pump installation in Norway. This heat pump was installed in a slaughterhouse providing hot water for cleaning purposes and has been in operation since 2007.

2 THE HYBRID HEAT PUMP TECHNOLOGY

The combination of an absorption process and a vapour compression process with ammonia-water as working fluid gives a flexible heat pump system. A hybrid heat pump with a 50% mixture of ammonia and water, can heat water to over 100°C with the same pressure

rating/equipment. Then this plant can cover quite different temperature ranges than conventional heat pumps and is particularly interesting in industrial processes.

The hybrid heat pumps (compression/absorption) exhibit some interesting possibilities when compared to conventional vapour compression heat pumps. High heat sink temperatures can be achieved at the design pressures of standard refrigerating components due to the boiling point elevation reached when mixing ammonia with water. The temperature glide of the ammonia-water mixture can be adjusted to the external heat sink/source fluids by adjusting the composition. Changing the average composition of the solution circulating between the absorber and the desorber allows for a change in the saturation pressures in the system, and a capacity control as the compressor is supplied with lower or higher density vapour.

3 SYSTEM DESCRIPTION

Figure 1 shows a sketch of the hybrid heat pump system. The working cycle consists of a solution pump pumping solution rich in water from low pressure to higher pressure, and a compressor which is pressurizing ammonia vapour from low pressure to high pressure. The solution rich in water is mixed with the ammonia vapour in the absorber, and heat is released to the heat sink during the ammonia absorption process. The resulting solution leaving the absorber is rich in ammonia, and is expanded to the low pressure side through the expansion valve before it enters the desorber. There ammonia is evaporated out of the solution by heat extraction from the heat source, and the process repeats itself. A solution heat exchanger is installed for internal heat recovery and increases the cycle efficiency. Figure 2 shows the hybrid heat pump cycle components in a pressure, temperature, concentration (PTX) diagram.

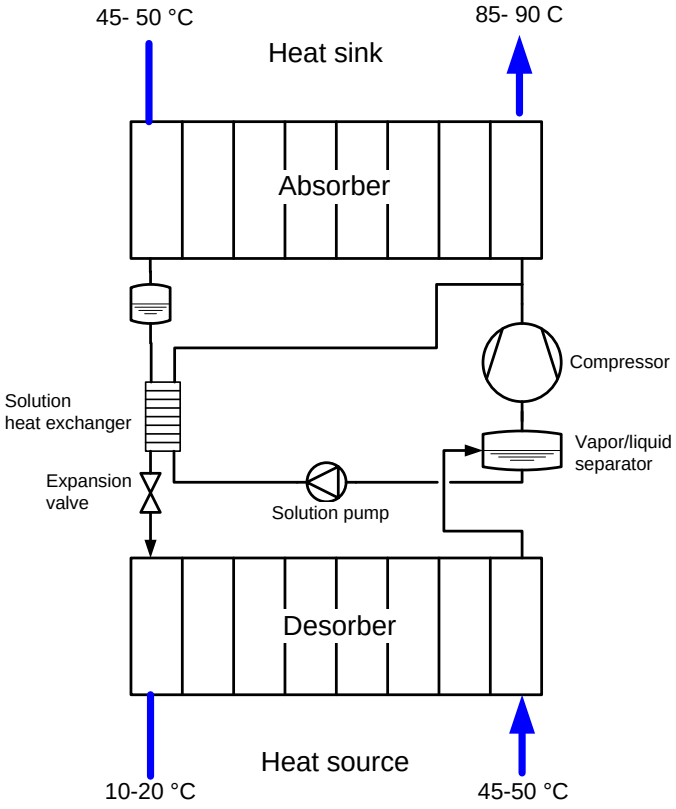

Figure 1: Hybrid heat pump sketch

As the working fluid is a mixture of ammonia and water the evaporation and condensation processes in the desorber and the absorber respectively, will occur at gliding temperatures. The ammonia concentration in the solution will increase in the absorber and the mixture temperature will decrease through the heat exchanger as the saturation temperature of ammonia is considerably lower than the saturation temperature of water. The process is reversed in the desorber where ammonia is evaporated out of the ammonia/water solution, and the saturation temperature in the solution will increase from the inlet to the outlet of the heat exchanger.

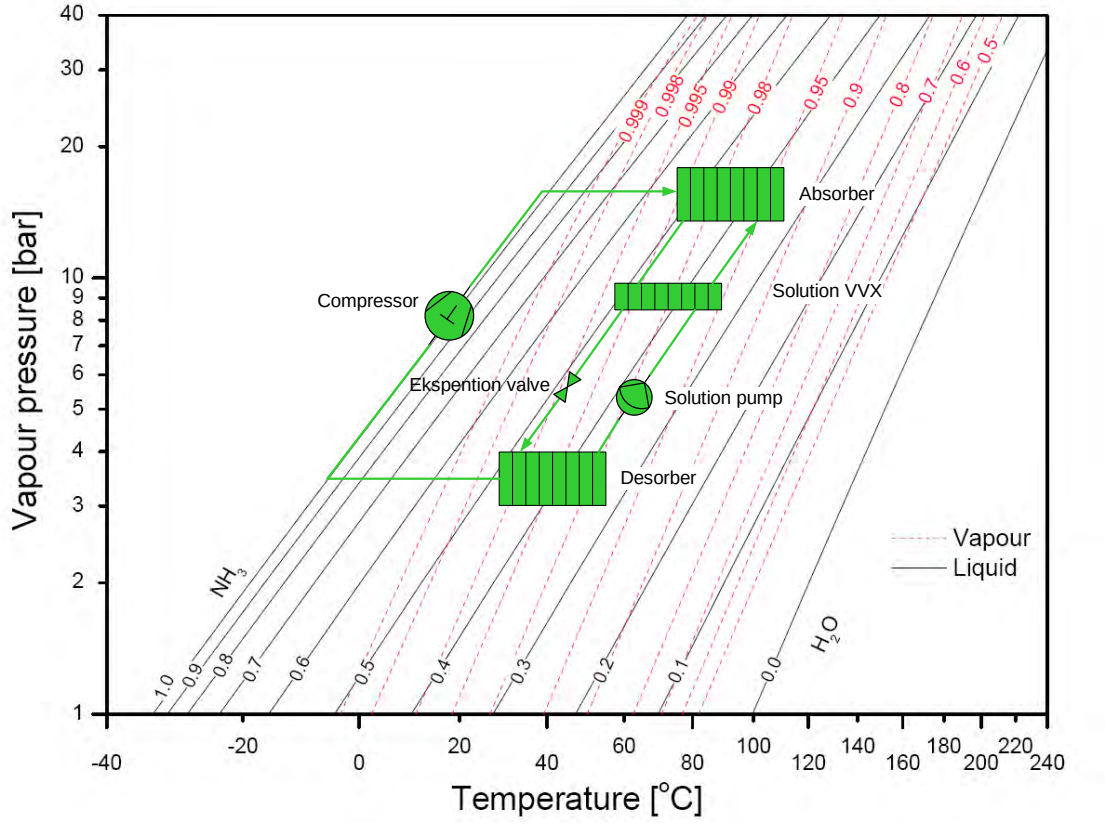

Figure 2: PTX diagram of ammonia-water mixture with hybrid heat pump components

The gliding temperatures of the working fluid mixture during heat extraction in the desorber and during heat release in the absorber can be an advantage in many processes. If the heat source is water that has to be cooled from 40 to 10°C, and the heat sink fluid is water that shall be heated from 50 to 90°C, the temperature glide of the working fluid mixture can be adapted to the temperature glide of the heat sink and heat source fluid. The compressor in the hybrid heat pump will then work against a lower temperature lift than the compressor in a conventional vapour compression heat pump using a pure fluid which experiences a constant temperature during evaporation and condensation.

4 THE HYBRID HEAT PUMP AT NORTURA RUDSHØGDA SLAUGHTERHOUSE

Nortura SA is one of the main suppliers of meat and eggs in Norway, and has 6,100 employees in different industries in 34 municipalities all over the country. The group is organized as a cooperative owned by 25,000 Norwegian farmers (Nortura 2011).

Nortura SA has a slaughterhouse at Rudshøgda in Norway. Nortura Rudshøgda slaughter cattle, pigs and sheep, and do cutting of cattle and pigs. The slaughterhouse produces

steaks/piece of meat, meat cakes, dough and salted/smoked and marinated products. The slaughterhouse need large amounts of hot process water at minimum temperature of 83°C.

In 2007 a hybrid heat pump with a capacity of 650 kW on the hot side was installed for this purpose. The hybrid heat pump is built using a standard reciprocating ammonia compressor and plate heat exchangers as heat exchange components. Figure 3 shows a system sketch of the heat pump installation.

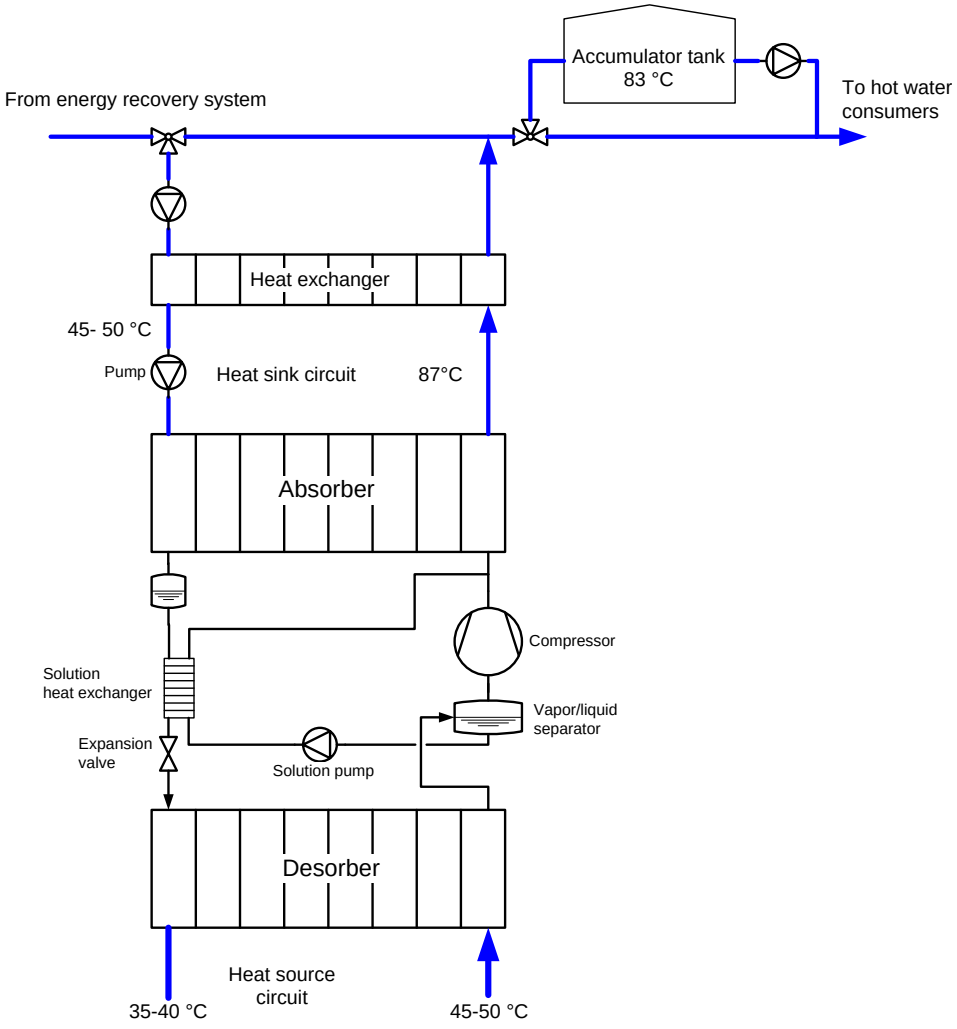

Figure 3: The hybrid heat pump installation at Nortura Rudshøgda

The energy recovery system at Nortura Rudshøgda recovers heat from the refrigeration system on site. Process water is preheated to approximately 50°C with a low-pressure ammonia heat pump system, and then further heated to approximately 83°C with the hybrid heat pump. The hybrid heat pump delivers heat at 87°C to at secondary circuit to avoid contamination of the water for consumption with ammonia in case of a leakage in a heat exchanger.

The heat source of the hybrid heat pump is surplus heat at a temperature of 45-50°C from the low-temperature ammonia compression heat pump plant and waste heat from the cooling/freezing plant.

As a part of the hybrid heat pump installation, a hot water accumulator tank with a capacity of 200 m^3 was installed. The accumulator tank gives the Nortura flexibility in the production, as

the hot water supply system manages large water withdrawals over periods without large peaks in the heating system. By heating tap water up to 83°C with recovered heat, the water can be stored without any danger of legionella problems.

The hybrid heat pump installation has showed an average efficiency of 4.5 over three years. The energy recovery system saves in total approximately 3.4 GWh annually.

5 REFERENCES

Nortura 2011. www.nortura.no

Nordtvedt, S.R. 2005. “Experimental and theoretical study of a compression/absorption heat pump with ammonia-water as working fluid,” *Doctoral Thesis*, Norwegian University of Science and Technology, 2005:82.

ANALYSIS OF A GAS-DRIVEN ABSORPTION HEAT PUMPING SYSTEM USED FOR HEATING AND DOMESTIC HOT WATER PREPARATION

Harald Moser, Rene Rieberer, Graz University of Technology, Institute of Thermal Engineering, Inffeldgasse 25 B, A-8010 Graz, Austria, rene.rieberer@tugraz.at

This paper was published in the proceedings of the 10th International Heat Pump Conference 2011 (www.heatpumpcentre.org/en/hppactivities/ieaheatpumpconference).

Abstract: In the building sector the use of thermally driven heat pumps can contribute substantially to energy conservation and the reduction of end-use energy. Within the IEA HPP Annex 34 a medium size absorption heat pump application installed in a storehouse in Graz has been monitored over a period of one year.

The system consists of two directly natural gas-driven ground source ammonia/water absorption heat pumps (each with ca. 40 kW heating capacity). Via a buffer storage space heating of an office building and a storage depot as well as domestic hot water preparation is provided.

During the monitoring period the system showed reliable operation and high energy performance. Based on the lower heating value of the natural gas the seasonal performance of the year 2010 was 1.54 which is approx. 60% higher compared to a condensing gas boiler with a seasonal performance of 96%. However, also room for improvements has been detected, especially at start/stop operation for domestic hot water preparation in summer.

Key Words: demonstration project, monitoring, IEA HPP Annex 34, ground source

1 INTRODUCTION

In the building sector the use of natural gas driven absorption heat pumps can contribute substantially to energy conservation and the reduction of CO_2-emmisions due to the reduction of the end-use energy demand. Especially the small-capacity range of absorption heat pumps for heating purpose are commonly considered as the logical next development step beyond the condensing gas boiler and thus the market potential is enormous. However, small-capacity applications still suffer from relatively low efficiencies and/or high investment cost compared to other technologies.

In the medium capacity range of around 50 kW heating capacity several absorption heat pumps are available on the market. Large scale AHP for heating purpose are relatively rare and mainly special designed systems based on chillers are used (Ziegler 2002).

The Annex 34 “Thermally Driven Heat Pumps for Heating and Cooling” within the IEA “Heat Pump Program” (HPP) aims to the reduction of the environmental impact of heating and cooling systems by the use of thermally driven heat pumps. One of the main objectives of the Annex 34 is to quantify the economic, environmental, and energy performance of integrated thermally driven heat pumps in cooling and heating systems in a range of climates, countries, and applications. Within this framework at Graz University of Technology (Institute of Thermal Engineering) a demonstration project has been started. The aim of the project is to

evaluate the seasonal performance of two ammonia/water absorption heat pumps for heating and domestic hot water preparation.

2 APPLICATION DATA

Two “Helioplus 40-S” absorption heat pumps from the company “Helioplus Energy Systems GmbH” are installed in a storehouse of a brewery in Graz, Austria (compare Figure 1 and Figure 2). These ammonia/water AHP are directly driven by natural gas, have a maximum supply temperature of 60°C and a heating capacity of 37.1 kW each. One feature of these AHP is that they include also a flue gas heat exchanger in order to condense water in the flue gas by rejecting condensing heat directly to the return flow of the heating circuit.

Figure 1: Storehouse building where the AHPs are installed

Figure 2: Photo of AHP installation

The AHP supply heat to a 1.2 m³ stratified thermal water storage tank (compare Figure 3). This storage tank supplies heating water to both the space heating distribution system and the domestic hot water tank. The outlet nozzle for the space heating system is located at an intermediate level and for domestic hot water preparation at the very top in order to receive the required temperature level.

The heating area comprises of an approx. 2000 m² storage depot and an office area with approx. 600 m². The storage depot has a nominal heating capacity of ca. 57 kW and is heated to 18°C. The office has a heating capacity of ca. 19 kW and is heated to 22°C room temperature. For domestic hot water (DHW) preparation a 0.5 m³ storage tank is used. It is charged by the heat from the heating water storage tank via a plate heat exchanger.

For space heating the heating water storage is controlled with respect to the ambient temperature and heating curve in order to achieve a temperature level in the storage approx. 2 K in excess of the required supply temperature (ca. 40°C at -12°C ambient temperature) for the heat distribution system.

If the temperature level of the DHW tank drops below a certain threshold the control of the AHP is switched to the DHW temperature set point in order to heat the upper part of the heating water storage to the required temperature level of more than 50°C. Using this heating water the domestic hot water tank is charged via a plate heat exchanger. After the temperature level of the domestic hot water tank has reached the temperature set point of 50°C the control of the AHP is switched back to the current space heating temperature set point.

The low temperature energy source for the AHP is provided by 7 ground probes each with a length of 100 m and a mixture of water and propylene glycol (ca. 20 wt%) is used as heat carrier. During summer the ground probes are used for free cooling of the office area. Therefore a plate heat exchanger is used in order to reject the heat from the heating water to the heat carrier of the ground probes. However, free cooling operation is not discussed in this paper and active cooling by the AHP is not provided.

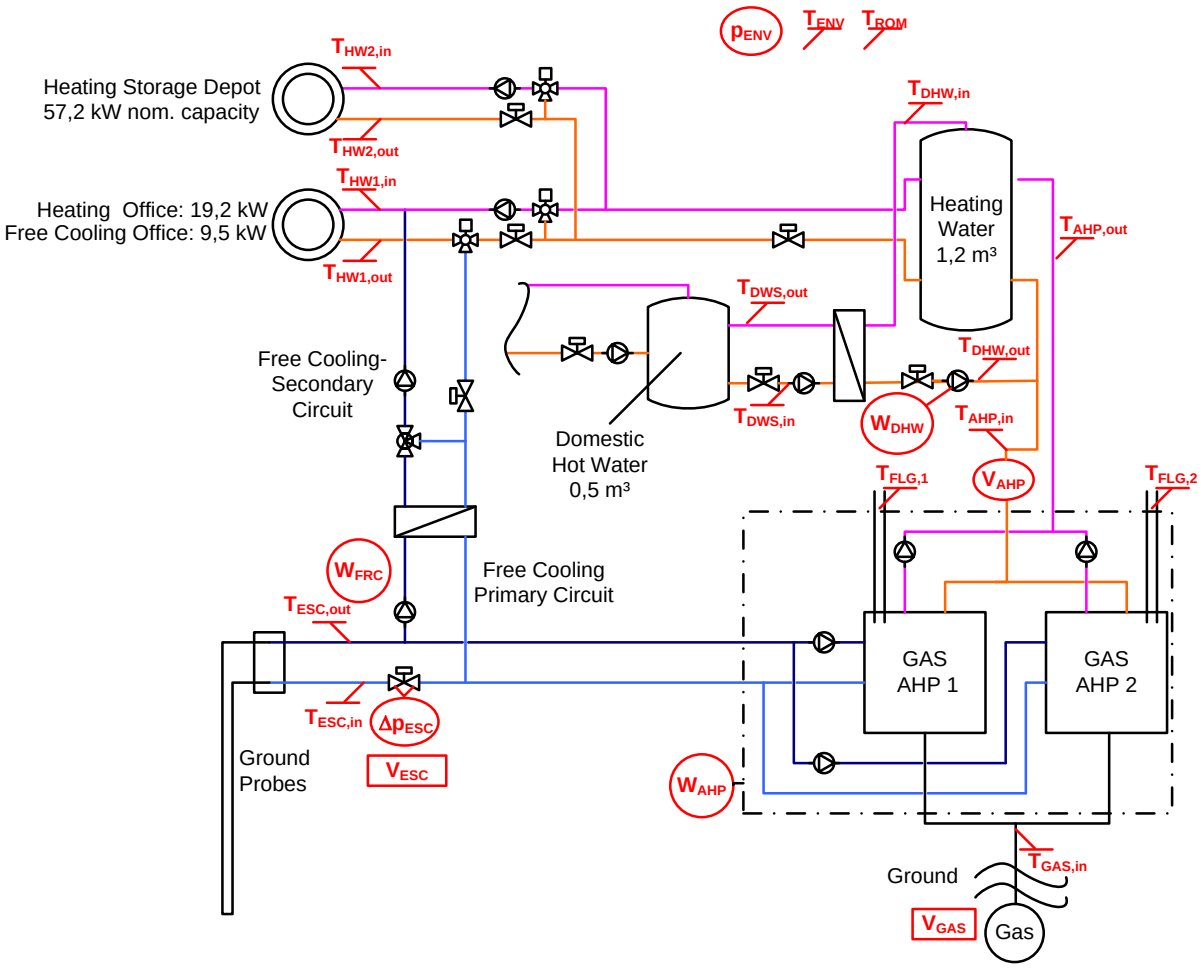

Figure 3: Schematic drawing of the heating system including measurement instrumentation (for legend symbols see Nomenclature)

3 MONITORING CONCEPT

The system has been monitored from 28.12.2009 until 03.01.2011 using a data logger (type “e.reader”) and all relevant data have been measured, processed and recorded within a measurement interval of 10 seconds. Due to some problems with the data transfer within the time period of week 17 to 19 and 23 to 25 the data sets are incomplete for these weeks. However, all available data have been used for system evaluation.

3.1 Measurement Instrumentation

The measurement instrumentation contains all relevant temperatures, the energy input of the heat source, natural gas and the electricity consumption as well as the delivered heat to the heating water storage tank. The measurement instrumentation is also indicated in the schematic drawing in Figure 3.

For the natural gas measurement a bellows-type gas flow meter is installed outside the building. In order to calculate the energy input of natural gas Eq. 1 and Eq. 2 have been used. For this the average upper heating value (Hv_{GAS}) was assumed to be 11.176 kWh/Nm³ (AGGM, 2011) as derived from the gas supplier (average Hv_{GAS} value for the period Jan. to Apr. and Sep. to Dec 2010). The ambient pressure has been measured and the gas pressure (p_{GAS}) has been assumed to be 22 mbar above the ambient pressure as controlled by the pressure reducing regulator upstream the gas flow meter. The standard pressure (p_{NORM}) is 1.013 $bar_{a,}$ the standard temperature (T_{NORM}) is 0°C. Because exact measurement of the gas temperature was not possible a temperature of 6°C has been assumed as it is also used for the gas billing procedure.

$$Q_{GAS} = Hv_{GAS} \cdot V_{GAS,NORM} \tag{1}$$

$$V_{GAS,NORM} = V_{GAS} \cdot \frac{T_{NORM}}{T_{GAS}} \cdot \frac{p_{GAS}}{p_{NORM}} \tag{2}$$

The heat coming from the ground probes have been calculated using Eq. 3 and Eq. 4. Due to the fact that the system was already installed and in operation when monitoring was decided within the IEA Annex 34 it was not permitted to insert flow meters in the hydraulic lines. That is why the volume flow has been measured indirectly by measuring the pressure loss via a balancing valve (compare Eq. 4).

$$Q_{ESC} = \rho_{ESC} \cdot \dot{V}_{ESC} \cdot cp_{ESC} \cdot (T_{ESC,out} - T_{ESC,in}) \cdot \tau \tag{3}$$

$$\dot{V}_{ESC} = \frac{Kv_{ESC}}{3600} \cdot \sqrt{\Delta p_{ESC}} \cdot \sqrt{\frac{\rho_{ESC}}{1000}} \tag{4}$$

The flow coefficient (Kv_{ESC} = 19.31 m³/h) of the balancing value has been determined on site using an ultrasonic flow meter. For calculation of the density and specific isobaric heat capacity a temperature depended polynomial curve fitting of the thermodynamic data has been used.

Electricity meters have been used for the electrical energy input to the AHP (which comprises of the heating water pumps, energy source pumps and AHP control), the pump for domestic hot water preparation and the pump for the primary free cooling circuit. The electrically consumption of the pumps for the heat distribution system have not been measured.

In the return flow line of the AHP heating water circuit a heat meter is installed which gives the possibility to use it as volume flow counter. Using this flow counter the heat output of the AHP has been calculated acc. to Eq. 5 for each measurement interval.

$$Q_{AHP} = \rho_{AHP} \cdot V_{AHP} \cdot cp_{AHP} \cdot (T_{AHP,out} - T_{AHP,in}) \tag{5}$$

All temperatures have been measured using PT100 sensors or thermocouples. In order to analyse the efficiency of the absorption heat pump the weekly Coefficient of Performance for heating (COP_H) has been calculated as indicated in Eq. 6. In order to analyse the absorbed energy from the energy source additional the COP for cooling (COP_C) has been calculated using Eq. 7.

$$COP_H = \frac{Q_{AHP}}{Q_{GAS} + W_{AHP}} \tag{6}$$

$$COP_C = \frac{Q_{ESC}}{Q_{GAS} + W_{AHP}} \quad (7)$$

3.2 Estimation of Measurement Uncertainties

In order to evaluate the combined standard uncertainties of the calculated heat flows and COP values the individual uncertainties of the measurement instrumentation have been estimated and combined by Gaussian error propagation as shown in Eq. 8 (ISO 1995).

$$u_y = \sqrt{\sum_i^N \left(\frac{\partial f}{\partial x_i}\right)^2 \cdot u^2{}_{x_i}} \quad (8)$$

For the natural gas energy consumption the measurement uncertainty of approx. 0.3 kWh/Nm³ has been estimated which correspond to the individual uncertainties given in Table 1.

Table 1: Estimated uncertainty for calculation of u(QGAS)

$u(Hv_{GAS})$	$u(V_{GAS})$	$u(T_{GAS})$	$u(p_{ENV})$
[MJ/Nm³]	[%]	[K]	[bar]
0.54	1	4	0.02

The measurement uncertainty for the low temperature heat source (Q_{ESC}), the delivered heat of the AHP (Q_{AHP}) and the electrical energy input (W_{AHP}) has been calculated for each measurement interval using the individual measurement uncertainties as given in Table 2.

Table 2: Estimated measurement uncertainty for calculation of $u(Q_{ESC})$, $u(Q_{AHP})$ and $u(W_{AHP})$

$u(cp_{ESC})$	$u(m_{ESC})$	$u(T_{ESC,out})$	$u(T_{ESC,in})$	$u(cp_{AHP})$	$u(m_{AHP})$	$u(\Delta T_{AHP})$	$u(W_{AHP})$
[kJ/kg K]	[kg/h]	[K]	[K]	[kJ/kg K]	[%]	[K]	[%]
0.05	350	0.1	0.1	0.02	1.5	0.4	1

It should be noted, that the temperature sensors of the low temperature heat source have been wet installed through drain nozzles, thus the process temperatures could be measured quite accurately. Unfortunately this was not possible at the heating water pipes of the AHP, thus these temperature sensors have been installed on the outside surface of the pipes. Subsequently these piping sections have been well insulated in order to limit the effect of the ambient air temperature. However, the measured temperature possibly deviates from the process temperature, especially at transient operating conditions. Because the temperature difference ($\Delta T_{AHP}=T_{AHP,out}-T_{AHP,in}$) which is relevant for calculation of the capacity can be measured with higher accuracy this difference has been used for uncertainty propagation.

For all data sets of every week the uncertainties of the COP have been calculated acc. to Eq. 9 and Eq.10.

$$u_{COP_{H,AHP}} = \sqrt{\left(\frac{1}{Q_{GAS} + W_{AHP}}\right)^2 \cdot u^2{}_{Q_{AHP}} + \left(\frac{-Q_{AHP}}{(Q_{GAS} + W_{AHP})^2}\right)^2 \cdot u^2{}_{Q_{GAS}} + \left(\frac{-Q_{AHP}}{(Q_{GAS} + W_{AHP})^2}\right)^2 \cdot u^2{}_{W_{AHP}}} \quad (9)$$

$$u_{COP_{C,AHP}} = \sqrt{\left(\frac{1}{Q_{GAS} + W_{AHP}}\right)^2 \cdot u^2{}_{Q_{ESC}} + \left(\frac{-Q_{ESC}}{(Q_{GAS} + W_{AHP})^2}\right)^2 \cdot u^2{}_{Q_{GAS}} + \left(\frac{-Q_{ESC}}{(Q_{GAS} + W_{AHP})^2}\right)^2 \cdot u^2{}_{W_{AHP}}} \quad (10)$$

4 MONITORING RESULTS

The system behavior for heating and domestic hot water preparation is discussed hereafter within the time frame of 07.03.2010 from 4:30 to 10:30 as shown in Figure 4a - 4d.
Figure 4a show the temperatures of the AHP, i.e. heating water and heat source in- and outlet. The temperature levels during domestic hot water preparation and the operation status information of the DHW pump are indicated in section b. The relevant temperature level of the two heat distribution systems (office building and storage depot) are shown in section c, and section d displays the operation status of the two AHP and the mass flow for heating water and heat source of the AHP.

At 4:30 one AHP is in heating operation. The AHP absorbs the heat from the cold water (6 to 2°C) which is the heat carrier from the ground probes to the AHP. The heating water enters the AHP with a temperature of 23°C and is heated up to approx. 35°C (compare Figure 4a). The supply flow temperature of both heat distribution systems is 32°C and the return flow is ca. 27°C for the office building and ca. 20°C for the depot area (compare Figure 4c).

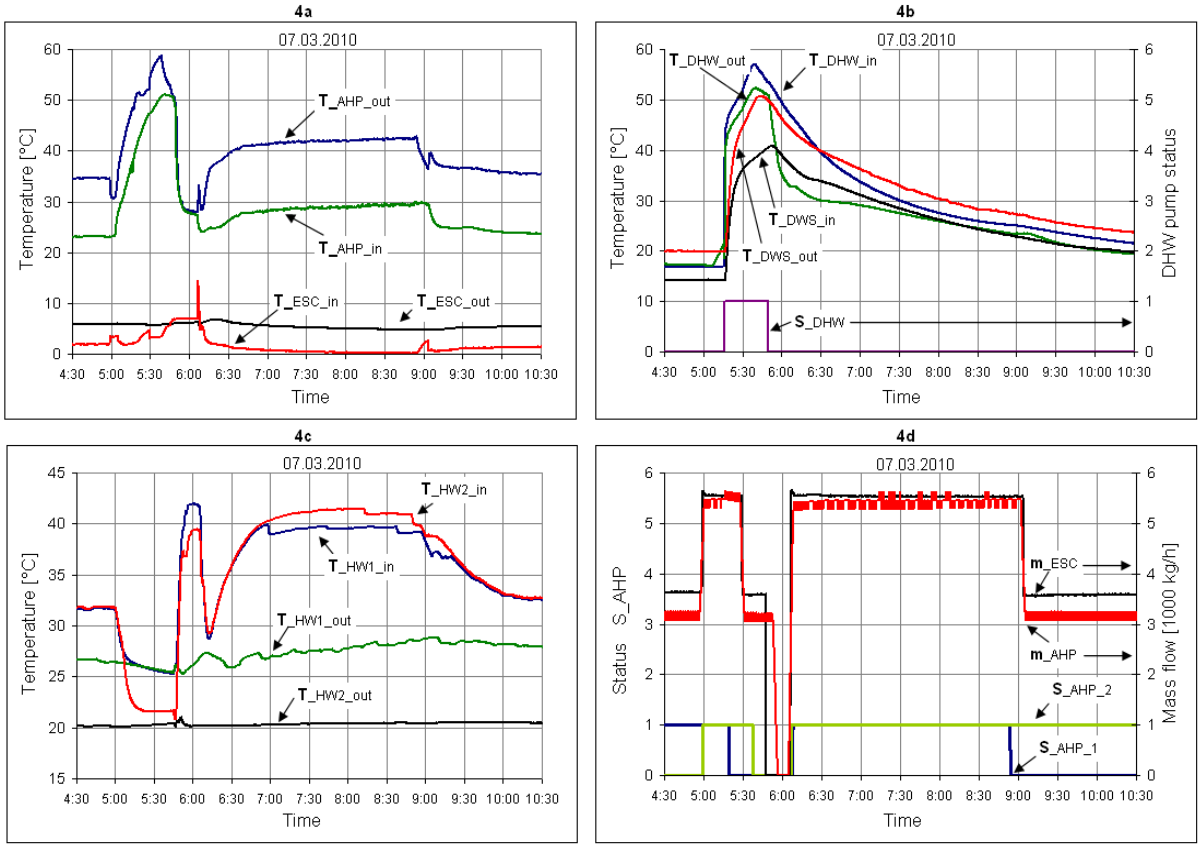

Figure 4: Temperature level, mass flow and operation status information for system operation during space heating and DHW preparation.

At approx. 5 o'clock the control is switched to DHW preparation mode, the second AHP is put into operation (Figure 4d) and the heat distribution for space heating is switched off (Figure 4c). Since the temperature level of the heating water tank rises, at approx. 05:15 the DHW pump is put into operation (Figure 4b) in order to deliver the heat via the heat exchanger to the DHW tank. At ca. 5:20 the first and at ca. 5:37 the second AHP is switched off while the pumps for the heating water and cold water remain in operation for approx. 10 more minutes. The DHW pump stops at 5:50 the heat delivery at a supply temperature to the DHW tank of ca 50°C (Figure 4b) and the space heating distribution systems start operation again at the same time (Figure 4c).

Due to heat supply for space heating without recharging the storage by the AHPs the temperature of the heating water storage tank and consequently the supply temperature for space heating drops (Figure 4c), and because of that at 06:07 both AHPs are put into operation. Then the heating water temperature of the AHP and the space heating distribution system rises to ca. 42°C. At approx. 8:50 AHP_1 is switched off and the supply temperature level drops to ca. 32°C. Subsequently one AHP remains in operation for space heating which was also the starting point of this discussion at 4:30.

As discussed above, the system has been monitored from 28.12.2009 until 03.01.2011 which are 53 weeks of operation. Figure 5 (left) shows the average values of the energy input to the AHP: natural gas (Q_GAS), low temperature heat source (Q_ESC) and electrical energy (including the AHP control, heating water pumps and heat source pumps - W_AHP) for every week. Figure 5 (right) shows the overall energy balance of the monitoring period. The energy consumption of the system ranged from ca. 1 GJ in week 29 where only DHW preparation has been used to nearly 45 GJ in week 51 where the main energy demand was space heating. The yearly energy balance shows a total energy input of 870 GJ (calculated with the upper heating value of natural gas) and a total energy output of 800 GJ. The difference between in- and output amounts to approx. 8.8% of the energy input. Apart from errors of measurement this can be dedicated to different kind of losses, i.e. heat losses, flue gas losses, start/stop losses and stand by losses. These comparably small losses (compared to e.g. 22% reported by Bakker and Sijpheer 2008) may likely be achieved because of the heat exchanger for flue gas condensation combined with the very low return temperature level of the heat distribution system between 18 and 32°C (compare Figure 4c).The electricity demand for the AHP amounts to approx. 3% of the heat output of the AHP which is a reasonable low value.

Figure 6 (left) shows the weekly overall energy balance (energy input - output) for the monitoring period and Figure 6 (right) shows the energy balance of week 29 in detail, subdivided into the different kinds of energy. In winter the energy balances are almost consistent (the deviation is below 10%). During summer the deviation rises up to over 70%, when only DHW preparation is in use as also shown in Figure 6 for week 29. This is because the operation period for DHW preparation is only ca. 40 min with long standby periods and therefore the stand by losses and start/stop losses are large. Especially the electricity demand becomes significant in summer and amounts to approx 21% which can mainly be dedicated to standby losses of the AHP control. However, as already discussed and shown in Figure 5 (right) due to the much higher energy consumption during the heating season the effect of summer operation on the total yearly energy consumption is minor.

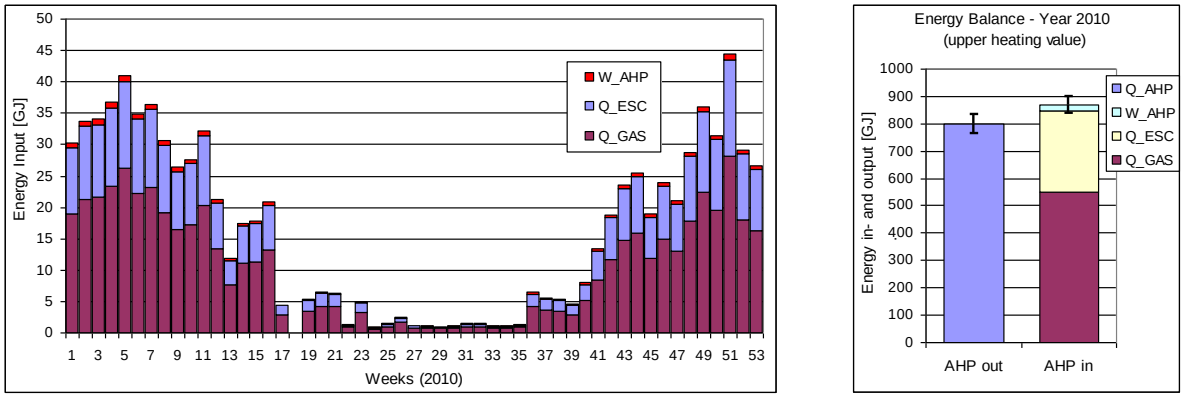

Figure 5: Average weekly energy input to the AHP (left) and energy balance of the AHP (right) for the year 2010

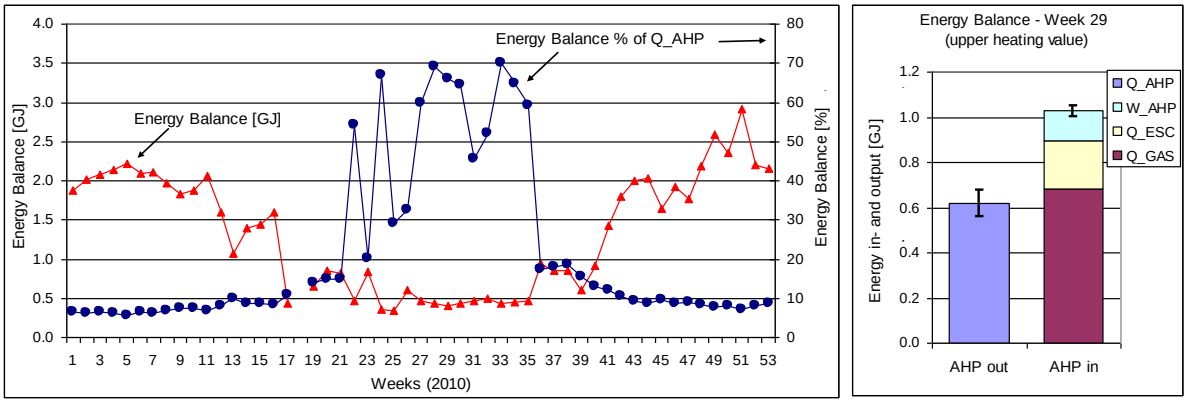

Figure 6: Average weekly energy balance based on upper heating value (input - output) for the year 2010 (left) and energy balance for week 29 - DHW preparation (right)

The average weekly COP for heating (COP_H) and cooling (COP_C) calculated with the lower heating value of the natural gas are shown in Figure 7 (left) where the calculated measurement uncertainties are shown with vertical bars. In winter, when the system is in continuous operation the COP_H is approx. 1.58 and the COP_C ca. 0.59. In summer when the system is mainly in start/stop operation for DHW preparation the COP_H drops to approx. 0.9 and the COP_C to ca. 0.3.

Even though the system is used for heating purpose only the COP_C shall be discussed in order to analyze the heat uptake from the heat source. If only the COP_H is analyzed one could come to the conclusion that the AHP process doesn't work correctly for DHW preparation in summer. The COP_C shows clearly that mainly losses are responsible for the low COP_H because even in summer the AHP absorbs approx. 30% of the energy input from the low temperature energy source.

The right diagram of Figure 7 shows the overall COP values for the year 2010 (which are equal to the yearly seasonal performance factors - SPF) for both calculated with the lower and upper heating value of natural gas. The overall COP for heating was 1.54 based on the lower heating value which is approx. 60% higher compared to a condensing gas boiler with a seasonal performance of 96%. The combined standard uncertainties for the seasonal performance factors for heating have been calculated to approx. ± 5.2% as shown in vertical bars.

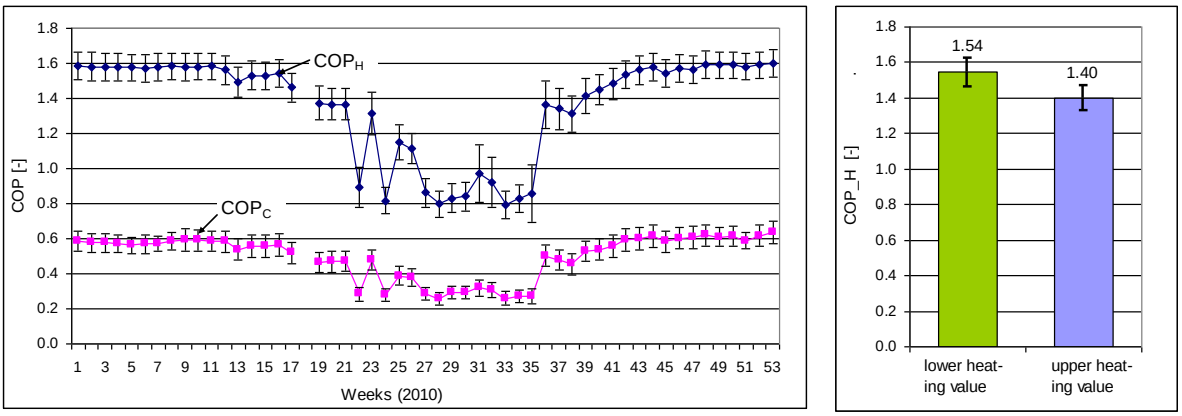

Figure 7: Average weekly COP (lower heating value) for heating and cooling (left) and overall COP for heating for the year 2010 calculated with the lower and upper heating value

5 CONCLUSION

The monitored medium size absorption heat pumping system for space heating and DHW preparation showed reliable operation and high energy performance over the monitoring period of one year. The energy consumption of the system ranged from ca. 1 GJ per week in summer when only DHW preparation has been used to nearly 45 GJ per week in winter when the main energy demand was space heating. In winter the energy balances are almost consistent (deviation below 10%). Apart from errors of measurement this can be dedicated to different kind of losses. The rather small losses in winter may likely be achieved because of the integrated heat exchanger for flue gas condensation combined with the very low return temperature level of the heat distribution system of max. 32°C.

In summer the deviation of the energy balances rises up to over 70%, when only DHW preparation is in use. These high losses are caused by relatively short operation periods for DHW preparation with long standby periods. Especially the electricity demand becomes significant in summer and amounts to approx 21% which can mainly be dedicated to electrical standby losses of the AHP control. However, due to the much higher energy consumption during the heating season the effect of summer operation on the total yearly energy consumption is minor.

Based on the lower heating value of the natural gas the seasonal performance for heating of the year 2010 was ca. 1.54 which is approx. 60% higher compared to a condensing gas boiler with a seasonal performance of 96%.

6 NOMENCLATURE

Symbols

COP	Coefficient of Performance	
c_p	Specific heat capacity	[kJ/(kg K)]
Δp	Pressure difference	[bar]
f	Functional relationship	
Hv	Heating value	[MJ/Nm³]
ρ	Density	[kg/m³]
Kv	Flow coefficient	[m³/h]
m	Mass	[kg]
$\dot{m}$	Mass flow rate	[kg/s]
p	Pressure	[bar]
Q	Thermal heat	[KJ]
$\dot{Q}$	Thermal capacity	[kW]
S	Status	
T	Temperature	[°C]
τ	Measurement interval	[s]
u	Standard uncertainty	
V	Volume	[m³]
$\dot{V}$	Volume flow	[m³/s]
W	Electrical energy	[KJ]
x	Variable x	
y	Variable y	

Subscripts

AHP	Absorption heat pumps
C	Cooling
DHW	Domestic hot water
DWS	Domestic hot water to supply tank
ENV	Environment
ESC	Low temperature energy source
FLG	Flue gas
FRC	Free cooling
GAS	Natural gas
H	Heating
HW1	Heating water distribution office
HW2	Heating water distribution depot
ROM	Room
i	index
in	inlet
out	outlet

7 ACKNOWLEDGMENT

This work has been carried out within the “IEA HPP Annex 34” and has been financed within the framework of the “IEA Forschungskooperation” on behalf of the “Austrian Federal Ministry for Transport, Innovation and Technology”. The authors also wish to thank the companies “Helioplus Energy Systems GmbH”, “Heliotherm Wärmepumpentechnik Ges.m.b.H.” and the “Obermurtaler Brauereigenossenschaft in Murau reg. Gen.m.b.H.” for their support and contributions.

8 REFERENCES

AGGM 2011. “Austrian Gas Grid Management AG“, http://www.aggm.at (14.01.2011, 15:37).

Bakker E. J. and Sijpheer N. C. 2008. “Testing a Prototype Gas-Fired Residential Heat Pump”, *Proc. 9th International IEA Heat Pump Conference*, Zürich, Switzerland.

ISO 1995. “Guide to the Expression of Uncertainty in Measurement”, International Organization for Standardization, first edition 1995.

Ziegler F. 2002. “State of the art in sorption heat pumping and cooling technologies”, *International Journal of Refrigeration*, 25, pp. 450-459.

APPLICATION OF CUSTOMIZED ABSORPTION HEAT PUMPS WITH HEATING CAPACITIES ABOVE 500 kW PROJECT: ACKERMANNBOGEN, MUNICH

Michael Radspieler, Peter Zachmeier, Christian Schweigler, Bavarian Center for Applied Energy Research (ZAE Bayern), Walther-Meißner-Str. 6, D-85748 Garching, Germany
Radspieler@muc.zae-bayern.de

Abstract: A solar heating system was installed at “Ackermannbogen” in Munich, where a residential area was built in 2007. To achieve a solar fraction larger than 50%, a large seasonal storage was installed to store solar surplus during summer and supply solar thermal heat in winter. To decrease the needed volume of this storage an absorption heat pump was installed into the system. This heat pump utilises heat from the storage and is driven by heat from a district heating grid. The low temperature heat is lifted to temperatures useable within the local heating grid to provide heat and domestic hot water to the residential area. Due to the demand on temperature levels of the system a “twin” absorption heat pump - consisting of two separate absorption heat pumps within a single shell - had to be installed for this application. In order to gain maximum benefit of the stored solar thermal energy the system controls change the mode of operation depending on the temperatures of the storage and the return temperature of the solar thermal collectors. The system was monitored and the collected data (capacities and temperatures of the absorption heat pump) of a representative day is shown in this paper.

Key Words: solar heating, seasonal storage, twin absorption heat pump

1 INTRODUCTION

In 2007, apartment houses (320 flats; gross area about 30,000 m²) were built at the Ackermann Street (“Ackermannbogen”) in Munich. Heating of the apartments is realised by radiators and floor heating systems. To realise energy supply with a solar fraction higher than 50% large solar thermal systems (Σ 3,600 m², Figure 1) working with water-glycol supported by seasonal heat storage (5,700 m³) were installed. The seasonal heat storage uses water as medium and is a subsurface, insulated storage.

Figure 1: Picture of a building at Ackermannbogen showing a part of the solar system

A local heating grid, working with water, supplies the generated heat to the apartments. In order to maximise the utilisation of the seasonal heat storage an absorption heat pump (thermally driven heat pump, TDHP) was installed into the system. This TDHP is driven by district hot water and lifts low temperature heat of the storage to temperatures useable for heating purposes and is therefore increasing the energy storage density of the system. The district hot water is used as backup system e.g. due to system breakdown, too. A scheme of the system is shown in Figure 2.

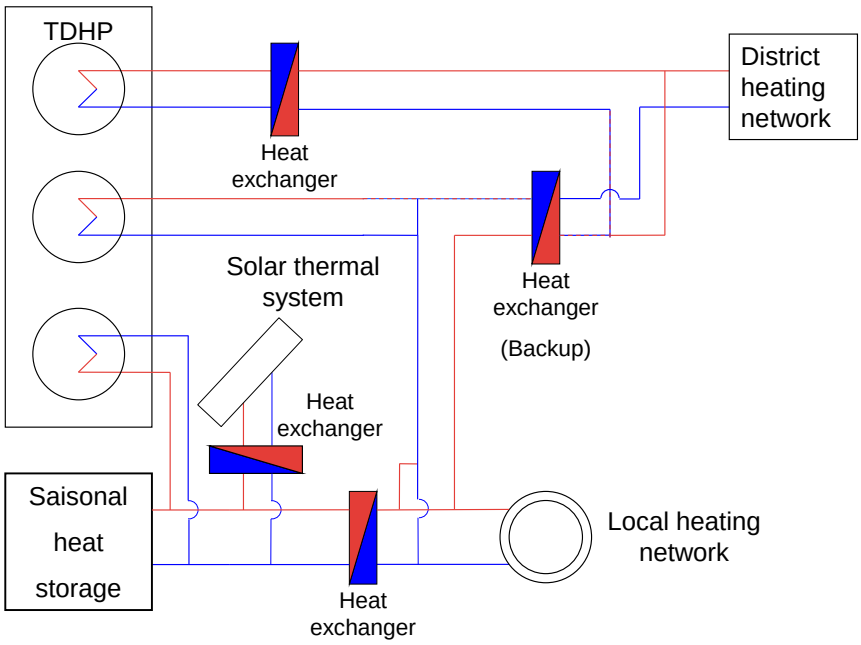

Figure 2: Simplified presentation of the system at Ackermannbogen

2 THERMALLY DRIVEN HEAT PUMP

The plant used at Ackermannbogen is a “twin” absorption heat pump, which is made of two separate heat pumps within a single shell. The external cycles pass serially through the individual components as shown in Figure 3.

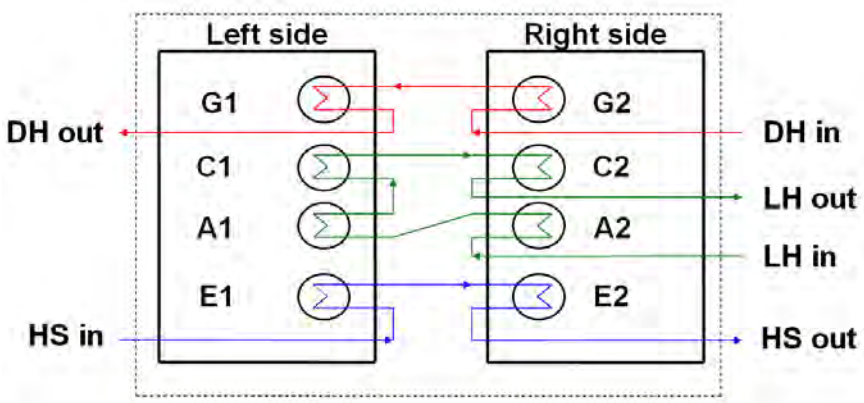

Figure 3: Scheme of the “Twin” TDHP and the external cycles

In this figure the main components of the heat pumps (generator G, condenser C, absorber A and evaporator E) are numbered to distinguish between the two plants. The absorption heat pump (4.6 m x 2.2 m x 3.2 m) is driven by hot water from the district heating network (driving

heat, DH). Depending on the ambient temperature the temperature of the district hot water ranges from 85°C up to 115°C. Low temperature source (heat source, HS) is the seasonal heat storage which is loaded by the solar thermal system. In nominal operation about 230 kW of low temperature heat are drained from the storage. The inlet temperature of the heat source varies between 33-12°C. Nominal heating capacity (local heat, LH) of the heat pump is about 550 kW with in- and outlet temperatures of 30/56°C. Figure 4 shows a picture of the plant.

Figure 4: Picture of the absorption heat pump at Ackermannbogen

The specification of the TDHP, as supplied by the manufacturer (Thermax ltd.) is shown in Table 1.

Table 1: Specification (nominal operation) of the absorption heat pump

	Driving heat (district hot water)			Local heat (residential heating)			Heat source (storage heat)		
Chilling capacity	Inlet temp.	Outlet temp.	flow	Inlet temp.	Outlet temp.	flow	Inlet temp.	Outlet temp.	flow
kW	°C	°C	m³/h	°C	°C	m³/h	°C	°C	m³/h
230	115	85,8	9,5	30	56,2	18	22,2	10	16,21

As shown in Table 1 the temperature spreading of the external circles during nominal conditions is large, especially for the local heat grid. This is the main reason to use a twin absorption heat pump. Figure 5 shows the internal and external temperatures in a Dühring plot as expected at nominal load and temperatures. This diagram shows the vapour-liquid-equilibrium states of water and aqueous lithium bromide solution, which is the working pair the THDP uses for its process, as grey lines.

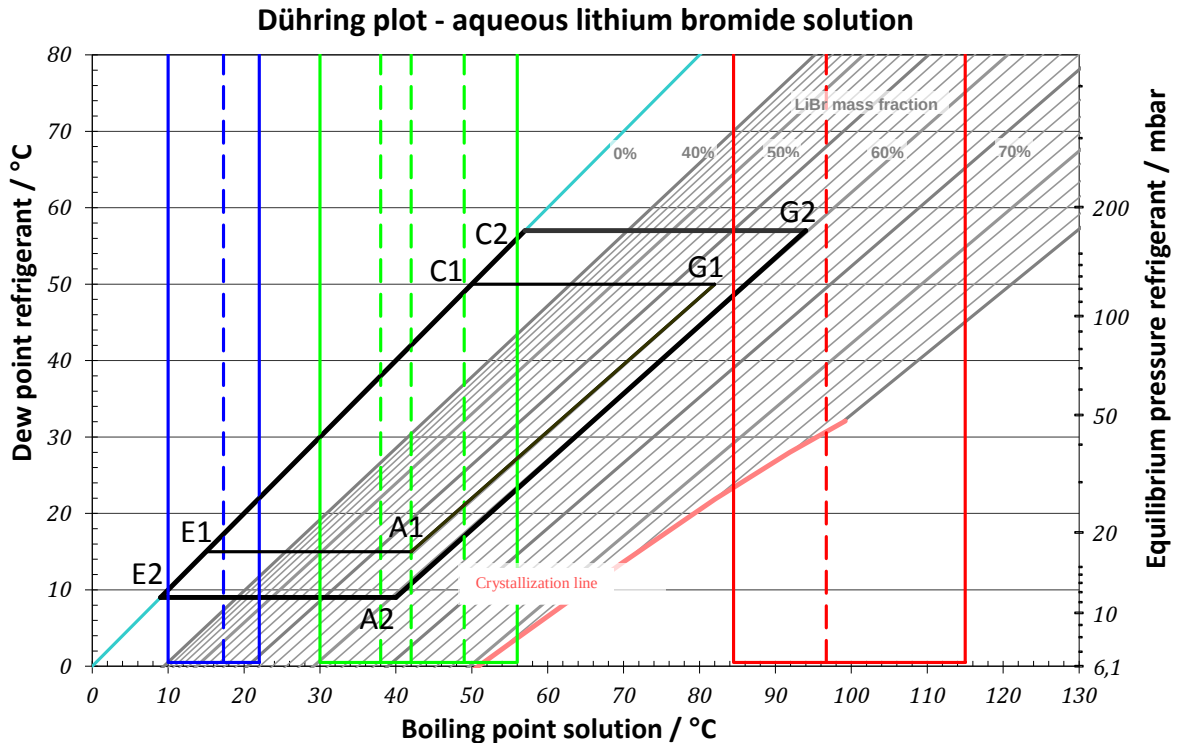

Figure 5: Operating conditions of the absorption heat pump

The thin and bold black lines show the internal state changes of the left and right part of the heat pump, as shown in Figure 5. The change in mass fraction from generator to absorber is neglected in this plot. The coloured upright lines show the temperatures of the external cycles. Dashed lines indicate external temperatures between the different components. It can be seen, a simple single effect absorption heat pump cannot be operated at the demanded external conditions. During winter the stored solar heat is used for space heating and domestic hot water preparation. As soon as the temperature of the storage drops below a certain set point the thermally driven heat pump utilises low temperature heat from the seasonal heat storage. The district heating grid provides additional heat as required.

3 CONTROL STRATEGY

During summer solar heat is used for domestic hot water preparation, the seasonal storage is charged with solar surplus. The heat pump is not in operation during summer time.

There are different operation modes to control the whole system. The system switches automatically between different modes, depending on temperature conditions as shown in Table 2.

Table 2: Operation modes of the system

Mode	Explanation	Required condition
BA 1	District heat only	Supplied temperature to residential buildings < 55°C
BA 2	Storage/ Direct solar	storage Temperature > 65°C Temperature solar > 65°C
BA 3	Storage with district heat	storage Temperature < 65°C
BA 4	Storage with TDHP and district heat	storage Temperature < 40°C
BA 5	TDHP with district heat	storage Temperature < 33°C

Mode BA1 is used as backup only. In case of system failure, maintenance of the system or periods when solar thermal energy (from solar radiation or storage) is not available this mode ensures supply of heat to the housing area.

If the temperature supplied by either the seasonal heat storage or the solar thermal system is higher than 65°C, the heating energy can be provided by the heat storage or the solar thermal system directly. Therefore in Mode BA2 heat for the residential buildings is supplied directly by the storage or the solar system.

As the storage temperature drops below 65°C, the system switches to Mode BA3. During BA3 warm storage water is used to preheat the return of the residential heating, while the district heating maintains the inlet temperature for the residential buildings at an appropriate level.

If the storage temperature drops below 40°C the THDP starts operating. After the preheating by the storage, the THDP lifts heat from additional storage water to further increase temperature of the residential building return. Afterwards, equivalent to mode BA3, the district heating controls the inlet temperature for the residential buildings.

When the storage temperature drops below 33°C, the system switches to mode BA5. The operation is similar to mode BA4, without the preheating by the storage heat.

Any solar heat surplus is stored in the seasonal storage. Due to the temperatures of the storage and the solar system and the low heating demand, the heat pump is not in operation during summer time.

The municipal utilities demand a return temperature of the district hot water below 50°C. Therefore after driving the heat pump the district hot water exchanges heat with the local heating grid. This means even though the heat pump, driven by district hot water, could fully supply the residential area with heat and domestic hot water, an additional fraction of the heat demand has to be provided by the district heating grid.

4 MEASURED DATA

Measured data of the 8th February 2012 will be discussed. Table 3 shows the calculated transferred heat of the system at this day.

Table 3: Measured heat converted by the absorption heat pump on the 8th of February 2012

Driving heat	kWh	5940
Local heat supplied by heat pump	kWh	9280
Heat source TDHP	kWh	3250
COP	-	1.56
Local heat supplied directly by district heat	kWh	4050

It can be seen that only about a quarter of the thermal energy demand is supplied by the solar energy from the storage (heat source THDP). The small solar fraction is caused by the forced heat input from the district hot water to the local heating grid as described above.

Figures 6 and 7 show the capacities and temperatures at the heat pump and the local heating network.

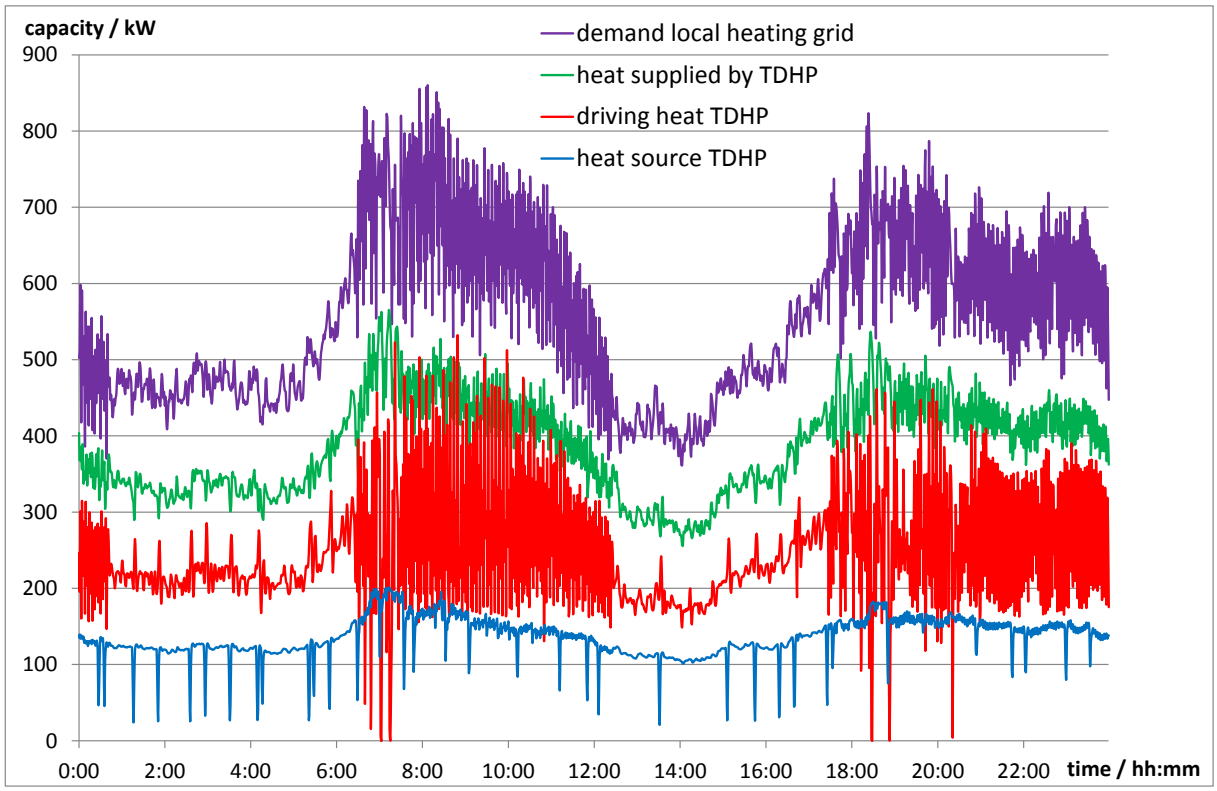

Figure 6: Capacities measured at the TDHP on the 8th Feb 2012

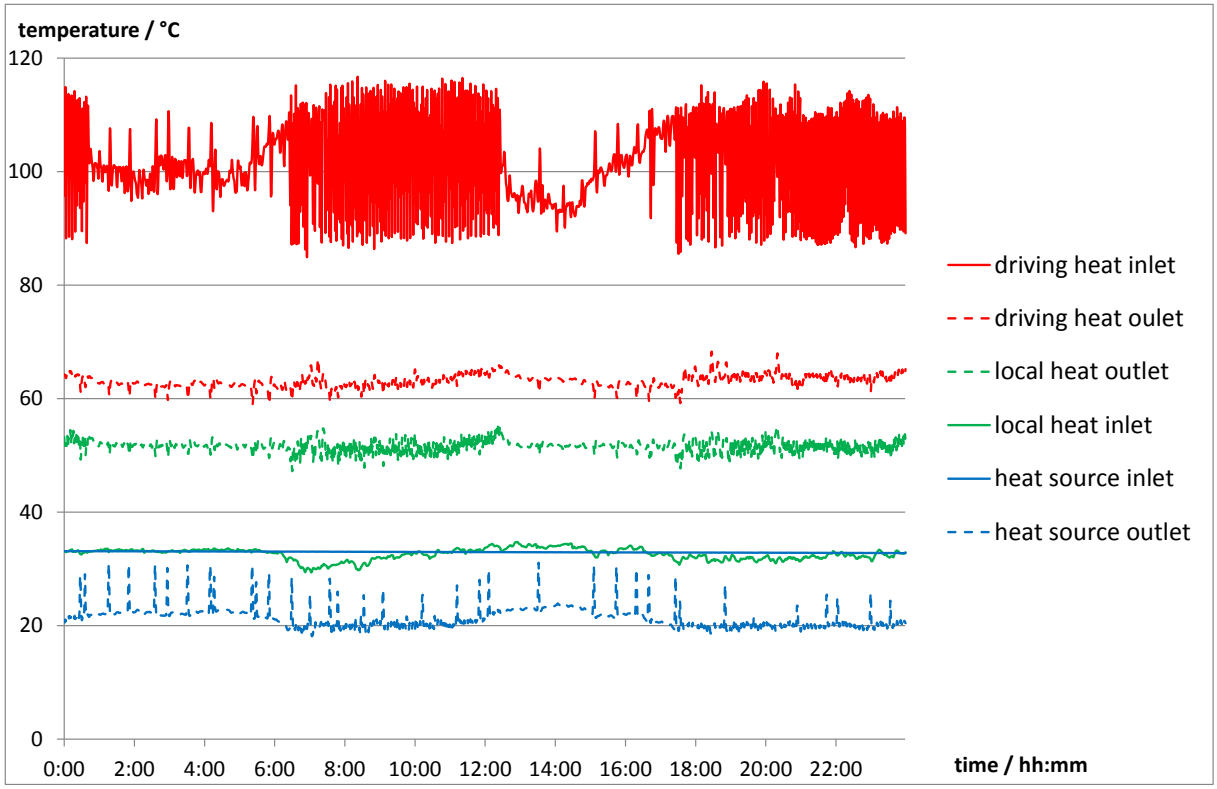

Figure 7: Temperatures measured at the TDHP on the 8th Feb 2012

In Figure 6 the increase of the heating load at morning and evening, the fluctuation of the heat load and the difference between heat demand and useful heat supplied by the heat pump can be seen. The fluctuation of the driving heat capacity is directly caused by the

controls trying to compensate the change of heat load. As the heat pump has a high thermal mass the heat provided to the local grid is more stable. The negative peaks of the heat source capacity are caused by the temperatures at the heat pump which are shown in Figure 7.

As this diagram indicates the temperature supplied by the storage (heat source inlet) and the return temperature of the local heating grid (local heat inlet) at this day have been nearly similar. This caused a very low lithium bromide concentration in the absorber and therefore a low level in the evaporator. The peaks in heat source outlet temperature occur when the level in the evaporator drops below the minimum set point and the internal refrigerant pump stops working to prevent cavitation.

The strong fluctuation in hot water inlet temperature is caused by the controls as the amount of district heating water supplied to the heat pump is controlled with respect to the temperature of the local heating net inlet and the pump circulating the hot water of the heat pump with respect to the outlet temperature of the district heating water. Due to this coupling the fluctuation of the local heating grid can be seen in hot water inlet temperature.

Especially Figure 6 shows an operation of the heat pump at about 300-450 kW heating capacity. Usually the heat pump is not working at more than 30 % part load due to an overestimation of the heat demand of the residential area during the system design. The continuous operation in small part load and the temperatures supplied by the system (causing the refrigerant pump to stop regularly) are the main reasons of the resulting COP of only about 1.55.

5 CONCLUSION

At “Ackermannbogen” in Munich a thermally driven “twin” heat pump has been installed to lift low temperature heat of a seasonal storage to temperatures useable for heating and providing hot water for a residual area. Due to the temperatures provided to the heat pump and the oversize of the heat pump it operates in small part load only, therefore not reaching its nominal COP.

This project has shown a TDHP can be used to increase the energy storage density of a seasonal storage by decreasing the lowest temperature utilisable. This combination of systems can therefore be useful to reach high solar fractions (≥ 50 %). At such complex systems the main issues to take care, besides the design of the main components and their implementation, are the controls and the correct sizing of the whole plant.

APPLICATION OF CUSTOMIZED ABSORPTION HEAT PUMPS WITH HEATING CAPACITIES ABOVE 500 kW PROJECT: VIVO, WARNGAU (NEAR MUNICH)

Peter Zachmeier, Michael Radspieler, Christian Schweigler, Bavarian Center for Applied Energy Research (ZAE Bayern), Walther-Meißner-Str. 6, D-85748 Garching, Germany
Zachmeier@muc.zae-bayern.de

Abstract: In 2005 a gas fired single effect absorption heat pump was installed at the area of VIVO GmbH, who runs a local civic waste collection point. Besides other recyclable materials, biodegradable waste is collected here and composted. During the composting process heat is generated due to aerobic biological processes. As the exhaust air from the rotting heaps has to be cooled down due to process reasons, the heat has to be transferred to an auxiliary medium. Until 2005 the heat was set free to the environment by free air cooling. The thermally driven heat pump instead utilises this heat and supplies heat on a useful temperature level to a local district heating grid. The local district heating grid supplies heat to office buildings of VIVO GmbH as well as to a nearby industrial area. Hence, the heat pump has two beneficial effects on this application, it cools down a process were cooling is needed and uses this energy for fuel saving in a heating grid, which runs basically on oil burners instead.

Key Words: gas-fired single effect, high temperature heat source, district heating

1 INTRODUCTION

The presented application is a communal composting plant in Warngau, about 50 km south of Munich, where bio waste decomposes to humus (see Figure 1). This composting takes place in a big industry hall. The decomposing is an aerobic process. To keep the process running, air is sucked through the bio waste to support the bacteria with oxygen. The exhaust air has a temperature between 30-65°C, depending on the rotting status of the bio waste. As this air has an offensive smell, it can't be blown directly to the atmosphere but has to pass a biological filter first. This filter can't take temperatures above 50°C for a longer time; therefore the air has to be cooled down. Since 2005, instead of cooling down the air and rejecting the heat to the atmosphere, the energy has been used as heat source for a thermally driven heat pump. Therefore the warm rotting air is passing a heat exchanger, where the energy of the air is transferred to a water circuit. A direct fired gas driven heat pump then utilises the energy of the composting air to supply a district heating system. The district heating system supplies nearby commercial buildings with heat. Due to the high temperatures of the heat source, the heat can be efficiently transferred to a temperature level useful for heating. A simplified scheme of the system is shown in Figure 2.

The low temperature heat is lifted from approximately 40°C to 80°C. The district heating system, connected to the heat pump, is the heat sink for the heat pump. How the consumers of the district heating system utilise the heat is unknown. As a backup for the district heating system two oil burners are available. Those burners are also used for medium and peak heat load in the district heating system during winter. Furthermore there is a combined heating and power (CHP) unit which also supplies heat to the district heating system. As the CHP unit is power led, the heat input from the CHP unit is not stable.

In the heat source water loop, a 3 m³ water storage tank is installed to flatten the temperature of the heat source. This is necessary, as the air is sucked intermittently through different parts of the rotting. While in the front part of the rotting the biological waste is very active, in the rear part it is already mainly decomposed and less active. As the air temperature increases with the activity of the rotting, the outlet temperature from the rotting alternates between 30-65°C. The storage is installed parallel in the system air/water heat exchanger and heat pump evaporator as shown in Figure 2.

Figure 1 left: Composting hall, which is used as heat source, the machine hall where the low temperature heat is exchanged from the air to the water of the evaporator circuit and the bio filter in the front of the photo, right: the absorption heat pump

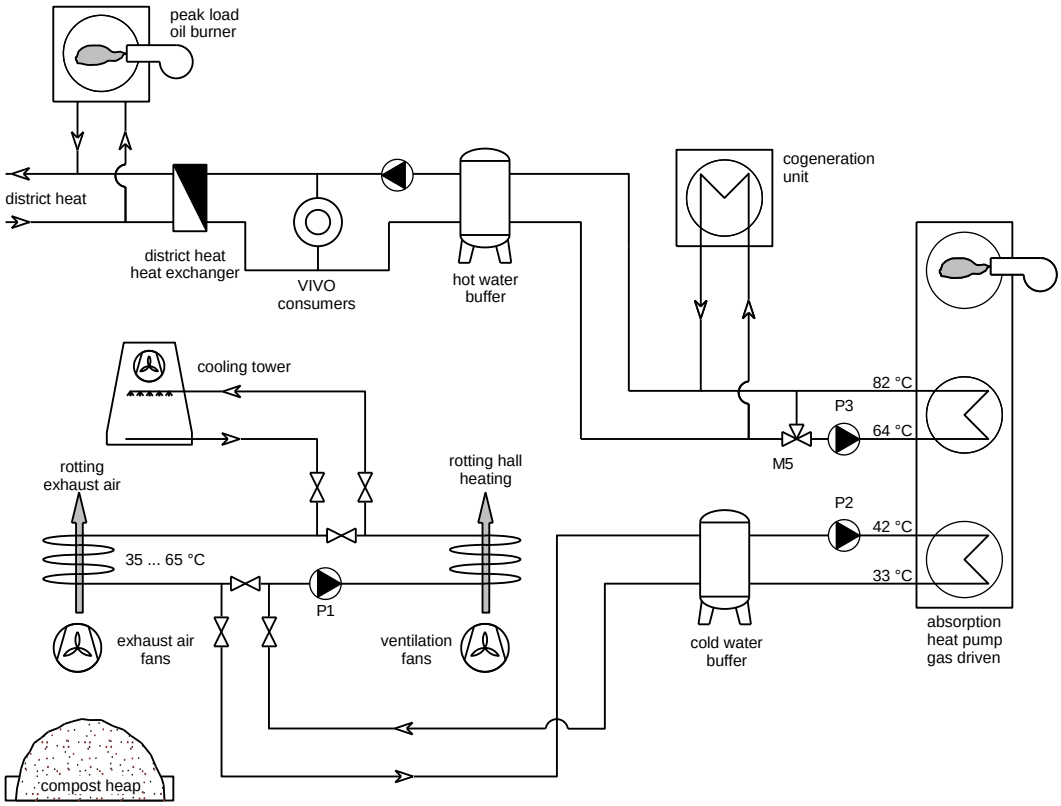

Figure 2: Hydraulic scheme of the system

2 THERMALLY DRIVEN HEAT PUMP

The thermally driven heat pump is manufactured by Thermax Ltd, India (model GHP A417). It is a standard model without special adaption to this plant. The TDHP is a direct gas fired single effect absorption heat pump with 607 kW nominal heating capacity and 240 kW nominal cooling capacity. The TDHP runs on natural gas and is controlled with a modulating burner. The working pair of the TDHP is water and aqueous lithium bromide solution. The refrigerant coming from condenser is cooled by the cooling water in a heat exchanger before entering the evaporator to reduce the flash losses.

The power of the TDHP is adjusted to the water temperature in the cold water storage, to keep this temperature in a defined range. While in operation the TDHP power is normally limited by the power of heat source, as the grid load is higher than the heat provided by CHP and the heat pump.

The nominal operation conditions of the TDHP are listed in Table 1.

Table 1: Nominal specification of the TDHP

	Heat source	Heat rejection	Driving heat
Temperature [°C]	42 - 33	64 - 82	-
Capacity [kW]	240	607	425

The capacity of the gas burner is higher than necessary to operate the TDHP in full load, but as the gas burner is capable to reduce the power down to 40% it fits and can reduce the power of the absorption heat pump down to about 50% cooling part load.

As the internal temperature lift is about 50 K and the heat rejection temperature is at about 80°C, the generator is working on temperatures of about 140°C. This leads to a high corrosion potential.

3 CONTROL STRATEGIES

The capacity of the low temperature heat source is fluctuating and depends on the filling of the heaps and the age of the biological waste. Due to the varying heat source, the power of the TDHP has to be controlled to avoid cooling down the heat source water to much. The temperature of the cold water storage tank is the control variable to increase or decrease the power of the TDHP. It has to be kept within a specified range. Furthermore, the TDHP controls the cooling water inlet temperature by a mixing valve to keep the cooling circuit in its specified range. As the heating demand decreases with higher ambient temperatures, the TDHP is shut down when the district heating grid load is too low. As free cooling of the waste heat is cheaper than operating a gas fired absorption chiller, the TDHP is not operating during summer period.

The basic decision, when to start the operation of the TDHP is made by the technical operators. Also shutdowns or restarts after unscheduled shutdowns are executed by the operation staff. To avoid problems in the district heating system the TDHP is restricted just to be started if the heat demand in the grid is high enough to absorb the heat produced by the TDHP.

4 MONITORING DATA

The measurement data of the 29th January 2007 are discussed in the following passage. The performance and abnormality are also checked and explained.

Table 2 shows the energy balance for the mentioned day. The COP is smaller than expected due to many start-stop cycles of the TDHP. A typical behaviour of the absorption heat pump is shown in Figure 3.

Table 2: Energy balance and performance on 29th January 2007

Energy input cold water [kWh]	Energy output cooling water [kWh]	COP [-]
2448	7560	1.48

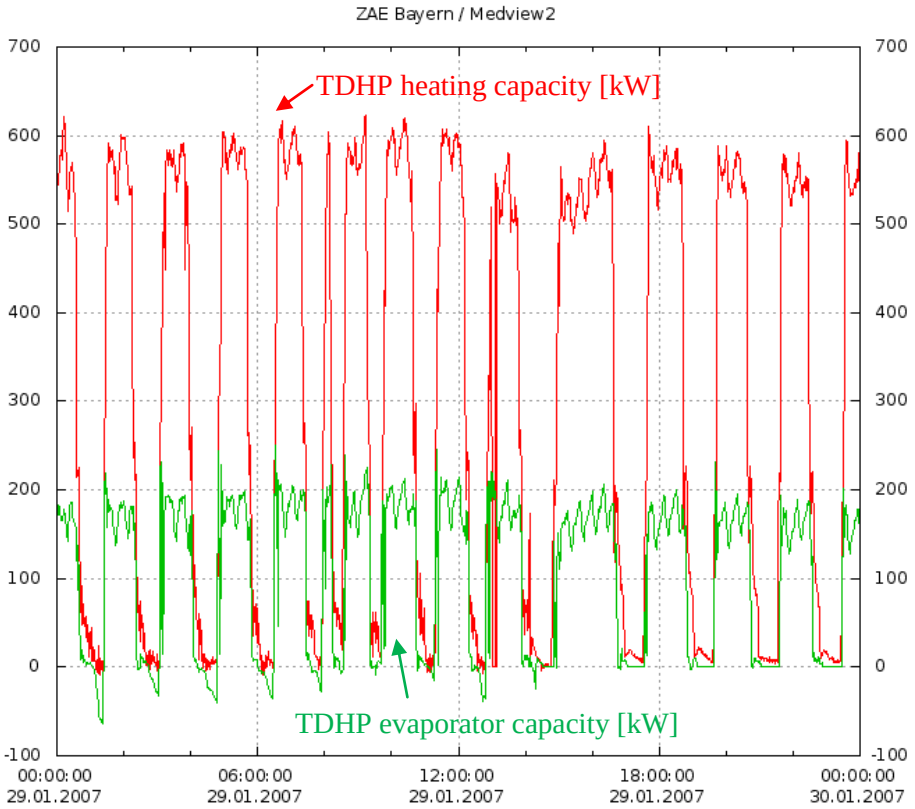

Figure 3 - Heat input and output of the TDHP

The chilled water temperature was always above 42°C (see Figure 4) on this day but the machine shuts down 14 times. The absorption heat pumps external parameters allowed operation in full load most of the time. As the gas burner is running on full load - which is a higher power than the TDHP requires- the concentration of the aqueous lithium bromide solution increased until a safety measure shuts down the TDHP. A shut down could also have been caused if the heat storage in the cool water loop was to warm, what leads to a loss of the external demand for the TDHP. Before this happens the power of the TDHP should be reduced. Although the natural gas burner was able to modulate its power according to the TDHP demands, the modulation was not noticeable because of an error in the communication between THDP and burner. As this was not fixed, neither by the operator nor the manufacturer, the TDHP was operating either in full load or not at all. This led to many dilution cycles with the typical losses. Those losses also decreased the seasonal performance.

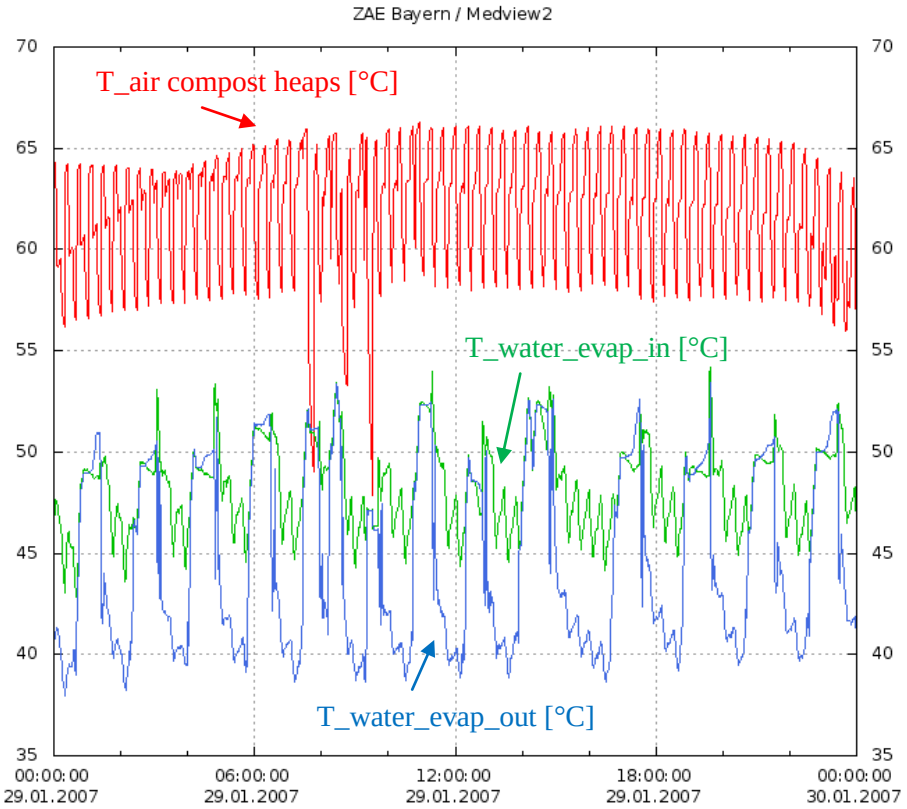

Figure 4 - Temperatures heat source

Figure 4 shows the temperatures of the heat source. In the beginning of the conversion path there is the air temperature from the compost heaps. It is the highest temperature and it alternates between 55-65°C. This is due to the air suction system, because compost heaps from different ages get ventilated one by one and the older the heaps are, the less heat is produced. After the warm air passed the air/water heat exchanger, the pulsation of the temperature signal can be found in the water. The heated water passes the cold storage and flows to the evaporator inlet, where the fluctuation can still be found although in a lower amplitude and frequency due to the cold water storage. The unsteady heat source temperature is one of the reasons why the TDHP is rarely operated in steady state condition. Especially when the compost is producing less heat than absorbed by the TDHP the cold water temperature drops because the modulation of the gas burner does not work. This enforces the machine to switch on and off more often. Low temperatures are the result of less biological activity or empty compost heaps. Those events are seen cumulative on weekends or holidays. If the TDHP didn't restart automatically on holidays and when no operators were around, it could cool down the whole TDHP to temperatures that lead to the risk of crystallization.

5 CONCLUSION

On the local civic waste collection point of VIVO GmbH a direct gas fired TDHP was installed. The TDHP had two beneficial effects. On the one hand, it provided cold for a composting process and on the other hand it supported a district heating system with heat. By delivering heat to a district heating system the fuel consumption of conventional oil burners, which are the main heat producers, is reduced.

The composting process has a high dynamic in heat production which is flattened by storage water tanks. The TDHP is supposed to follow the available heat by adapting its power

according to temperatures in the cold water loop. Due to problems in the communication between TDHP and gas burner the power of the absorption heat pump was not reduced automatically. This led to a cycle operation of the TDHP and caused typical dilution losses. Therefore the measured COP of the THDP was lower than dimensioned. Nevertheless it was in the range of 1.3 – 1.5 which is a considerable improvement compared to a normal fuel burner. This is even more true as in this application the heat from the TDHP is replacing heat from an oil burner.

SOLAR COOLING - STATE OF THE ART OF SOLAR THERMALLY DRIVEN HEAT PUMPS FOR COOLING

Dr. Uli Jakob, Green Chiller Association for Sorption Cooling e.V.
Solem Consulting, Postfach 2127, D-71370 Weinstadt, Germany
uli.jakob@solem-consulting.com

Abstract: An attractive alternative to conventional electricity driven cooling systems is solar cooling, which combines thermally driven heat pumps/chillers with solar thermal collectors. Solar cooling is especially interesting if the solar thermal system is also used for other applications such as heating, hot water, etc. Thus, maximum operation time and low-cost driving heat for sorption chillers are the key for economic efficiency of solar cooling systems. Several small and medium-scale sorption chillers are developed in the last few years, some of them especially for solar cooling applications. Today about 1,000 solar cooling systems are installed worldwide, where the market has grown in the last 8 years between 40 and 70% per year.

Key Words: Solar Cooling, thermally driven heat pumps, absorption, adsorption

1 INTRODUCTION

Worldwide, the energy consumption required for cold and air conditioning is rising rapidly. Usual electrically driven compressor chillers (split units) have maximum energy consumption in peak-load periods during the summer. In the last few years in Southern Europe this has regularly led to grids working to maximum capacity and blackouts. Particularly in recent years, the sale figures of split units with a cooling capacity range up to 5 kW have risen rapidly. The Japan Refrigeration and Air Conditioning Industry Association (JRAIA) has estimated worldwide sales of 94.5 million units in 2011 (JARN 2011). In Europe, the number of units sold per year has risen about 235% from 2.8 million in 2002 to predicted 6.6 million in 2011.

Conventional split-units have a high-energy consumption and using non-environmentally friendly refrigerants. The refrigerants that are currently used in the split-units no longer have an ozone depletion potential (ODP), but they have a considerable global warming potential (GWP), because of leakages of the split units in the area of 5 to 15% per year.

Against it, sorption chillers use environmentally friendly refrigerants (water or ammonia) and have only very low electricity demand. Therefore the operating costs of these chillers are very low and the CO_2 balance compared to compressor chillers is considerably better. In case of solar cooling the main advantage is the coincidence of solar irradiation and cooling demand.

In general, the solar thermally driven cooling processes can be divided into two main groups: Closed systems for cold water generation (absorption and adsorption) and open systems for air-conditioning (DEC and liquid sorption systems).

2 HISTORY

The world first solar cooling system was running in Paris, France (Figure 1) during the world exhibition 1878 (Mouchot 1987). This system has consisted of an ammonia/water absorption chiller and a parabolic reflector to produce ice.

The first commercial solar cooling systems for air-conditioning were developed in Europe and the USA one hundred years later in the 1970s, e.g. by the companies Dornier-Prinz Solartechnik, Germany, Arkla Industries (today Robur, Italy) and Carrier, both from USA. These systems have been realized in several demonstration projects. Due to the lack of demand on the market for solar cooling during this time, the production of these solar cooling systems was stopped in the late 1980s (Grossman 2002). In the 1990s companies like Yazaki, Japan and Thermolux, Germany have realized only a few costume-made solar cooling systems. After the year 2000 the first solar cooling system suppliers have started again the solar cooling business like CitrinSolar, Conergy, SolarNext all from Germany and SOLID, Sol-ution both from Austria. Some of these companies have already stopped again their activities.

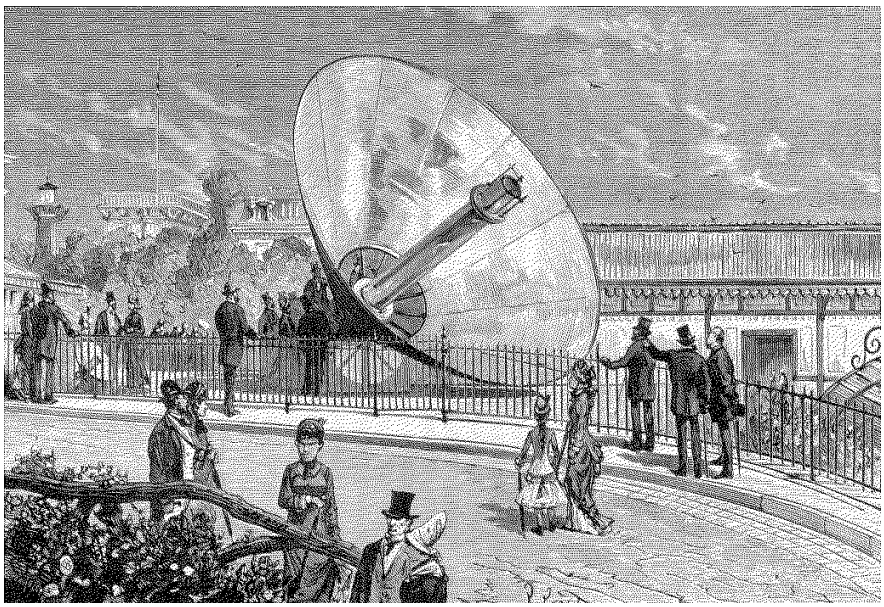

Figure 1: World exhibition 1878, Paris: Augustin Mouchot produced the first ice block through solar energy (Source: Olynthus Verlag)

3 MARKET READY SOLAR COOLING KITS

Medium and large-scale sorption chillers with cooling capacities above 35 kW are available since several years. Today these chillers are mainly manufactured in China, India, Japan and South Korea and used for costume-made solar cooling systems.

In contrast new small and medium-scale sorption chillers were developed in the last 5 to 10 years, which are used for standardized solar cooling kits. These absorption chillers have cooling capacities from 10 kW to 500 kW (working pair water/lithium bromide or ammonia/ water) produced by companies like EAW, Jiangsu Huineng, Sakura, Thermax, Yazaki, AGO, Pink and Tranter Solarice. The market available adsorption chillers have capacities from 8 kW to 370 kW (working pair water/silica gel or water/zeolite) produced by companies like SorTech, Shuangliang, InvenSor, Mayekawa and Mitsubishi Plastics. According to the latest figures from the year 2009, the market shares of various solar cooling technologies are as follows: approximately 71% absorption chillers, adsorption chillers 13%, 14% and 2% DEC systems and liquid sorption systems (Mugnier 2010), as shown in Figure 2.

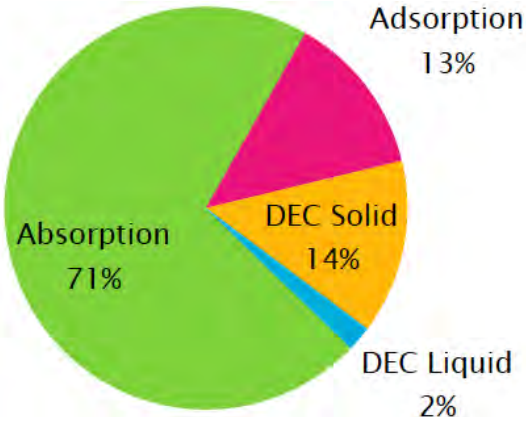

Figure 2: Market shares of solar driven sorption technologies in 2009 (Source: Tecsol)

For the simplification of the installation of solar cooling systems companies like Jiangsu Huineng from China offer an integrated absorption system, which is a combination of water/lithium bromide absorption chiller, wet cooling tower and pumps in one enclosure. InvenSor from Germany has developed a water/zeolite adsorption chiller with an integrated chilling station, which makes the installation essentially comes down to the pipework systems, as the necessary pumps, mixers and valves are already integrated into the machine (Figure 3).

Figure 3: 10 kW water/zeolite adsorption chiller with integrated chilling station and integrated absorption system with 23 kW water/lithium bromide absorption chiller and wet cooling tower (Sources: InvenSor [left], Jiangsu Huineng [right])

During the last few years, a few companies in the solar business have positioned themselves on the market as complete system providers for solar cooling. In the small and medium-scale capacity range up to 200 kW, the companies SolarNext (8-175 kW), Schüco (15 and 30 kW), Kloben (17.5-105 kW), Sol-ution (8-54 kW) and Jiangsu Huineng New Energy Technology (11-175 kW) are active. Their solar cooling systems basically contain solar thermal collectors and support structure, hot water storage tank, pump-sets, a sorption chiller, a heat rejection unit, sometimes cold water storage and a system controller. Figure 4 shows two examples of such solar cooling kits, which can be supplemented by cold storage package, cold distribution package, etc.

New system suppliers are also large companies such as Thermax (India) and Hitachi (Japan), both using in-house developed concentrating collectors, which are offered together with absorption chillers as solar cooling kit (Malaviya and Epp 2011; Augsten and Epp 2011).

Figure 4: Solar cooling kits (Sources: SolarNext [left], Schüco [right])

For solar cooling kits, the average value of specific collector surface of all market available kits is 4.2 m^2/kW cooling capacity (Epp 2009). SolarNext recommends collector areas with 4.5 m^2/kW and Schüco recommends the smallest areas with 3.2 m^2/kW. The average value of all installed small to large-scale solar cooling systems in Europe until the year 2006 was 3.0 m^2/kW (Henning 2007).

An all-season use of renewable energy sources for domestic hot water, space heating and solar cooling is advantageous. As a rule of thumb, the solar fraction for the solar cooling kit should be greater than 70%.

4 SOLAR COOLING MARKET

Today about 1,000 solar cooling systems were installed (Jakob 2012), where the market has grown in the last 8 years between 40 and 70% per year (Figure 5). The total number of installations shows that the solar cooling market is still a niche market, which is under development.

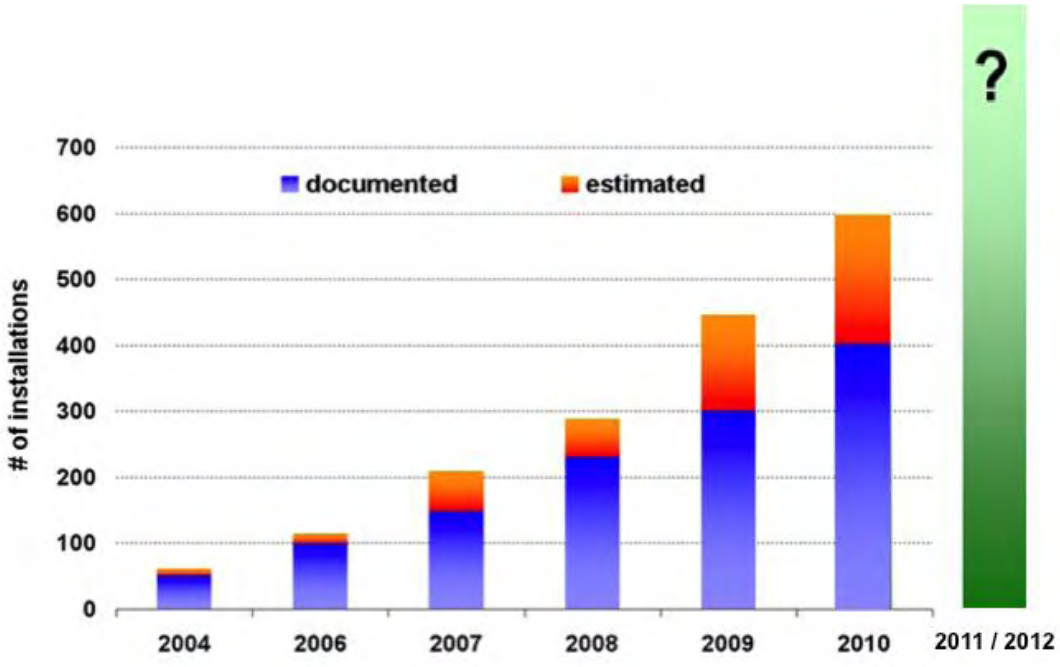

Figure 5: Market development of small to large-scale solar cooling systems worldwide (Source: Tecsol, Solem Consulting)

So far, according to a survey from the year 2009, most solar cooling systems are installed today in Spain (42%), Germany (17%) and Italy (10%) (Sparber and Napolitano 2010). Until 2004, the top three solar cooling markets were Germany (39%), Spain (28%) and Greece (9%) (Henning 2007). The picture has changed, because of many new small-scale installations in Spain during the last few years.

5 SYSTEM COSTS AND ECONOMICS

Today, solar cooling systems are often not yet economically viable. The solar thermal system is usually the largest cost factor, the operating and maintenance costs of the sorption chillers are lower than conventional systems, the investment costs due to the small numbers even higher. Is actively cooled, then long running hours of the sorption chiller are crucial for the efficiency of solar cooling. While in the residential sector in Central Europe only about 50 to 200 cooling hours occur, in the southern Mediterranean around 1,000 full load hours are required.

The specific investment costs of solar cooling in the power range of 8 to 175 kW cooling capacity (no installation cost and cold distribution included) are currently between 4,500 EUR/kW for small-scale kits and 2,250 EUR/kW for medium-/ large-scale kits (SolarNext 2012). Today, the cost share for the solar thermal collectors is about 45% to 65% of the total investment costs for the small-scale and medium-/ large-scale capacity range, respectively. Since 2007, a cost reduction of about 50% was realized within the last six years, because of the further standardization of the solar cooling kits (Jakob 2012), as shown in Figure 6.

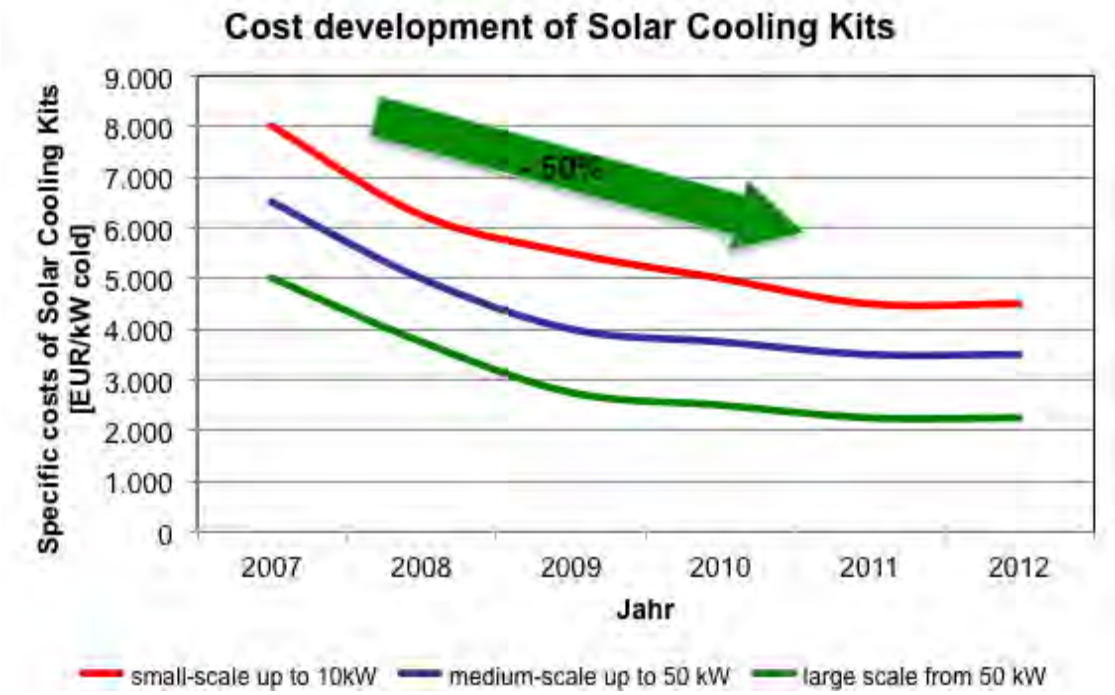

Figure 6: Specific total costs of solar cooling kits (Source: Solem Consulting / SolarNext)

Basically, in Europe at large solar cooling systems, e.g. possible today for administrative buildings, a ROI (Return on Investment) of about 10-15 years, in some cases with high electricity costs or long operating times even under 10 years is possible. For solar cooling kits for residential buildings or small offices, the ROI is depending on the boundary conditions between 12 and 18 years. The analysis of a solar cooling kit implemented in a single family house in Germany with 7.5 kW cooling capacity shows that the specific net cost including cold distribution are about 6,900 EUR/kW (Jakob 2009).

6 GREEN CHILLER

The increased interest in the technology also becomes apparent that more and more system suppliers to position themselves with solar cooling kits on the market and these are not just companies in the solar industry. That the industry is trying to organize could be shown that in March 2009, the Green Chiller - Association for Sorption Cooling e.V. was founded in Berlin. The objective of the association is the promotion and development of solar cooling and the thermal cooling market in Europe (Figure 7). The association brings together about 60% of all European manufacturers of sorption chillers in the small and medium cooling capacity range.

Figure 7: Website of Green Chiller Association (Source: Green Chiller)

During 2006 and 2012, the Green Chiller members have produced and commissioned together about 630 absorption and adsorption chillers with an accumulated cooling capacity of 18.8 MW. About 34% of these chillers are used for solar cooling systems and 44% for CHPC systems. The rest is installed in district heating networks (8%) or is using waste heat e.g. from industrial processes (14%).

7 CONCLUSION

Active air-conditioning of buildings is necessary, if high internal and external loads cannot be removed by efficient night ventilation. Therefore, thermally driven sorption chillers can often provide an environmentally sound alternative to electricity driven technologies. This is because sorption chillers use environmentally friendly refrigerants (water or ammonia) and they have a very low electricity demand for the chiller itself.

In the small and medium-scale cooling capacity range up to 500 kW several novel single-effect water/lithium bromide and ammonia/water absorption chillers as well as water/zeolite and water/silica gel adsorption chillers are now available on the market. The market potential for solar cooling is very large, so that different companies have developed complete solar cooling kits (sorption chiller, heat rejection, etc.) for the product business. Solar cooling is especially interesting if the solar thermal system is also used for other applications such as

heating, hot water, etc. Thus, maximum operation time and low-cost driving heat for sorption chillers are the key for economic efficiency of solar cooling systems. Other heat sources like district heat is particularly of interest if cheap excess heat in summertime is used for decentralized sorption cooling systems. Furthermore, if waste heat from a cogeneration unit (CHP unit) is used for sorption cooling, then this leads to longer operating times and increased electricity production of the cogeneration unit itself.

The Green Chiller – Association for Sorption Cooling e.V. is helping to develop and promote the solar cooling and thermal cooling markets in Europe to get solar cooling out of its niche existence.

8 REFERENCES

Augsten E., B. Epp 2011. “Solar Cooling Market to experience big Changes”, Global Solar Thermal Energy Council, www.solarthermalworld.org, 18.07.2011.

Epp B. 2009. “Solar Cooling Kits for Europe”, Global Solar Thermal Energy Council, www.solarthermalworld.org, 05.01.2009.

Grossman G. 2002. “Solar-powered systems for cooling, dehumidification and air-conditioning”, *Solar Energy*, Vol. 72, No. 1, pp. 53-62.

Henning H.M. 2007. “Overview on solar cooling”, *Proc. of the 3rd European Solar Thermal Energy Conference – estec, 19-20 June 2007*, Freiburg, Germany.

Jakob U. 2009. „Solar Cooling in Europe”, *Proc. of the ausSCIG Conference, 19 May 2009, CSIRO*, Newcastle, Australia.

Jakob U. 2012. “Marktentwicklung und Rahmenbedingungen thermisch angetriebener Kältetechnik und solarer Kühlung, *Proc. of the BMU Statusworkshop Solare Kühlung, 06.11.2012*, Berlin, Germany.

JARN 2011. “World Air Conditioner Market: The 2010 Overview”, JARN, Serial No. 508-S, pp. 49-62.

Malaviya J., B. Epp 2011. “India - Innovative Solar Cooling System at Solar Energy Centre”, Global Solar Thermal Energy Council, www.solarthermalworld.org, 10.08.2011.

Mouchot A. 1987. “Die Sonnenwärme und ihre industriellen Anwendungen“, Olynthus-Verlag.

Mugnier D. 2010. “Solar Cooling Economics”, *Proc. of the Task 38 Solar Air-Conditioning and Refrigeration Workshop – AHR Expo, 27 January 2010*, Orlando, Florida, USA.

SolarNext 2012. “chilli® Prices 2012”, price list SolarNext, May 2012.

Sparber W., A. Napolitano 2010. “Review on existing solar assisted heating and cooling installations”, *Proc. of the Task 38 Solar Air-Conditioning and Refrigeration Workshop – AHR Expo, 27 January 2010*, Orlando, Florida, USA.

DEVELOPMENT OF AN INNOVATIVE 2.5 kW WATER-SILICA GEL ADSORPTION CHILLER

Ernst-Jan Bakker, Robert de Boer, Simon Smeding, Niels Sijpheer, Michel van der Pal
Energy research Centre of the Netherlands, PO Box 1, 1755 ZG, Petten, The Netherlands
r.deboer@ecn.nl

Abstract: Besides (better) utilization of available solar heat or waste heat, and thereby reduction of fossil fuel consumption, sorption cooling offers several other advantages compared to conventional compression cooling. Such as reduction of summer peaks in the electricity grid, use of natural refrigerants, and low noise & maintenance. Sorption cooling in itself is not a new development. However, the development of small scale sorption chillers (2-20 kW) is new. This development allows sorption cooling to enter the markets for individual homes, small collective systems and small commercial applications. A second trend is gradual reduction of the driving temperatures of the sorption cycles allowing more solar and waste heat to be used. This article describes the design and performance of a new, innovative 2.5 kW adsorption chiller, developed by ECN.
This system was built and tests have been performed in a laboratory and in one of ECN's full-scale research houses.

Key Words: adsorption chiller, silica gel, prototype, performance

1 INTRODUCTION

Triggered by the potential of waste heat (e.g. from industry) and renewable heat (e.g. from the sun), the Energy research Centre of the Netherlands (ECN) initiated development of sorption cooling technology several years ago. Recent work was done within the framework of the European (FP6) PolySMART project (www.polysmart.org).

Water-silica gel was chosen as a working pair for the cooling machine: a choice that has proven to be successful so far. Compared to conventional compression cooling, thermally driven cooling (TDC) offers several advantages, e.g.:

- Using heat instead of electricity reduces peaks on the electricity grids
- Using renewable heat reduces carbon emissions.
- Many sorption cycles are based on natural refrigerants.
- TDC's have low noise levels and low maintenance and installation requirements.

Just like a conventional compression chiller, an adsorption chiller uses a cycle where a refrigerant condenses at high pressure/temperature and evaporates at low pressure/ temperature. However, this cycle is not driven by a mechanical compressor but uses thermal compression, based on the sorption reaction of silica gel and water, using heat as the driving force. Dry silica gel (a porous, glass-like solid) attracts and adsorbs water vapour until it is saturated, and must then be regenerated. Heating the silica gel releases the water vapour at a pressure that allows it to condense at ambient temperatures, after which the cycle of adsorption and de-sorption can be repeated. This cycle is not unlike absorption cycles (with e.g. LiBr-solution), there are two important differences:

1. The silica gel can be regenerated efficiently at lower driving temperatures
2. The silica gel is a solid that cannot be pumped from generator to absorber

The silica gel is applied to the surfaces of heat exchangers, which are supplied intermittently with hot and cooling water. The adsorption cycle is therefore a batch process, and for quasi-

continuous cooling at least two silica gel beds (reactors) are needed, operating in counter-phase. A schematic system lay-out of an adsorption chiller is shown in Figure 1.

The lowest possible chilled water temperature of this adsorption cycle is about 4°C, making it perfectly suited for air-conditioning and chilled water systems in the built environment and in industry.

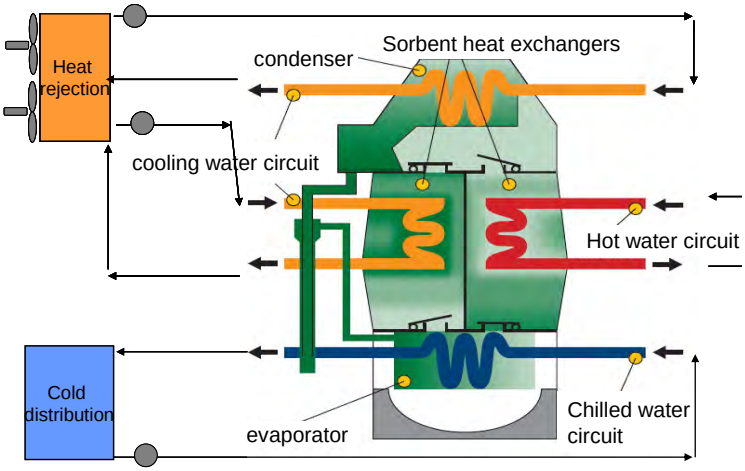

Figure 1: Schematic adsorption chiller lay-out

2 DESIGN AND CONSTRUCTION OF THE 2.5 kW ADSORPTION CHILLER

As part of the European PolySMART project (www.polysmart.org), ECN has developed a small-scale adsorption chiller using water-silica gel as working pair, which is tested and demonstrated. The starting point for this chiller is to supply sufficient cooling power (2.5 kW) for a modern single-family house. A common (challenging!) standard for household appliances is used to determine the physical size limits: a 60 x 60 cm footprint, and a height of about 100 cm.

Compact light-weight aluminium heat exchangers from the automotive industry have been used to carry the silica gel, creating a large surface while maintaining low weight and volume. For the same reason, this type of heat exchanger has also been used for the condenser and for the evaporator. Figure 2 shows the layout of the new chiller: the evaporator at the bottom, two silica gel reactors above the evaporator, and the condenser on top.

Water vapor flows at low pressure from the evaporator (creating a cooling effect) and is adsorbed in one of the two silica gel reactors (adsorption phase). At the same time, water vapor flows from the other reactor to the condenser (desorption phase) at a higher pressure. Special check valves have been placed between these components to prevent the water vapor from flowing back. This (low pressure) process requires that the system does not contain any gases or vapors other than water vapor, and that all components are hermetically sealed. The water from the condenser flows back to the evaporator via a condensate return line. The flow for heating and cooling of the silica gel is controlled by eight valves, which intermittently supply both reactors. A PLC unit is included in the chiller to control these valves and to monitor temperatures and pressures.

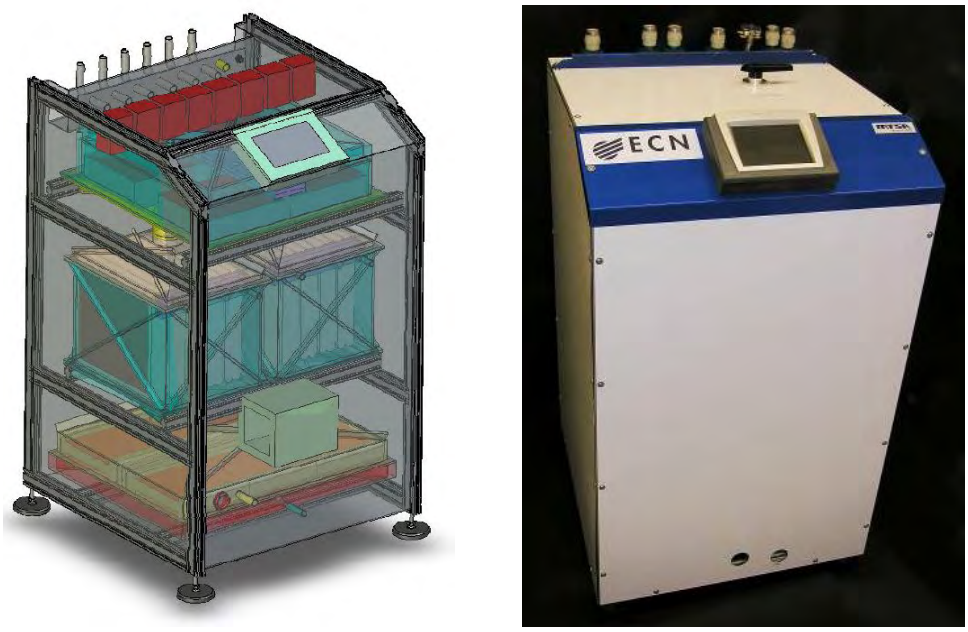

Figure 2: Design drawing and picture of the ECN 2.5 kW adsorption chiller

3 PERFORMANCE MEASUREMENTS

The performance of the chiller was first determined in the laboratory and afterwards in a micro-trigeneration setup in one of ECN's research dwellings.

3.1 Laboratory measurements

The prototype adsorption chiller has been tested in an ECN laboratory, with the facilities to control flow rates and temperatures for hot, cooling and chilled water. Hot, cooling and chilled water temperatures strongly influence the chillers' performance. The following inlet temperatures are used as nominal operating conditions for driving heat, regeneration and chilling: 80°C, 30°C and 15°C respectively. The influence of cycle time on thermal performance has been determined for these operating conditions. The cycle time is the duration of a complete cycle of heating up and cooling down of one reactor. Figure 3 shows the cooling power (left axis) and coefficient of performance (right axis, ratio of cooling power and driving heat). For this application, the coefficient of performance is defined as:

$$\mathrm{COP} = \frac{Q_{\mathrm{evaporator}}}{Q_{\mathrm{heatsource}}} \qquad (1)$$

Figure 3 shows that cycle times under six minutes are not useful, because both cooling power and COP show a decrease (because this short cycle time does not allow all the silica gel to go through the complete temperature cycle). With increasing cycle times (>10 minutes), a decrease in cooling power is compensated by an increase in efficiency (because fewer changes between heating and cooling of a reactor mean less thermal losses).

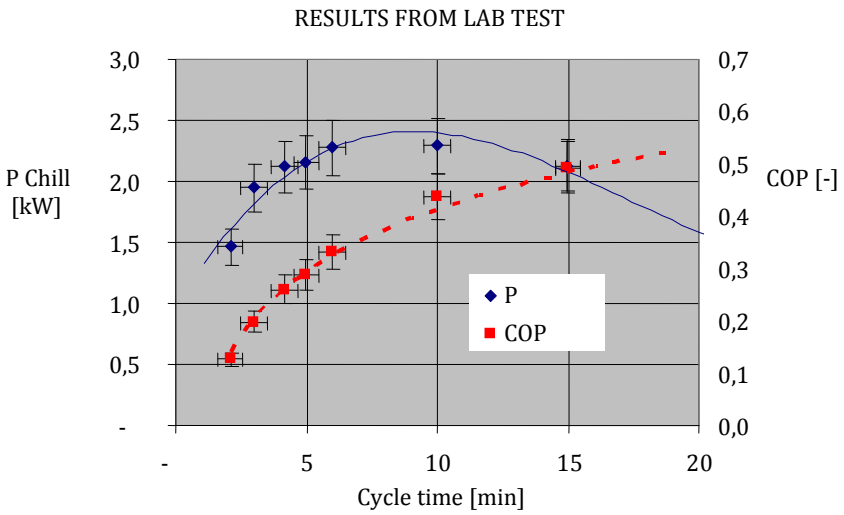

Figure 3: Influence of cycle time on the thermal performance of the adsorption chiller

Figure 4 shows the influence of the cooling water and chilled water inlet temperature on the chiller performance. The measurements were all performed with a fixed cycle time of 12 minutes. Chiller performance clearly benefits from “high chilled water temperatures” and relatively low cooling water temperatures. The laboratory tests show that the ambitious design specifications for this prototype have been achieved. Nearly 2.5 kW cooling power can be produced with a compact machine (power density of 7 kW/m^3) at a respectable COP.

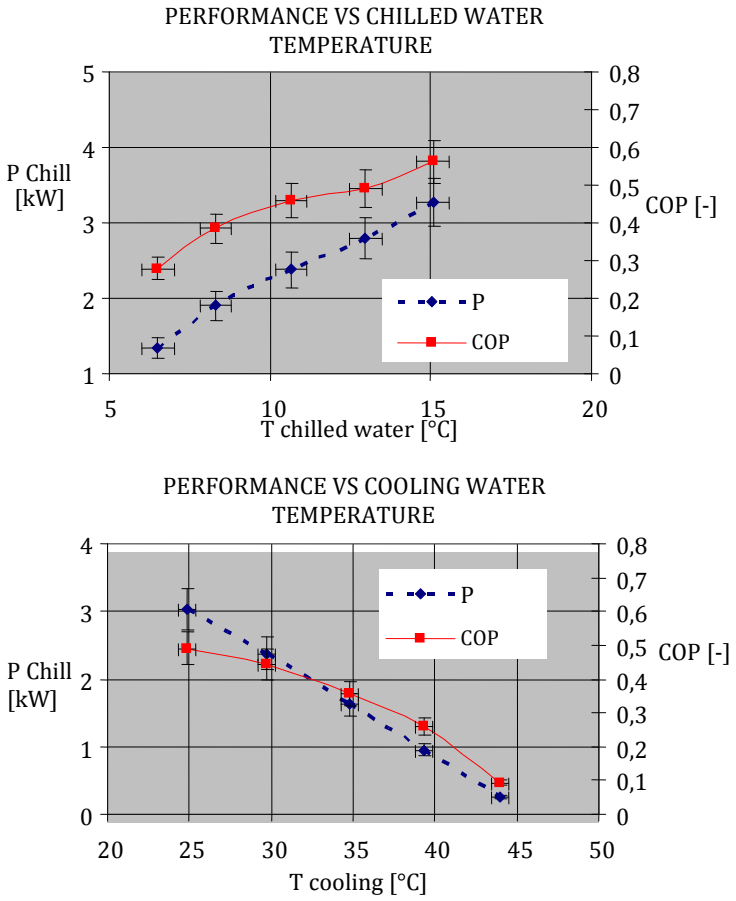

Figure 4: Influence of cooling water (below) and chilled water (upper) inlet temperature on the chiller performance

3.2 Measurements in research dwellings

The research dwelling that is used, is in one of the four full-scale single family dwellings at ECN in Petten, Netherlands as shown in Figure 5. The size of these dwellings represents the Dutch average for new dwellings. The research dwellings are equipped with an extensive data acquisition system, logging every 10 minutes more than a 100 sensors. These systems register energy flows such as passive (windows) and active (collector) solar radiation, electricity use but also temperature, humidity and if necessary carbon dioxide levels. The data acquisition also allows to measure on the component level such as: electricity use of circulation pumps or controls, heat supplied by heating systems, temperature and humidity (comfort aspects) etc. The measurements with the adsorption chiller are performed with the installation setup as shown in Figure 6.

Figure 5: The four single family dwellings. The second house to the left is used for measurements with the adsorption chiller

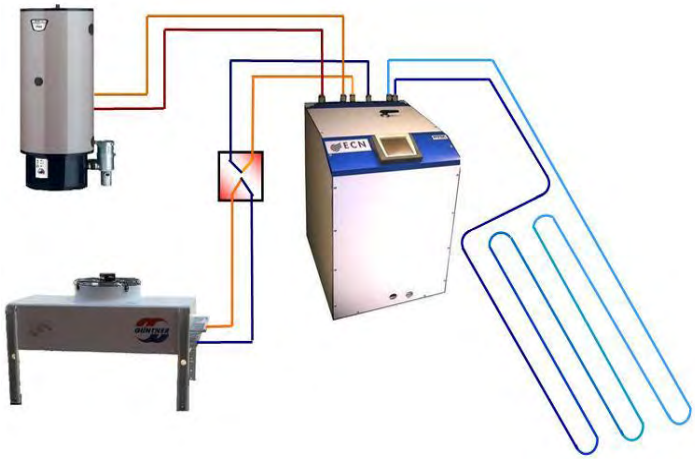

Figure 6: Installation setup of the adsorption chiller and a gas-fired boiler as heat source

In Figure 6 a gas fired boiler is used to supply the heat to the chiller. A dry cooler is positioned outside the building to reject the heat of condensation and the heat of adsorption coming from the chiller. The boiler was applied as a forerunner for the intended micro-chp system (combined heating and power), to provide the driving heat for the chiller. The installation of the micro-chp was delayed due to limited pre-commercial availability.

As can be seen in the graphs in Figure 4, the performance of the chiller is strongly influenced by the chilled water temperature and the cooling water temperature. To be able to compare measurements that are performed under different conditions, COP and cooling power can be plotted against the so-called reduced temperature. The reduced temperature is defined as:

$$T_{reduced} = \frac{T_{cooling(in)} - T_{chilledwater}}{T_{hot(in)} - T_{cooling(in)}} \quad (2)$$

The following graphs (Figure 7) show the results from measurements in the research dwelling and the laboratory. The horizontal axes represent the reduced temperature, allowing comparing the results from lab and research dwelling.

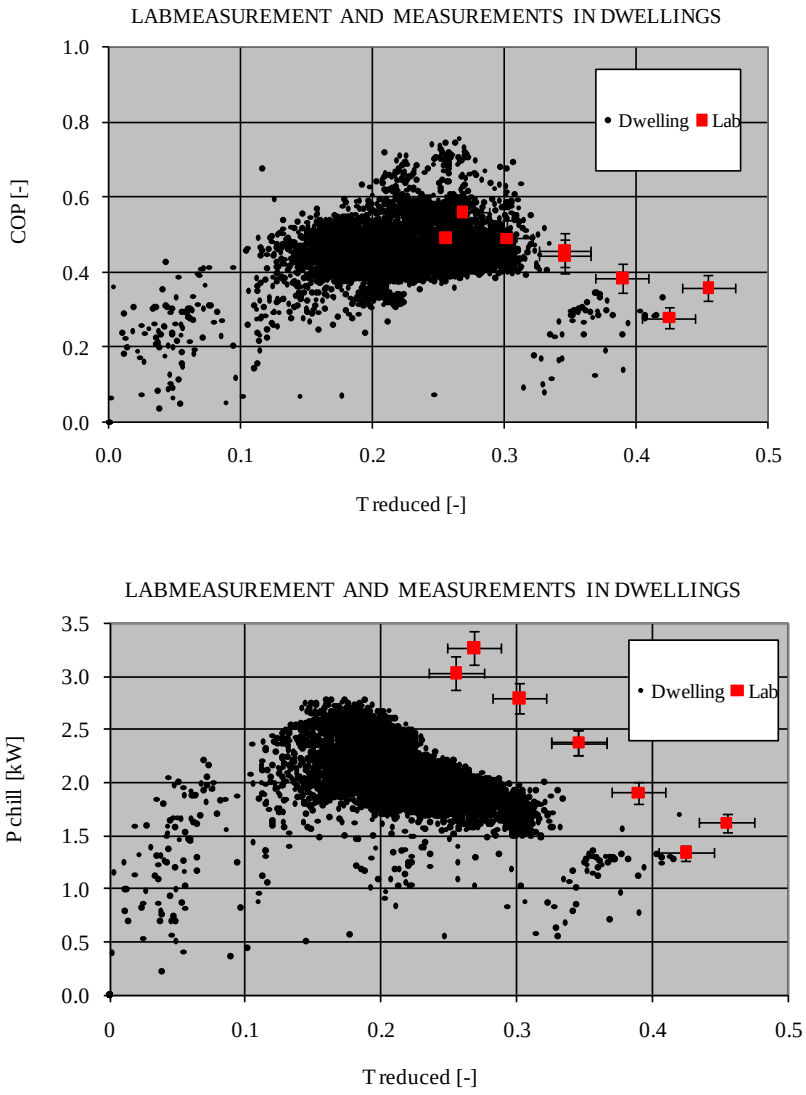

Figure 7: Comparison of the adsorption chiller performance between laboratory and research dwelling measurements

The measurements in the research dwelling demonstrate that the prototype adsorption chiller can also operate successfully under realistic operating conditions. Also, the difference in performance from measurements in the laboratory and the research dwelling is shown.

3.3 Measurement analysis

The comparison of the measured data shows reduction in performance of the chiller under operating conditions in the dwelling compared to the performance under laboratory conditions. The available cooling power was reduced by 25 to 30% compared to the laboratory results. The performance of the prototype chiller under operating conditions in the dwelling can be improved by the following design adjustments:

- improvement of the refrigerant valve design;
- improvement of the refrigerant liquid level control in the evaporator;
- reconsider evaporator design to avoid pool boiling;
- reconsider material use to reduce any corrosion.

If these adjustments are being incorporated in a second prototype, the expectation is that the performance will increase with 10%. Also the difference in performance between lab and practical conditions will be reduced.

4 CONCLUSION AND OUTLOOK

A new adsorption chiller prototype was successfully developed, designed, built, commissioned and tested in laboratory conditions and in more real life conditions in a research dwelling. The laboratory measurements indicated a nominal cooling power of 2.5 kW with a COP of 0.5, in accordance to the design targets. The thermal performance increases with higher chilled water delivery temperatures and with lower heat rejection temperatures. Measurements results under the operating conditions in one of ECN's research dwellings, showed a lower cooling power and COP in comparison to the laboratory measurements. The two sets of measurements helped to address future adjustments to the design that can improve a commercial version. The adsorption chiller that is developed by ECN is ready to be commercialized.

5 REFERENCES

Bakker, E.J., N.C. Sijpheer 2004. "Ecobuild Research: full-scale testing of innovative technologies for energy efficient houses", *Report Energy Research Centre of the Netherlands (ECN)*, Petten, The Netherlands.

Bakker, E.J., N.C. Sijpheer 2008. "Testing a prototype gas-fired residential heat pump", *Proc. 9th Int. Heat Pump Conference 2008*, Zurich, Switzerland.

Boer, R. de., E.J. Bakker 2010. "Development of a new 2.5 kW adsorption chiller for heat driven cooling", *IEA Heat pump Newsletter*, Vol. 28, 1/2010, pp. 39-42.

Boer, R. de., R.J.H. Grisel, S.F. Smeding 2010. "Waste heat driven silica gel/water adsorption cooling in trigeneration", *Applied Thermal Engineering*, Vol. 30, pp. 1039-1046.

Sijpheer N.C. et al. 2007. "Floor cooling and air-cooling, the effects on thermal comfort of different cooling systems"*, Report Energy Research Centre of the Netherlands (ECN)*, Petten, The Netherlands.

SOLAR COOLING WITH ADSORPTION CHILLERS

Ingo Daßler, Walter Mittelbach, SorTech AG, Zscherbener Landstraße 17
D-06126 Halle, Germany, walter.mittelbach@sortech.de

Abstract: Solar cooling for small-scale application is quite a new topic if it comes to practical applications. SorTech AG, founded in 2002, is one of the few manufactures of small scale adsorption chillers and on the market for 5 years now. Within this time over 200 projects were established all over the world. With these projects a lot of experience in planning, installation, and operations of thermal cooling systems has been gathered.
As an example a solar cooling installation in Austria will give an insight of performances, efficiencies, and potentials of this technology.

Keywords: solar cooling, thermal cooling, adsorption chiller, SorTech AG, SolCoolSys, solar cooling installation

1 OVERVIEW

The following paper shows an example of the strong influence of installation on the performance of a solar air-conditioning system. The data given are drawn from a project which was carried out within the German funded project “SolCoolSys”, targeting at the development of standard solar cooling applications. The installation was performed in Mürzzuschlag, Austria with the collaboration of the companies SOLVIS and PINK. The system was monitored by Fraunhofer ISE.

The paper exhibits the performance data after the first installation and again after a subsequent adaption of the hydraulics and the control strategy, which lead to a significant increase in cooling capacity and electrical COP. Furthermore, a detailed analysis is given how installation conditions are affecting the performance data of the adsorption chiller.

2 COMPANY’S PROFILE

SorTech AG, founded in 2002 as a spin-off of the German Fraunhofer-Institut für Solare Energiesysteme ISE, is one of the first companies in Europe which offers commercial products for small scale solar cooling application. Since 2007, SorTech offers silica gel based adsorption chillers with cooling capacities starting from 5 kW to 15 kW per unit (see Figure 1). In the meantime more than 200 projects mainly in Europe, but as well in Africa, North America, Asia, and Australia could be realized with cooling capacities up to 150 kW (e.g. Patent Office in Munich).

In addition to the adsorption chillers SorTech AG product portfolio covers:

- standard cooling packages, consisting of chiller, heat dissipation unit, and hydronic pump station,
- customized cooling systems,
- detailed planning and installation support.

Figure 1: Adsorption chiller ACS 08 / ACS 15

Besides silica gel technology SorTech acquired a deep know-how in zeolite coating technology (Figure 2), which provides coating of almost any aluminium (Al) alloy based three dimensional structures. Unique feature of this technology is the crystallization of zeolite directly on aluminum based surfaces. This provides high energy density and therefore compact heat exchanger for SorTech's next generation sorption chillers and heat pumps.

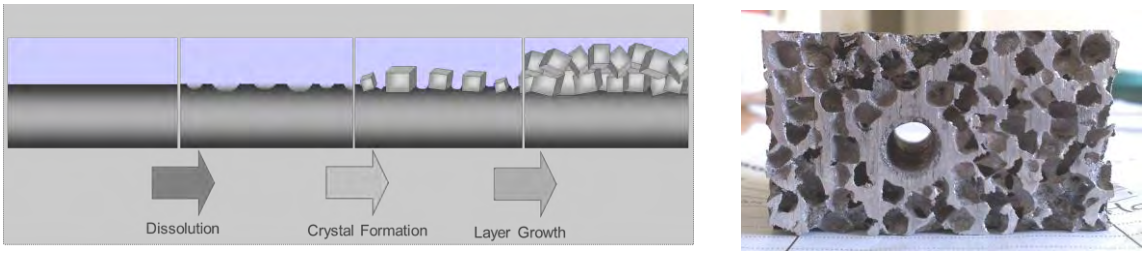

Figure 2: Crystallization process (left); Al-alloy sponge suitable for zeolite coating (right)

3 EXAMPLE OF SOLAR COOLING INSTALLATION

The following example of a solar cooling application provides an idea of the potential and performance of such a system. This solar cooling application has been established within the German funded project "SolCoolSys", targeting at the development of standard solar cooling applications.

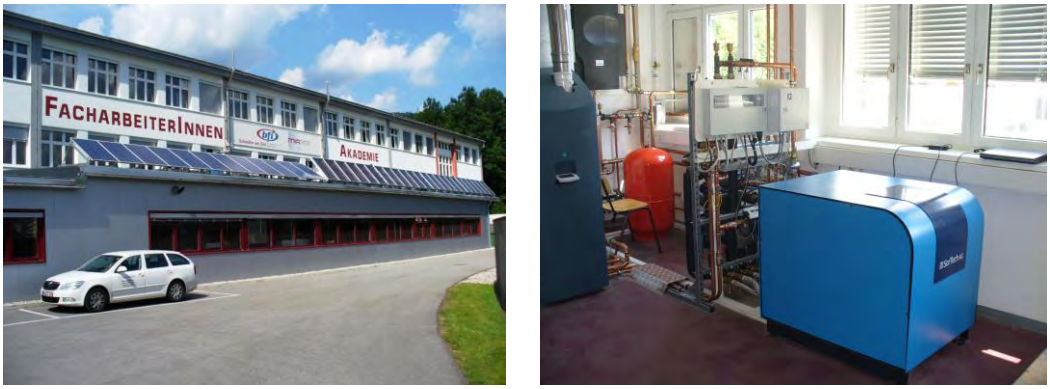

Figure 3: Solar Cooling Professional School, Mürzzuschlag, Austria (left: Solar thermal collector; right: Adsorption Chiller ACS08)

3.1 Technical facts

Basic technical facts of the installation are shown in Table 1.

Table 1: Technical facts of installation

Chiller type	ACS08; 8kW cooling capacity at nominal conditions
Primary Heat (hot temperature) source	31 m²; flat panel
Secondary Heat source	gas burner
Heat (middle temperature) sink	heat dissipation unit with spraying system (type RC08)
Cooling task (chilled water):	Workshop studio and bureau via fan coil units
Year of commissioning	June, 2011

A gas burner and two hot water storages have been installed to provide the system with heat, independently of solar radiation and to bridge operation phases with high thermal energy consumption (e.g. at the beginning of each sorption cycle).

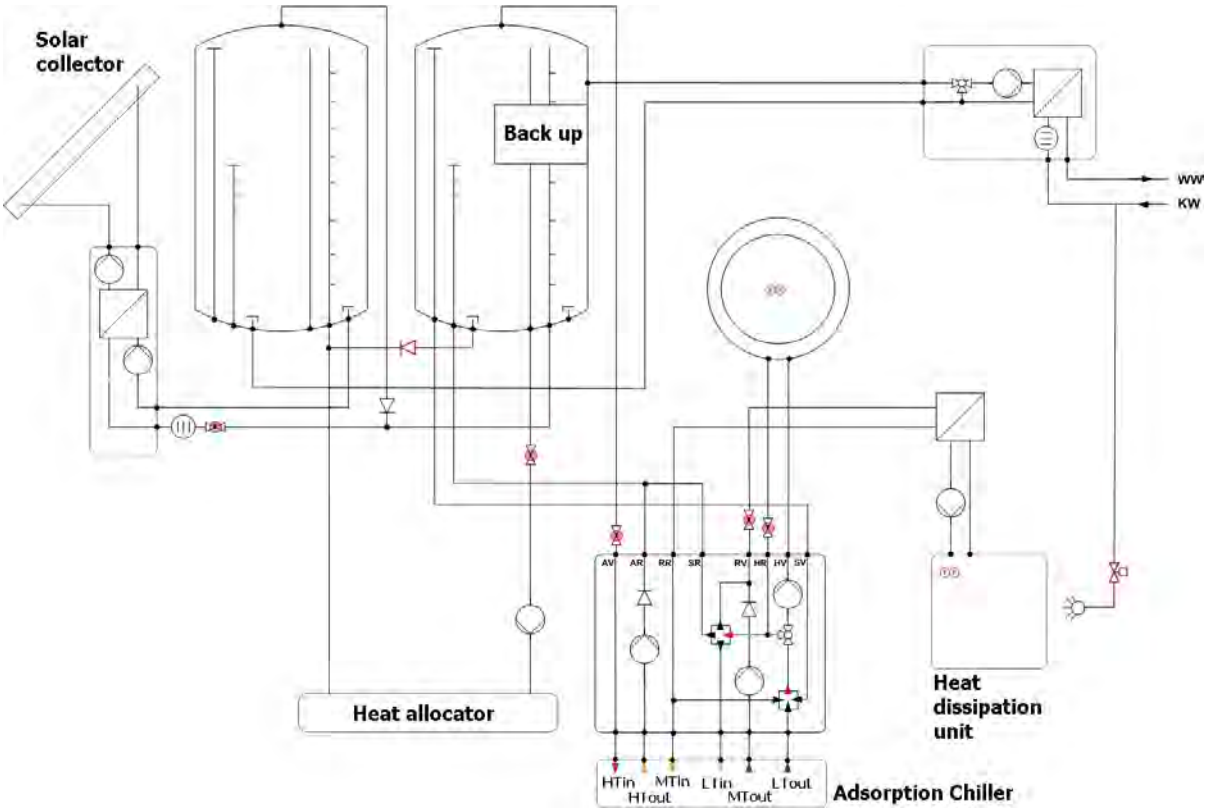

Figure 4: Hydronic diagram of connections

The system has been equipped with additional components to provide free cooling (using the heat dissipation unit for cooling at low ambient temperatures) and heating as well. Due to the lack of practical and performance experiences of solar cooling systems this system has been monitored. Therefore temperature sensors, flow meters, electric meters, etc. were installed in order to measure the behavior and the performance of the system. The results were analyzed and provide the basis for improvements of the system. The results of this monitoring are given in the next paragraph.

3.2 Results

The main focus of the monitoring is set to cooling capacity and electrical COP as performance and efficiency parameters. The cooling capacity is determined by the three temperature levels of the adsorption process. The electrical COP, as the ratio of cooling power and electrical consumption of common auxiliaries, is mainly determined by the heat dissipation unit with the highest electrical consumption of the system.

The definition of the electrical COP is similar to the definition of the COP of conventional systems and shows the main advantages of thermal cooling systems: electrical energy is only used for common auxiliaries (e.g. pumps, heat dissipation units, controlling). The electrical COP of thermal systems, therefore, can reach a multiple of conventional systems.

Figure 5 shows typical charts of the monitoring (displayed period: approx. 4 hours around midday):

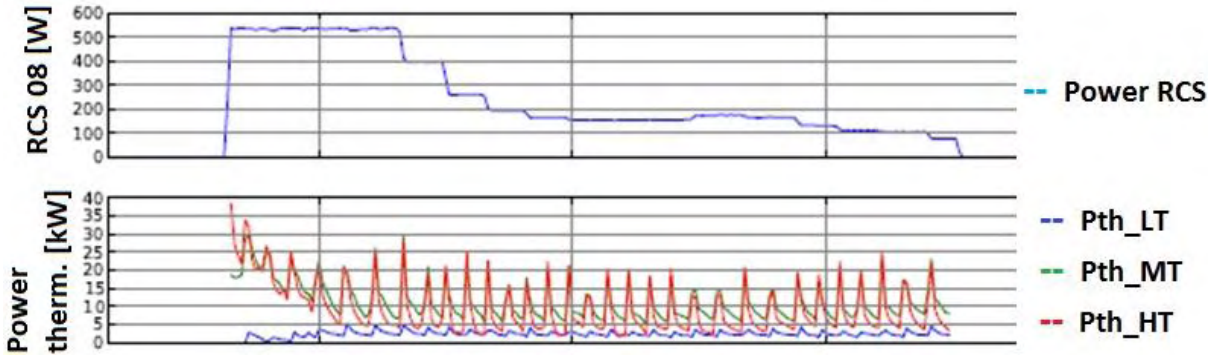

Figure 5: Chart example: characteristic of the solar cooling system

Upper diagram - electrical consumption of the heat dissipation unit:
To reduce the electrical consumption the heat dissipation unit adapts the speed of its fans to the cooling load – the lower the load, the lower the speed and electrical consumption. At the beginning of operation the heat dissipation unit runs at maximum speed to achieve the cooling task. Along with operation time the speed is reduced to a minimum due to lower cooling loads.

Lower diagram - heat flows:
Here the typical characteristic of the heat flows (driving heat – red chart, dissipation heat – green chart, and cooling power – blue chart) are shown with its high peaks at the beginning of each sorption cycle.

In the following the improvement of the solar cooling system is shown. Therefore, the results for cooling capacity and electrical COP before and after system improvements are compared to each other. The results have been achieved under similar weather conditions and representing average values of a one day monitoring. The monitoring of the system started in summer 2011. During winter and spring 2012 the improvement of the system took place.

The results after commissioning of the solar cooling system are shown in Table 2.

Table 2: Results before improvements

Cooling capacity	max. 3 kW
Electrical COP	< 5

The performance and efficiency is below expectation. In order to improve the system's performance and efficiency both, constructional and control oriented adaptations have been done based on the monitoring results. Basic adaptations of the systems are shown in Table 3.

Table 3: Monitored effects and adaptation of the system

Monitored effect	Effect on the system	Reason & System adaptation
High temperature differences between heat dissipation unit and ambient temperature	• High heat dissipation temperature and therefore low cooling power and electrical COP	• Heat exchanger was connected wrongly → reconnecting heat exchanger • Wrong control strategy of heat dissipation unit → control algorithm has been updated
Cooling power to low	• Risk of condensation on cooling devices due to low temperature • Low electrical COP	• Full cooling load was not yet available → expanding cooling task

After the first monitoring phase the system could be improved due to the adaptations. Actual performance and efficiency of the system is shown in Table 4.

Table 4: Results after improvement

Cooling capacity	3 to 5 kW
Electrical COP	6 to 15

4 FACING CHALLENGES

These results and the experiences with other solar and thermal cooling systems show, performance and efficiency depend, like in any other applications, on correct planning, installation, and operation. Table 5 shows different operation parameters and the effect on performance and efficiency. To give an idea of the effects the impact of each parameter on performance and efficiency is given in numbers for a concrete example.

Example:
A cooling task is given with 5.5 kW cooling load and a predicted electrical COP of approx. 11.2.

Table 5: Effects on performance and efficiency

Parameters influencing the performance	Effect on performance
Flow rate of driving and cooling circuits are less than nominal flow rate (e.g. – 200l/h each)	- 10% (5kW instead of 5.5kW)
Insufficient air bleeding of hydronic system	- 5% (5,3kW instead of 5.5 kW)
Driving Heat temperature is less than planned (e.g. 65°C instead of 75°C)	- 25% (4.1kW instead of 5.5kW)
All effects	- 40% (3.3kW instead of 5.5 kW)

Parameters influencing the efficiency	Effect on efficiency
wrong pumps (e.g. low end pumps instead of high efficiency pumps)	- 10% (10.1 instead of 11.2)
higher ΔT in heat dissipation cycle due to wrong installation (e.g. heat exchanger)	- 38% (7 instead of 11.2)
All effects	-42% (6.5 instead of 11.2)

Our experiences of more than 5 years solar cooling for small scale application in Europe show:

- Robust operation mode of the adsorption chiller and good performance are shown in over 200 SorTech installations
- Solar Cooling means today: detailed planning
- Concept and dimensioning are crucial factors for the energetic and monetary outcome: „rules of thumb“ do not work!
- Not every application is suited for thermal cooling! (e.g. very low cold water temperatures are reached only efficiently under certain conditions.

5 SUMMARY AND POTENTIAL

Experiences show that solar cooling can be a good alternative to conventional cooling systems. The market for thermal cooling, however, is still small but high potential due to ecological and economical advantages. Besides solar cooling application the market for thermal cooling using waste heat at low temperature level (<100°C for absorption systems; <80°C for adsorption systems) and the combination of co-generation units with sorption chiller is promising. Nevertheless, for market development the following issues are crucial for the success of thermal cooling in future:

- Reducing cost for both, chiller and components
- Increasing power-to-mass-ratio
- Developing of standard systems for easy installation and operation
- Increasing awareness level of solar cooling technology.

6 NOMENCLATURE

ACS08	Adsorption Chiller Silica Gel, 8 kW nominal cooling capacity
Electrical COP	ration of cooling power and electrical power of auxiliary equipment
Pth_MT	(thermal) dissipation heat
Pth_HT	(thermal) driving heat
Pth_LT	cooling power
RCS08	heat dissipation unit

7 ACKNOWLEDGEMENTS

We would like to thank:

Projekträger Jülich PtJ for supporting the research within the “SolCoolSys”- Project

Solvis GmbH for installation support

Fraunhofer Gesellschaft ISE, Freiburg for installing the monitoring system and data analysing

Pink GmbH for supervising the installation in Mürzzuschlag, Austria

NEW ABSORPTION CHILLERS FOR CHCP OR SOLAR COOLING SYSTEM TECHNOLOGY

Stefan Petersen, Alexander Beil, Christian Hennrich, Wolfgang Lanser, Walther Guido Hüls,
Technische Universität Berlin, KT2, Marchstraße 18, D-10587 Berlin, Germany,
Stefan Natzer, Bayerisches Zentrum für angewandte Energieforschung (ZAE Bayern),
Walther-Meissner-Straße 6, D-85748 Garching, Germany, stefan.petersen@tu-berlin.de

Abstract: Sorption cooling technologies are well known as best practice energy efficient cooling supplying apparatus where heat as driving source is delivered by waste heat, trigeneration systems, solar thermal plants, etc. Recent European demonstration projects could not match this prospect due to parasitic electric consumptions.

A research project under participation of science and engineer researchers (TU-Berlin, ZAE Bayern) and an energy provider (Vattenfall Europe) was set up to develop high efficient absorption chillers in the range of 50-320 kW. System set ups for the entire cooling generation including reject heat and hydraulic components and control are within the focus. While a 160 kW absorption chiller is on the test bench, 50 kW absorption systems are already running in 2 demonstration plants.

The chiller operates in between 25 and 140% of load at thermal COP´s in the range of 0.80 and can stationary deliver cold down to part load of 5%. While driving heat can be used from 55°C up to 110°C at the inlet (standard operation point is at 90/72°C in/out), reject heat inlet temperatures up to 45°C are feasible for normal operation mode. Even higher reject heat temperatures are viable without crystallization, only limited by lower power density. Operation figures of new 50 and 160 kW absorption chillers as well as energy efficiency ratios of demonstration plants are presented. System layout, including market available dry reject heat systems, gains parasitic electric EER values lower than 6% of cooling load. New volumetric/energetic density benchmarks up to 23 l/kW are proven.

Results of 50 kW absorption system overreached thermodynamical targets while proposing a lower price than market available. System demonstration and development up to 320 kW cooling load systems are actually undertaken in Lab and will be lead to real estate installations in 2013.

Keywords: optimization, efficiency, control, demonstration, tri-generation

Supported by:
Federal Ministry of Economics and Technology
on the basis of a decision by the German Bundestag

1 INTRODUCTION

More than 25% of the space heating demand in some European countries as Germany, Sweden, Denmark or Finland is covered by district heat. Some cities in northern Europe even reach a ratio of more than 70% (Randløv 1997). In summer months, most of the district heating systems in Europe are running on low capacity as shown in Figure 1. On the other hand, there is an increasing demand of cooling supply for air-conditioning. Sorption chillers working with low driving temperatures are especially suitable for using district heat in summer to meet the demands of cooling loads. This way, the efficiency of district heating networks is improved, the provider of the heating networks encounters new key markets and the operator of the chiller obtains a cheap, reliable and ecologically worthwhile driving energy (Naß et al. 2010, Zegenhagen et al. 2010). But not only district heat networks can be used to drive absorption technology. Even solar thermal systems already used for heating tap water or support heating systems during winter period are viable to deliver the heat for producing cold in summer season (Petersen et al. 2006, Henning 2010). The main obstacle for sorption cooling by district heat is the lack of viable machines on a moderate price level on the market.

These considerations led to a collaboration project between the Technical University of Berlin (TU Berlin), the Bavarian Center for Applied Energy Research (ZAE Bayern) and Vattenfall Europe, who operates large district heating systems, to develop a low temperature driven water/lithium bromide absorption chiller. The focus was set on an efficient system for the whole cooling generation process, including heat rejection, hydraulic components (together with parasitic energy demand) and control.

An expedient capacity range was seen in 50 - 320 kW cooling power. This is suitable for average sized residential blocks. So, in a first step a 50 kW chiller was designed, built and installed in several demonstration sites. In a later step, a 160 kW machine is being developed.

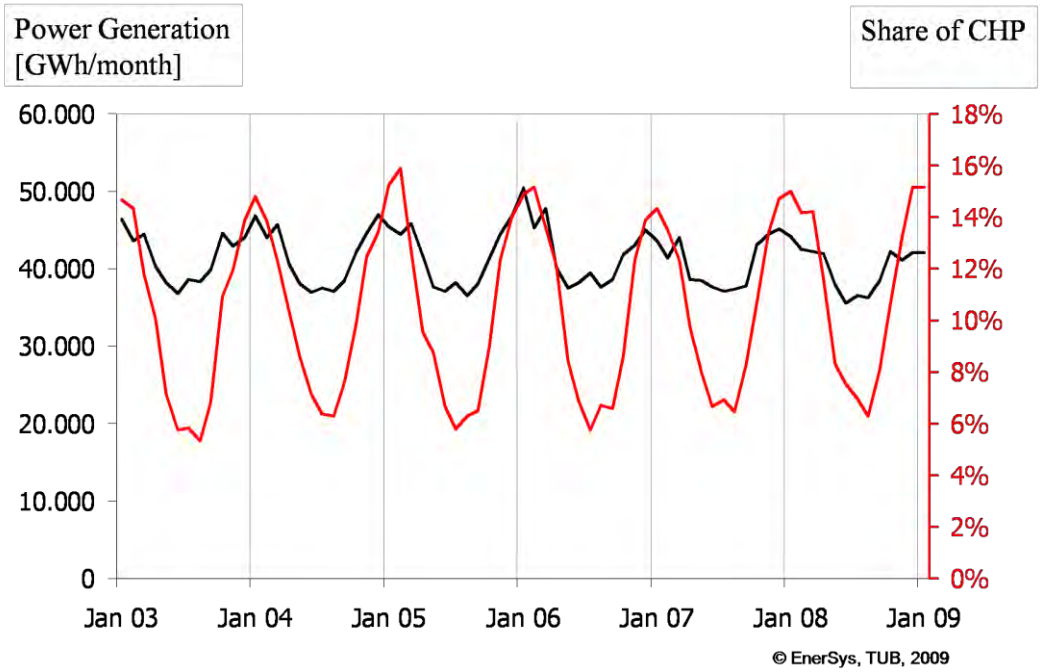

Figure 1: Share of CHP (combined heating and power) electricity in Germany 2003-2009

2 ABSORPTION CHILLERS

Main focus of the project as well as in market availability and necessity are single effect absorption chillers. In case of facility cooling water/lithium bromide is the most used working pair.

Most of the commercially available water/LiBr absorption cooling machines are working on a capacity range from 300 kW and up. Here, shell and tube heat exchanger are state of the art. Copper tubes are rolled into heavy front plates, assuring the inner refrigerant atmosphere to be vacuum proof. The direction change of the heat transfer medium is done by water boxes fixed outside onto the front plates. Transferring this technique on smaller capacity ranges below 200 kW leads to high specific cost, because with smaller tube lengths the fix costs of the fringe effects dominate (Estiot et al. 2007).

Other approaches, developed for small machines that are available from few manufacturers, like coiled tube heat exchangers, led to different problems including high size ratio and high external pressure drops. On the other hand, this pressure drops lead to high parasitic energy demands, reducing the advantage of heat driven cooling machines (Aprile 2010).

Another point is the part load behavior of common chillers. With fixed volume flows on the heat transfer medium side and a fix fan speed for the heat rejection unit (both set for nominal power), the resulting parasitic electric consumptions dominate at part load. Thus, again, the advantage of low electric energy consumption for sorption systems is reduced, leading to a low electric energy efficient ratio (electric EER).

Focusing on these aspects, the goals for a new development of an efficient and economic absorption chiller were set. Among those, a high COP on a wide capacity range was also set as target for the system. Inter alia, this can be achieved by low heat losses through reduced thermal bridges. Of course, also the number of working steps for construction (i.e. price), the compactness and the weight was to be looked at.

As a result, a new and promising idea of U-shaped bended tubes, arranged in a face-to-face adjustment for absorber and evaporator and cross-shaped parallel for generator and condenser, with a split condenser right and left of the generator, came to be.

3 NEW ABSORPTION CHILLER CHARACTERISTICS

Focus of the project has been the development of absorption chillers in small and medium capacity up to 320 kW. A first 50 kW lab functional model was erected in 2010 being analyzed for 18 month till late 2011. Based on these results conception studies for the 160 kW model were undertaken, gaining in a new 160 kW lab functional model which is actually analyzed at the test rig of TU Berlin.

3.1 50 kW lab model

Thermophysical characteristics of the first 50 kW chiller has been well described in 2011 (Petersen et al. 2011). It is stressed that the new chiller design, focusing on heat exchanger optimization due to pressure losses and surface usage combined with new control strategies can lead to efficiencies of 0.8 in cooling mode. The new absorption chiller overcomes limitations of low driving heat temperatures and can therefore start operation at 55°C up to 110°C.

New results do even claim to pull down a second prejudice. Designed for low maintenance costs there was a need to identify most expensive cost objects. Even in a country like Germany, where water is not really a limited source, costs for water treatment and bacteria

treatment in evaporative reject heat cooling towers can be responsible for 30-40% of operation costs for small systems. Main concept of the new development has therefore been the combination with dry reject heat systems, taking into account that reject heat temperatures therefore do increase in normal load conditions. New benchmarks in reject heat temperatures have been reached not any more limited by 35°C as state of the art, and no crystallization problems at high reject heat temperatures. Even as there is no need for the chiller to shut down at high reject heat inlet temperatures as shown in Figure 2, capacity is limited if driving heat and used cold temperatures are kept constant and lead to 15 kW cooling capacity at 45°C. In part load there is a theoretical potential of saving pump energy in the reject heat cycle. As defined in European Seasonal Energy Efficiency Ratio (ESEER) around 40% of load hours are at 50% of installed capacity. Reducing volume flow while reducing pump speed will save up to 98.5% of electric consumption of the pump if efficiency of the pump keeps constant. Of course this is a scientific analysis, nevertheless it remains obvious that increasing reject heat temperature and therefore lowering fan speed simultaneously to control pump speed can lead to parasitic energy savings of 80-90% compared to full load if control strategies do system control and not each component on its own.

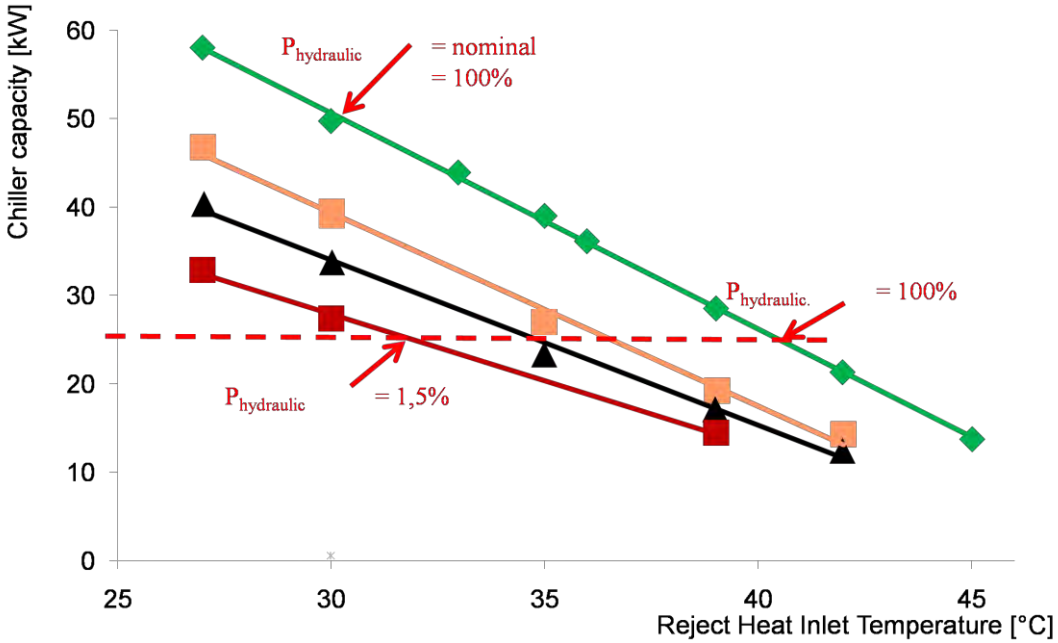

Figure 2: Reject heat variation

As a result of experimental characterization of the 160 kW functional model the 50 kW small capacity chiller was rearranged. The volumetric energy density was again increased by 30%. Results of an experimental characterization of the small size chiller should be available by late 2013.

3.2 160 kW "Bumble Bee"

Adapting and enhancing the heat exchanger concept of the 50 kW model the 160 kW model was established. Main goals, beside of the capacity, were keeping the weight of the chiller or the modules below 1000 kg (stair up- and downward transportability) and size limits below 1.9 m x 1.6 m x 0.88 m (floor transfer bottlenecks as doors and corner sizes) due to facility limitations. Finally, the new concept reached out to figures given in Table 1. As shown in Figure 3 the concept allows to divide the chiller into 2 main modules consisting each of 2 main heat exchangers, the low pressure part of evaporator, absorber, solution heat exchanger, pumps and base frame and the upper pressure vessel hosting desorber and condenser.

Figure 3: Modularized 160 kW "Bumble Bee"

Characteristic measurements started in April 2012. Results up to now fulfilled the expectations - not mandatory - but after particular on site construction changes. Chiller capacity varies in between 154 kW and 162 kW in nominal load conditions as shown in table 1, while COP is in the range of 0.79. Further thermodynamic characteristics will be analyzed till summer 2012. Simultaneous simulation models are varied to predict all kind of usage, temperature and volume flow conditions to discuss field tests, which should start in 2013. In figure 4 the new chiller is compared to top market available chillers. Even as one complete system it is lighter and smaller than “one vessel” market products which are pooled in the circle. One vessel chillers are not divisible, not in weight and not in size. Taking into account the possibility of modularizing the new chiller the advantage gets obvious. As a compact and complete chiller it is with only 0,86 m width the slimmest chiller of the capacity range above 15 kW nominal capacity and the first one passing through doorways.

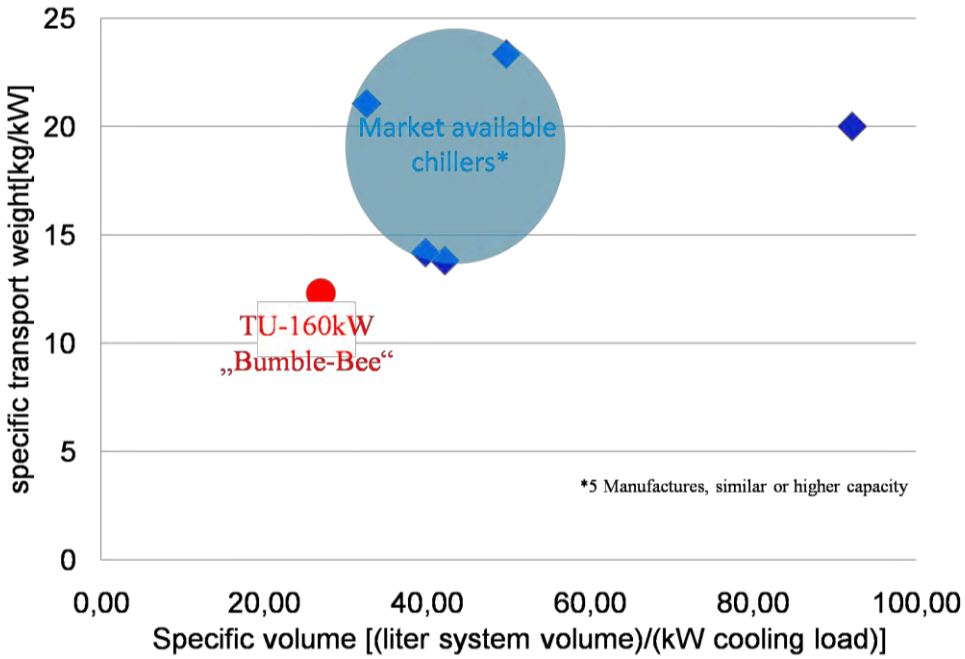

Figure 4: specific sizing benchmarks of absorption chillers

3.3 Results

First economic analyses propose system costs to be 50-70% lower than available by now. Figure 5 shows the expected costs in comparison to results based on a literature review given by IUTA (2002) for compression systems and absorption chillers. Considering the

uncertainty due to system equipment the benefit of the new construction and system design is evident. System costs based on the new development including the absorption chiller, a dry reject heat system, supplying pumps and a system controller will be available at a reduced rate compared to market available absorption chillers. Compression chillers, still being price competitive or cheaper, loose significantly margin, which will finally lead to higher cold generation costs due to maintenance costs.

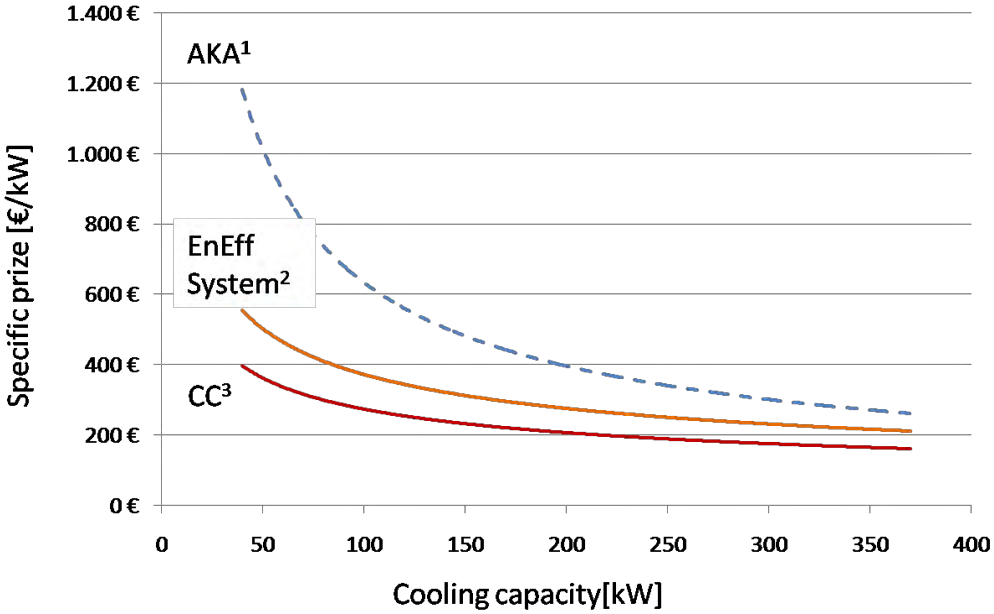

Figure 5: comparison of specific costs of cooling devices

In Table 1 geometrical data of the new absorption chillers are summarized. Beside of the compactness the modularity in terms of single module weights offers the opportunity to step with this chiller types not only in new building construction sites but also in the retrofit market which dominates the actual construction market all over Europe and where therefore the main necessities of energy saving heating and cooling devices are needed.

Table 1: Chiller size

	Bee Redesign (50 kW)	Bumble Bee (160 kW)
size of entire machine		
length [m]	1.75	1.95
width [m]	0.68	0.86
height [m]	1.59	2.05
total transportation weight [kg]	650	1750
max. modules	2(+4)	2+4
size of biggest module		
length [m]	1.75	1.82
width [m]	0.68	0.86
height [m]	0.98	1.21
transportation weight [kg]	< 350	<850

Table 2 gives an overview to operation standard conditions of the two models. Currently the 160 kW chiller is examined in the lab for its part load characterization. Both chillers provide chilled water in between 6°C and 25°C, using hot water from 55°C to 110°C, types for hot water temperatures up to 135°C will be viable. Hot water temperature spreads at standard flow rates of 0.014 l/s/kW (standard operation conditions, decentralized CHP) are in the range of 18 K but also spreads up to 40 K are feasible at low flow system flow rates of 0.006 l/s/kW as used in district heat networks or solar thermal systems.

Table 2: Standard operation conditions

		Bee	Bumble Bee	unit
Nominal cooling capacity		50	166	kW
Heat demand		63	208	kW
Reject heat		113	374	kW
COP			0.79	
Chilled water	temperature inlet		21	°C
	temperature outlet		16	°C
	volume flow	8.5	27.7	m³/h
	pressure drop	0.27	0.25	bar
	max. pressure		6.0	bar
Hot water	temperature inlet		90	°C
	temperature outlet		72	°C
	volume flow	3.0	9.7	m³/h
	pressure drop	0.12	0.36	bar
	max. pressure		16	bar
Reject heat water cycle	temperature inlet		30	°C
	temperature outlet	37	38	°C
	volume flow	14.4	39.0	m³/h
	pressure drop	0.70	0.57	bar
	max. pressure		6.0	bar

4 SUMMARY

The investigative development described in this paper shows up the potential for modernization of an old fashioned cooling technology. Sorption cooling or heat pump systems have been a niche-market during electrification period in Europe and northern American States. Within the actual discussion of energy usage efficiency, solar power usage and combined heat and power sorption cooling systems offer the possibility to make use of heat during summer season, diminish additional electric loads caused by compression cooling systems and with the goal of delivering cold. Within this topic market available systems suffer by volumetric size, efficiency and prize to be competitive. A new heat exchanger concept is elaborated.

With respect to research results of the last 15 years specific energy densities are increased by at least 30% for cooling capacities in the range from 30 kW to 320 kW. Cost reduction is expected to be in a range of 50% to 70% compared to current cooling costs.

The new generation overcomes conventional operating limits of absorption chillers. Former limitations regarding minimum hot water temperatures or maximum reject heat temperatures have been mainly based on construction parameters. Starting operation at 55°C hot water

inlet there are no limitations to reject heat inlet temperatures up to 50°C. Nevertheless, system design will be different for high reject heat conditions than for lower ones.

The first 50 kW model is operating in two field tests in Germany, supplying cold for a 44 kW office cooling driven by district heat and a 35 kW solar cooled datacenter installation. Further field tests with the final developments in the range of 30 to 200 kW are expected to be set up in 2013.

5 ACKNOWLEDGEMENT

Authors wish to thank all supporting companies and the scientific community in the field of absorption technology. Special thanks do belong to our main project partner Vattenfall Europe and the German Federal Ministry of Economics and Technology represented by Project Management Jülich (PTJ) under the project number 0327460B.

6 REFERENCES

Aprile M. 2010. “The market potential of micro-CHCP. POLYgeneration with advanced Small and Medium scale thermally driven Air-conditioning and Refrigeration Technology”, Final report, www.polysmart.org.

Estiot E., S. Natzer, C. Schweigler 2007: “Heat Exchanger Development for Compact Water/LiBr Absorption Systems”, *Proc. 22nd Int. Congress of Refrigeration, 21-26 August 2007*, Bejing, China.

Henning H.M. 2010. “Solar Air Conditioning and Refrigeration - Achievements and Challenges”, *Proc. Int. Conf. on Solar Heating, Cooling and Buildings, Eurosun 2010*, Graz, Austria.

Institut für Energie- und Umwelttechnik e.V. (IUTA) 2002. Preisatlas. Ableitung von Kostenfunktionen für Komponenten der rationellen Energienutzung. Duisburg, Germany.

Naß S., W. Lanser, S. Petersen, F. Ziegler 2010. “Einfluss thermischer Kälteerzeugung auf den Einsatz von KWK-Anlagen in Fernwärmenetzen“, *Proc. 11. Symposium Energieinnovationen*, Graz, Austria.

Petersen S., C. Caporal, F. Ziegler 2006. “Solar Cooling - results of a 10 kW absorption chiller combined with simulated solar thermal systems”, *Proc. Water and Energy for Sustainable Development, CIERTA 2006*, Camara de Almeria, Spain.

Petersen S., A. Hansske, C. Hennrich, W. Hüls, J. Stangl, M. Mittermaier, M. Helm, P. Zachmeier, S. Natzer, W. Lanser, F. Ziegler 2011. “Development of a 50 kW absorption chiller”, *Proc. 23rd Int. Conf. of Refrigeration*, Prague, Czech Republic.

Randløv P. 1997. Fernwärmehandbuch. European District Heating Pipe Manufacturers Association, Fredericia, Denmark. ISBN 87-90488-02-4.

Zegenhagen T., J. Corrales, S. Petersen, C. Ricart, F. Ziegler 2010. “Best Practice: Data Center Cooling using CHCP Technology”, *Proc. Sustainable Refrigeration and Heat Pump Technology Conf., 13-16 June 2010*, Stockholm, Sweden.

ACTIVITIES IN THERMAL DRIVEN COOLING AT FRAUNHOFER UMSICHT

Peter Schwerdt, Fraunhofer UMSICHT, Department of Energy-Efficiency-Technologies
Osterfelder Str. 3, D-46047 Oberhausen, Germany, peter.schwerdt@umsicht.fraunhofer.de

Abstract: Thermally actuated cooling processes have reached a promising maturity to offer an environmentally acceptable solution to the growing demand for air conditioning. Using solar thermal energy, district heating or waste heat from cogeneration or industrial processes avoids the large electricity of conventional compression chillers, prevents grid overloads in summer and helps to save primary energy.

Several thermal driven refrigeration processes have been investigated and realized by Fraunhofer UMSICHT since the 1990s, with cooling capacities of 1 to 1000 kW. Some examples of steam jet ejector chillers, an adsorption system set up in Egypt and a novel membrane-absorption process as well as thermal storage with PCS/PCM are presented.

Key Words: Thermal driven cooling, Solar cooling, Steam-Jet-Ejector chiller, Absorption cooling, Membrane pervaporation, Water-Lithium bromide

1 INTRODUCTION

In most OECD economies buildings account for about 40% of all energy use and are the largest single usage sector, more than industry or transport. Therefore, with respect to climate change and declining fossile energy resources, strong efforts have to focus on the improvement of energy efficiency and savings of primary energy in the building sector. In residential and commercial buildings the provision of thermal comfort and air quality accounts for the greatest energy use. Beside better insulation of the building envelope, improvements should focus on HVAC equipment and utilize non-electric energy sources such as solar energy, district heating water or waste heat of small CHP-plants.

2 REFERENCES AND PROJECTS IN THERMAL DRIVEN COOLING

Fraunhofer UMSICHT develops applied and custom-made process engineering technologies. Assuming a leading position in the fields of environmental and material technologies, process engineering and energy technology, Fraunhofer UMSICHT is committed to sustainable economic development and environmentally friendly technologies. The department Energy-Efficiency-Technologies focuses on the intelligent integration of energy systems into existing and new supply structures as well as their efficient utilization. Besides strong activities in Energy Efficiency, Renewable Energies and Electric Energy Storage there is continuous R&D work in the fields of thermal energy storage and thermal, resp. solar cooling.

In the 1990s researchers at Fraunhofer UMSICHT worked on several thermally driven refrigeration processes. In 1998 a first steam jet ejector chiller system (SJEC) with a maximum cooling capacity of about 600 kW was put into operation in the city of Gera, driven by steam of a municipal power station and serving a district cooling network in the city centre (Figure 1).

Figure 1: District cooling in the city of Gera with 600 kW steam jet ejector chiller

This system was also included in the “Study on Measurements of operational Optimization of Solar-thermal Driven Plants for Cold Generation”, which was embedded in the IEA Task 38 “Solar Air-Conditioning and Refrigeration”. Later on a SJE cooling system with a cooling capacity 1000 kW was designed and realized at a paper mill in Germany, driven by waste heat from a combined heating power plant.

Since 2002 a solar driven cooling system with vacuum tube collectors is being operated as a demonstration project at UMSICHT itself, feeding chilled water into the institutes air-conditioning (AC) network (Figure 2). The system consists of a collector field of about 100 m², supplying a 35 kW Yasaki WFC10 absorption chiller, and buffer tanks for heating water and chilled water. The system also allows free cooling and direct supply of hot water for heating purposes in spring or fall.

Figure 2: Solar Cooling demonstration plant at Fraunhofer UMSICHT with Yasaki WFC10 absorption chiller

Other projects focused on the development of a prototype SJEC with a small cold capacity of ~1 kW (with support by the Deutsche Bundesstiftung Umwelt), and two similar processes with ~5 kW (Pollerberg et al. 2009) and about 80 kW cooling power, see Figures 3 and 4

(supported by the Bundesministerium für Bildung und Forschung). The principle process diagram of a solar driven SJE chiller is given in Figure 5.

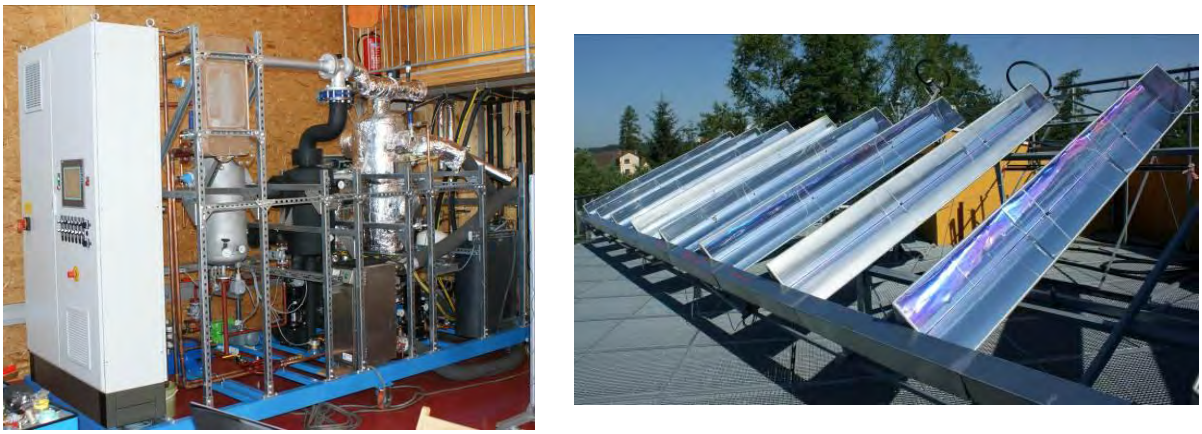

Figure 3: SJE chiller with 5 kW by Fraunhofer UMSICHT, as a contribution to the German-Austrian demonstration project "Solar Cooling" at Gleisdorf, Austria (Source: AEE Intec)

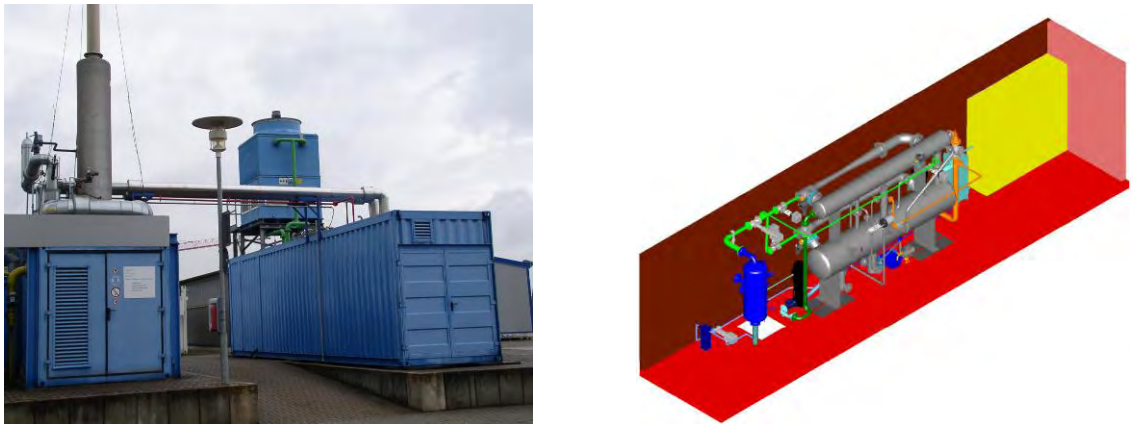

Figure 4: SJE chiller (cooling capacity of 80 – 200 kW) at Fraunhofer UMSICHT in standard container, driven by waste heat from a CHP unit

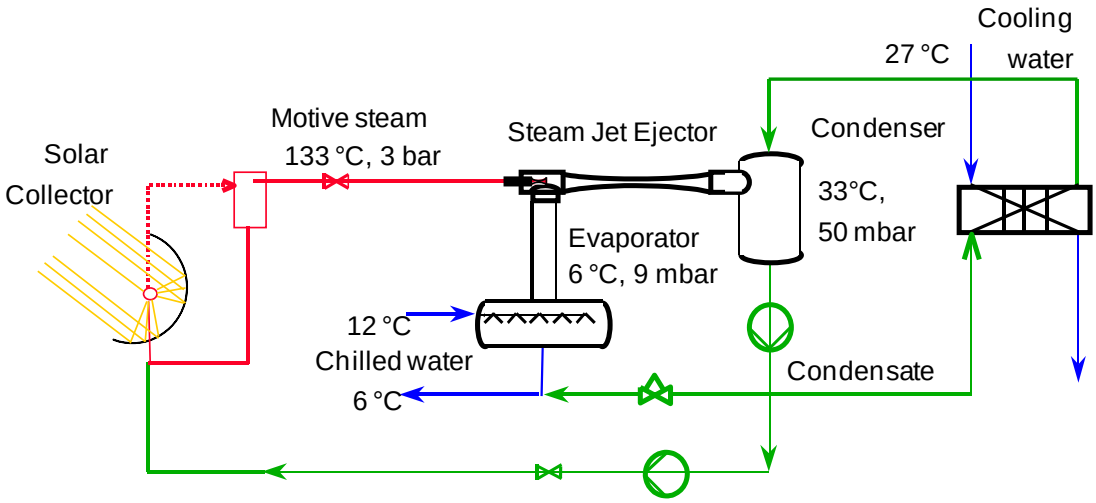

Figure 5: Process scheme of solar driven steam jet ejector chiller

In order to establish solar cooling of buildings as an energy-efficient and electricity saving technology in the Indian market, Fraunhofer UMSICHT and its cooperation partner »VSM Energy« founded the spin-off company VSM Solar PLC in 2011.

For demonstration purposes a solar driven cooling system of 60 kW will be installed at the companies building in Bangalore, supplying the AC with chilled water (Figure 6).

Figure 6: Design concept of company building with solar cooling – with roof mounted collector field (Fraunhofer JV VSM Solar, Bangalore, India)

In the frame of the German-Egyptian Joint Research Fund activities (GERF, supported by the Bundesministerium für Bildung und Forschung) a cooperation project was performed by the University of Assiut and UMSICHT. It aimed at the realization of an AC system powered by solar-thermal energy from a 40 m² vacuum tube collector field. The system with a 7.5 kW adsorption chiller as the key component was successfully put into operation in summer 2012, followed by long-term monitoring and performance measurements.

Figure 7: Solar cooling system at Assiut University (GERF demonstration project)

In continuing the R&D activities in thermal driven cooling processes a test bench for sorption heat pumps and chillers was set up in the department lab. For the time being it is used for experimental work with water/lithium bromide absorption cycles and their components, especially for the development of a membrane absorption process (as described below).

Figure 8: Test bench for sorption heat pumps and chillers at Fraunhofer UMSICHT lab

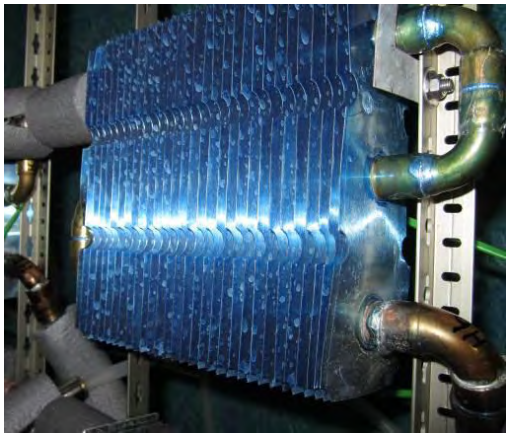

Figure 9: Long-term spray and performance tests on hybrid cooling towers for improved heat rejection of thermally driven chillers

To improve thermal transport and storage capacity of water based cold supply systems, intensive research work is being performed in the field of Phase Change Materials (PCM) respective slurries. Two demonstration plants are already realized based on ice-slurries for cold storage. Several actual projects are concentrating on Paraffin/water-dispersions for cold and heat storage, in various capacities, and with concern to e.g. thermal management of power batteries, mobile cooling, capillary tubes for wall/ceiling cooling, cold and heat storages with a small temperature shift (Kappels et. al. 2011).

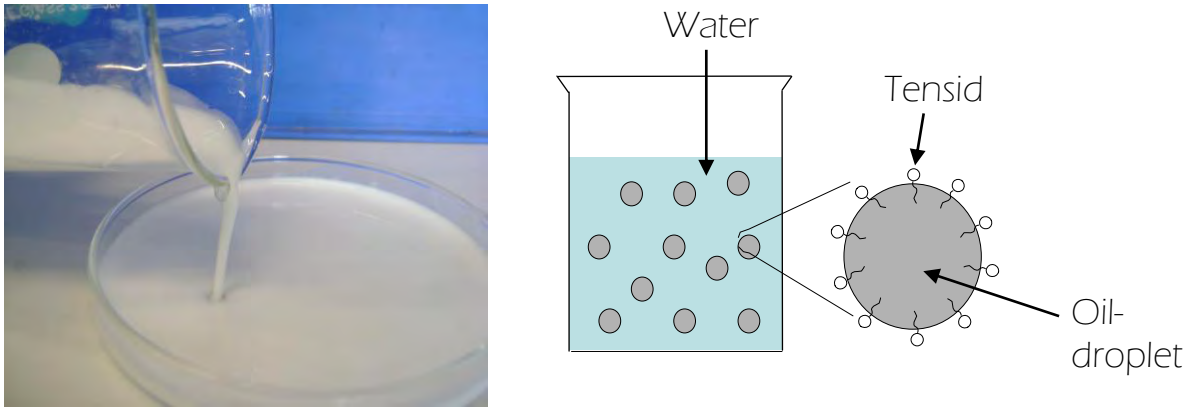

Figure 10: Paraffin/water-dispersion as phase change slurry for latent heat storage and transport

3 DEVELOPMENT OF A MEMBRANE ABSORPTION CHILLER

Since some years and mainly in Europe there is a strong scope on the development and market entry of small thermally driven heat pumps (i.e. cooling capacity 5-15 kW or more) which can be used for residential heating and cooling purposes.

Especially the water/lithium bromide (LiBr) absorption cycle, which is environmentally friendly and traditionally well established in large scale applications, still offers great promise as a high-efficient cooling process for small capacities as well. This technology could be used for non-electric driven residential cooling, driven by widely available low temperature heat. As a precondition, these units should be easy to install and to operate, which requires a significant reduction in size and weight, because space in private houses is strictly limited. Furthermore, reducing the initial costs is necessary to enable small absorption chillers entering the residential building market.

Fraunhofer UMSICHT is working on a new absorption process technology, aiming at replacing the traditional falling film shell and tube heat exchangers by a compact, stack-like design, using a pervaporation process with microporous membranes. A significant reduction of the unit size is expected by using flat plate modules. In this arrangement the refrigerant vapor (water) is passing through flat semipermeable membrane sheets to be absorbed in very thin LiBr-solution films, thus achieving large contact surfaces per volume for improved heat and mass transfer. To enable constant absorption, the heat of absorption is simultaneously transferred to the cooling water plate, forming the backside of the solution film. To achieve a certain absorption capacity several modules are integrated to one stack.

3.1 Membrane selection

Today a large variety of membranes is available for medical purposes or technical processes, such as filtration, desalination or sewage treatment plants. Also in the field of HVAC membrane technologies become more present, i.e. in so called enthalpy heat exchangers, recovering both heat and humidity in building ventilation systems or for cooling and air dehumidification in chilled ceilings.

In the beginning the focus was on selection of membranes which also meet the special requirements for use in a membrane absorber, as they especially must be compatible with the LiBr solution, reliably hydrophobic, mechanically stable and have a high refrigerant vapor transport capacity (flux). Like in conventional falling film absorbers also in a membrane sorption process the partial pressure difference is the driving force for the refrigerant mass transfer into (absorption) or from the solution (desorption). In pervaporation the driving force additionally has to cover the pressure drop caused by the membrane pores, which was evaluated in previous simulations of membrane absorption (Ali and Schwerdt 2009). A large variety of membranes from several manufacturers were investigated and characterized in a test cell to select the most suitable types.

Based on these results a modular stack design for membrane sorption was developed by adapting basic principles of plate heat exchangers and membrane filtration (Figure 11). The active membrane area was set to 180 x 250 mm (8 x 10“), corresponding to a common sheet format. From the results of previous screenings with various hydrophobic membranes a PTFE membrane with 0.45 µm pore size and 80% porosity was selected, which had had shown the best vapor flux, sufficient hydrophobicity and good mechanical stability. Design and assembling of the module components had to meet challenging requirements like being vacuum tight on the process side, leakproof and stable against the cooling water pressure.

After function testing of basic single-membrane-units a membrane sorption module with two active membranes, one cooling module and several variable features was built and tested.

3.2 Module design and experimental results

The performance of the membrane sorption process was experimentally investigated under realistic conditions of the external temperatures: T cold water : 9-17°C, T cooling water 28-32°C, T driving hot water 50-60°C. The external temperatures were supplied by two laboratory thermostats (Figure 12.). To cover both absorption and desorption conditions the operation parameters were varied in a wide range: starting from favorable absorption conditions the partial pressure difference was stepwise reduced and then inverted by increasing the solution and reducing the refrigerant temperature. This resulted in changing the absorption process smoothly to desorption, without interrupting the operation (Figure 13). The concentration of the supplied LiBr solution was in a range of 53-55 %.

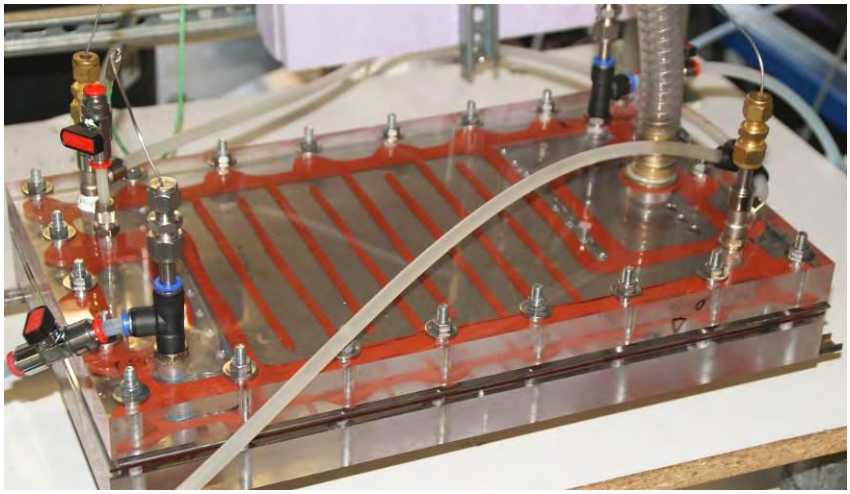

Figure 11: Membrane module for sorption performance testing in LiBr/H_2O-system

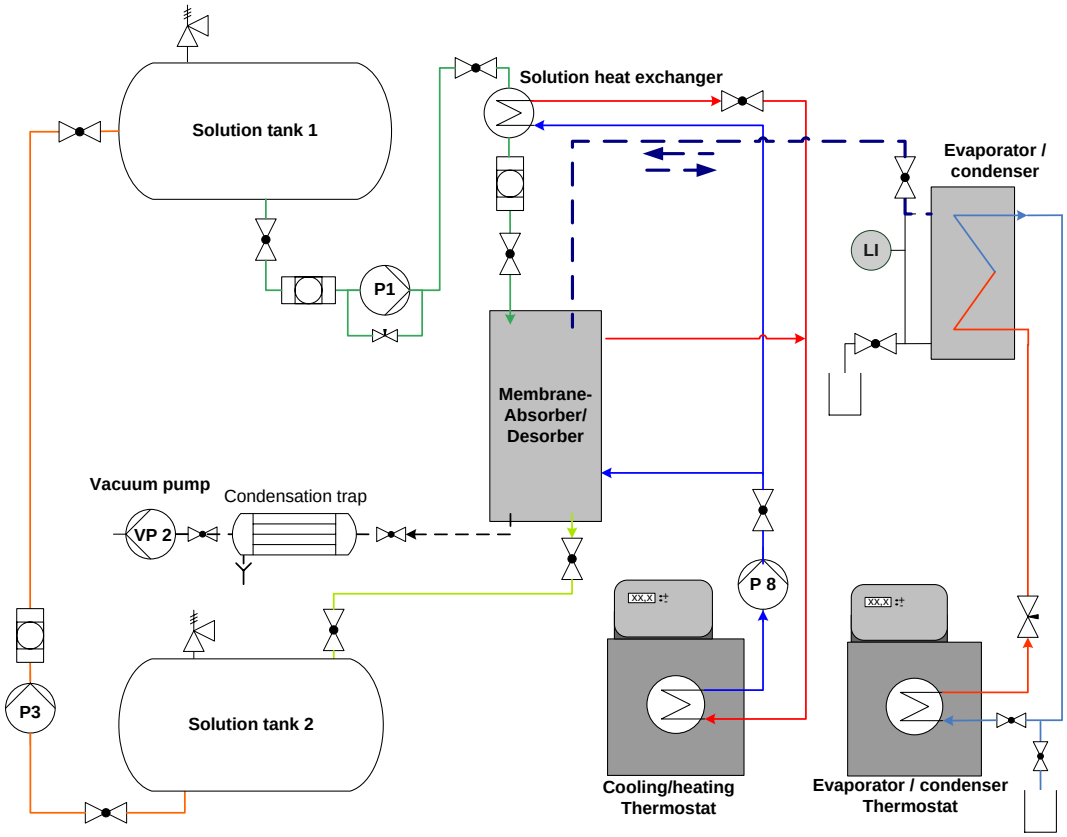

Figure 12: Experimental set up for membrane module investigation

The partial pressure difference as the driving force is calculated from the actual refrigerant vapor pressure p_v and the partial pressure of vapor in the solution p_s according to

$$\Delta p_{part.} = p_V - p_s \qquad (1)$$

The solution partial pressure is determined from the solution concentration and temperature. The vapor flux was measured to 2.25 kg/m²/h at driving pressure Δp_{part} of just 0.9 kPa for absorption and 1.5 kg/m²/h for desorption conditions and Δp_{part} of 1.6 kPa.

It is obvious that these relatively low flux values are in line with the low partial pressure difference as the driving force.

The measurements of the trans-membrane vapor flux (represented by the exchanged heat) were performed with several parameters varied, e.g. the solution flow, the solution concentration, the film thickness and the spacers used in the vapor and solution channels.

The membrane process allows both absorption and desorption, with a slightly better performance of absorption, as displayed in Figure 13. Although different types of membranes were used, their results almost show similar trends. From these first results the total absorber membrane area of the scheduled LiBr-Water sorption chiller of 5 kW cooling power could be estimated to about 3.3 m² at Δp_{part} of 7 mbar. The desorber would need about 4.2 m² at 11 mbar Δp_{part}.

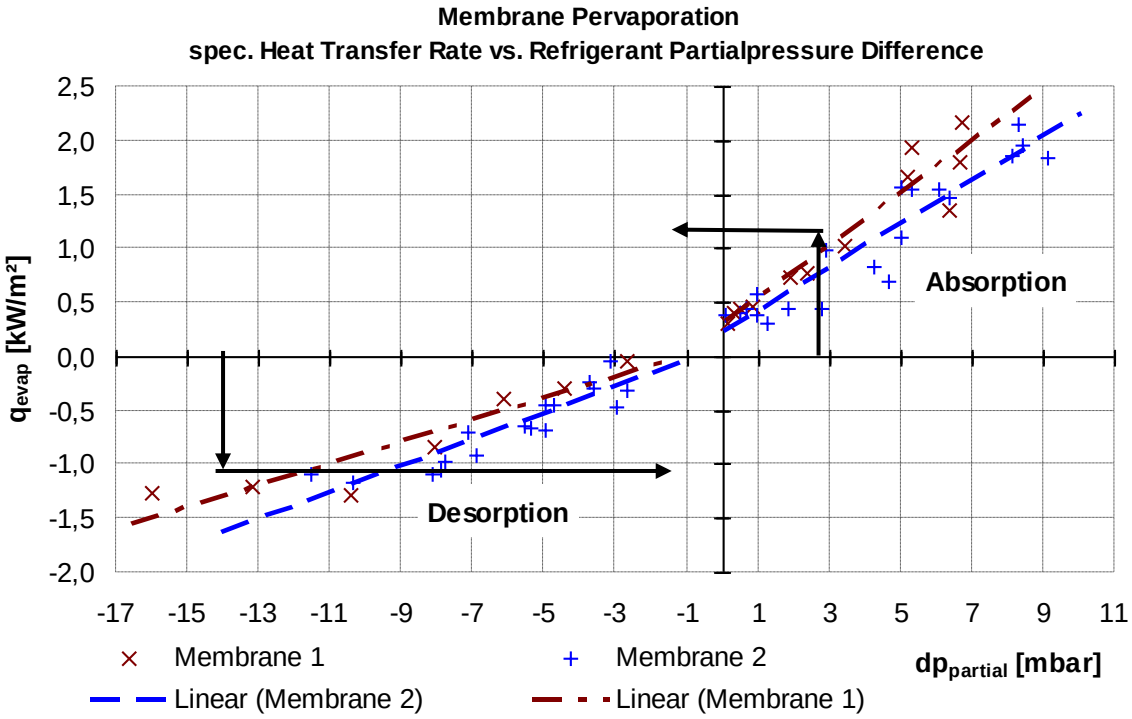

Figure 13: Performance of heat transfer rate vs. refrigerant partial pressure difference

3.3 Design concept for membrane-absorber and -desorber

For the layout-concept of a membrane sorption unit, like it is shown in Figure 14, some basic edge conditions were considered:

- absorption capacity of about 5.5 kW, desorption heat load of 5.9 kW
- flat plate stack with just a few different components made of stainless steel and non-metal materials
- all media connections (solution in/out, cooling/heating water in/out, refrigerant vapor) on the end plates
- cooling water module as a stable, pressure tight sandwich plate
- possible use of different types of membranes
- easy access of all media channels and spacers inside

With the required membrane area of about 3.3 m² and the actual component layout the membrane stack would consist of 76 membranes (absorber). To reduce this large number several modifications will be included to improve the module performance, like e.g. reducing the pressure drop of the vapor channel spacer. By a modified design the module thickness will be reduced additionally, so that the absorber stack will just have 56 membranes and a volume of 26 liters. The desorber would need 90 modules and 41 liters respectively. This

could be drastically reduced by allowing an increased heating water temperature, which is available from solar thermal plants or other heat sources.

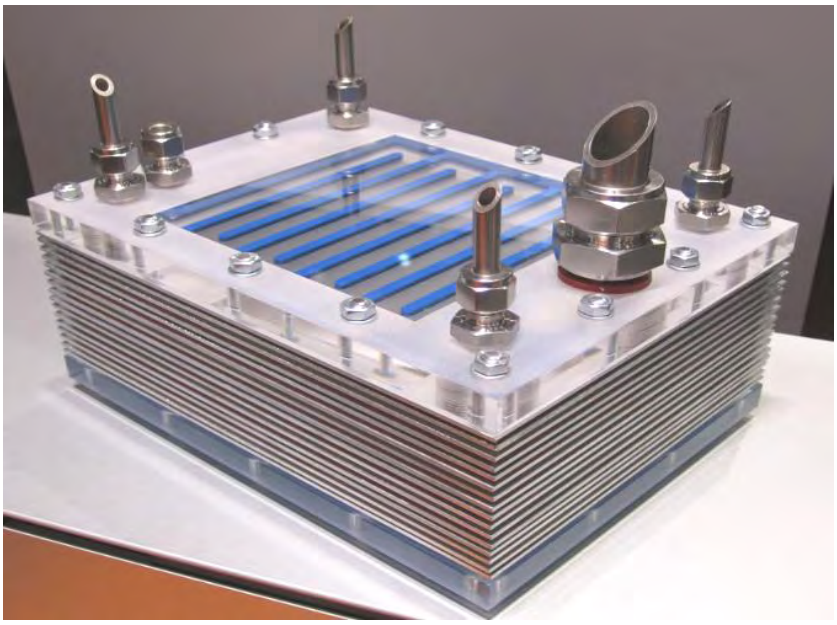

Figure 14: Design study of a multiple cell membrane stack for both absorption and desorption

3.4 Outlook

The membrane pervaporation process, realized in compact stack design with flat sheet membranes could replace the conventional falling film absorption and desorption apparatus in small scale chillers. The actual experiments with very low partial process driving pressures resulted in a vapour flux of 2.2 kg/m²/h heat flux, representing about 1.6 to 2.1 kW/m². The drafted module design seems promising as a basis for multiplication to achieve a nominal cooling capacity of 5 kW, producing chilled water of 17°C. Nevertheless the membrane module is subject to further modification concerning the membranes and the solution channel spacers. Emphasis will be put on increasing the vapour flux to reduce the number of required modules of the absorber and desorber stack.

4 SUMMARY

The worldwide growing demand for air conditioning requires the use of thermally driven cooling processes in order to save primary energy and to avoid overloads of the electrical grids. As an alternative to electrically driven compression cycles thermally actuated chillers could supply buildings and processes, powered by solar thermal energy, district heating or waste heat. Several technologies have been investigated and realized by Fraunhofer UMSICHT. In 1998 a steam jet ejector chiller (SJEC) with a cooling capacity of about 600 kW was erected in Gera (Germany). The system is driven by steam of a municipal power station and is serving a district cooling network. A similar process with about 1 MW was realized in a paper mill for cooling purposes. Small scale solar driven SJEC were built and tested at Fraunhofer UMSICHT and within an IEA cooperation project.

The institute´s solar cooling demonstration plant with a 35 kW Yasaki absorption chiller is operating since 2002. The system driven by solar energy from 100m² of vacuum tubes collectors and supplies cold water to the institute´s labs or feeds hot water into the heating system.

Recently Fraunhofer UMSICHT has started a joint venture with an Indian partner to promote solar/thermal cooling technology for the Indian Market. Actual research is focusing on PCM and PCS for heat or cold storage, thermo active building systems, thermal battery management etc.

A novel absorption process with water/lithium bromide is being developed for low capacity residential cooling, based on membrane pervaporation in compact, stack-type heat and mass exchangers.

5 REFERENCES

Ali A.H., P. Schwerdt 2009. “Characteristics of the membrane utilized in a compact absorber for lithium bromide-water absorption cooling chillers”, *Int. J. of Refrigeration*, Vol. 32, pp. 1886 – 1896.

Kappels T., C. Pollerberg, L. Hanu, Z. Youssef, A. Delahaye, L. Fournaison 2011. ”Phase change slurries as cold storage fluid with high energy density for solar cooling”, *ISES Solar World Congress (SWC)*, Kassel, Germany.

Pollerberg C., D. Jähnig, C. Dötsch 2009. ”Prototype of a solar driven steam jet ejector chiller”, *3rd Int. Conf. on Solar Air-Conditioning,* Palermo, Italy.

NEW ABSORPTION CHILLER AND CONTROL STRATEGY FOR THE SOLAR ASSISTED COOLING SYSTEM AT THE GERMAN FEDERAL ENVIRONMENT AGENCY

Jan Albers, Technische Universität Berlin, Institute of Energy Engineering, KT 2, Marchstraße 18, D-10587 Berlin, Germany, jan.albers@tu-berlin.de

Abstract: Typically the cooling capacity of absorption chillers is controlled by adjusting the driving hot water temperature according to the load. Meanwhile the cooling water temperature is controlled to a constant set value. In order to increase the solar cooling fraction and/or to decrease the operating costs of solar assisted cooling systems (SAC-systems) a new control strategy has been developed which controls hot and cooling water temperature simultaneously. Hereby the specific cost of cold – generated from solar or conventional heat – can be reduced. The basic concept of the strategy is explained and first results are shown for the SAC-system at the German Federal Environment Agency in Dessau. Here a recently developed absorption chiller is now used instead of a former adsorption chiller. With the new absorption chiller and the control strategy a seasonal energy efficiency ratio SEER above 0.75 is achieved. In addition the replacement of the adsorption chiller results in a 35% higher electric efficiency and a reduction of about 70% of the costs for spray water consumption in the reject heat device.

Key Words: Absorption Chiller, Adsorption Chiller, Monitoring, Control strategy, Cold Price

1 INTRODUCTION

The Federal Environment Agency is the scientific environmental authority that comes within the remit of the Federal Ministry of Environment, Nature Conservation and Reactor Safety (BMU). The main objectives of the agency are (see Umweltbundesamt (2006) for further information):

- to protect and nurture the natural basis for life now and for future generations,
- to promote sustainable development,
- to encourage everyone to consider environmental protection as a matter of course.

The Federal Environment Agency (UBA) relocated its main office from Berlin to Dessau in 2005. The architecturally unique headquarter of the Agency is located at a historic site in Dessau-Roßlau, the former ”Gas Quarter”. The number of employees here is approximately 750 (Umweltbundesamt 2006). The building itself is extremely well insulated. The energy demand is in between a low energy house and a passive house. The energetic requirements exceed those of the German Heat Protection Regulations by more than 50% and those of the Energy Conservation Regulations by some 40%. Mainly the heat demand for the building is supplied from a district heating network. The building ventilation system can be controlled separately for various areas. In order to reduce energy consumption, outside air is fed through a ground heat exchanger, one of the world’s largest. The pipes have a total length of 4800 meters and are used for pre-treatment of the air, which is heated in winter and cooled in summer. For certain ambient air conditions it is possible to bypass the ground heat exchanger.

Due to the ground heat exchanger the office rooms do not need any additional air conditioning. But for the high cooling loads of an IT-centre, teaching rooms and the lecture hall a solar-assisted cooling system has been designed. In addition electricity is supplied by a photovoltaic system integrated in the multi-pitched glass roof. Renewable energy sources (in the form of

solar power, solar heating and cooling as well as heat extracted from the ground) account for about 15% of the total energy demand (Umweltbundesamt 2006).

2 SOLAR COOLING CONCEPT

On first sight the cold demand of the Federal Environmental Agency seems to be unsuitable for solar cooling application, because it is relatively constant throughout the year and does not show up coherence with solar irradiation since it is dominated by the IT-centre. Therefore the basic idea of the cold supply concept was to use a hybrid dry/wet cooling tower in wintertime for direct cold supply in combination with a thermally driven chiller for summertime. Hereby a promising coherence of cold demand and available solar heat is re-established. During summertime the thermally driven chiller is powered either by district heat from a central CHP-plant in Dessau or by solar heat from a field of vacuum tube collectors (heat pipes, 216 m² absorber area, 3 x 7.5 m³ storage volume). A compression chiller is used for peak loads (e.g. at full occupation of the lecture hall) and as redundancy for the IT-centre. During wintertime the reject heat device is used directly for cold supply. In this case neither the compression chiller nor the thermally driven chiller is running (free cooling mode).

Due to a low supply temperature in the district heating network of Dessau (which is often below 75°C, e.g. in summertime) the decision was made to install an adsorption chiller in the beginning of the planning process. Using the experiences from a previous project (Wiemken and Henning 2005), an additional storage of 1 m³ size was installed in the hot water return flow from the chiller in order to dampen the temperature amplitude, which occurs during the heat recovery phase inside the adsorption chiller. Hereby a reliable operation of the system (with and without solar heating) was possible.

On the other hand the efficiency of the adsorption chiller was considerably lower as expected from manufacturer's data. In average the Nishiyodo adsorption chiller (type NAK-C 20) provided only about 60% of the expected cooling capacity and reached only about 70% of the expected coefficient of performance (COP). The low efficiency resulted in higher operating costs caused by an increased electricity and water consumption of the reject heat device in addition to the higher heat demand. Therefore, the adsorption chiller has been replaced in summer 2011 by a new H_2O/LiBr absorption chiller developed by the TU Berlin and ZAE Bayern (without any other change of the cold supply concept). This chiller was designed especially for district heating application and can be operated with driving temperatures below 65°C. Moreover a wet cooling tower is not necessary anymore (Petersen et al. 2011). Nevertheless, within the replacement project of the chiller at UBA the existing hybrid dry/wet cooling tower was retained and only the damping storage has been removed. The general control strategy for the whole SAC-system was kept unchanged.

2.1 System Control

Winter period (free cooling mode)
During wintertime the chiller is switched off and the cooling load is covered by free cooling operation of the heat rejection system. Consequently, there is no heat pump operation.

The heating demand is covered by district heating from a nearby CHP-plant mainly. During spring and autumn solar heating is also possible, if the temperature in the hot water tank is higher than the set value of the heating system. This set value depends on ambient temperature.

Summer period (chiller mode)
During summertime the heating system is switched off and the cold supply is performed mainly by the absorption chiller with peak load support from the electrical driven chiller. At nighttime the absorption chiller is normally driven by district heating. During day time the following control sequence is applied:

1) Starting the collector pump when global horizontal irradiation is higher than e.g. 200 W/m².
2) Switch on secondary solar pump, if collector outlet temperature is higher than the storage temperature in order to load the hot water storage tanks.
3) Switch off district heating and start with solar operation, when the storage temperature in first tank has reached the set value for driving the ad- or absorption chiller or is higher than the available temperature of the district heating system.
4) Solar operation is stopped, when the temperature in first storage tank is e.g. two degrees below the set value. After that, district heating is used until the next day.

2.2 Control strategy for the ad- and absorption chiller

The control strategy for the thermally driven chiller is independent of solar or district heating. In both cases the intention is to minimize the specific cost or the price p_{cold} for the generation of cold E_E. In general the strategy can be applied to any thermally driven cooling process, but has been explained first for the solar driven adsorption chiller at the Federal Environment Agency (Albers et al. 2009).

The price for cold is the ratio of operating costs C_{op} and generated cold E_E during a certain time period.

$$p_{cold} = \frac{C_{op}}{E_E} = \frac{\int \dot{Q}_D \cdot p_{th}\, d\tau + \int P_{el} \cdot p_{el}\, d\tau + \int \dot{M}_{mat} \cdot p_{mat}\, d\tau}{\int \dot{Q}_E\, d\tau} \approx \frac{\dot{Q}_D \cdot p_{th} + P_{el} \cdot p_{AC}}{\dot{Q}_E} = p_{cold,\,th} + p_{cold,\,el} \quad (1)$$

Here $\dot{Q}_E$ is the cooling capacity, $\dot{Q}_D$ the necessary heat flow to drive the chiller and P_{el} the necessary electricity (e.g. for the fans in any reject heat device) to reject the heat $\dot{Q}_{AC} = \dot{Q}_D + \dot{Q}_E$ from condenser and absorber to the environment. If a wet cooling tower is used an additional mass flow (e.g. water, chemicals etc.) may be necessary. Prices of thermal energy p_{th}, electricity p_{el} and of utilized material p_{mat} are applied to monetize these efforts. To derive the total price for cold generation in a certain moment, the specific costs of all input values have been divided by the load, which is assumed to be equal to the actual cooling capacity $\dot{Q}_E$ of the chiller.

For the basic concept of the control strategy some simplifications will be used:
- No electrical back-up system is considered.
- Electricity demand for supply pumps is neglected.
- Storage effects are neglected, i.e. quasi-steady state operation is assumed.
- Non-energetic or material input values are assumed to be proportional to the power P_{el} of the cooling tower. They are considered by a constant mixed price $p_{AC} = f(p_{el}, p_{mat}) = const.$

With these simplifications the right hand side of equation (1) is valid and might be re-written as

$$p_{cold} = p_{cold,th} + p_{cold,el} = \frac{p_{th}}{COP_{AKA}} + \frac{p_{AC}}{COP_{el}} \quad (2)$$

The total price for cold depends on the coefficients of performance (COP) which describes the part load behavior of chiller and reject heat device (RKW), in combination with the prices for materials as well as electrical and thermal energy.

For SAC-systems the price of thermal energy is also a mixed price. It can be derived from the price for back-up heat (e.g. district heat, gas consumption etc.) and the specific capital costs for the solar collector field p_{sol}. Thus it depends on the solar fraction D_{sol}. Without solar (i.e. $D_{sol} = 0$) the thermal price p_{th} equals the price for conventional back-up heat p_{conv}.

$$p_{th} = p_{sol} \cdot D_{sol} + p_{conv} \cdot (1 - D_{sol}) \quad (3)$$

The part load behavior of an absorption chiller can be described by the method of characteristic equations. It has been shown in Ziegler et al. (1999) that the cooling capacity is approximately a linear function of a so called characteristic temperatures difference $\Delta\Delta t$. This temperature difference combines the mean temperatures t_X (where X=D, A, C, E holds for Desorber, Absorber, Condenser and Evaporator of the chiller) with a constant Dühring parameter B. The Dühring parameter gives the slope of a mean sorbens isostere in a Dühring chart where the boiling temperature of the sorbens is plotted with respect to the dew point of pure refrigerant.

$$\Delta\Delta t = t_D - t_A - B \cdot (t_C - t_E) \quad (4)$$

A characteristic straight line for the cooling capacity of adsorption chillers is available also, if a modified characteristic temperature difference $\Delta\Delta t^*$ is used with inlet and outlet temperatures (instead of mean temperatures) in combination with a pseudo Dühring parameter B* (see label of x-axis in Figure 1). In contrast to B the parameter B* includes not only the boiling property data but also some information about the thermodynamic losses of the process. In Albers (2012) the determination of pseudo Dühring parameters B* for single stage cycles is described more in detail.

According to the characteristic equation

$$\dot{Q}_E = s_E \cdot \Delta\Delta t^* + r_E \quad (5)$$

the load condition (fixed by $\dot{Q}_E = \dot{Q}_{E,wanted}$ and $t_{Eo} = t_{Eo,set}$) can be matched by an arbitrary value of either t_{Di} or t_{ACi} (as long as both are inside the allowed operation interval). The only restriction for the remaining temperature is that it has to yield a certain $\Delta\Delta t^*_{set}$ which is determined by the demand $\dot{Q}_E = \dot{Q}_{E,wanted}$ and the part load behavior of the chiller (i.e. the characteristic equation). This degree of freedom in one temperature can be used to minimize the operating costs in any thermally driven chiller or heat pump.

For example it is seen from Figure 1 that the driving heat flow $\dot{Q}_D$ of the former adsorption chiller can be described by a characteristic equation also. But when plotted against the modified characteristic temperature, especially the loss parameter r_D shows up to be variable and not constant. This means that the necessary driving heat for a certain cooling capacity of e.g. 30 kW varies at fixed chilled water outlet temperature $t_{Eo,set}$ = 10°C as a function of driving and cooling water inlet temperature (in Figure 1 between approx. 80 and 90 kW). This variation of the loss parameter can be explained and described by an improved method of characteristic equations, which does not assume constant thermodynamic losses anymore, see Albers and Ziegler (2009), Albers and Ziegler (2011), and Albers (2012) for further information.

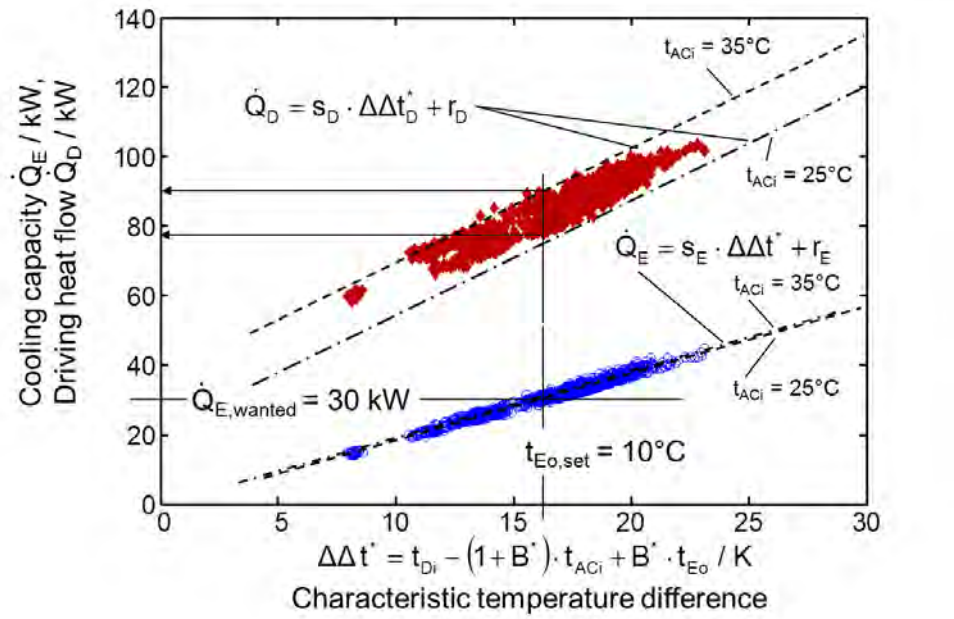

Figure 1: Characteristic lines and measured data of the adsorption chiller Nishiyodo NAK-020 at the German Federal Environment Agency

In the improved method of characteristic equations the loss parameters r_E and r_D are derived as explicit functions of the external inlet temperatures and the heat permeability (i.e. the UA-value) of each heat exchanger in the chiller.

$$\dot{Q}_E = s_E \cdot \Delta\Delta t^* + r_E(t_{Di}, t_{ACi}) . \tag{5}$$

$$\dot{Q}_D = s_D \cdot \Delta\Delta t^* + r_D(t_{Di}, t_{ACi}) . \tag{6}$$

From the energy balance of the chiller the reject heat flow can be described by the sum of these two equations, i.e. $\dot{Q}_{AC} = -(\dot{Q}_D + \dot{Q}_E)$. Moreover the outlet air temperature of the RKW $t_{air,out}$ is determined by the heat transfer effectiveness Θ_{air} and a ratio R'_{air} of air properties $(c_p \cdot \rho)_{air}$ with respect to the heat capacity flow rate of cooling water, $\dot{W}_{AC}$. Consequently, for a fixed load condition the power of the fans in a dry cooler is also a function of t_{Di} and t_{ACi} only.

$$P_{el} = e_{fric} \cdot \dot{V}_{air}^3 = e_{fric} \cdot \left(\frac{\dot{Q}_{AC}}{c_{p,air} \cdot \rho_{air} \cdot (t_{air,in} - t_{air,out})} \right)^3 = \left(\frac{\dot{Q}_{AC} \cdot \sqrt[3]{e_{fric}}}{R'_{air} \cdot \Theta_{air} \cdot [\dot{Q}_{AC} + \dot{W}_{AC} \cdot (t_{air,in} - t_{ACi})]} \right)^3 \tag{7}$$

Inserting the characteristic equations of the chiller (5) and (6) and of the dry air cooler (7) into equation (1) the price for cold generation can be derived as function of driving and cooling water inlet temperature (t_{Di} and t_{ACi}).

$$p_{cold} = \overbrace{\frac{\dot{Q}_D(t_{Di}, t_{ACi})}{\dot{Q}_E(t_{Di}, t_{ACi})} \cdot p_{th}}^{\text{thermal price}} + \overbrace{\frac{P_{el}(t_{Di}, t_{ACi})}{\dot{Q}_E(t_{Di}, t_{ACi})} \cdot p_{AC}}^{\text{electrical price}} = p_{cold,th}(t_{Di}, t_{ACi}) + p_{cold,el}(t_{Di}, t_{ACi}) \tag{8}$$

But only one of these temperatures is independent (t_{Di} is used here) because the other one (here t_{ACi}) is fixed by the required characteristic temperature difference or load, respectively.

$$t_{ACi} = \frac{1}{(1+B^*)} \cdot (t_{Di} - B \cdot t_{Eo,set} - \Delta\Delta t^*_{set}) = \frac{1}{(1+B^*)} \cdot (t_{Di} - B \cdot t_{Eo,set} - \frac{\dot{Q}_{E,wanted} - r_E}{s_E}) \quad (9)$$

To achieve a minimum price, the first derivative of equation (8) has to become zero, i.e.

$$\frac{dp_{cold}}{dt_{Di}} = 0 = \frac{dp_{cold,th}(t_{Di})}{dt_{Di}} + \frac{dp_{cold,el}(t_{Di})}{dt_{Di}} \quad . \quad (10)$$

This additional equation takes up the degree of freedom and determines the combination of $t_{Di} = t_{Di,opt}$ and $t_{ACi} = t_{ACi,opt}$ which gives the minimum total cold price p_{cold}. Consequently neither t_{Di} nor t_{ACi} are free to choose anymore. Both have to be adjusted to distinct values ($t_{Di,opt}$/$t_{ACi,opt}$) where the load $\dot{Q}_E$ is matched and at the same time the minimum price condition is fulfilled.

In Figure 2 the development of the total cold price p_{cold} is shown schematically as function of hot water inlet temperature t_{Di} together with the fractions $p_{cold,th}$ and $p_{cold,el}$ for given load and ambient conditions ($\dot{Q}_E$, t_{Eo}, and t_{amb}). Hence, these values can be used as constants in the derivative (10). With increasing driving temperature t_{Di} the cooling water temperature also increases (otherwise the cooling capacity or chilled water temperature would change). In addition the thermal price for cold $p_{cold,th}$ is increasing. This is a consequence of the increasing irreversibility in the sorption chiller (i.e. increasing $\dot{Q}_D$ for the same load $\dot{Q}_E$). Consequently the reject heat flow $\dot{Q}_{AC}$ is increased also. Nevertheless the specific electricity costs $p_{cold,el}$ are decreasing due to an increasing cooling water temperature t_{ACi}, which results in a higher driving temperature difference in the dry air cooler (since t_{amb} is constant).

It has to be mentioned that the location and the value of the minimum price depends not only on the governing technical variables (such as s_X, e_{fric}, Θ_{air} etc.) or economic variables, such as first costs and energy prices (p_{th}, p_{el} etc.), but also on the current load and ambient condition ($\dot{Q}_{E,wanted}$, $t_{Eo,set}$, t_{amb}). Consequently, both temperatures t_{Di} and t_{ACi} have to be controlled simultaneously to set values $t_{Di,set} = t_{Di,opt}$ and $t_{ACi,set} = t_{ACi,opt}$ at any time the chiller is in operation.

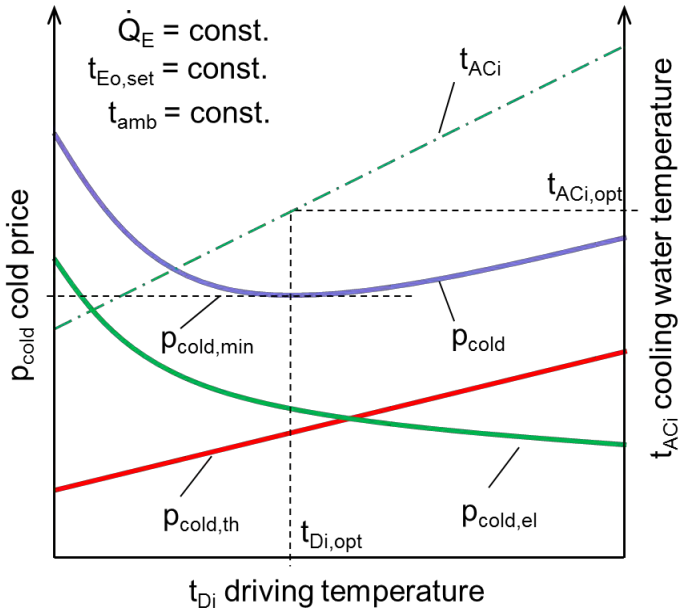

Figure 2: Hot and cooling water temperatures for a minimum cold price

3 MONITORING CONCEPT

The SAC-system at the Federal Environment Agency was monitored from the beginning of operation. The data acquisition is in full operation since August 2005. In addition to the conventional plant management system, for the control of pumps, valves, flaps etc. mainly heat flow meters have been installed for monitoring (see Figure 3). The aim was to achieve complete energy balance for all hot, chilled and cooling water circuits especially for the thermally driven chiller.

The temperature probes for heat flow measurements are paired and calibrated Pt-100 sensors. Together with ultrasonic or magnetic inductive flow meters they are connected to heat-meters, where the heat flow is calculated according to the implemented property data. Standard signals of 4-20 mA are provided by the heat-meters for the values of

- t_{Xc} cold flow temperature in °C
- t_{Xh} hot flow temperature in °C
- $\dot{V}_x$ volume flow rate in m³/h
- $\dot{Q}_x$ heat flow in kW

where X holds for the positions of the heat flow meter (e.g. X = K = solar collector, see Figure 3). In addition to t_{Xh} and t_{Xc} inlet and outlet temperatures t_{Xi} and t_{Xo} are measured by NTC-sensors in parallel. They have a lower accuracy, since they are used only by the plant management system to operate the HVAC units, chillers etc. but not to calculate heat balances. For the acquisition of global horizontal solar irradiation a pyranometer (WMO secondary standard) has been installed on the roof. Electricity consumption is measured by smart electric meters, which also provide the power P in some positions. All data can be visualized on a PC-monitor and a SQL data base is generated in a 1-minute time interval, which is used for data evaluation.

4 RESULTS

The control strategy has been adapted from the adsorption chiller to the absorption chiller just by implementing new slope and loss parameters of the characteristic equations (i.e. s_X and r_X) into the control system. Figure 4 shows a typical summer day in 2012 with a daily sum of global horizontal irradiation q_{gh} = 6.4 kWh/m² and a mean ambient temperature of t_{amb} = 19°C (min/max: 13/25°C).

According to the load and the available supply temperature (from solar heating t_{PSh} or district heating t_{FWh}) the driving and cooling water temperature of the chiller is controlled simultaneously in a range of 55°C < t_{Di} < 75°C and 20°C < t_{ACi} < 28°C, respectively. In contrast the chilled water outlet temperature t_{Eo} is relatively constant and close to the set value.

Due to a high storage temperature t_{PS11}, from the previous day, solar operation is ongoing until 5 a.m. When the storage tank temperature t_{PS11} is not high enough anymore and below the district heating supply temperature t_{FWh}, the solar operation is stopped. It is re-started at 11:30 a.m. where t_{PS11} is sufficiently high enough anew. In the very beginning around 11:30 a.m. the solar supply temperature t_{PSh} is considerably lower as t_{PS11} because of heat losses in the pipe section between solar heat storage and chiller. Thus, for a short moment the available supply temperature is lower than the necessary one to match the load (i.e. $t_{PSh} < t_{Di,opt}$). The lag of heating capacity is balanced by a lower set value for the cooling water (i.e. $t_{ACi,set} < t_{ACi,opt}$). Thus the RKW can be used for back-up purposes also. Since the deviation between $t_{Di,opt}$ and t_{PSh} is large during this switching phase, $t_{ACi,set}$ is calculated so low that the humidifier of the hybrid dry/wet cooling tower is switched on for a moment ($\gamma_{wet} > 0$). This happened again at approximately 8 p.m. where the solar operation was stopped for a short moment after the primary collector pump was switched off. In turn this is a complex effect of hydraulics and heat losses during idle periods in the hot water circuit.

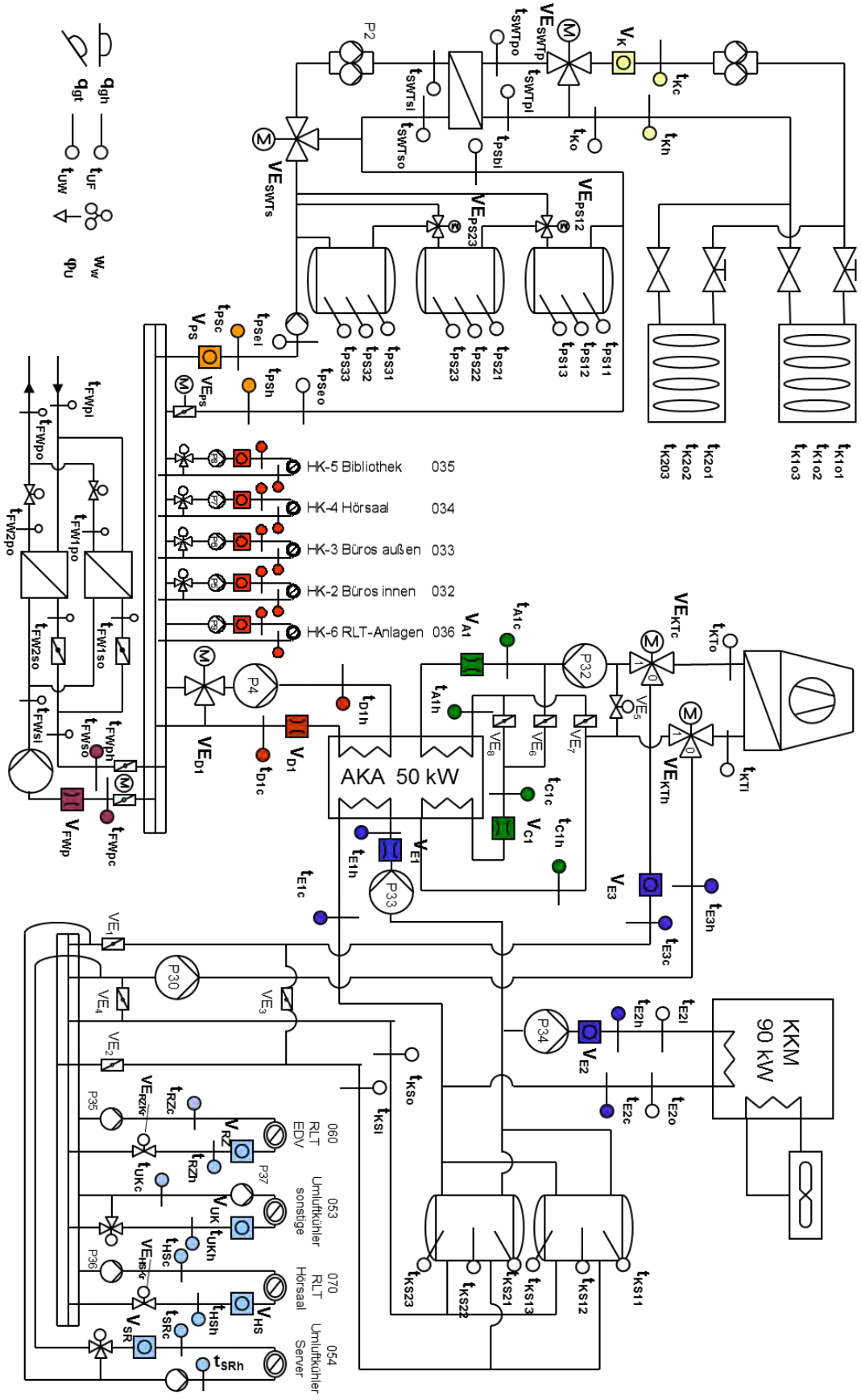

Figure 3: Monitoring scheme for the SAC-system at the Federal Environment Agency in Dessau

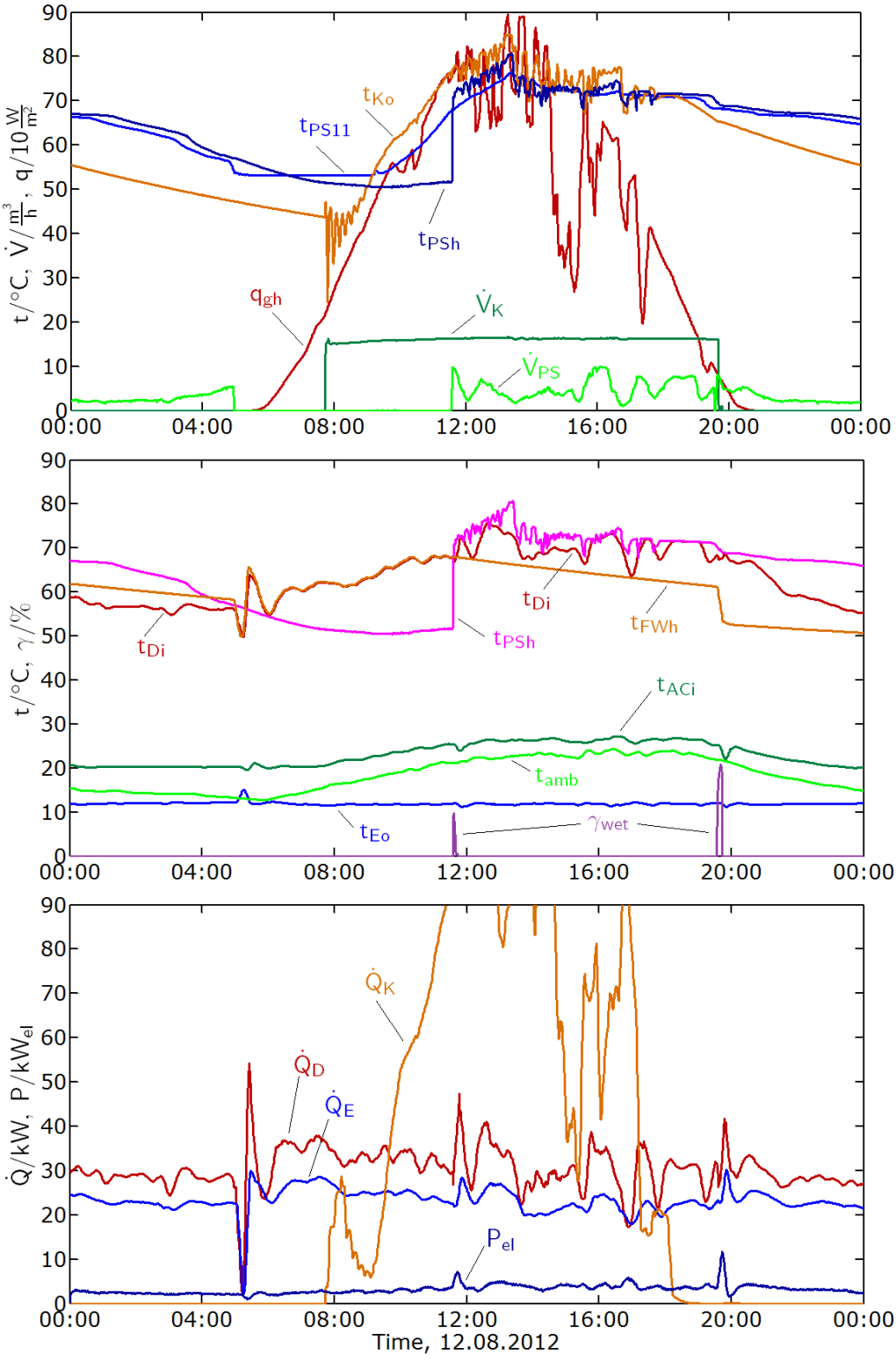

Figure 4: Monitoring Data of new absorption chiller and improved control strategy

At higher ambient temperatures the humidifier was also operated continuously in order to match the optimum cooling water temperature. Nevertheless the spray water consumption has been reduced considerably without any change of the humidifier control itself. Especially during months with moderate ambient temperatures the reduction due to the new absorption chiller in combination with variable cooling water temperatures is large (see Figure 5).

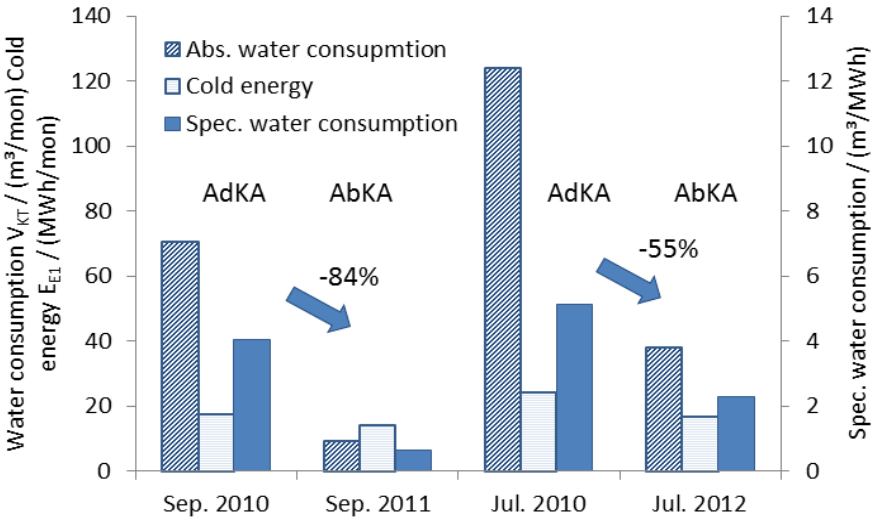

Figure 5: Reduction of water consumption for the hybrid dry/wet cooler (AdKA=adsorption chiller, AbKA=absorption chiller)

The operation of the new absorption chiller started in July 2011. Thus, for a summarizing evaluation of the chiller replacement the operating data of the first year (i.e. from 01.08.2011 to 31.07.2012) are used. Unfortunately a frost damage occurred inside the hybrid dry/wet cooling tower during a very cold time period in February 2012, where $t_{amb} < -18°C$. As a consequence thermally driven cooling was not possible until mid of June 2012 and the total amount of generated cold from the new absorption chiller is significantly lower as in the previous year (upper part in Table 1).

Tab. 1: Evaluation of operating data after chiller replacement

	Previous year with adsorption chiller Aug. 2010 – Jul. 2011	First year with new absorption chiller Aug. 2011 – Jul. 2012	Change
Cold generation	104 MWh_0	59 MWh_0	
Driving heat	221 MWh_{th}	80 MWh_{th}	
Thermal efficiency	0,47 MWh_0/MWh_{th}	0,76 MWh_0/MWh_{th}	+62%
Electrical efficiency	2,3 MWh_0/MWh_{el}	3,1 MWh_0/MWh_{el}	+35%
Water consumption	4,0 m^3/MWh_0	1,3 m^3/MWh_0	–68%

Nevertheless the specific data in Table 1 show that the seasonal thermal efficiency of the absorption chiller is remarkably higher in comparison to the former adsorption chiller. In addition the electrical efficiency has been improved by approx. 35%. But as seen from Table 2 the total specific electricity demand for (solar) thermal cold generation is still in the same range as for the compression chiller.

This has two reasons: On the one hand side, free cooling operation with a low electricity consumption of $e_{RKW} < 0.05 – 0.1$ as in the previous years was not possible during the breakdown period of the reject heat device. On the other hand the relatively high specific electricity demand for thermally driven cooling during June and July due to high ambient temperatures is not balanced by the lower values which could have been achieved in spring 2012. Therefore a further reduction in specific electricity consumption is expected for the following period.

Tab. 2: Specific electricity demand with absorption chiller

Electricity consumer		kWh_{el}/kWh_0
Reject heat device	e_{RKW}	0,17
Chilled & cooling water p.	e_{P32+33}	0,09
Hot water pump	e_{P4}	0,01
Pumps in solar circuits	e_{P1+2}	0,05
Compression chiller	e_{KKM}	0,29

5 CONCLUSIONS

The replacement of an adsorption chiller by a new developed absorption chiller at the German Federal Energy Agency in Dessau has increased the energy and cost efficiency considerably. In addition a control strategy with simultaneously controlled hot and cooling water temperature has been implemented successfully. Despite of variable driving temperatures from the solar collector field and limited supply temperatures in the district heating network during summer-time, the chilled water outlet temperature was kept sufficiently constant. A lower cooling water set value for the reject heat device is used for this purpose if necessary. As a consequence the optimum temperature combination of hot and cooling water could not be reached continuously under these conditions. Nevertheless the advanced control algorithm tracked the chiller in the direction of minimum costs as far as possible. But due to the increasing electricity demand with decreasing cooling water temperature the possibility of primary energy savings with the SAC-system is limited under the economic constraint of minimum price. Therefore future work will concentrate on a higher overall electrical efficiency – especially of the hybrid dry/wet reject heat device. On the other hand the economic optimum temperature combination is not expected to be the same as necessary for maximum primary energy savings. Consequently an objective function has to be included which combines both goals.

6 ACKNOWLEDGEMENT

The investigation was carried out with financial support from German Ministry for Economics and Technology (BMWi-Project 0327460B) and Federal Energy Agency (FKZ 363 01 222).

7 REFERENCES

Albers J., H. Kemmer, F. Ziegler 2009. “Solar-driven adsorption chiller controlled by hot and cooling water temperature”, *Proc. 3rd Int. Conf. Solar Air-Conditioning*, Palermo, Italy, pp. 338-343.

Albers J., F. Ziegler 2009. “Influence of internal irreversibilities on the characteristic equation of absorption chillers”, *Proc. Heat Powered Cycles Conference*, Berlin, Germany, paper 420.

Albers J., F. Ziegler 2011. “Heat transfer calculation for absorption heat pumps under variable flow rate conditions”, *Proc. Int. Sorption Heat Pump Conf*, Padua, Italy, pp. 813-822.

Albers J. 2012. “Improvement of a calculation method for the control of absorption chillers”, PhD-thesis in German, Technische Universität Berlin, Fakultät III Prozesswissenschaften, Institut für Energietechnik, to be published.

Petersen S., A. Hansske, C. Hennrich, W. Hüls, J. Stangl, M. Mittermaier, M. Helm, P. Zachmeier, S. Natzer, W. Lanser, F. Ziegler 2011. “Development of a 50 kW absorption chiller”, *Proc. 23rd Int. Conf. of Refrigeration*, Prague, Czech Republic.

Umweltbundesamt (Ed. Möcker V.) 2006. Federal Environment Agency – For people and the environment, Umweltbundesamt Dessau, Germany.

Wiemken E., H.-M. Henning 2005. “Solar assisted cooling at the University Hospital Klinikum Freiburg”, *Proc. Int. Conf. Solar Air-Conditioning*, Staffelstein, Germany, pp.178-182.

Ziegler F., C. Schweigler, H.-M. Hellmann 1999. “The characteristic equation of sorption chillers”, *Proc. Int. Sorption Heat Pump Conf.*, Munich, Germany, pp. 169-172.

SOLAR HEATING AND COOLING WITH ABSORPTION CHILLER AND LATENT HEAT STORAGE

Martin Helm, Kilian Hagel, Stefan Hiebler, Christian Schweigler
Bavarian Center for Applied Energy Research (ZAE Bayern), Walther-Meissner-Str. 6
D-85748 Garching, Germany, helm@muc.zae-bayern.de

Abstract: Performance figures and control strategies of an innovative solar heating and cooling system (SHC-System) composed of an aqueous lithium bromide-water single-effect absorption chiller with 10 kW cooling capacity, a dry heat rejection system and a low phase change temperature (28-29°C) latent heat storage based on salt hydrates are given. During cooling season the latent heat storage serves as a secondary heat sink supporting the dry air cooler at high ambient temperatures to ensure 32°C coolant to the absorption chiller at any time. In the heating season the latent heat storage buffers heat surplus of the solar collectors latently by melting the phase change material (PCM) calcium chloride hexahydrate. As a result of the constant temperature during charging, solar thermal collector efficiency is increased and furthermore the overall heat dissipation is reduced. The results on the one hand show a positive effect on the cooling capacity, electrical and thermal Coefficient of Performance (COP) of the absorption chiller, which are significantly increased especially at hot days compared to solely dry air cooled systems. On the other hand a high solar fraction in the heating period, due to constantly low storage temperatures, is achieved.

Key Words: dry air cooler, low temperature latent heat storage

1 INTRODUCTION

In SHC-Systems, solar heating as well as solar cooling are provided synergistically yielding a complete annual utilisation. The solar gain during the cold season serves for space heating. In order to cope with the mismatch of solar gain and building heat demand voluminous heat storages with up to 100 litre per square meter collector area are necessary. Increasing storage temperature during the loading process results in high thermal losses of the collector system and reduced system efficiency.

During the warm season the solar heat is converted into useful chilled water for air conditioning by means of sorption cooling devices. These devices typically require an open wet cooling tower to dissipate the reject heat to the ambient. Yet, water consumption, the need for water make-up and cleaning, formation of fog, and the risk of legionella bacteria growth are hindering factors for their use. If a dry air cooler is applied, the chilling capacity of the same sorption machine decreases up to 40 % due to significant higher coolant temperatures.

To overcome both problems a low-temperature latent heat storage based on phase-change-materials (PCM) can be applied to cope with the given system requirements: During heating operation the storage temperature of the latent heat storage remains constant while gathering solar surpluses. Thus a low operating temperature of the solar thermal system is accomplished yielding efficient operation with optimum solar gain. In cooling mode the latent heat storage serves as an additionally reject heat sink for the absorption chiller in addition to the dry cooling system and allows a staggered reject heat dissipation. By that means a part of the heat rejection of the chiller is shifted to periods with lower ambient temperatures, i.e. night time or off-peak hours, and thus the necessity of a wet cooling tower is eliminated allowing for a substantial reduction in operational effort, water consumption and cost.

2 INNOVATIVE CONCEPT

Open wet cooling towers are designed for coolant supply/return temperature 27/35°C. When a dry air-cooler is to be used, cooling water temperature increases to 40/45°C in Mediterranean climate. As a consequence of the increased cooling water temperature, the temperature level of the driving heat supplied to the regenerator of the absorption chiller has to be increased to about 105°C accordingly. Finally, the low collector efficiency at this temperature has to be compensated for by installing more than 20% additional collector area. Otherwise the cooling capacity of the chiller decreases by about 40%. The application of a latent heat storage supporting the dry air cooler allows a reduction of the coolant temperature to 40/32°C, avoiding a major decrease of the chiller's capacity during hot ambient conditions. At ambient temperatures of 32°C the dry air cooler provides a coolant temperature of 36°C and the latent heat storage serves for additional cooling of the cooling water from 36°C down to 32°C. Independently from the operation of the latent heat storage, the dry air cooler may provide a further reduction of the coolant cycle temperatures during off-peak hours with moderate ambient air temperatures. The stored reject heat is then discharged during off-peak operation or night time when more favorable ambient temperature conditions are available. A simplified system structure for a solar cooling system with a latent heat storage supporting a dry air cooler in the reject heat cycle is given in Figure 1.

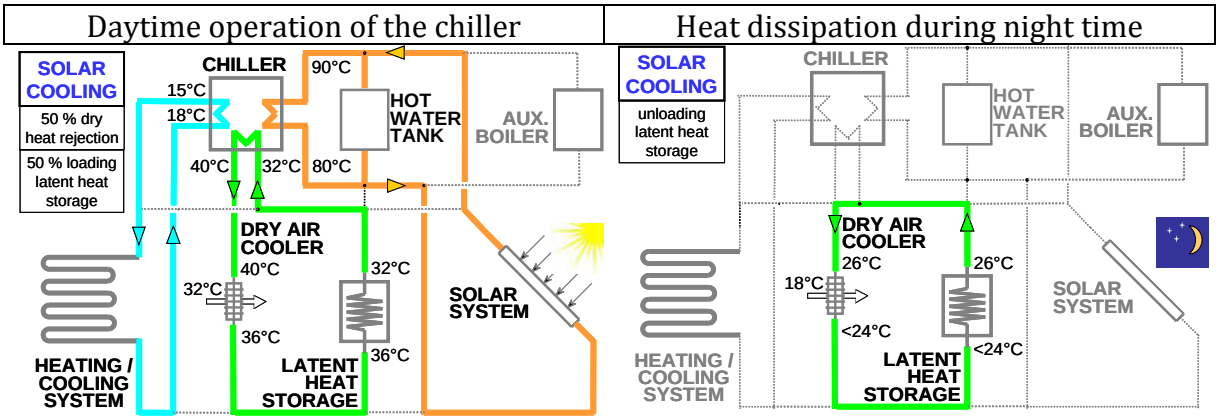

Figure 1: System scheme for solar cooling supported by a latent heat storage

During the heating season, the latent heat storage buffers the solar surplus heat and balances the heat supply to the consumer by boosting the return temperature of the heating system (see Figure 2). The design of the latent heat storage is based on an internal phase-change temperature of about 29°C. Thus, a low operating temperature of the solar thermal system is accomplished yielding efficient operation with optimum solar gain.

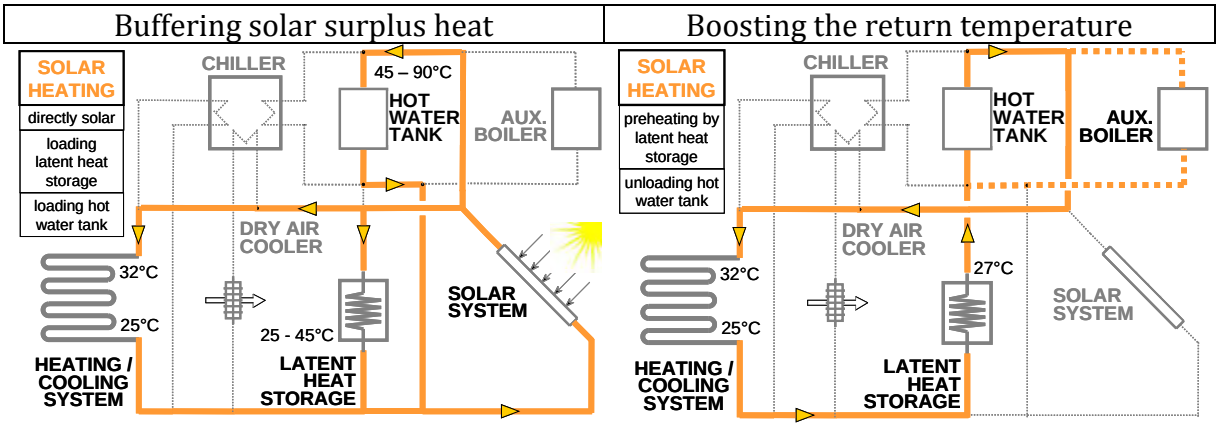

Figure 2: System scheme for solar heating with latent heat storage

3 PILOT INSTALLATION

Within the framework of the German “Solarthermie 2000plus” Program a pilot installation of an innovative solar heating and cooling (SHC-System) has been erected at the office building of the Bavarian Centre for Applied Energy Research (ZAE Bayern) in Garching (near Munich), Germany in 2007. The installation simultaneously serves as a field test project for a compact water/LiBr absorption chiller with 10 kW nominal capacity designed by ZAE Bayern in collaboration with SK Sonnenklima and TU Berlin (Schweigler et al. 2002, Kühn et al. 2005). Furthermore, the performance, cycle stability and the material's chemical resistance/durability of a new developed low temperature latent heat storage based on the salt hydrate calcium chloride hexahydrate is tested.

The two-floor office building (see Figure 3) was completed in the year 2000. At this time its wooden wallboard construction exceeds the prevailing German low-energy standard. The thermal insulation for the building envelope is dimensioned to U = 0.18 to 0.20 $W \cdot m^{-1} \cdot K^{-1}$. The glazing has insulating properties of U = 0.4 and 0.9 $W \cdot m^{-1} \cdot K^{-1}$. Passive utilization of solar energy is done by storing heat from solar radiation in the concrete core and in the insulated base plate. Therefore, the building heat demand is comparable to the German "3-liter-house" class, which limits the annual correspondent domestic fuel oil consumption for space heating to 3 liters per square meter living area.

Figure 3: ZAE Bayern office building and solar thermal flat plate collectors on the rooftop

As heating and cooling equipment, for the in total 400 square meters of office space, activated ceilings are installed. This allows moderate system temperatures in both modes. In the heating season the maximal supply temperature is set dependently on the ambient conditions based on a characteristic heating curve gradient of 0.5 and in cooling mode to 15°C by default, but at least 1.5 K above dew point temperature. As backup system in times of insufficient solar energy a pellet boiler for heating and a well for additional chilled water during the cooling season are available.

The pilot installation provides solar assisted heating and cooling with a total of 57 square meters of aperture area consisting of 24 anti-glare coated flat plate collectors oriented +10° to the south with 40° inclination.

The solar-driven single-stage absorption chiller with working pair aqueous lithium bromide as sorbent and water as refrigerant with a nominal chilled water capacity of 10 kW is designed to cover a base load coverage of 50% referred to the maximum cooling load of the building (20 kW). The chiller provides chilled water supply/return temperatures 18/15°C in full load, driven by solar heat gained from the flat plate collectors at supply/return temperatures of 90/80°C. The occasional fluctuations in radiation and heat consumption are buffered by a hot water tank connected in parallel to the solar thermal collectors.

In conventional absorption cooling installations, wet cooling towers designed for coolant supply/return temperature 27/35°C are applied as heat rejection system. Water consumption and high maintenance costs as well as the risk of bacteria notably legionella growth and legal restrictions are hindering facts for an extensive use of this kind of solar cooling. When an almost maintenance-free dry air-cooler is to be used, cooling water temperature has to be increased above ambient air temperature for sensible heat dissipation.

Having regard to an economic size of the heat exchanger area of the dry air cooler (195 m²) a driving temperature difference of 8 K between cooling water outlet and ambient air temperature is required. In view of this fact and considering the hottest weather data for the location Garching (Munich) of +32°C the temperature level in the reject heat circuit rises to 40°C. This increase of the cooling water temperature negatively affects the performance of the chiller especially on days with high cooling load.

By integrating a latent heat storage with a phase change temperature between 28°C and 29°C in serial to the dry air cooler a second heat sink is available to ensure a constant coolant temperature level of 32°C yielding constant chilling capacity even at rising ambient temperatures. The latent stored reject heat can be discharged during off-peak operation or night time when more favorable ambient conditions, i.e. lower ambient temperatures or electricity tariff, are available. The melting temperature of the aqueous salt solution calcium chloride hexahydrate ($CaCl_2$•$6H_2O$) fits perfectly for the given application (see Figure 4). This low-cost technical phase change material (PCM) provides a latent heat of about 150 J/g or 240 J/L and is used in food industry, medicine and farming for several purposes as well.

The heat storage capacity is set to cover 50 % of the nominal reject heat capacity of the chiller and a heat content of 120 kWh in the temperature range between 22 °C and 36 °C. Within the current project a matrix of polypropylene capillary tubes with an outer diameter of 4.3 mm serves as heat exchanger between the polypropylene glycol coolant and the phase change material. Despite the total heat exchanger area of more than 30 m² the capillary tubes occupy less than 5% of the whole storage volume.

Melting range	28... 29°C
Melting Enthalpy (by weight)	150 kJ·kg^{-1}
Melting Enthalpy (volumetric)	240 kJ·Litre^{-1}
PCM costs	0.30 €·kg^{-1}
Volume	1.4 m^{-3}
Mass	2.2 tons

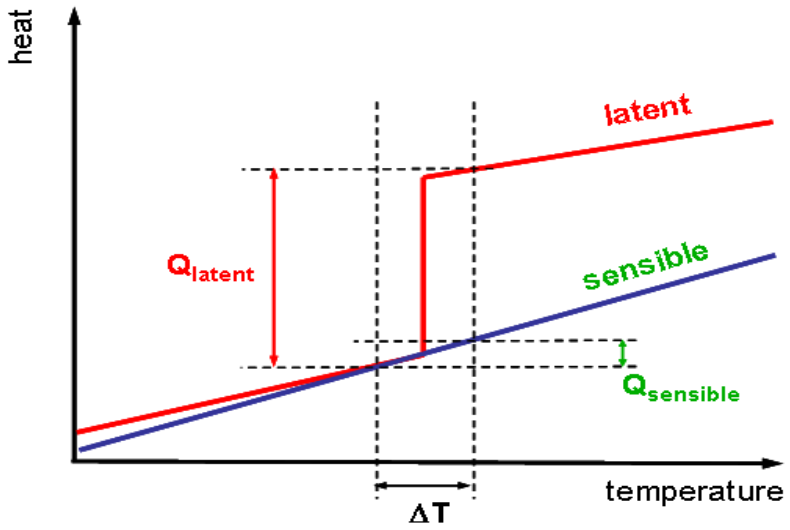

Figure 4: Selected storage data and principle of latent and sensible heat storage

The heat exchanger is finally enclosed by a modified PVC plastic bag and immersed in a cubic sandwich-panel structure which contains 1400 liters of phase change material (see Figure 5). Based on the low specific cost of 0.30 Euro per kilogram calcium chloride hexahydrate the investment costs for the complete filling does not exceed 500 Euro.

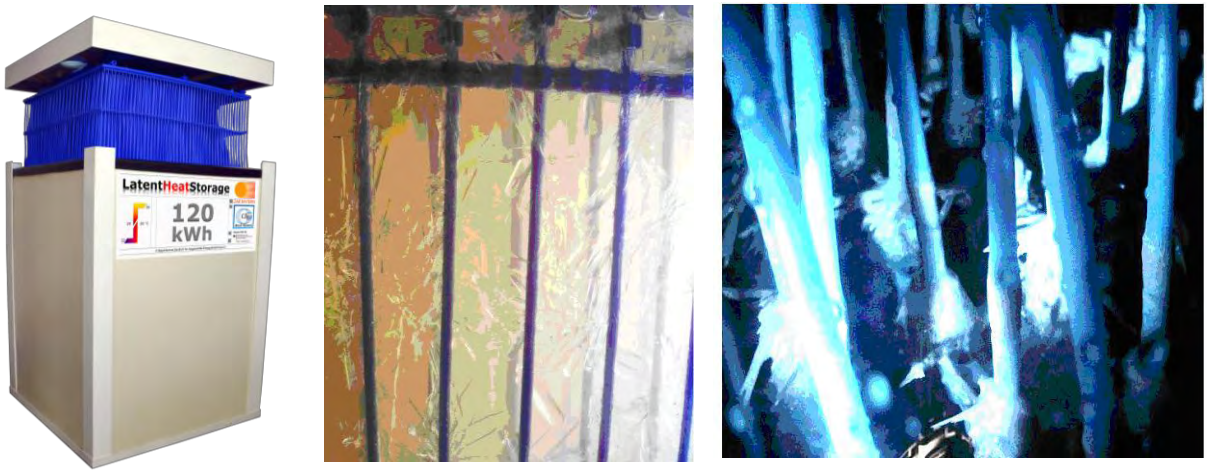

Figure 5: Latent heat storage and capillary matrix surrounded by crystallized salt hydrate

In heating mode the available solar thermal energy is used for direct heating or preheating of the building's heating system. Solar surpluses are primarily stored at constant low temperature (29°C) in the latent heat storage. Thus a low operating temperature of the solar thermal system is accomplished yielding efficient operation with optimum solar gain. In addition to the latent heat the phase change material can be heated up sensibly to 45°C. Further solar surpluses are stored in the buffer tank by increasing the water temperature from 45°C to 90°C. Due to the low return temperature of the activated ceilings (~25°C) and the constant latent storage temperature (29°C) the heat pump mode of the absorption machine in combination with the solar thermal collectors as heat sink only affects the solar coverage ratio negligibly and is therefore not implemented. A detailed hydraulic scheme including all main components and sensors of the system is given in Figure 6.

4 CONTROL STRATEGIES

Depending on the three days average of the ambient temperature (TIC001) the building management system (BMS) of the ZAE Bayern office in Garching chooses cooling or heating mode (see Figure 6). When ambient and certain room temperatures exceed the set point values the main distribution pump starts and the individual control equipment conditions each single room to custom settings by regulating the mass flow rate through the activated ceilings. Notwithstanding the above, a pellet backup boiler keeps the buffer tank (TIC406) on a temperature of 60°C for hot water preparation at any times. If the upper buffer tank temperature (TIC406) falls below 60°C the pellet boiler starts firing and continues until the lower buffer tank temperature (TIC410) reaches 60°C.

The SHC system itself is controlled by a low-cost (600 €) universal programmable logic controller. Except the chillers internal processes, which are regulated by a PLC (Beckhoff), all valves, pumps, fan etc. of the whole system are connected to this device.

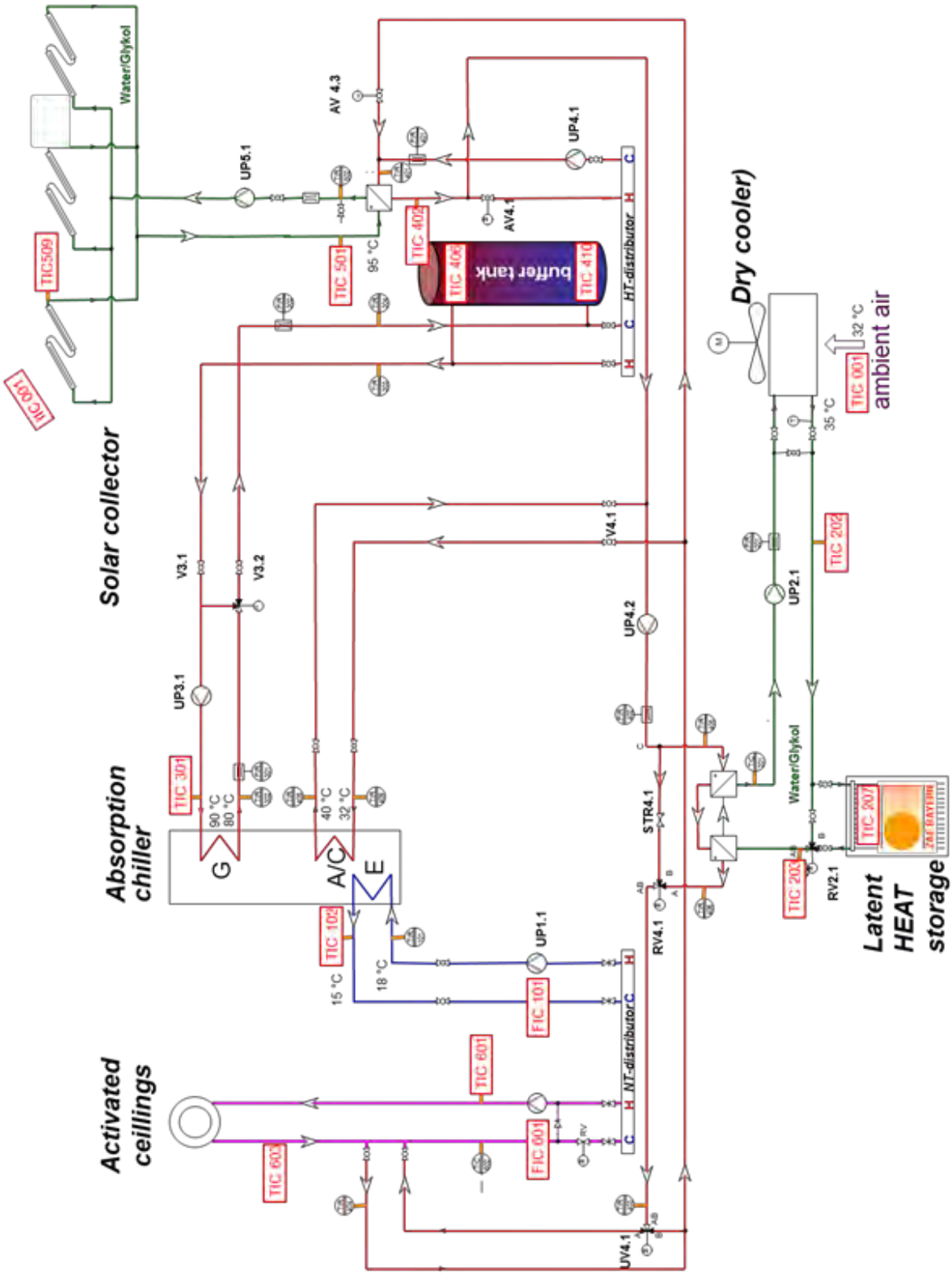

Figure 6: Piping and instrumentation diagram (P&ID) of the solar heating and cooling system

Winter Period:
In heating mode the current supply temperature (TIC601) to the activated ceilings is calculated with a heating curve gradient of 0.5 referred to the ambient air temperature (TIC001) and adjusted by injecting hot water from the buffer tank into the heating circuit. Due to the low return temperatures around 25°C the absorption machine is not used as a heat pump. Thus, Evaporator (E) and Absorber/Condenser (A/C) hydraulic circuit are shut off and solar energy is directly used to preheat the return flow of the heating system in several steps. When the collector aperture temperature (TIC509) exceeds the return flow temperature (TIC603) +3 K with a hysteresis of -1 K the solar primary pump (UP5.1) starts with a rotary speed directly proportional to the insolation on the solar plant (IIC001). After the required temperature at the solar heat exchanger (TIC501) is reached, one of the solar secondary pumps (UP4.2) feeds the heating system with the corresponding flow (FIC601). In the case that the solar gain exceeds the building heat demand, the latent heat storage circuit (UP2.1) is activated to store heat at all times the internal phase change material temperature (TIC207) is 5 K lower than the collector temperature (TIC509) with a hysteresis of -2 K. This stored heat is delivered to the heating system during night-time or insufficient insolation if the storage temperature (TIC207) is 2 K higher than the return flow of the building (TIC603). Thereby the pumps UP4.2 and UP2.1 generate a flow corresponding to the circulating water in the activated ceilings. The adequate supply temperature (TIC601) is ensured by the mixing valve (UV4.1) in both cases.

If the temperature in the solar circuit (TIC501) exceeds 65°C due to minor heat demand and/or full loaded latent heat storage (TIC207=50°C) the system switches to load the high temperature buffer tank via the HT-distributor and the pump UP4.1 with the current buffer tank temperature (TIC406), but at least 60°C. Buffer tank charging stops when its bottom temperature reaches 85°C (Hysteresis -5 K).

An overheating of the collector plant is avoided by dissipating any surplus heat to the ambient air. In this rare case the pumps UP4.2 and UP2.1 operate at maximum speed, the mixing valve RV4.1 limits the temperature in the solar secondary circuit (TIC402) to 90°C and the dry air cooler cools the brine (TIC202) to 50°C.

Summer Period:
In the cooling season chilled water at 15°C and 1.5 K above dew point respectively is provide to the building from 8 a.m. to 7 p.m. A well as backup cold source ensures continuous chilled water for the activated ceilings in times of insufficient solar energy necessary to drive the thermally driven chiller, which is design to operate in base load with a capacity (10 kW) of 50% of the maximum cooling demand (20 kW).

During the cooling mode the switching valves AV4.3 and UV4.1 separate the reject heat circuit from the solar and the building circuit respectively.

When the collector aperture temperature (TIC509) exceeds 65°C and the upper buffer tank temperature (TIC406) +2 K the solar primary pump (UP5.1) starts with a rotary speed directly proportional to the insolation on the solar plant (IIC001). After the required temperature at the solar heat exchanger (TIC501) is reached, the solar secondary pump (UP4.1) feeds the buffer tank via the HT-distributor. Thereby the maximum flow rate is limited to 1 m³/h, which corresponds to the generator flow rate of the chiller. This improves the chiller performance at startup, due to higher driving temperatures up to 92°C. There over, the limitation is negated and the hot water surplus charges the hot water buffer tank.

In case of cooling demand the chiller and chilled water pump (UP1.1) start, but only when the upper buffer temperature (TIC406) or the solar collector temperature (TIC402) is higher than the minimum driving temperature; here 65°C. The generator pump (UP3.1) operates at constant speed and the mixing valve RV3.1 reduces the heat flow from the buffer to the chiller in part load conditions to ensure 15°C chilled water.

The variable rotary speed of the reject heat pump UP2.1 is linked to UP4.2, which operates as a function of the difference between driving and ambient temperature. In a first step the coolant is cooled by the activated dry air cooler to 32°C. Above 24°C ambient air temperature the valve RV2.1 opens proportionally and the latent heat storage is used as a secondary heat sink to guarantee 32°C coolant, if the phase change material temperature (TIC207) is lower than the outlet temperature (TIC202) of the dry air cooler.

Chilled water preparation stops at 7 p.m. or insufficient driving heat from the solar plant or buffer tank. Due to the low internal lithium bromide concentrations a solution dilution procedure is not required for indoor applications.

If energy has been stored in the latent heat storage in the course of cold production the discharging of the latent heat storage is activated at 12 p.m. at the earliest when ambient temperature falls below 22°C and continued until the phase change material temperature is cooled down to 2 K below phase change temperature. In the process the pump (UP2.1) and fan operate at constant speed to ensure a economic discharging with high heat transfer rates and low auxiliary power consumption, which have been determined earlier on a test rig.

In the near future a new developed energy meter for the stored latent heat replaces this algorithm. Then discharging starts depending on the current latent energy content, weather forecast, ambient temperature and available timeframe in the night. By doing this, reject heat dissipation is shifted in times of lowest ambient temperatures and the electricity consumption for discharging is reduced to a minimum.

5 PERFORMANCE EVALUATION

The system has been operated and monitored for four complete years (2008-2011). Due to the low system temperatures for heating and moderate chilled water temperatures supplied to the activated ceilings in summer a high collector yield of about 400 $kWh \cdot m^{-2} \cdot a^{-1}$ is obtained. The absorption chiller itself operates about 600 hours each year, producing cold at 15°C by means of solar heat about 90°C with an average thermal Coefficient of Performance of 0.70.

By replacing some ineffective pumps with high efficiency components in spring 2009 the overall seasonal electrical COP increased significantly (about 20%) and reaches values above 10 at the moment. Almost 60% of the primary energy has been saved compared to a conventional compression cooling system supplying the same amount of cold.

During the monitoring period 2008 until 2011 (Helm et al. 2009) the two latent heat storage prototypes have undergone over 800 charging and discharging cycles under real conditions. In 2011 these two modules were replaced by a single module with improved compact design. Since then a total of over 300 charge- and discharging cycles have been completed without any indication of degradation in capacity and heat content. Figure 7 and 8 show inlet and outlet temperatures of the latent heat storage during charging at 36°C and discharging at 22°C with a flow rate of 3 $m^3 \cdot h^{-1}$. The quarterly measured constant temperatures clearly show the effect of latent heat storage over a long period where the phase change material melts and solidifies, respectively. Subcooling of the phase change material is observed during discharging by only about 1.5 K below the phase change temperature of 28…29°C, facilitating a reliable operation of the system.

In heating mode about one third of the overall heat demand had been covered by solar energy. Due to the use of the latent heat storage in cooling mode the cooling water return temperature did not exceed 32°C despite the dry heat rejection at ambient temperatures above 32°C.

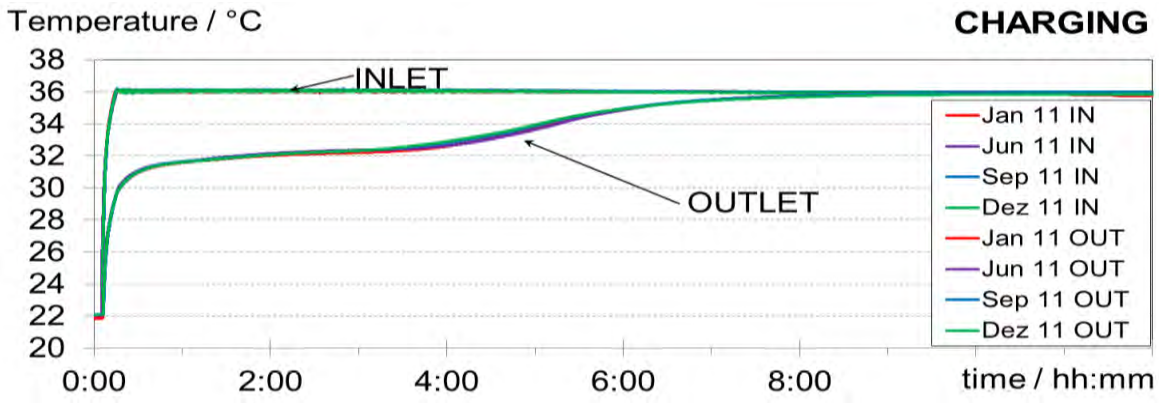

Figure 7: Quarterly reference measures of the latent heat storage while charging at 36 °C

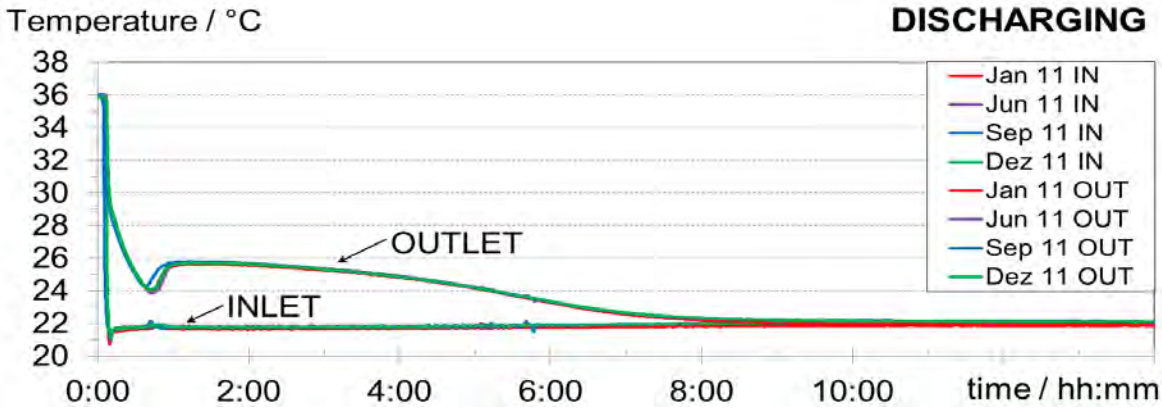

Figure 8: Quarterly reference measures of the latent heat storage while discharging at 22 °C

Figure 9 shows a typical temperature chart in the course of a day when the latent heat storage supports the dry air cooler and ensures constant cooling water temperatures to the absorption chiller below 32°C even at higher ambient temperatures. During hot (34°C) ambient conditions up to 50% of the daily reject heat load is covered by the latent heat storage (see Figure 10). During night time the lower ambient temperatures down to 15°C suffice to regenerate the latent heat storage within 6 hours.

6 CONCLUSION

A new innovative and patented concept of a solar cooling and heating system comprising an absorption chiller (10 kW chilled water capacity, $COP_{thermal}$ ~ 0.72) with dry air cooler and a latent heat storage has been observed over a period of four years. In cooling mode the latent heat storage stabilizes the cooling water temperature at 32°C independently from the ambient temperature. During the heating period a significant increase of the solar gain has been observed, due to the lower collector temperature compared to sensible heat storages. It has been proven that despite the low storage temperature, the buffered solar heat can be transferred efficiently to the building heating system. It may be concluded, that especially in low capacity applications the absence of a wet cooling tower substantially facilitates the introduction of absorption technology and contributes significantly to the performance of the solar heating system.

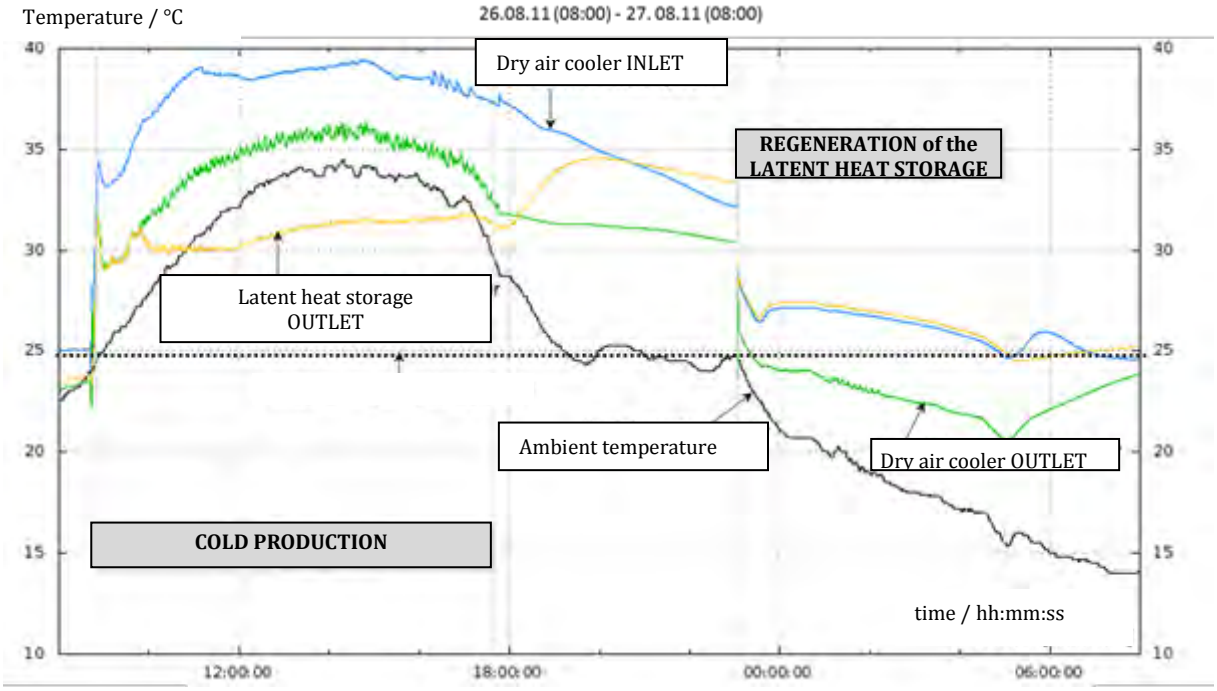

Figure 9: Temperatures of the dry air cooler and latent heat storage in the course of a day

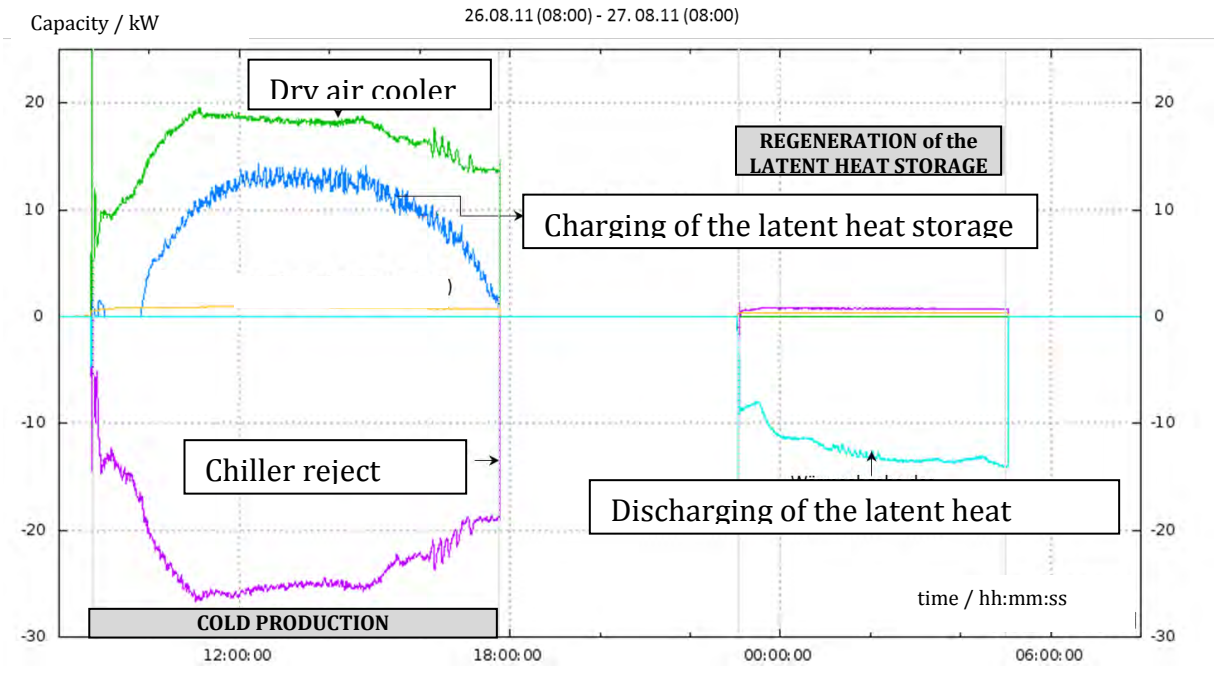

Figure 10: Power of the dry air cooler and latent heat storage in the course of a day

7 ACKNOWLEDGEMENT

This project has been supported by the German Federal Ministry for the Environment, Nature Conservation and Nuclear Safety under the project number (FKZ) 0329605D and 0329605O.

8 REFERENCES

Helm M., C. Keil, S. Hiebler, H. Mehling, C. Schweigler 2009. “Solar heating and cooling system with absorption chiller and low temperature latent heat storage: Energetic performance and operational experience”, *Int. J. of Refrigeration*, Vol. 32 (4), pp. 596-606.

Kühn A., S. Petersen, F. Ziegler, P. Kohlenbach, M. Harm, C. Schweigler 2005. ”Operational Results of a 10 kW Absorption Chiller for Low-Grade Driving Heat”, *Proc. of the Int. Sorption Heat Pump Conf., June 22-24*, Denver, USA.

Schweigler C., A. Costa, M. Högenauer-Lego, M. Harm, F. Ziegler 2001. “Absorptions-kaltwassersatz zur solaren Klimatisierung mit 10 kW Kälteleistung“, *Tagungsbericht der Deutschen Kälte-Klima-Tagung 2001, Ulm*, Deutscher Kälte- und Klimatechnischer Verein, Stuttgart.

MICRO COMBINED COOLING AND POWER

Kyle Gluesenkamp, Oak Ridge National Laboratory, Oak Ridge, TN
Reinhard Radermacher, Yunho Hwang, Center for Environmental Energy Engineering, University of Maryland, College Park, MD, USA, gluesenkampk@ornl.gov

Abstract: Thermally driven chillers can be driven by waste heat from prime movers (engines, turbines or fuel cells) to form combined cooling and power (CCP) systems. In this chapter, a method of matching chillers to prime movers is presented. CCP configurations with and without backup cooling are described, along with first-order estimates of the energy efficiency of each combination of configuration and prime mover. Some experimental results for micro combined cooling heating and power (CCHP) are presented. Based on the analytical and experimental work, it is concluded that CCP and CCHP performance depend heavily on the choice of prime mover. CCP systems based on fuel cells can use less energy than grid-driven electrical cooling systems. CCP with combustion-based prime movers has potential to save energy in off grid applications.

Key Words: prime mover, trigeneration, CCP, CCHP, CHP

1 INTRODUCTION

An important use for thermally driven chillers is to combine them with electricity production for co-production of cooling and power. When do such combined cooling and power (CCP) systems save primary energy compared to conventional, separate systems? This question can be addressed as a function of several important variables. In a first-order analysis, the efficiencies of a particular prime mover and a particular chiller can be treated as constant. This type of analysis is sufficient to reveal broad trends about combined cooling and power systems based on different prime movers. It provides perspective on technology potential and limitations, and a fundamental metric against which experimental results can be compared.

This chapter emphasizes micro-scale prime movers (<5 kW_{elec}), although some are included that are not available at this size range (microturbines and molten carbonate fuel cells). The analysis is applicable to any size system by referring to the underlying expressions (Gluesenkamp 2012) and substituting the component efficiencies desired by the reader. Internal and external combustion-based prime movers become significantly more efficient at larger scale, while the efficiency of fuel cells will be relatively constant.

This chapter also emphasizes combined cooling and power (CCP). Similar important possibilities exist, with the same basic equipment, for combined thermally driven heat pumping and power, or for combined cooling, heating and power (CCHP). For simplicity, the focus of this chapter remains on CCP, with some recent results for residential CCHP presented at the end of the chapter.

2 MATCHING PRIME MOVERS AND THERMALLY DRIVEN CHILLERS

One essential element for combined cooling and power is matching prime mover waste heat resources with thermally driven chiller requirements. A convenient tool for this analysis is the temperature vs. cumulative heat transfer (T-Q) diagram. The composite curve, a concept from pinch analysis which combines all forms of heat into a single line or curve (Kemp 2007), is shown for the waste heat resources of several micro-scale prime movers in Figure 1

(Gluesenkamp 2012). The prime movers shown are the spark ignition internal combustion engine (SI-ICE), molten carbonate fuel cell (MCFC), compression ignition internal combustion engine (CI-ICE), solid oxide fuel cell (SOFC), microturbine (MT), Stirling engine (SE), organic Rankine cycle (ORC), high temperature proton exchange membrane fuel cell (HT-PEMFC), and low temperature proton exchange membrane fuel cell (LT-PEMFC).

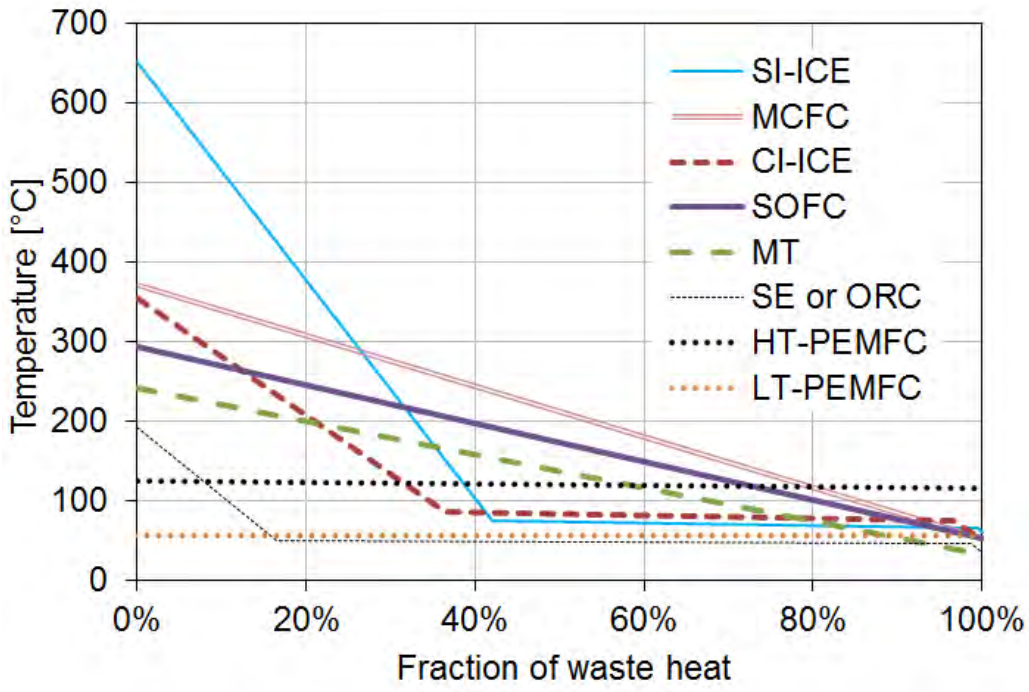

Figure 1: Waste heat resources for several micro prime movers

Figure 1 shows how much of each prime mover's waste heat is available at a given temperature. For example, about 67% of waste heat for a MT, 40% for a SI-ICE, and 0% for a LT-PEMFC are available above 100°C. The MT can provide about 83% of its waste heat above 60°C, compared to 100% for the SI-ICE and 100% for the LT-PEMFC.

The different thermally driven cooling options are shown in Figure 2 (Gluesenkamp and Radermacher 2011). Each technology covers a range of temperatures, since the driving temperature will change with external conditions. Most technologies are characterized by a narrow range of thermal COP. The region in the figure for adsorption cycles covers a very wide range of both temperature and COP since that region represents a wide diversity of working pairs. In general, when higher driving temperature is available, a higher COP technology can be used.

One way to show the match between prime movers and chillers is shown in Figure 3. Figure 3 places each prime mover on a plot of its electrical efficiency vs. the product $\varepsilon_{exh}COP_{th}$. COP_{th} is the thermal COP of the matching chiller, and ε_{exh} is the exhaust heat recovery effectiveness, if applicable (equal to 1 if not applicable). Prime movers with waste heat entirely in the form of exhaust (MT, MCFC and SOFC) have a pinch penalty represented by a red arrow. This accounts for the exhaust energy that cannot be utilized since it would be below the regeneration temperature of the chiller, resulting in $\varepsilon_{exh}<1$.

The way of displaying matched systems used in Figure 3 has the advantage that contours can be overlaid on it. The contours in Figure 3 represent primary energy consumption equivalent to conventional separate generation (Gluesenkamp 2012). A CCP system lying above a contour will have better primary energy ratio (PER) than the baseline conventional system. One contour has entirely optimistic assumption; the other pessimistic. The green

contour assumes that there are no heat losses from the prime mover (λ=0, where λ is defined as the fraction of fuel not converted to a useful product by the prime mover), no parasitic electricity consumption of the chiller (κ=0, where κ is defined as electrical consumption per unit of cooling), a low-efficiency baseline alternative (η=20%), and low efficiency baseline vapor compression system (COP_{VCS}=3). Compared to this baseline, all CCP systems have better PER. The other extreme baseline is shown in gray: a new combined cycle power plant driving a high efficiency vapor compression system, with high prime mover heat losses and high chiller parasitic consumption. In that scenario, only the SOFC and MCFC have better PER. All other baseline systems will lie between these two extremes, meaning that most CCP systems may or may not save energy, depending on the application.

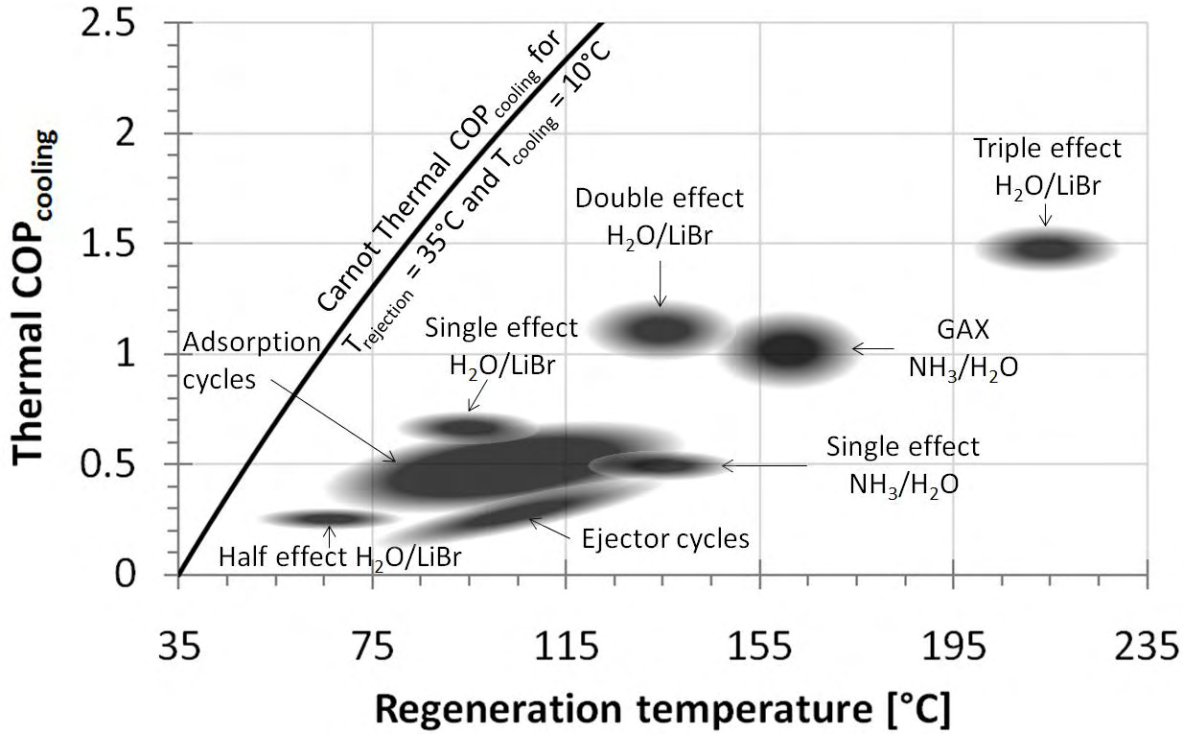

Figure 2: Thermally driven cooling technologies

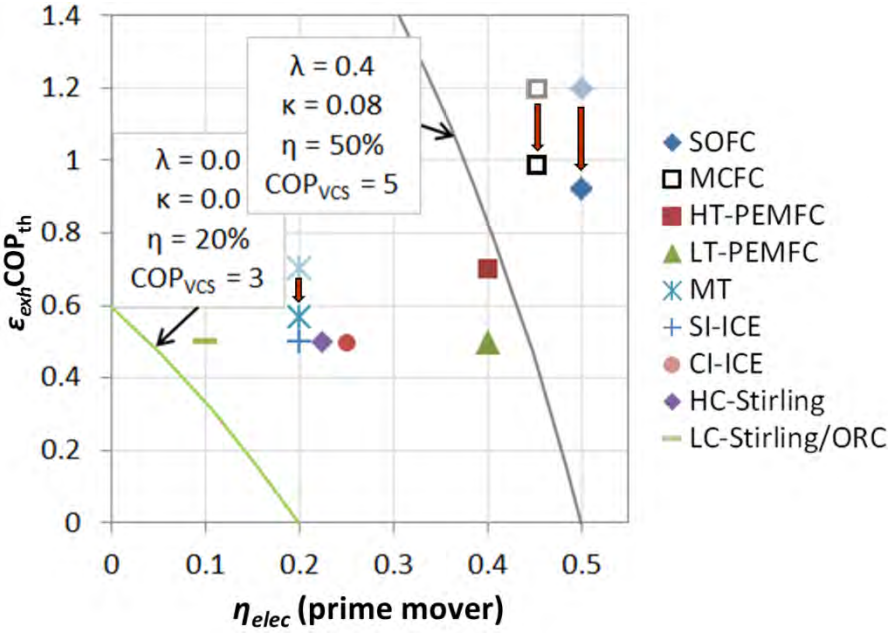

Figure 3: Matched systems and equivalent PER contours

Another way to represent matched systems is shown in Figure 4. Here the x-axis is the fuel energy consumed by the prime mover, and the y-axis is the work produced (i.e. electricity) or saved (i.e. electricity that no longer need be produced since thermally driven cooling has displaced it). Thus, the area under each curve is the net benefit of a CCP system using the given prime mover.

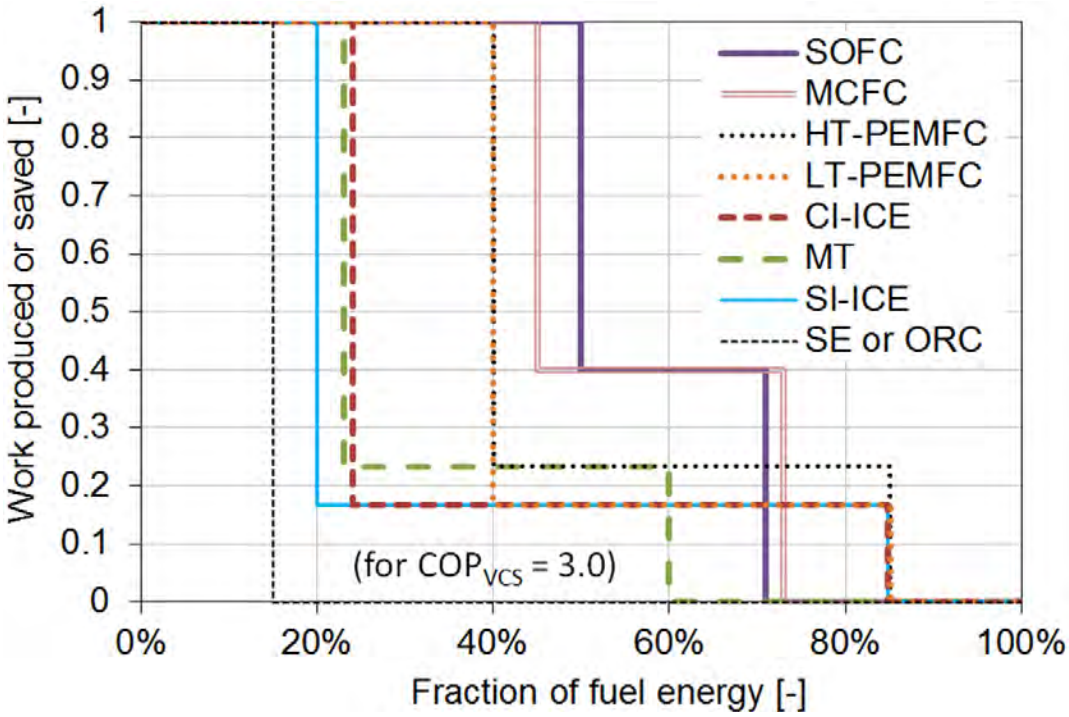

Figure 4: Work produced and saved for different CCP systems

Note that the preceding figures are optimistic since they assume that all electricity and cooling produced by a CCP system are utilized – in other words, the systems operate at the cooling fraction that naturally results from the component efficiencies. However, the relative amounts of cooling and power required by a building or process does not always match the relative amounts of cooling and power produced by a prime mover. The performance with mismatch is addressed in the next section.

3 PRIMARY ENERGY RATIO OF COMBINED COOLING AND POWER SYSTEMS WITH LOAD MISMATCH

So far, CCP systems have been assumed to operate at their natural cooling load fraction. However, the cooling demand as a fraction of the sum of cooling and electric demands (denoted f_{clg}), is highly variable with application, time of year and time of day, and thus will now be treated parametrically.

Note that, for a given match of prime mover and thermally driven chiller, there are different configurations possible. Figure 5 shows the conventional electrically-driven vapor compression cycle, and Figures 6 through 8 show three important CCP configurations.

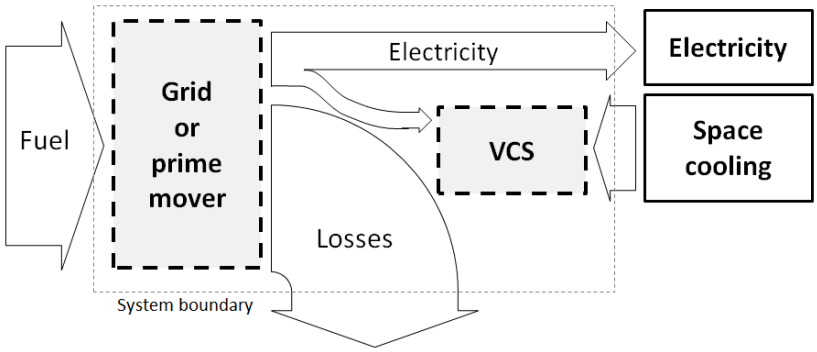

Figure 5: Conventional electrically-driven vapor compression system (VCS)

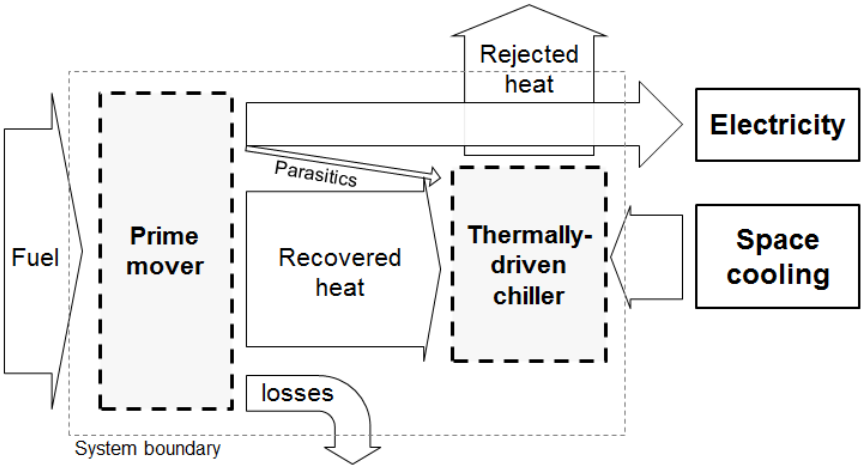

Figure 6: CCP system without backup cooling

The simple CCP schematic of Figure 6 (no backup cooling) was assumed for Figure 3. Figures 7 and 8 show two possibilities for systems with backup cooling.

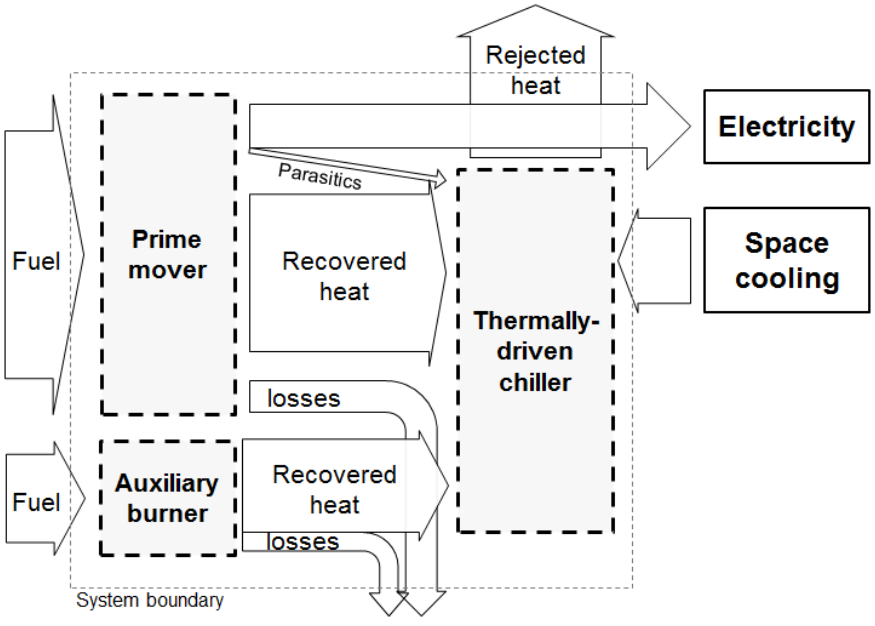

Figure 7: CCP system with auxiliary burner backup

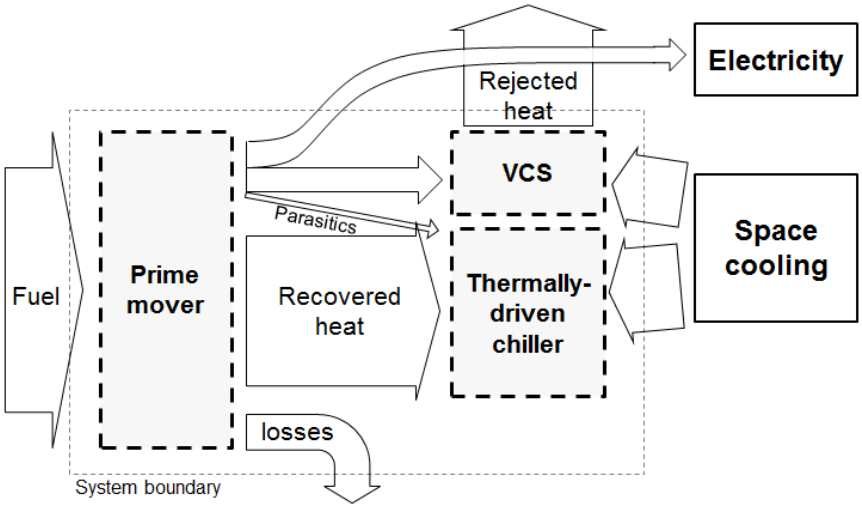

Figure 8: CCP system with backup VCS

Following the configurations shown in Figures 5 to 8, expressions can be derived for the PER of each configuration as a function of component efficiencies and the cooling demand relative to the electrical demand (Gluesenkamp 2012). In this analysis the cooling as a fraction of total load is denoted f_{clg} [-], where the total load is the sum of electrical and cooling demand [kW]. Thus f_{clg}=0 represents a demand for electricity alone, and f_{clg}=1 represents demand for cooling alone.

Using the example of a HTPEMFC prime mover, Figure 9 shows the comparison of fuel consumption (inverse PER) for conventional on-grid separate generation ("grid-VCS"), conventional off-grid separate generation (HTPEMFC-VCS), and the three CCP configurations (noAB=no auxiliary burner, wAB=with auxiliary burner). Note that inverse PER has the unit of primary energy (e.g. fuel) per unit delivered energy (cooling plus electricity): lower values represent higher efficiency systems. Using the inverse of PER allows for linear curves in the plot.

From Figure 9 it can be seen that CCP systems perform best relative to separate generation when operating at the natural cooling fraction. The value of the natural cooling fraction will vary depending on the CCP component efficiencies; for HTPEMFC it is about 0.46.

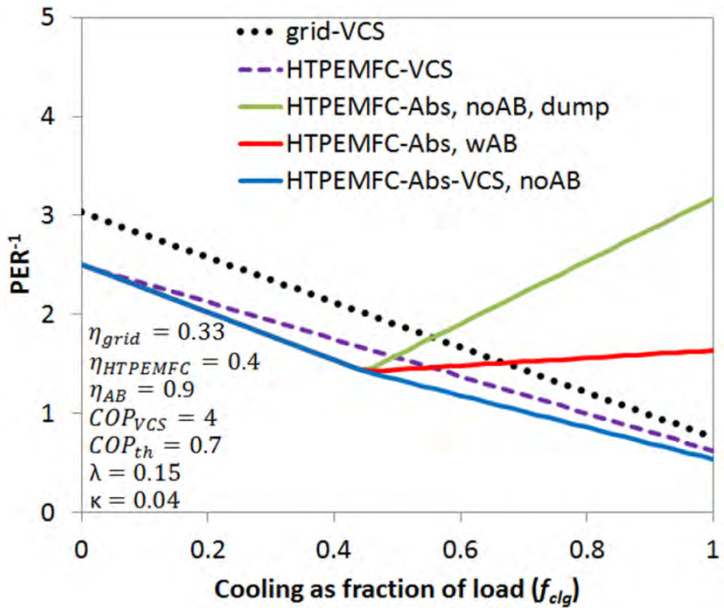

Figure 9: Inverse PER for two conventional and three CCP configurations using HTPEMFC

Figure 10 shows the same set of curves as Figure 9. For rapid visual comparison, several prime movers are shown in simplified plots. All prime movers have been assumed to have λ=0.15, and all chillers to have κ=0.04. As would be expected for typical micro (<5 kW_{elec}) devices, the prime mover electrical efficiencies are assumed to be 50% for SOFC, 40% for PEMFC, 23% for MT (assuming 25 kW_{elec} in this case), 20% for ICE, and 10% for low cost (LC) Stirling engine.

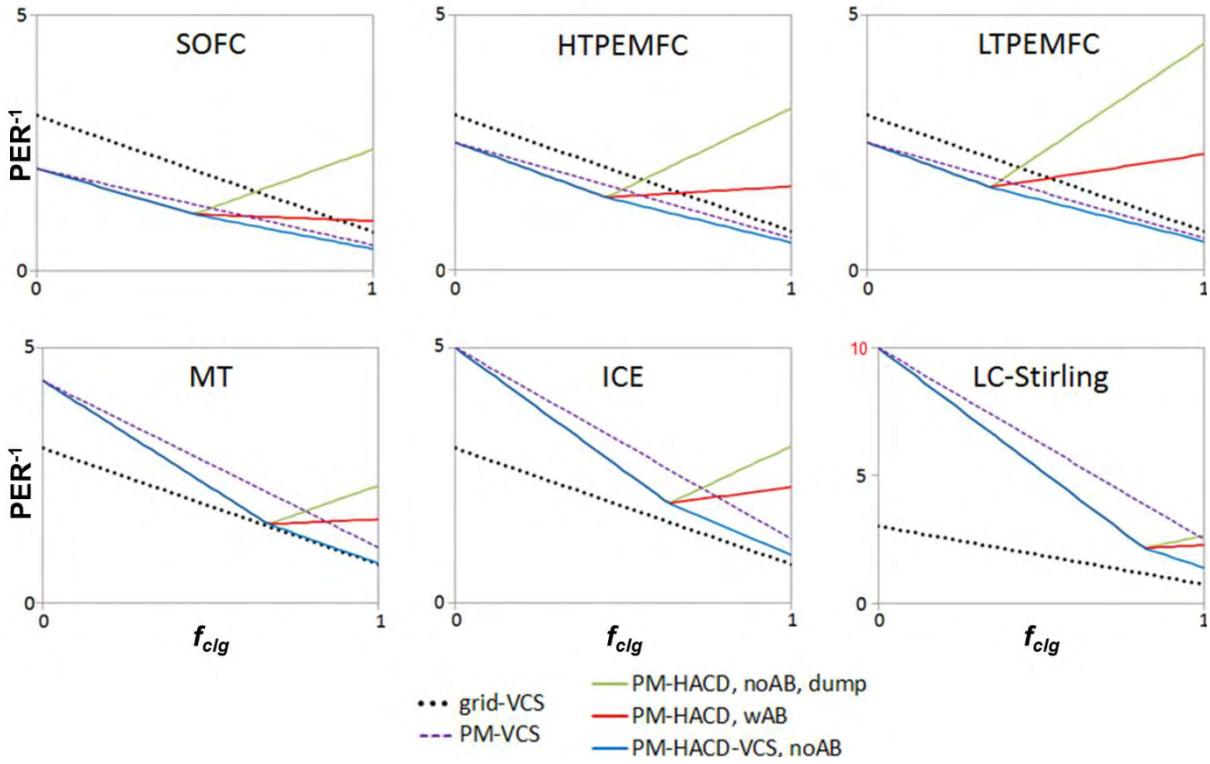

Figure 10: Inverse PER comparisons for CCP systems with various prime movers

In each plot within Figure 10, the natural cooling fraction can be seen as the point where the PER of the different CCP backup options begin to diverge with increasing cooling load fraction. Below the natural cooling fraction, systems with thermally driven cooling always have the lowest energy consumption. Above the natural cooling fraction, the VCS backup always performs best. When no backup is present, the thermally driven cooling very quickly loses its advantage above the natural cooling fraction. The burner backup is in between.

Prime movers with low electrical efficiency have the most potential for improvement by the addition of thermally driven cooling. However, the prime movers with high electrical efficiency have the best performance relative to the grid. From this it can be concluded that the greatest potential for combined cooling and power is in off-grid engines and microturbines, or on grid with fuel cells.

4 EXPERIMENTAL CCHP FACILITY AT UNIVERSITY OF MARYLAND

A prototype adsorption chiller (Qian et al. submitted) based on water and FAM-Z01 zeolite (Kakiuchi et al. 2004) was constructed and driven by waste heat from a commercially available Ecopower residential CHP engine. The engine also supplied domestic hot water to form a combined cooling, heating and power (CCHP) system. Waste heat was captured from the generator, oil cooler, cooling jackets, and exhaust, and delivered at 70°C to the chiller. The system is shown in Figure 11.

Figure 11: Photograph of combined cooling, heating and power system at UMD

The measured outputs and fuel input for the CCHP system over a 5-day load following test are shown in Figure 12 (Qian et al. 2013).

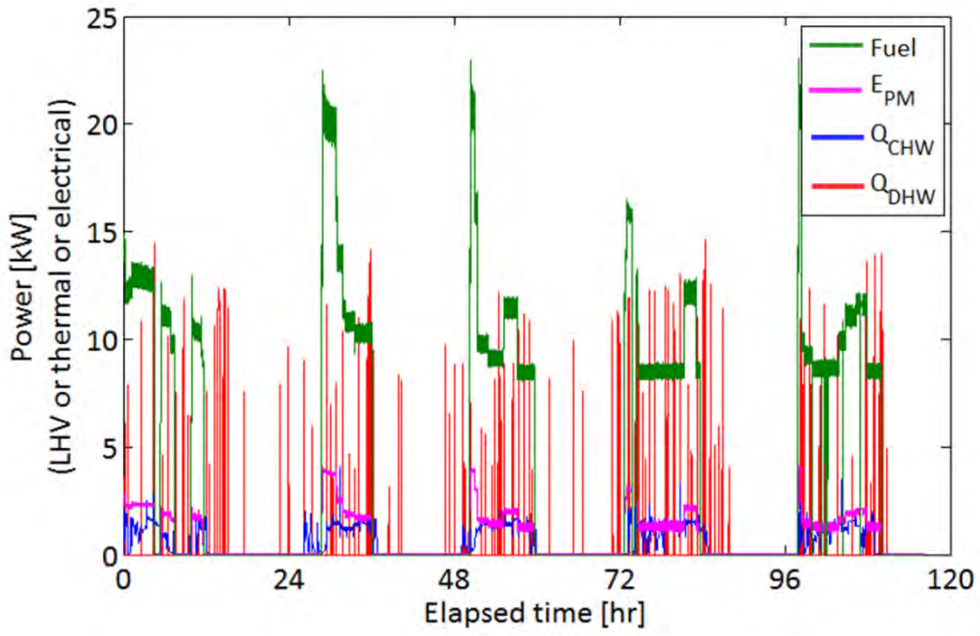

Figure 12: Measured inputs and outputs of CCHP system over 5-day load-following dynamic test

By summing the cumulative totals in Figure 12 and comparing to the primary energy that three different conventional systems would use to produce the same outputs, the savings of CCHP can be calculated, as shown in Table 1 (Qian et al. 2013). As expected from the preceding analysis, the SI-ICE based system did not save energy relative to the grid, but had substantial savings relative to a conventional off-grid system. The CCHP system also had significant savings relative to an off-grid combined heat and power system with VCS cooling.

Table 1: Fuel consumption of experimental CCHP vs. three baseline scenarios

Baseline scenario				CCHP savings
name	*electricity from:*	*DHW from:*	*cooling from:*	
grid-VCS	grid	boiler	VCS	**-15.6%**
off-grid conventional	generator	boiler	VCS	**36.1%**
off-grid CHP, VCS	CHP engine	CHP engine	VCS	**28.6%**

5 CONCLUSIONS

Thermally driven chillers can be matched with prime movers by choosing the chiller that maximizes the sum of work produced and work saved by the match. Depending on the choice of baseline system, most CCP systems may or may not save energy. Simple expressions for the PER of CCP systems can be derived as a function of the cooling load as a fraction of total load. The prime movers with the strongest potential for high efficiency are the fuel cells, especially high temperature fuel cells (SOFC, MCFC, and HTPEMFC). Conventional prime movers (ICE and MT) can save fuel in off-grid CCP systems. This was shown experimentally for an SI-ICE-based CCHP system with prototype adsorption chiller.

6 REFERENCES

Gluesenkamp, K. and Radermacher, R. 2011. “Heat Activated Cooling Technologies for Small and Micro CHP Applications,” Beith, R., ed., *Small and Micro CHP Systems*, Cambridge, UK: Woodhead Publishing Ltd.

Gluesenkamp, K. 2012. “Development and analysis of micro polygeneration systems and adsorption chillers,” PhD dissertation, University of Maryland, College Park. ProQuest/UMI. (Publication No. 3553078).

Kakiuchi, H., Iwade, M., Shimooka, S., Ooshima, K., Yamazaki, M. and Takewaki, T. 2004. “Novel zeolite adsorbents and their application for AHP and desiccant system,” *IEA Annex 17, Energy Conservation through Energy Storage, 7th Expert Meeting and Workshop*, October 8-12, Beijing, China.

Kemp, I. C. 2007. Pinch analysis and process integration: a user guide on process integration for the efficient use of energy, 2nd ed., Oxford: Butterworth-Heinemann.

Qian, S., Gluesenkamp, K., Hwang, Y., Radermacher, R. submitted to Energy. "Characterization of cyclic steady state performance and development of control strategy for adsorption chiller driven by engine coolant waste heat".

Qian, S., Gluesenkamp, K., Hwang, Y., Radermacher, R. 2013. "Experimental study on performance of a residential combined cooling, heating and power system under varying building load", *Proc. of ASME 2013 7th Int. Conf. on Energy Sustainability and 11th Fuel Cell Science, Engineering and Technology Conference*, Minneapolis, July 14-19, MN, USA.

EXPERIMENTAL RESULTS AND MODEL CALCULATIONS OF A HYBRID ADSORPTION-COMPRESSION HEAT PUMP BASED ON A ROOTS COMPRESSOR AND SILICA GEL-WATER SORPTION

Michel van der Pal, Robert de Boer, Anton Wemmers, Simon Smeding, Jakobert Veldhuis, Jan-Aiso Lycklama a Nijeholt, Energy research Centre of the Netherlands (ECN)
P.O. Box 1, 1755 ZG, Petten, The Netherlands, vanderpal@ecn.nl

Abstract: Thermally driven sorption systems can provide significant energy savings, especially in industrial applications. The driving temperature for operation of such systems limits the operating window and can be a barrier for market-introduction. By adding a compressor, the sorption cycle can be run using lower waste heat temperatures.

ECN has recently started the development of such a hybrid heat pump. The final goal is to develop a hybrid heat pump for upgrading lower (<100°C) temperature industrial waste heat to above pinch temperatures.

The paper presents the first measurements and model calculations of a hybrid heat pump system using a water-silica gel system combined with a Roots type compressor. From the measurements can be seen that the effect of the compressor is dependent on where in the cycle it is placed. When placed between the evaporator and the sorption reactor, it has a considerable larger effect compared to the compressor placed between the sorption reactor and the condenser. The latter hardly improves the performance compared to purely heat-driven operation. This shows the importance of studying the interaction between all components of the system. The model, which shows reasonable correlation with the measurements, could proof to be a valuable tool to determine the optimal hybrid heat pump configuration.

Keywords: sorption, heat pump, compressor, hybrid

1 INTRODUCTION

In The Netherlands more than 100 PJ of heat in the refining and chemical industry is actively disposed (Spoelstra et al. 2002). More than 40 PJ of this heat has a temperature of more than 100°C and can be used in a heat-driven heat pump to upgrade this industrial waste-heat to useful process heat, thereby reducing the industrial primary energy demand. After a review of potential heat pump technologies, a heat pump based on chemisorption of ammonia on solid salts was selected for further development at ECN. Industrial waste heat with a temperature between 100°C to 150°C can be upgraded to 180°C to 220°C to create medium-pressure steam. The sorption cycle is shown schematically in Figure 1 with the colored arrows showing the heat flows into (at middle temperature) and out (at ambient and high temperature) of the system.

The temperature lift that can be achieved using this cycle is determined by the chosen sorbents and waste heat temperature. The temperature lift decreases with decreasing waste heat temperatures. For a single-stage heat pump type II, a waste-heat temperature of more than 100°C is required to achieve a temperature lift of 50°C. Multi-stage heat pumps can achieve >50°C temperature lifts using lower waste heat temperatures but have poor efficiency. A 50°C temperature lift is considered the minimum temperature lift that is required

for reusing waste heat. For temperature lifts smaller than 50°C, compressors form an attractive alternative, both in terms of energy efficiency and economy.

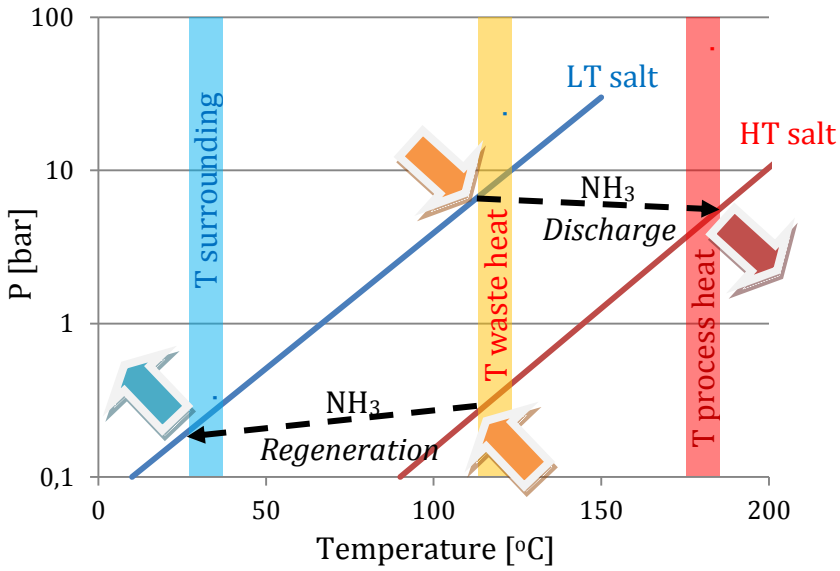

Figure 1: Schematic diagram of a heat-driven heat pump type II for upgrading (industrial) heat to a higher temperature. The blue and red lines show the sorption line of respectively low and high temperature sorbent. The colored arrows show heat flows into (at middle temperature) and out (at ambient and high temperature) of the system.

About 40 PJ of industrial waste heat in The Netherlands has a temperature between 70°C and 100°C. Extending the operating window of the sorption cycle to these lower waste heat temperatures would contribute significantly to the efficiency of the industrial energy use in The Netherlands. This extension can be achieved by adding a compression step to the cycle. This hybrid adsorption – compression cycle is schematically shown in Figure 2. The increase in pressure during the discharge phase of the cycle, allows the use of waste heat with a lower temperature. Model calculations have shown this hybrid cycle can reduce required waste-heat temperature (for a temperature lift of at least 50°C) to as low as 70°C and still yield net primary energy savings (van der Pal et al. 2010).

In order to make this cycle work, it is required to combine the continuous operation of the compressor with the sorption cycle. For solid sorbents, such as the ammonia salts, the latter is a batch operation. The combination of a batch-process with the continuous operation of the compressor could result in unforeseen problems and/or lower than expected performance. The objective of this study is to determine the effects of the hybrid operation, and therefore a combination of compressor with a sorption reactor has been tested. Although our study (van der Pal et al., 2010) showed the ammonia-salt reactions of $CaCl_2$ and $MnCl_2$ as most energy efficient, for practical reasons a water-silica gel system was tested.

Unlike ammonia-salt reactions, the adsorption of water vapor to the silica gel is a physisorption reaction. The performance of this process depends on an isosteres-field rather than the discrete transition between the adsorbed and the desorbed state that is found in chemisorption cycles. Also the temperature range the system can be operated is different than the foreseen application. Waste-heat with a maximum temperature of 90°C is used to create cooling rather than heating. This means the cycle as shown in Figure 1 is operated in reverse. In this mode, it is equal to a heat-driven cooling cycle. This paper shows the results of the measurements of the heat-driven and hybrid system based on adsorption of water vapor on silica gel. To get a better understanding of the measurements, an existing adsorption model has been adapted to describe the measurements. Also the model results are presented.

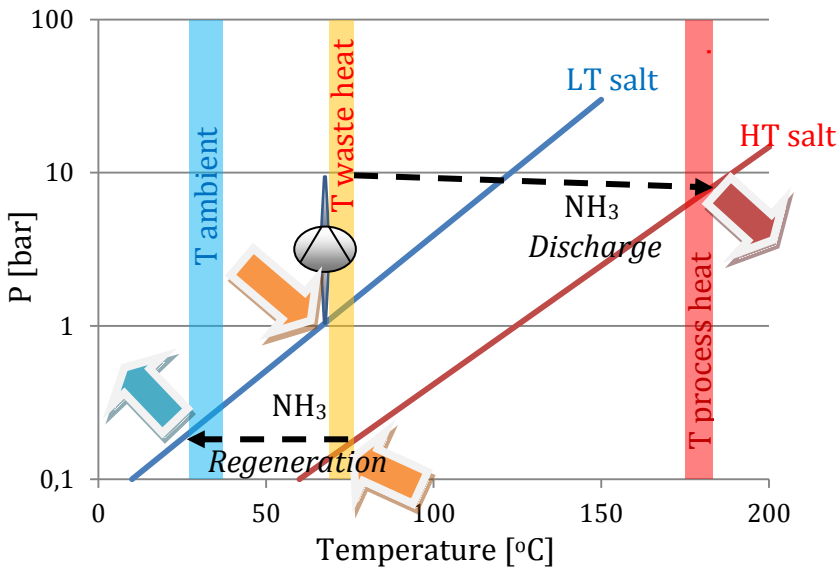

Figure 2: Schematic diagram of a hybrid adsorption - compression heat pump for upgrading (industrial) heat to a higher temperature. The blue and red lines show the sorption line of respectively low and high temperature sorbent. The colored arrows show heat flows into (at middle temperature) and out (at ambient and high temperature) of the system.

2 MATERIALS AND METHODS

2.1 Experimental set-up

The system consists of a condenser, evaporator and a reactor vessel. This setup has been described by Boer et al (Boer et al. 2005). The reactor vessel contains a sorption reactor consisting of four silica gel filled plate-fin heat exchangers (Grisel et al. 2010). Each heat exchanger contains 1.5 kg of silica gel, so the sorption reactor contains 6 kg of silica gel in total. A heating and cooling rig is used to provide the sorption reactor, condenser and evaporator with water at the desired temperature. During the regeneration phase of the cycle the sorption reactor is heated to high temperature (60 to 90°C) while the condenser is kept at ambient temperature. During the discharge phase of the cycle the sorption reactor is cooled down to ambient and the evaporator kept at desired cooling temperature. Valves with a timer are used to switch between the two phases. By measuring the temperature of the water entering and leaving the components (evaporator, condenser and sorption reactor) and its flow rate, the amount of heat consumed or released can be calculated. Furthermore the temperatures and pressures inside the components are measured.

The compressor, type Falco WY1000B from Busch Ltd, is a roots-type compressor that provides a volume flow of up to 1200 m^3h^{-1}. The frequency of the compressor is controlled by a Vacon NXL frequency controller and can be varied between 0 and 60 Hz. The maximum power consumption is 3 kW electricity and is monitored with a Sineax P530 power meter. The compressor has a leak rate of less than $1 \cdot 10^{-6}$ $mbar \cdot l \cdot s^{-1}$. On the gas side of the compressor, the pressure and the temperature of the compressed gas are measured.

2.2 Measurements

The following four configurations (see Figure 3) were used in the measurements:

1) In configuration 1, the compressor is placed between the condenser and the evaporator. The performance of this regular compressor cycle is determined for a temperature of 10°C and 20°C on respectively the evaporator and the condenser. The frequency of the compressor was varied in 5 Hz steps between 15 and 30 Hz;

2) In configuration 2, the system contains the condenser, evaporator and the sorption reactor. The performance of this pure heat-driven system is determined. The conditions were identical to those in the measurements of the hybrid configurations;
3) In configuration 3, all components are used. The compressor is placed between the evaporator and the sorption reactor. Its effect on the discharge phase of the cycle is measured. The temperature of the evaporator and condenser are kept at respectively 12°C and 35°C whilst the sorption reactor cycled in 2x6 minute intervals between 35°C and 85°C. The compressor frequency was set to 30 Hz;
4) In configuration 4, all components are used. The compressor is placed between the sorption reactor and the condenser. Its effect on the regeneration phase of the cycle is measured. The temperature of the evaporator and condenser are kept at respectively 12°C and 26°C whilst the sorption reactor cycled in 2x6 minute intervals between 26°C and 71°C. The compressor frequency was set to 30Hz.

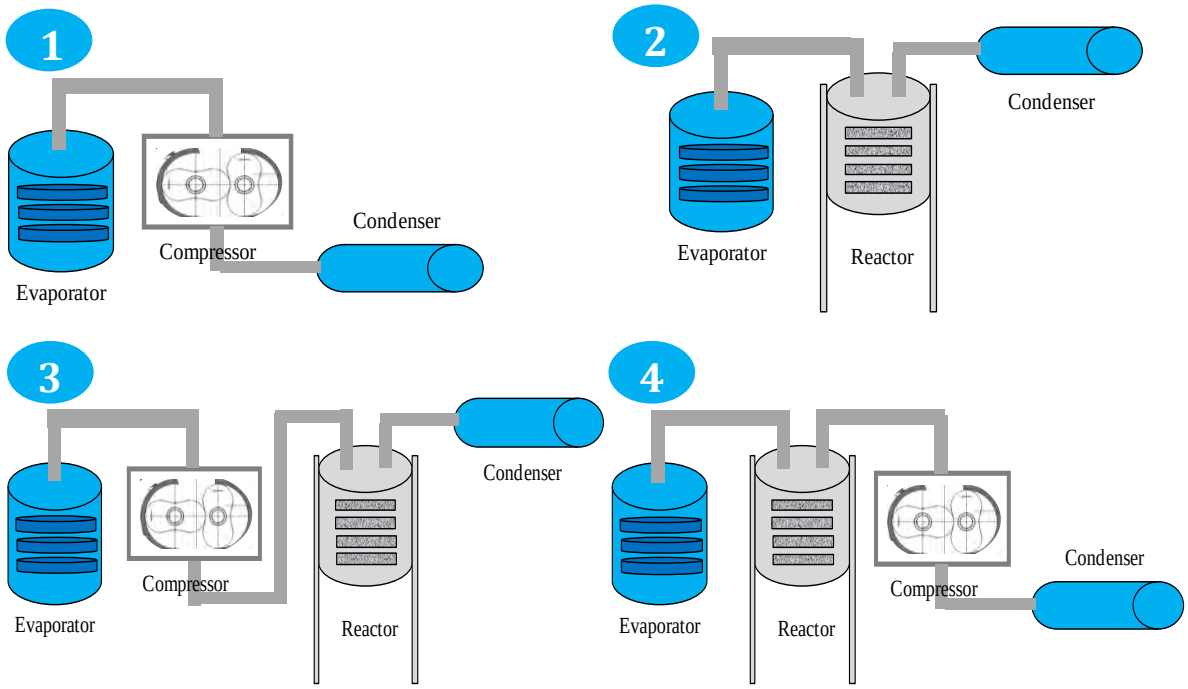

Figure 3: The four configurations for measuring system performance: 1 - continuous 'standard' compression, 2 - purely heat-driven sorption system, 3 - hybrid system with compression at low pressure and 4 – hybrid system with compression at high pressure

2.3 Model calculations

For the model calculations, an adapted version of the Matlab-Simulink model developed by the University of Valencia (Verde et al. 2010) was used. This model originally described the heat and mass transfer in a water-zeolite vapor sorption heat pump for automobile applications. The model is a transient model with (among others) the following assumptions:

- Non-equilibrium conditions with a simple kinetic model
- Zero-dimensional (i.e. uniform temperature distribution in each operating unit).
- The pressure at the sorption reactor depends on the instantaneous mass of vapor contained inside.
- The flow of water vapor between the sorption reactor, the condenser and evaporator is governed by the pressure difference between them and the position of the valves.
- The heat exchangers are characterized by their global UA value (W/K). For the sorption reactor heat exchangers, a detailed analytical study was carried out in order to estimate an adequate UA value depending on the sorbent thermal properties as well as the geometrical characteristics of the sorption reactor.

A detailed description of the model can be found here (Verde et al. 2010).

To use the model for our measurements, some changes in the model were required. These include:

- The original model used two sorption reactors to provide continuous cooling. The measurements were conducted on 1 sorption reactor. Therefore the number of active sorption reactors was reduced to one by setting the vapor flow to the second sorption reactor to zero;
- The isosteres data for zeolite were substituted with the data of the silica gel isosteres (Restuccia et al. 1999);
- The dimensions of the automobile sorption reactor were substituted with the dimensions of the sorption reactor based on the four plate-fin heat exchangers;
- The thermal masses of the sorption reactor were adapted to current system;
- The evaporator and condenser properties were adapted to current system.

To use the model for hybrid operation, some additional changes were made. The pressure step created by the compressor was used as a transient input parameter for the model calculations. Depending on the configuration, this pressure step was set between the evaporator and the sorption reactor (configuration 3) or the sorption reactor and the condenser (configuration 4). Because the pressure step was a set parameter, the flow resistance between the components was set (close to) zero. Also, the original model would directly connect the condenser and evaporator in case the pressure of the condenser is lower than in the evaporator. This option was disabled for the (hybrid) system because such shortcut was not made in the measurements.

3 RESULTS

3.1 Measurement results

Figure 4 shows the results of the measurements with the compressor between the evaporator and condenser (configuration 1). The trends are according to expectations. The power used by the compressor increases with frequency. The increase in frequency also results in higher pressure ratios and increased condenser and chilling power. The compressed gas temperature also rises. This is due to both increased pressure ratio (= ratio pressure discharge/suction gas) as well as increased volume flow. For an adiabatic process, the latter should not affect the compressed gas temperature. In practice, however, the gas loses a considerable amount of its heat before its temperature is measured. The overall electric efficiency of the compressor is low: the $COP_{electric}$ (ratio of chilling power/compressor power) is about 1.5 at 30 Hz operation. This is likely due to the poor properties of water vapor as refrigerant under given conditions and the Roots-type compressor, which is not energy efficient.

Table 1 shows the results for hybrid operation with compressor between evaporator and sorption reactor compared to heat-driven operation. The $COP_{thermal}$ is defined as the amount of heat extracted by the evaporator divided by the amount of heating required for the regeneration of the reactor (at $T_{heating}$). The $COP_{electric}$ is defined as the amount of heat extracted by the evaporator divided by the amount of electricity consumed. The compressor has a significant effect on the performance compared to the heat-driven system. The chilling power increases from 0.7 kW to 1.2 kW and the - for heat loss corrected - thermal efficiency ($COP_{thermal}$) increases from 0.41 to 0.59.

Conditions:	Frequentie Hz	15	20	25	30
	T cond in °C	20.67	21.05	21.31	21.39
	T evap in °C	10.17	10.09	10.09	10.10

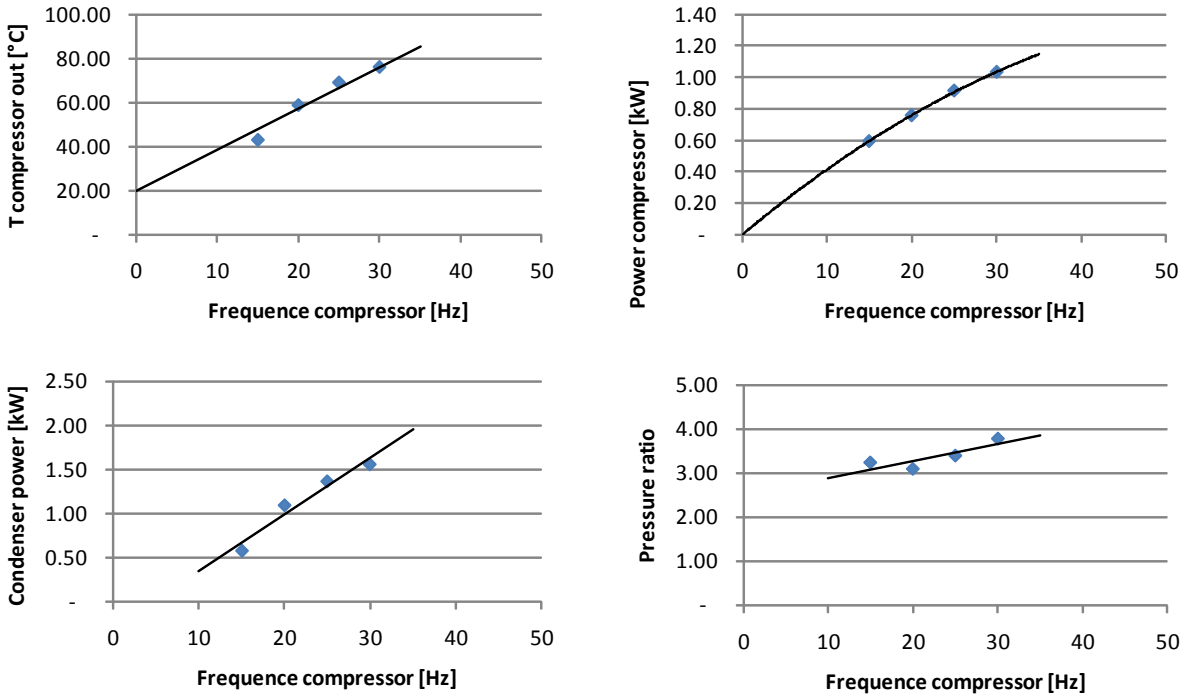

Figure 4: The compressed gas temperature, compressor power, condenser power and pressure ratio as a function of the compressor frequency for condenser and evaporator temperatures of respectively 20°C and 10°C

Table 1: Results for hybrid operation with compressor between evaporator and sorption reactor (configuration 3) compared to heat-driven operation (configuration 2).

	heat-driven	hybrid configuration 3
$T_{heating}$ (°C)	84.7	84.6
$T_{cooling}$ (°C)	35.1	35.3
$T_{evaporator}$ (°C)	12.6	11.7
pressure ratio	1.0	1.5
power compressor (kW)	0	0.9
chilling power (kW)	0.7	1.2
$COP_{thermal}$	0.41	0.59
$COP_{electric}$	na	1.3

Table 2 shows the results for hybrid operation with compressor between sorption reactor and condenser compared to heat-driven operation. The effect of the compressor seems only to be reflected in the increased pressure ratio and the compressor power. Despite this considerable effect on the pressure levels, no significant effect on the chilling power is observed and there is only a slight increase in thermal efficiency. This effect could possibly be explained by a reduced thermal conductivity of the reactor bed (van der Pal et al. 2011).

Although the performance of this system is very poor for generating cooling in terms of $COP_{thermal}$ as well as $COP_{electric}$, one needs to bear in mind that the goal of these measurements is not to create an efficient cooling system. It is a first step in the development of a hybrid heat pump for upgrading waste heat to useful process heat that will use ammonia and salts rather than water vapor and silica gel.

Table 2: Results for hybrid operation with compressor between sorption reactor and condenser (configuration 4) compared to heat-driven operation (configuration 2).

	heat-driven	hybrid configuration 4
$T_{heating}$ (°C)	71.4	71.3
$T_{cooling}$ (°C)	26.2	26.2
$T_{evaporator}$ (°C)	12.3	12.3
pressure ratio	1.0	2.9
power compressor (kW)	0	1.1
chilling power (kW)	1.0	1.0
$COP_{thermal}$	0.32	0.33
$COP_{electric}$	na	0.9

3.2 Model calculations

The measured and calculated temperatures, pressures and thermal powers for the heat-driven operation are shown in respectively Figure 5, Figure 6, and Figure 7. Figure 5 shows a good correlation between the measurements and the model calculations. Only some deviations are found around when switching between the discharge and the regeneration phase. The good correlation is somewhat deceiving: to achieve large deviations in out-going temperatures, the amount of heat released or adsorbed by the components must increase considerably.

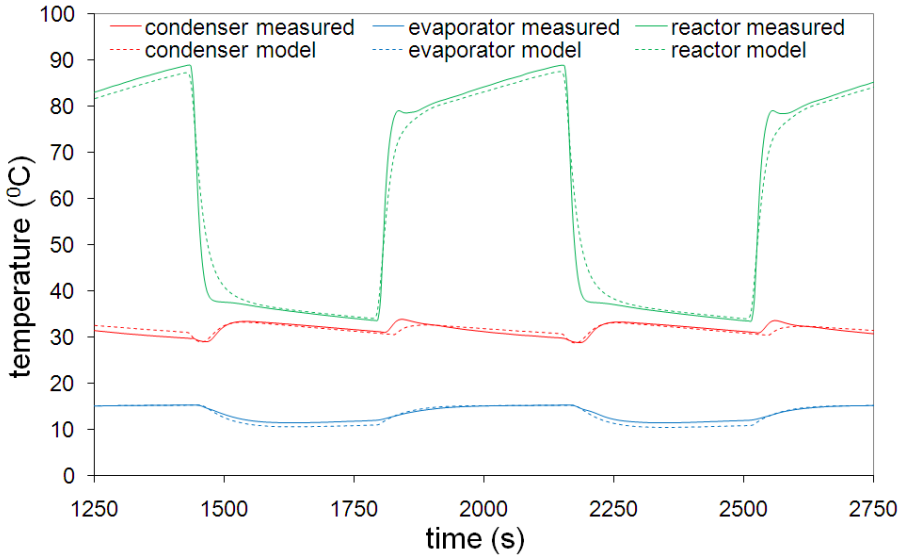

Figure 5: Heat-driven operation: the temperature from the measurement and model calculations of the condenser, evaporator and sorption reactor as a function of time

More information can be obtained from the pressure as a function of time as shown in Figure 6. For the evaporator pressure and the sorption reactor pressure during the low pressure part of the cycle, a good correlation is found between measured values and calculated values. For the pressure in the condenser and the sorption reactor during the high pressure part of the cycle, the correlation is not as good. It can also be observed that the measured pressure in the condenser increases each cycle whilst the model value remains constant. This suggests an increasing presence of non-condensables in the condenser.

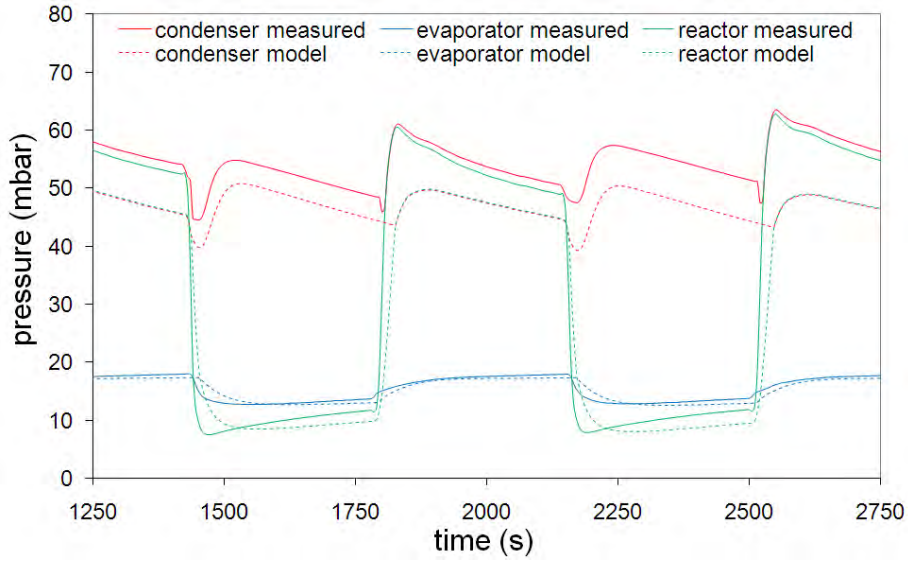

Figure 6: Heat-driven operation: the pressure from the measurement and model calculations of the condenser, evaporator and sorption reactor as a function of time

Figure 7 shows the measured and calculated thermal powers. The measured power of the sorption reactor shows a considerable quicker response compared to model calculations when switching between the discharge and regeneration phases. Also the total amount of heat input/output of the sorption reactor is per cycle considerable smaller than calculated. These effects could be caused by overestimating the thermal mass. Considering the masses of the heat exchangers, the water and the metal components were carefully determined, it is more likely the fraction of the mass varying in temperature was overestimated by the model which might be related to the uniform temperature assumption of the model. The calculated heating powers are, however, close to the measured values. The measured cooling power is somewhat smaller than calculated which could be explained by the presence of non-condensables in the system.

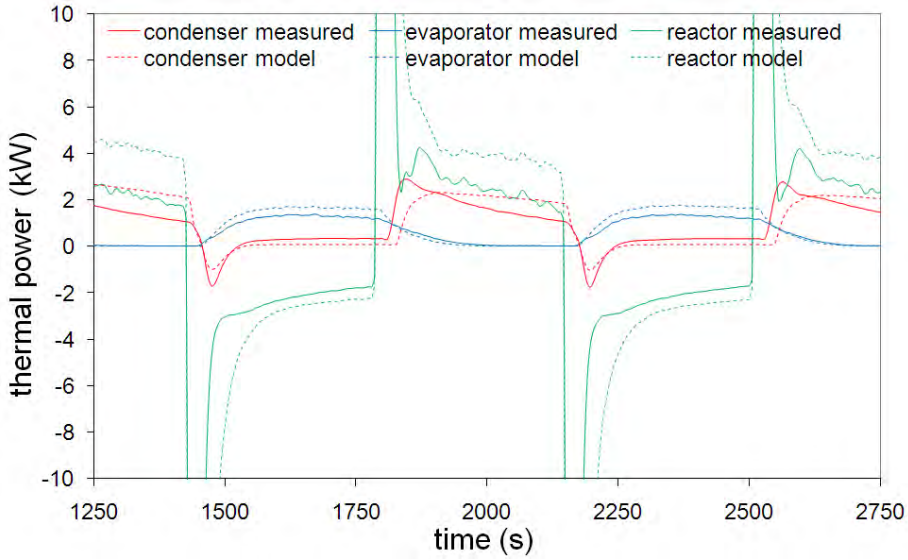

Figure 7: Heat driven operation: the thermal power, the temperature from the measurement and model calculations of the condenser, evaporator and sorption reactor as a function of time

Figure 8 shows the measured and calculated pressures of the hybrid configurations as a function of time. As can be expected, the pressure in the sorption reactor is increased when the compressor is placed between the evaporator and sorption reactor (left) and reduced

when the compressor is placed between the sorption reactor and the condenser (right). The maximum pressures measured on the evaporator are higher than calculated. The condenser pressures correlate reasonably well. Because the sorption reactor pressure depends on the phase of the cycle, closely related to the evaporator or the condenser pressure (in hybrid mode increased or decreased with the measured pressure step), the measured pressure of the sorption reactor performs according to expectations for the discharge phase and shows an overshoot compared to the model during the regeneration phase.

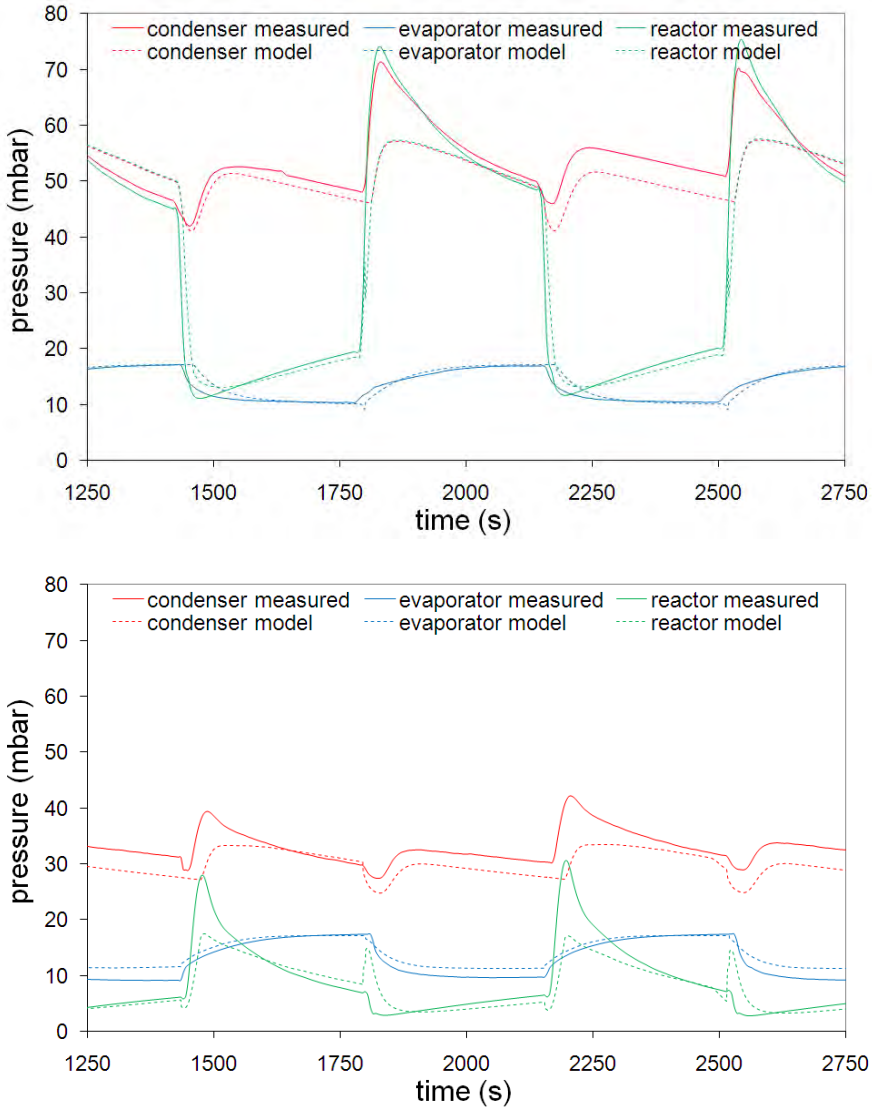

Figure 8: Measured and calculated pressures as a function of time for hybrid heat pump operation with the compressor placed between evaporator and sorption reactor (top: config 3) and placed between sorption reactor and condenser (bottom: config 4)

Figure 9 shows the measured and calculated powers of the hybrid configuration as a function of time. Similar to the heat-driven configuration, the thermal power of the sorption reactor has been somewhat overestimated. The cooling power for the hybrid operation has, similar to heat-driven configuration, been slightly overestimated. The model calculates a 58% increase in cooling power for configuration 3 which is close to measured values. For configuration 4, however, the model estimates a 28% increase in cooling power where hardly any improvement is found in the measurements.

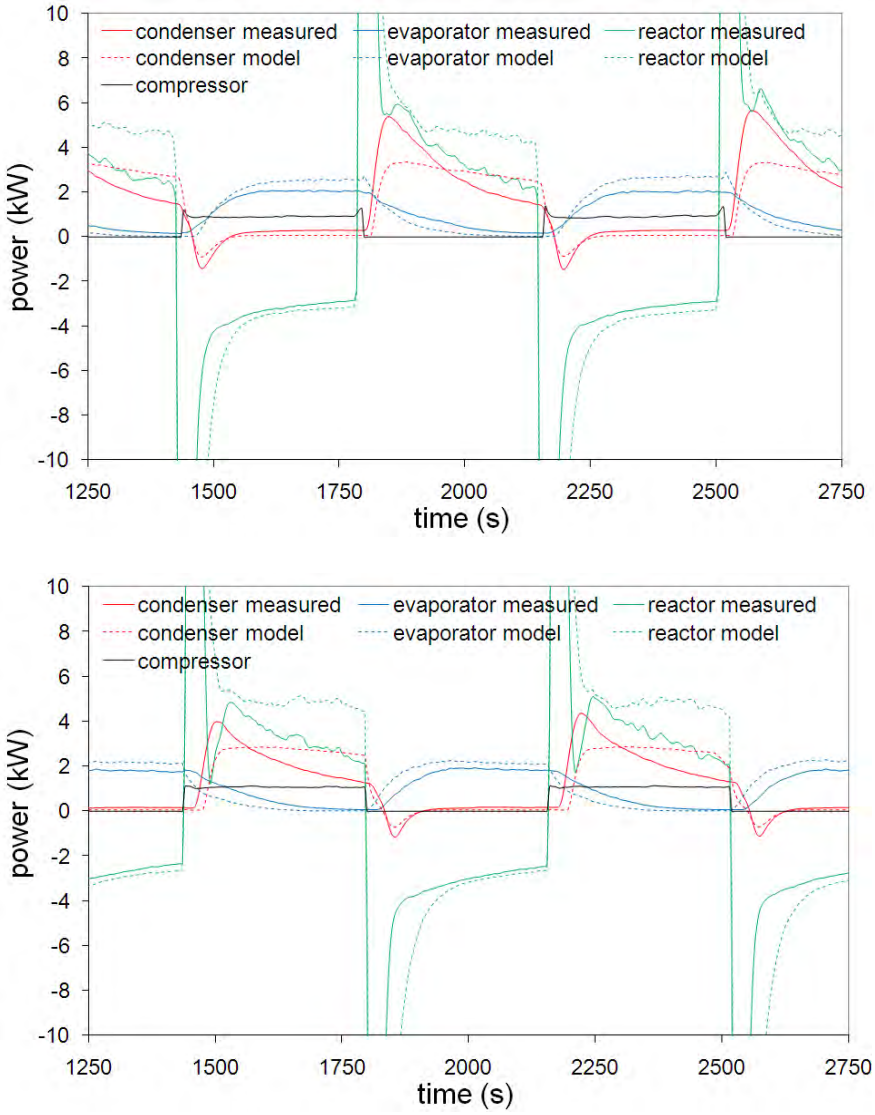

Figure 9: Measured and calculated powers as a function of time for hybrid heat pump operation with the compressor placed between evaporator and sorption reactor (top: config 3) and placed between sorption reactor and condenser (bottom: config 4)

4 CONCLUSIONS AND RECOMMENDATIONS

From the measurements and model calculations can be seen that the hybrid operation of the sorption-cycle can yield considerably higher chilling powers and $COP_{thermal}$ compared to the purely heat-driven cycle. However, this improvement does not necessary always occur as the results for configuration 4 show.

There are some differences between the measurements and the model calculations. The differences show mainly in the pressure and thermal power and are similar for both the heat-driven as well as the hybrid operation of the heat pump. These differences can (partly) be explained by differences in the amount of thermal mass and/or its temperature variation, which might be related to the uniform temperature assumption of the model. Despite the differences, the calculated evaporator (cooling) and condenser (heating) powers are close to the measured values.

A better correlation between model calculations and measurements could be obtained by tweaking the input parameters such as the thermal mass. However, to be able to use the model

as a tool for accurately predicting the performance of a heat-driven and/or hybrid heat pump, it is recommended to look into the effect of the model assumptions on the calculations.

5 ACKNOWLEDGEMENT

This work has been funded by AgentschapNL (Dutch agency for sustainable development and innovation) within the EOS-LT program, contract number EOSLT08026. We would like to thank Maria Verde and José Miguel Corberán Salvador of the University of Valencia for providing us with the model and their support.

6 REFERENCES

Boer R. de, S. F. Smeding, R. J. H. Grisel 2005. "Development and testing of a sorbent filled heat exchanger for use in compact solid sorption cooling systems", ECN-RX--05-121, 2005.

Grisel R.J.H., S.F. Smeding, R. de Boer 2010. "Waste Heat Driven Silica Gel/Water Adsorption Cooling in Trigeneration", *Appl.Thermal Eng.*, 30 [8-9], pp. 1039-1046.

Restuccia G., Y.I. Aristov, G. Maggiot, G. Cacciola, M.M. Tokarev 1999. "Performance of sorption system using new selective water sorbents", *Proc. of the Int. Sorption Heat Pump Conf., March 24-26*, ZAE Bayern, Munich, Germany, pp. 219-223.

Spoelstra S., W.G. Haije, J.W. Dijkstra 2002. "Techno-Economic Feasibility of High-Temperature High-Lift Chemical Heat Pumps for Upgrading Industrial Waste Heat", *Appl.Thermal Eng.*, 22 [14], pp. 1619-1630.

van der Pal M., A. Wemmers, S. Smeding, K. van den Heuvel 2010. "Study on performance of hybrid adsorption-compression type II heat pumps based on ammonia-salt adsorption", *9th Int. Conf. on Sustainable Energy Technologies (SET 2010)*, paper CO13.

van der Pal M., A. Wemmers, S. Smeding, J. Veldhuis 2011. “Measurement results of a hybrid adsorption-compression heat pump based on a roots compressor and silica gel-water sorption cycle”, *Proc. of the Int. Sorption Heat Pump Conf.,* April 4-6, Padua, Italy.

Verde M., L. Cortés, J.M. Corberán, A. Sapienza, S. Vasta, G. Restuccia 2010. “Modelling of an Adsorption System Driven by Engine Waste Heat for Truck Cabin A/C. Performance Estimation for a Standard Driving Cycle”, *Appl.Thermal Eng.*, 30 [13], pp. 1511-1522.

A 10 kW INDIRECTLY FIRED ABSORPTION HEAT PUMP: CONCEPTS FOR A REVERSIBLE OPERATION

Annett Kühn, Christian Özgür-Popanda, Felix Ziegler
Technische Universität Berlin, Institute of Energy Engineering, KT 2, Marchstraße 18, D-10587 Berlin, Germany, annett.kuehn@tu-berlin.de

This paper was published in the proceedings of the 10th International Heat Pump Conference 2011 (www.heatpumpcentre.org/en/hppactivities/ieaheatpumpconference).

Abstract: In the last decade several small and medium sized solar or waste heat driven chillers have been developed and brought to market. Nevertheless, in Central Europe where many of these chillers are installed, the required cooling period of buildings is rather short. By using them as a heat pump during winter time their operating period can be extended in order to shorten the payback period and increase the cost effectiveness, and at the same time, the benefit to the environment is increased.

From a thermodynamical point of view it is possible to run a chiller also as a heat pump, but in practice there are restrictions in application due to the dependency of the driving temperature and the temperatures of heat source and heat sink. Using the example of a 10 kW H_2O/LiBr absorption chiller, constraints of and demands on different possible peripheral systems (heat sources and heat sinks) for the reversible operation have been investigated. In the paper we present combinations which are favorable, and others which should be avoided from a primary energy point of view.

Key Words: absorption heat pump/chiller, reversible operation, heat sources/sinks

1 INTRODUCTION

The energy consumption for air-conditioning equipment is rising strongly worldwide. For this reason, in the last decade the development of thermally driven absorption or adsorption heat pumps and chillers has regained importance. Particularly, small and medium sized solar or waste heat driven chillers have been developed. In Germany alone, there were seven sorption chillers between 10 and 50 kW brought into market. But in most cases such systems are not yet competitive to compression chillers, especially in moderate climates where cooling seasons are rather short. Their market share can only be increased by improvement of the economic efficiency. This can be achieved by an extension of the operating period. In moderate climates sorption systems should not only be used for space cooling but primarily for space heating.

Up to now, there are two major approaches in the field of sorption systems: on the one hand solar or waste heat driven sorption chillers developed for space cooling (e.g. Association for sorption cooling e.V. (ASC 2011)) and on the other hand gas driven sorption heat pumps developed for space heating (e.g. Initiative Gaswärmepumpe (IGWP 2011)). From a thermodynamical point of view every chiller can also be applied as a heat pump; only the use of heat source and heat sink circuits is reversed, as for reversible compression heat pumps. But in practice there are restrictions in the application due to the dependency of the driving temperature and the temperatures of heat source and heat sink.

This paper explicates the interdependencies of the three temperature levels (driving heat, heat sink and heat source) and their impact on the operation in heating or cooling mode using the example of a small scale H_2O/LiBr absorption heat pump. Two exemplary concepts for the use of a reversible absorption heat pump are presented.

2 BASIC SPECIFICATION OF THE HEAT PUMP

The absorption system presented here has been developed as small scale chiller with focus on compactness and low driving temperatures for solar cooling (Schweigler et al. 2001). Figure 1 shows the prototype and summarizes the technical data for nominal load.

Cooling mode	
Working pair	H_2O/LiBr
EER	0.76
Cooling capacity	10 kW
chilled water in/out	18/**15**°C
flow rate	2.9 m³/h
Driving heat flow	13.2 kW
hot water in/out	**75**/65°C
flow rate	1.2 m³/h
Reject heat flow	23.2 kW
cooling water in/out	**27**/35°C
flow rate	2.6 m³/h

Figure 1: Prototype of a 10 kW absorption chiller and technical data

Even without changing the temperatures, the chiller can also be used as a heat pump. As can be seen from the technical data, under nominal conditions the heat pump already supplies water of 35°C for the use in panel heating systems such as floor heating. In this case (heat source temperature of 18°C, e.g. sewage water) a coefficient of performance (COP=useful heat/driving heat) of 1.76 would be achieved. Of course, heating supply temperature can be increased and heat source temperature level can be decreased adapting e.g. the driving temperature. To cope with a lower heat source temperature of 10°C (e.g. ground water) the driving temperature has to be increased to approximately 88°C.

3 INFLUENCE OF TEMPERATURES

3.1 The characteristic curve

Using the method of the characteristic equation (Ziegler 1997) a large range of potential operating conditions can be evaluated. The characteristic equation for the presented chiller has been determined by fitting measurement data (Kühn et al. 2005) to

$$\dot{Q}_E = 0.42 \cdot \Delta\Delta t' + 0.9 \,. \qquad (1)$$

The corresponding characteristic temperature function is

$$\Delta\Delta t' = t_D - 2.5\, t_{AC} + 1.8\, t_E \qquad (2)$$

where t_D, t_A, t_C, t_E are the external arithmetic mean temperatures at desorber, absorber, condenser and evaporator, and t_{AC} is the arithmetic mean value of t_A and t_C. To calculate also the heat output $\dot{Q}_{AC}$ and the COP/EER, characteristic equations for $\dot{Q}_{AC}$ and $\dot{Q}_D$ have also been fitted to

$$\dot{Q}_D = 0.53 \cdot \Delta\Delta t'' - 2.5 \quad (3)$$

$$\dot{Q}_{AC} = 0.94 \cdot \Delta\Delta t''' - 0.4\,. \quad (4)$$

The corresponding characteristic temperature functions are

$$\Delta\Delta t'' = t_D - 2.1\ t_{AC} + 1.5\ t_E \quad (5)$$

$$\Delta\Delta t''' = t_D - 2.3\ t_{AC} + 1.6\ t_{E.} \quad (6)$$

The sum of the three heat flows does not necessarily result to zero, because - depending on load and ambient conditions - heat losses to the environment, heat input from the environment, and the internal pumps (solution and refrigerant pump) have to be accounted for when using the fits of all three characteristic equations.

Figure 2 presents the characteristic curves of cooling capacity (chiller mode) and heat output (heat pump mode).

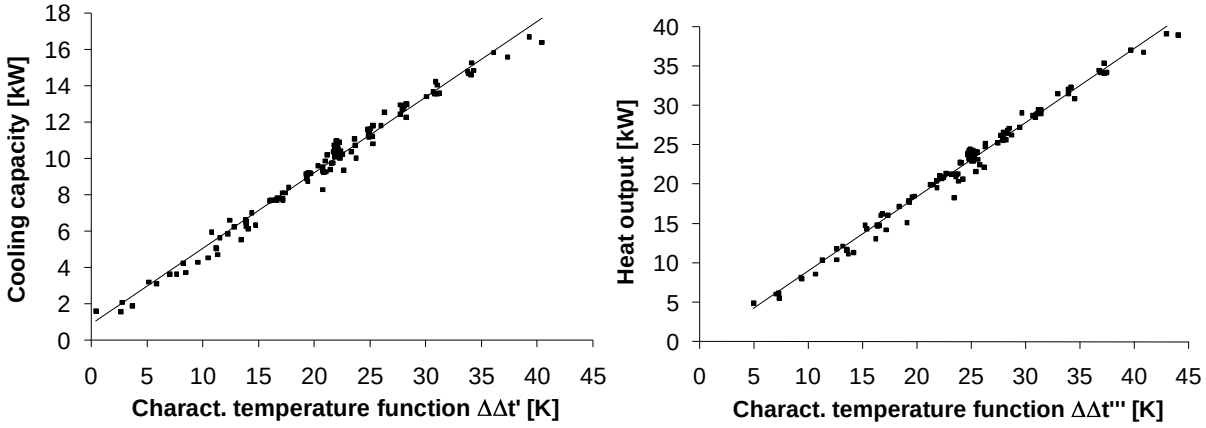

Figure 2: Characteristic curves of cooling capacity and heat output

Evidently, the characteristic equation method provides a simple linear correlation to describe the behavior of the heat pump at design flow rates and at a large range of possible external temperatures. Deviation of 96% of the measurement points from this equation is below 1 kW (in cooling mode) or below 2 kW (in heating mode) which is in each case around 10% of the nominal capacity. The characteristic equations (Eq. 1, 3 and 4) can be used to determine the load behavior and efficiency when changing the characteristic temperature function. It is even exact enough to serve as a control algorithm. As the heat output or cooling capacity does not change if the characteristic temperature function remains constant, it follows immediately how changes of an external temperature can be compensated by control of another external temperature. That means for example, a drop of the heat source temperature by 5 K can be compensated by an increase of the driving temperature by 8 K to keep the heat output constant (Eq. 6).

3.2 Improvement of the method

Using mean temperatures in the characteristic temperature functions (Eq. 2, 5 and 6) has the disadvantage that they usually are not known. They change with the heat flows. Usually only

inlet or outlet temperatures are known by the user. This is different in heating and cooling mode. In the case of heating mode, the given values in equations (7) to (9) normally are the driving inlet temperature t_{Din}, the heat source inlet temperature t_{Ein}, and the heating supply temperature t_{Cout}. In the case of cooling mode, the driving inlet temperature t_{Din}, the chilled water outlet temperature t_{Eout}, and the cooling water inlet temperature t_{Ain} are given.

$$\Delta\Delta t' = \frac{t_{Din} - t_{Dout}}{2} - 2.5\frac{t_{Cout} - t_{Ain}}{2} + 1.8\frac{t_{Ein} - t_{Eout}}{2} \quad (7)$$

$$\Delta\Delta t'' = \frac{t_{Din} - t_{Dout}}{2} - 2.1\frac{t_{Cout} - t_{Ain}}{2} + 1.5\frac{t_{Ein} - t_{Eout}}{2} \quad (8)$$

$$\Delta\Delta t''' = \frac{t_{Din} - t_{Dout}}{2} - 2.3\frac{t_{Cout} - t_{Ain}}{2} + 1.6\frac{t_{Ein} - t_{Eout}}{2} \quad (9)$$

In both cases, we still have three unknown temperatures. They can be derived from the well-known equations (10) to (12) which determine the heat flows:

$$t_{Ein} - t_{Eout} = \dot{m} \cdot c_p \cdot \dot{Q}_E = 0.30\,\mathrm{K/kW} \cdot \dot{Q}_E \quad (10)$$

$$t_{Din} - t_{Dout} = \dot{m} \cdot c_p \cdot \dot{Q}_D = 0.74\,\mathrm{K/kW} \cdot \dot{Q}_D \quad (11)$$

$$t_{Cout} - t_{Ain} = \dot{m} \cdot c_p \cdot \dot{Q}_{AC} = 0.33\,\mathrm{K/kW} \cdot \dot{Q}_{AC} \quad (12)$$

By numerically solving the system of equations we can determine either the cooling capacity or the heat output and the EER/COP from any set of known external inlet or outlet temperatures.

The method of the characteristic equation in principle allows an extrapolation. However, a good accuracy in the order of less than 10% of nominal capacity can only been guaranteed if the temperature values are not too far off the measurement range the equations have been fitted for. Else, further refinement of the method is required (Albers et al. 2011). Measurements have been carried out in the following ranges: t_{Ein}=8...20°C, t_{Eout}=5...18°C, t_{Din}=50...105°C, t_{Ain}=23...40°C and t_{Cout}=27...46°C.

In order to ensure save and stable operation, freezing of the refrigerant has to be avoided. To this end, the evaporation temperature T_E must be determined as well. It can be derived from the heat transfer equation

$$\dot{Q}_E = U_E \cdot A_E \cdot \Delta\vartheta_{log,E} = U_E \cdot A_E \cdot \frac{t_{Ein} - t_{Eout}}{\ln\frac{t_{Ein} - T_E}{t_{Eout} - T_E}}\,. \quad (13)$$

Since the temperature difference in the chilled water circuit in most cases is small, the arithmetic temperature difference can be used as an approximation of the logarithmic one which simplifies the equation to

$$\dot{Q}_E = U_E \cdot A_E \cdot ((t_{Ein} + t_{Eout})/2 - T_E)\,. \quad (14)$$

In Figure 3 the temperature difference $(t_{Ein}+t_{Eout})/2-T_E$ is plotted against the cooling capacity. From all measurement data we get the linear equation

$$(t_{Ein} + t_{Eout})/2 - T_E = 0.35\ \mathrm{K/kW} \cdot \dot{Q}_E \quad (15)$$

where 0.35 K/kW is the nearly constant overall heat transfer resistance ($1/U_E A_E$). It should be kept in mind that the approximation is not valid for very low cooling capacity.

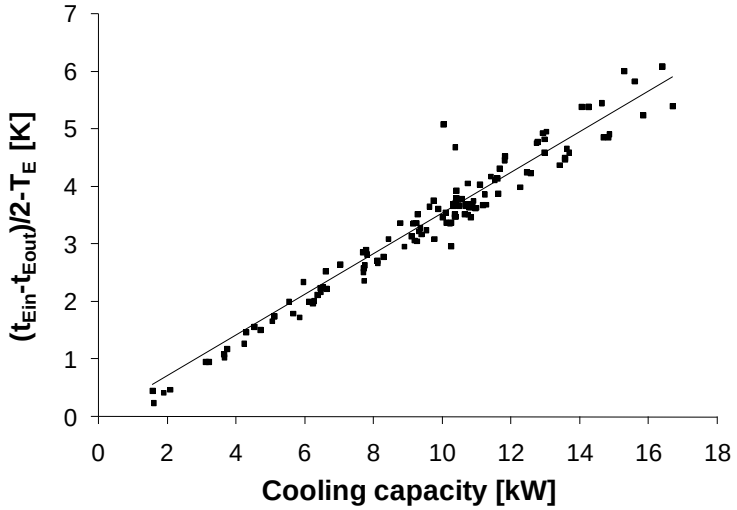

Figure 3: Arithmetic temperature difference $(t_{Ein}+t_{Eout})/2-T_E$ as function of the cooling capacity

4 REVERSIBLE OPERATION

As explained in chapters 1 and 2, the absorption heat pump is able to supply cold in summer time and heat in winter time. In the case of cooling mode, the heat source is the system which serves to distribute the cold in the building. It is connected to the evaporator of the heat pump. In terms of economic feasibility, the same system should be used to distribute the heat in the building in winter time. It is the heat sink, then. Thus, in heating mode this water circuit has to be connected to absorber and condenser. Equally, the heat sink of the cooling mode (water circuit between absorber/condenser and environment) should be the same as the heat source of the heating mode (water circuit between evaporator and environment). The switching of these two water circuits (heat source and heat sink) can easily be done by a valve, in the same way as in reversible compression heat pumps.

4.1 Operating conditions

Before evaluating the heat pump operation with different heat sources and heat sinks for cooling and/or heating mode operating conditions have to be specified. Two mandatory requirements have to be kept in mind in order to ensure a proper operation of the heat pump:

- The LiBr solution must not crystallize. Therefore, a minimum distance from the crystallization line of 3 percentage points has to be maintained.
- The refrigerant (water) must not freeze. Therefore, a minimum evaporation temperature of 3°C has been defined.

For reasons of energy efficiency we specified the following additional boundary conditions:

- In cooling mode, a minimum cooling capacity of 5 kW (50% of the nominal load) has been defined. It is also possible to achieve 25% part load or even less (see Figure 2, left), but even though cooling capacity is low, electric power consumption e.g. for the external pumps does not drop proportionally. This boundary condition is not mandatory for the operation but may be specified, depending on the system in order to achieve reasonable electrical EERs.
- In heating mode, a minimum thermal COP of 1.3 has been defined. Compared to a condensing boiler an additional energy input for external pumps like the heat source pump is required. To ensure a reasonable operation in terms of primary

energy use a high COP value is essential. Again, this condition is to be specified depending on the system.

Finally, we defined the following maximum differences between supply and return temperature of the air-conditioning equipment:

- 5 K for panel heating or cooling equipment like floor heating or chilled ceilings,
- 10 K for heating systems with supply temperatures above 40°C.

The last four conditions are not specific for the heat pump itself but they depend on the system.

4.2 Operational alternatives

Possible types of heat sources for the cooling mode have been classified into three groups based on the chiller outlet temperature:

- 7°C: central ventilation and air conditioning (VAC) systems (without downstream fan-coils), fan-coils (without upstream VAC system),
- 16°C: chilled ceilings or walls, passive cooling convectors, induction units and fan-coils with upstream VAC system, façade ventilation units,
- 20°C: concrete core cooling, floor cooling, radiators.

Possible heat sinks for the heating mode have been classified into five groups based on the heating supply temperature:

- 30°C: ceiling heating, concrete core heating,
- 35°C: floor heating,
- 40°C: wall heating, passive convection heaters,
- 45°C: central heating, ventilation and air conditioning (HVAC) systems, induction units and fan-coils with upstream HVAC system, fan-coils without upstream HVAC system, façade ventilation units, radiators,
- ≥ 50°C: central heating, ventilation and air conditioning (HVAC) systems, induction units and fan-coils with upstream HVAC system, fan-coils without upstream HVAC system, façade ventilation units, radiators.

As heat sinks for the cooling mode or heat sources for the heating mode respectively, air, water, and ground have been considered. While ground, surface or sewage water, bore holes, ground collectors, or dry or hybrid cooling towers can be used both for the cooling as well as for the heating mode, an open wet cooling tower is only feasible as a heat sink for the cooling mode. To increase the temperature of the heat source air, in the heating period a solar or air collector can be used.

The different possibilities have been combined in a matrix. For all combinations the heating and cooling power has been calculated for the presented heat pump using the model of chapter 3. Further assumptions have been made as follows:

- A constant driving temperature of 95°C has been assumed for cooling and heating mode. Doing so, of course, the power output of heat pump and chiller are restricted. The full potential of the chiller is not exploited as higher driving temperatures up to 120°C can be applied. However, in heating mode the driving temperature in some cases has been decreased below 95°C (e.g. by recirculation of the hot water return flow) if there was the risk of the evaporation temperature dropping below 3°C or the temperature difference in the heating system exceeding the maximum value of 5 or 10 K. In the case of cooling mode additionally an increase of the cooling water inlet temperature has been investigated in order to save the refrigerant from freezing. In this case the cooling tower fan speed is reduced. Considerable power savings can be achieved applying this alternative control strategy (Kühn et al. 2008a).
- The closest approach temperature difference of all heat exchangers in the peripheral systems, e.g. the dry cooler or bore hole heat exchanger, has been assumed to be 2 K.

- A heating limit temperature of 15°C has been assumed.
- In a first attempt, no heating characteristic has been regarded for the consumer. The heating supply temperatures have been assumed to stay constant with varying ambient temperature. Thus, the results turn out to be conservative.

As not all combinations can be presented in detail here we decided to demonstrate the most representative examples.

4.2.1 Bore holes/ground water as heat source/heat sink

A constant soil respectively ground water temperature of 10°C was assumed all year round. With this assumption water instead of brine can be used, also in case of bore holes. This assumption is reliable as the ground is cooled down (regenerated) during winter time. However, a detailed study on the ground temperature has not been performed yet.

Accordingly, in cooling mode we get a constant absorber inlet temperature of t_{Ain}=12°C. For cooling systems working with chilled water supply temperatures of 16°C or higher the ground water can be used directly; an operation of the heat pump in chiller mode is not required.

In case of 7°C chilled water supply temperature (i.e. for air dehumidification) the chiller is able to provide a cooling capacity of nearly 23 kW with an EER of 0.82. As the evaporation temperature drops below 3°C to 2.4°C, we have to limit the cooling capacity. This can be achieved either by decreasing the driving temperature to 84.6°C (e.g. by recirculation of the desorber outlet, see Figure 4, left side) or by increasing the cooling water temperature to 15.9°C (e.g. by recirculation of the condenser outlet, see Figure 4, centre). Cooling capacity in both cases is 20 kW. As the thermal EER has its maximum at medium driving temperatures, the EER in the first case is 0.83 and drops at rising cooling water temperatures to 0.80. But as already mentioned, the second control strategy can offer considerable advantages in terms of the electrical EER. Another possibility which was not investigated in this work is to reduce flow rates.

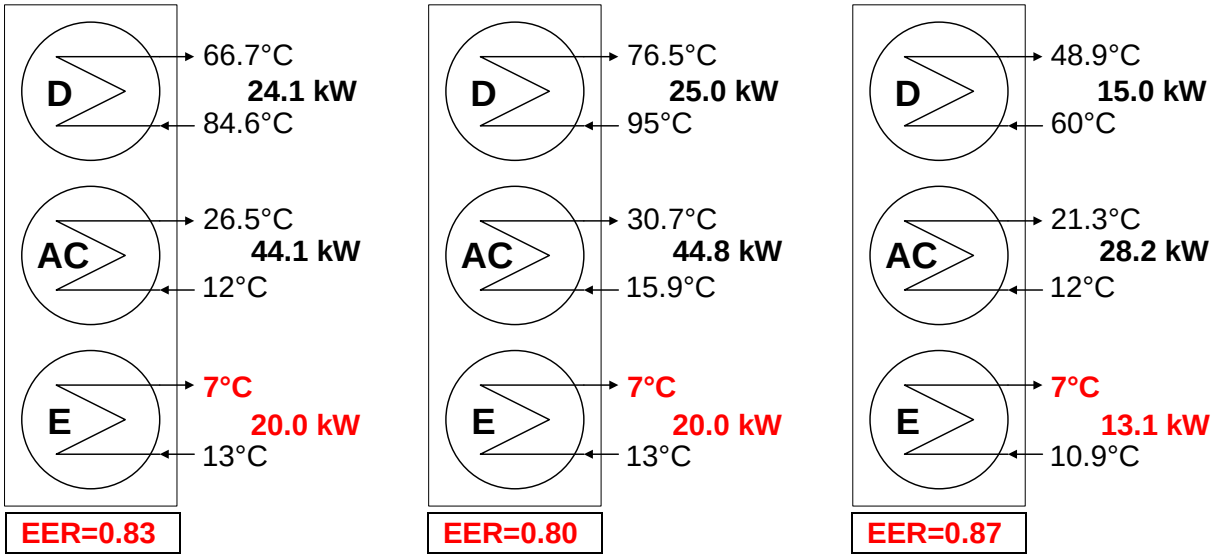

Figure 4: Chiller operation (t_{Eout}=7°C) with bore holes or ground water as heat sink (left: driving temperature decreased, centre: cooling water temperature increased, right: solar cooling)

If a solar collector is used as driving source instead of waste heat from e.g. CHP units or district heat, driving temperature in moderate climate like in Central Europe will not be that high (especially when using economic flat plate types). A chiller with only 60°C driving temperature, 12°C absorber inlet and 7°C evaporator outlet temperature delivers a cooling

capacity of 13 kW with an EER of 0.87 (see Figure 4, right side). It has to be admitted that these calculations have not been validated experimentally yet. The minimum absorber inlet temperature applied so far was 23°C. In this example, we assume an absorber inlet temperature of only 12°C. So the quoted EER might be too high. Nevertheless, the temperature lift in such point of operation is very small so a high EER is reasonable.

In heating mode (Figure 5), a minimum evaporator inlet temperature of t_{Ein}=5°C has been assumed (in case of bore holes). With this boundary condition a maximum heat supply temperature of 40°C can be achieved. Heat output in this case is around 10 kW; the COP is still acceptable with a value of 1.4. It increases with decreasing heating supply temperature to 1.65 at t_{Cout}=30°C. In the cases of 30°C and 35°C heating supply temperature the heat output had to be limited (by decreasing the driving temperature) as the evaporation temperature fell below the lower limit of 3°C. Measures to depress the freezing point of the refrigerant would help to use the full potential of the heat pump but have not been implemented here.

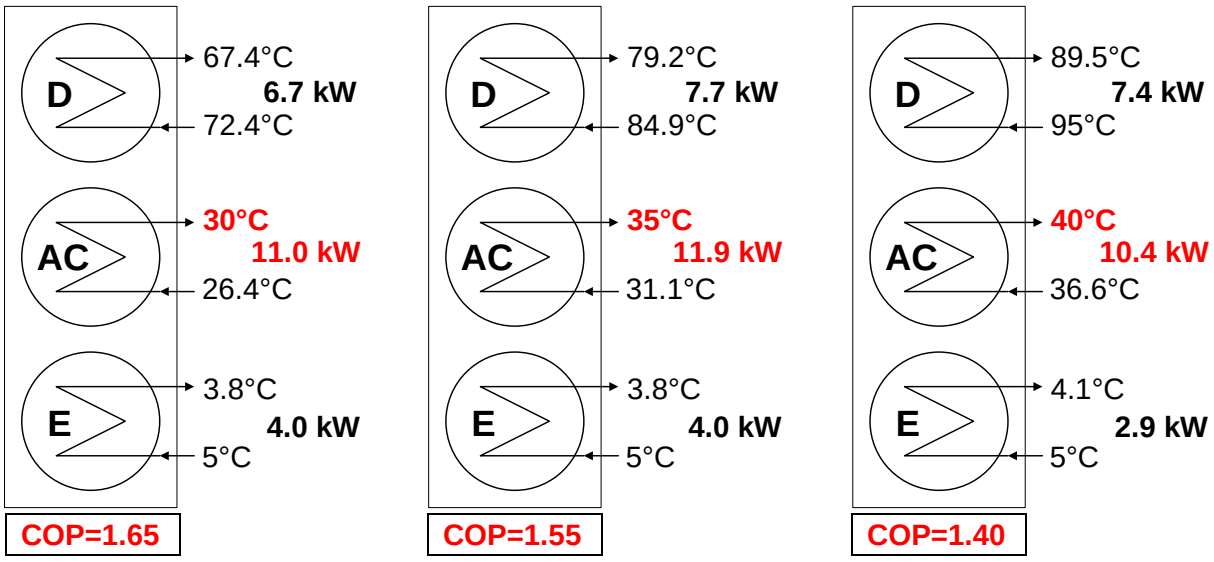

Figure 5: Heat pump operation with bore holes as heat source (t_{Ein}=5°C, heating supply temperature left: 30°C, centre 35°C, right: 40°C)

An increase of the heat source temperature has a significant influence (compare Figures 5 and 6). With an increase of only 3 K in the evaporator inlet temperature from 5°C to 8°C (e.g. ground water) the heat output is roughly between 30% and 45% higher. The COP is also increasing considerably.

The all year round use of bore holes is favourable as the ground which cools down during heat pump operation is regenerated in summer by the reject heat of the chiller. Nevertheless, heat transferred to the ground and heat removed from it should be balanced. Cooling capacity and heat output first have to be adapted to the building's requirements. There are buildings with very good insulation standard. There, cooling load might be higher than heating load. In this case the reject heat flow transferred to the ground in cooling mode is much higher than the heat source flow removed from it in heating mode. Consequently, the ground temperature will increase which is favourable for the heating mode; the system will adapt. However, there are also cases where heating load will be considerably higher. The number of bore holes required fits better for the reversible operation in the latter case. This applies in particular given that in moderate climate the heating period is longer than the cooling period. It further has to be considered that in cases of 16°C or 20°C chilled water

supply temperature where the heat source is directly used to cool the building only approximately half of the heat is transferred to the ground.

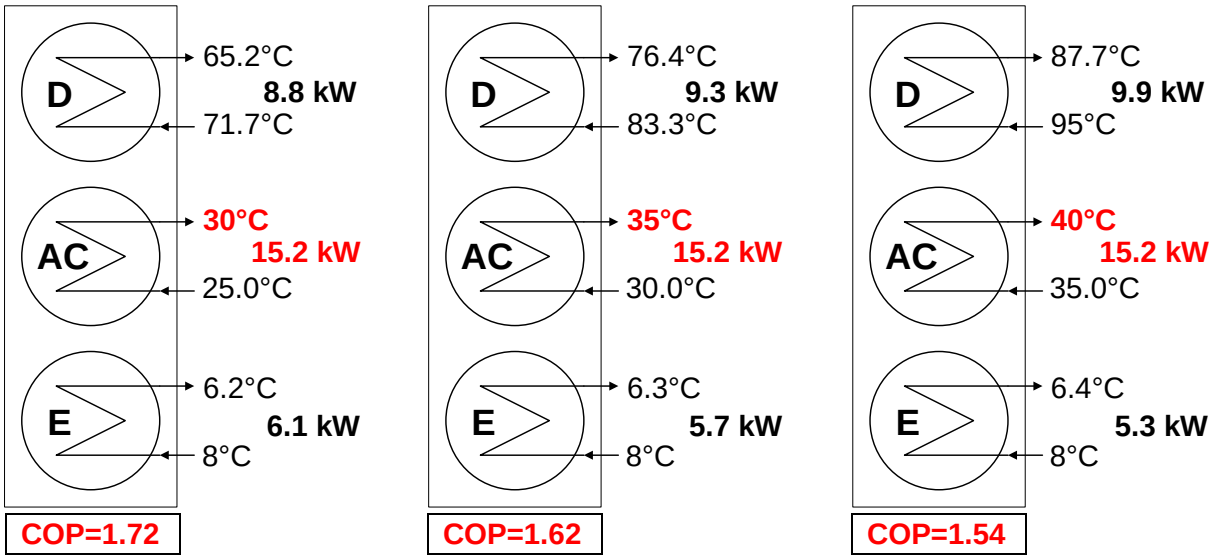

Figure 6: Heat pump operation with bore holes or ground water as heat source (t_{Ein}=8°C, heating supply temperature left: 30°C, centre 35°C, right: 40°C)

4.2.2 Air as heat source/heat sink

Ambient air can be used as a heat source or heat sink by means of a cooling tower. A wet cooling tower presents a very effective possibility to reject heat in cooling mode as cooling water temperatures below ambient temperature can be provided. Nevertheless, the design of an open wet cooling tower does not allow the use of ambient air as a heat source in winter time. Therefore, only dry or hybrid coolers (which also offer the advantages of a wet cooling tower at hot summer days) or closed cycle wet cooling towers can be applied for a reversible operation of the heat pump.

Cooling operation has been defined to start at an ambient temperature of 24°C (corresponding to an absorber inlet temperature of 26°C). Up to this ambient temperature window ventilation has been assumed to be sufficient. The cooling capacity delivered by the chiller and the EER depending on ambient temperature are presented in Figure 7. The parameter t_{Eout} is the chilled water temperature delivered to the building's cooling system.

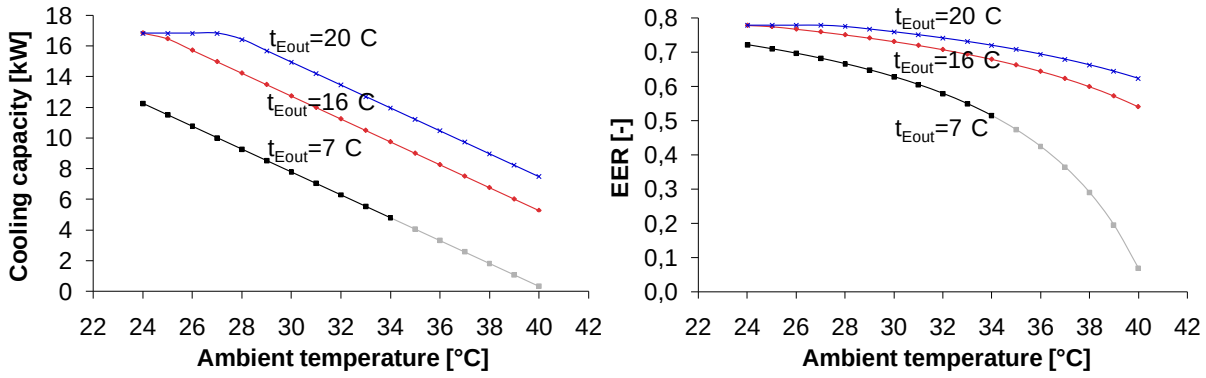

Figure 7: Chiller operation with air as heat sink (dry or hybrid cooler)

In the cases of 16°C and 20°C chilled water temperature a maximum temperature difference in the chilled water circuit of 5 K has to be maintained. Therefore, the maximum cooling capacity is limited to approximately 17 kW at 24°C ambient temperature (EER=0.8). Minimum cooling capacity is 5.3 kW at 16°C chilled water und 40°C ambient temperature (EER=0.5), and 7.5 kW at 20°C chilled water temperature (EER=0.6), respectively. Maximum cooling capacity at 7°C chilled water temperature is 12.3 kW at 24°C ambient temperature (EER=0.7). In this case, the cooling capacity falls below the defined minimum value of 5 kW at ambient temperatures above 34°C. That means that in hot climate HVAC-systems or fan-coils used for air humidification cannot be combined with a dry cooler but a hybrid cooler has to be used. The EER of the chiller at 7°C chilled water temperature and 34°C ambient temperature is still above 0.5.

In heating mode, air can only be used as a heat source at ambient temperatures from 6°C and above which limits application considerably. This is due to the impending freezing of the refrigerant water. In (Kojima et al. 2003, Richter et al. 2007, and Kühn et al. 2008b) a possibility to enlarge the operation limits to heat source temperatures even below 0°C has been presented. This method is not considered in this paper, as stated before.

In case of low temperature heating systems (30°C and 35°C heating supply temperature) the temperature difference in the heating circuit is limited to 5 K. This is achieved by a decrease of the driving temperature. Therefore, the heat output is limited to maximum 15 kW (COP=1.8 at t_{Cout}=30°C and 1.7 at t_{Cout}=35°C, see Figure 8). In case of heating systems with supply temperatures of 40°C (or higher) a temperature difference of 10 K is allowed. Therefore, the maximum heat output of such a system at 15°C ambient temperature (corresponding to an evaporator inlet temperature of 13°C) is 23 kW (COP=1.7). The lowest heat output in all three heating systems is between 7 and 9 kW at 6°C ambient temperature (corresponding to an evaporator inlet temperature of 4°C). The COP at this operating point is higher than the requested 1.3 in case of 40°C heating supply temperature and nearly 1.6 in case of 30°C heating supply temperature. A heating supply temperature of 45°C can only be delivered at ambient temperatures near to the heating limit temperature and is therefore not very reasonable.

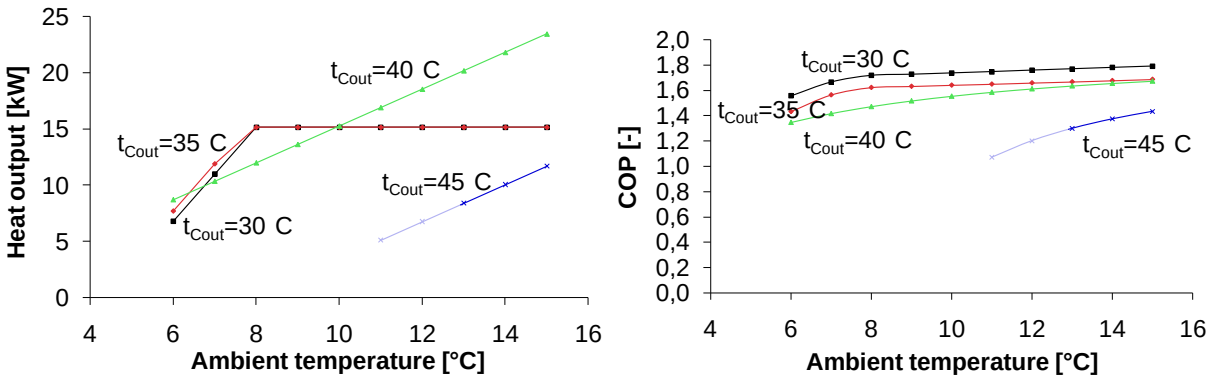

Figure 8: Heat pump operation with air as heat sink (dry or hybrid cooler)

An option in case of solar cooling, i.e. if a solar collector is used to provide the required driving heat in cooling mode, is to use the collector as heat source equipment, also. It is supposed that the operating range with air as a heat source can be extended considerably. In a draft of the German norm VDI 4650-2 a temperature increase of 5.6 K above ambient temperature is reported when using a collector with an aperture area of 8 m² (VDI 2010).

5 SUMMARY

In this paper a reversible H_2O/LiBr absorption heat pump is presented for which all possible combinations of heat source and heat sink have been evaluated using an improved version of the characteristic equation method. The most representative examples have been presented in detail; influencing parameters have been described.

The reversible water-water absorption heat pump can be classified in accordance with the EN 12309-2 (CEN 2000) as W10/W35 with a heat output of 15.2 kW and a COP of 1.6 (heating mode) and as W30/W7 with a cooling capacity of 9.4 kW and an EER of 0.7 (cooling mode). The use of the heat pump is possible up to heating supply temperatures of 40°C (W10/W40) without limitations. The supply of higher heating supply temperatures is not reasonable. Air can also be used as a heat source or heat sink, respectively, but not directly. Heat has to be transferred to/from a water circuit. The use of air as a heat source has been limited to a minimum ambient temperature of 6°C if pure water is used as a refrigerant. Below this temperature the driving heat must directly be used to heat the building. The use of a solar collector as a heat source can extend the operating time of the heat pump considerably. The use of air as a heat sink in summer is limited to an ambient temperature of 34°C only in case of a low chilled water supply temperature of e.g. 7°C. In cases of higher chilled water supply temperatures, like e.g. 16°C, heat of the chiller can efficiently been rejected up to an ambient temperature of 40°C. The prototype can also be used as a brine-water heat pump as explained in (Kühn et al. 2008b) but to a limited extent.

It can be concluded, that the absorption chiller is very flexible and is able to deliver a heat output and a cooling capacity very different from the rated conditions. The integration into a building energy supply system consisting of a heat source and a heat sink imposes some restrictions, especially if a reversible operation is requested. There, deliverable useful heat flows have to be adapted to the requirements of the peripheral circuits, e.g. a maximum temperature difference of the heating or cooling system. The heat pump already allows the use of many combinations of heat sink and heat source, but by using an intelligent system integration there are still more options (e.g. the use of a solar collector as driving source in cooling mode and as heat source in heating mode).

For a final assessment, in a further step seasonal COPs (SCOP) and seasonal EERs (SEER) of the reversible absorption heat pump will be calculated and the different possibilities will be evaluated regarding cost, applicability and comfort for the user of the heating and cooling system.

6 NOMENCLATURE

		Indices	
t, T	temperature [°C]		
$\dot{Q}$	heat flow [kW]	D	desorber
$\Delta\Delta t$	characteristic temperature functions [K]	A	absorber
$\dot{m}$	mass flow rate [kg/s]	C	condenser
c_p	specific heat capacity [kJ/kgK]	AC	absorber/condenser in series
U	heat transfer coefficient [kW/m²K]	E	evaporator
A	heat transfer area [m²]	in	inlet
$\Delta\vartheta_{log}$	logarithmic temperature difference [K]	out	outlet

7 REFERENCES

Albers J., F. Ziegler 2011. “Heat transfer calculation for absorption heat pumps under variable flow rate conditions”, *Proc. of the Int. Sorption Heat Pump Conf. (ISHPC)*, 6-8 April 2011, Padua, Italy.

ASC 2011. www.greenchiller.eu, 28.01.2011.

CEN 2000. “EN12309-2 Gas-fired absorption and adsorption air-conditioning and/or heat pump appliances with a net heat input not exceeding 70 kW – Part 2: Rational use of energy”, CEN, Brussels.

IGWP 2011. www.igwp.de, 28.01.2011.

Kojima, M., T. Fujita, T. Irie, N. Inoue, T. Matsubara 2003. “Development of Water-Lithium Bromide Absorption Machine Operating Below Zero Degrees”, *Proc. of the Int. Congress of Refrigeration 2003*, Washington, D.C., USA.

Kühn A., F. Ziegler 2005. “Operational results of a 10 kW absorption chiller and adaptation of the characteristic equation”, *Proc. of the 1st Int. Conf. Solar Air Conditioning*, 6-7 October 2005, Bad Staffelstein, Germany.

Kühn A., J. L. Corrales Ciganda, F. Ziegler 2008a. “Comparison of control strategies of solar absorption chillers”, *Proc. of the 1st Int. Conf. on Solar Heating, Cooling and Buildings (Eurosun)*, 7-10 October 2008, Lisbon, Portugal.

Kühn A., T. Meyer, F. Ziegler 2008b. “Operational results of a 10 kW absorption chiller in heat pump mode”, *Proc. of the 9th Int. Energy Agency Heat Pump Conf.,* 20-22 May 2008, Zürich, Switzerland.

Richter, L., M. Kuhn, M. Safarik 2007. “Kälteerzeugung unter 0°C mit einer Wasser/LiBr-Resorptionskältemaschine“, *Tagungsbericht der Deutschen Kälte-Klima-Tagung 2007 Hannover,* Deutscher Kälte- und Klimatechnischer Verein, Stuttgart, Germany.

Schweigler C., A. Costa, M. Högenauer-Lego, M. Harm, F. Ziegler 2001. “Absorptions-kaltwassersatz zur solaren Klimatisierung mit 10 kW Kälteleistung“, *Tagungsbericht der Deutschen Kälte-Klima-Tagung 2001 Ulm,* Deutscher Kälte- und Klimatechnischer Verein, Stuttgart, Germany.

VDI 2010. “VDI 4650-2 Simplified method for the calculation of the annual coefficient of performance and the annual utilization ratio of sorption heat pumps - Gas heat pumps for space heating and domestic hot water”, VDI, Düsseldorf.

Ziegler F. 1997. “Sorptionswärmepumpen“, *Forschungsberichte des DKV Nr. 57, Habilitationsschrift*, Erding, Germany.

EJECTOR APPLICATIONS IN REFRIGERATION AND HEATING: AN OVERVIEW OF MODELING, OPERATION AND RECENT DEVELOPMENTS

Zine Aidoun, Daniel Giguère, David A. Scott, Sophie Hosatte, CanmetENERGY, Natural Resources Canada, 1615 boul. Lionel-Boulet, CP 4800, Varennes, Québec, J3X 1S6, Canada
shosatte@nrcan.gc.ca

This paper was published in the proceedings of the 10th International Heat Pump Conference 2011 (www.heatpumpcentre.org/en/hppactivities/ieaheatpumpconference).

Abstract: The utilization of ejectors in heat pump systems as compression components, alone or in combination with other equipment, have gained renewed interest as a thermally driven solution for low temperature heat recovery and upgrading and more efficient energy use. This paper summarizes the main findings and trends, in the area of heat driven ejector based machines using low boiling point working fluids. An overall view of such systems is provided by presenting the ejector principles of physics and the latest developments on ejector design, operation and modeling approaches. Aspects related to the analysis of the complex interacting phenomena taking place in these systems for high performance are highlighted. Conventional and improved ejector heat pump cycles of interest employing ejectors alone or boosted combinations are presented and discussed, and their potential applications are indicated. Finally, sample theoretical and experimental results obtained at CanmetENERGY on ejector operation and design are reported.

Key Words: ejector modelling, design, simulation, experiments, thermal activation, cycle

1 INTRODUCTION

An ejector is a form of thermally activated jet-pump that is generally used for pumping gases from systems to produce vacuum or compressing vapours. They have been in application for many years (ASHRAE 1969), but mainly restricted to industrial applications using steam as the working fluid. They are commercially available in different sizes and geometries to match different power requirements. The ejector as a component is simple, low cost, and without moving parts, which makes it attractive for many applications. However, the fundamental mechanisms involved during their operation are complex due to the interactions during mixing of two fluid streams in sub-sonic and super-sonic conditions.

The utilization of ejectors for heat pump applications (heat upgrading, cooling and refrigeration) has been limited until now because of the lack of knowledge on their performance over a wide range of operating conditions and using different refrigerants, and also because of their low energy efficiency compared to mechanical vapour compression systems. However, in the current energy and environmental context, there is a renewal of interest for ejectors as a thermally driven technology which may provide a reliable and low-cost solution for recovering and upgrading thermal energy.

As a thermally driven heat pumping technology, ejectors may be considered in many applications. For heating and cooling in buildings, houses and communities, ejectors may be used in combination with renewable energy systems or distributed generation systems in tri-generation applications. In industry, they represent an attractive solution for waste heat

upgrading. They may be used as a stand-alone system or in hybrid vapour compression-ejector or absorption-ejector systems.

The availability of more sophisticated modeling tools (e.g. Computational Fluid Dynamics) combined with experimental analysis, provides new opportunities to develop advanced knowledge on the internal phenomena occurring in the ejector, to identify solutions that reduce internal losses, to optimize ejector performance by varying design, geometry, and refrigerants and to evaluate the performance of innovative cycles based on a combination of ejectors with vapour compression or absorption systems for different applications.

This paper presents the principles of ejectors, different application cycles, performance obtained through modelling and experimental work, and a discussion on some promising applications for ejectors.

2 EJECTOR OPERATION

Basic ejector operation is briefly described here but a more detailed account can be found in journal publications (Ouzzane and Aidoun 2003). The principle of operation of all supersonic ejectors is the same, regardless of the application. As shown in Figure 1, a high energy refrigerant stream is expanded in a primary nozzle (1), converting pressure and temperature to velocity.

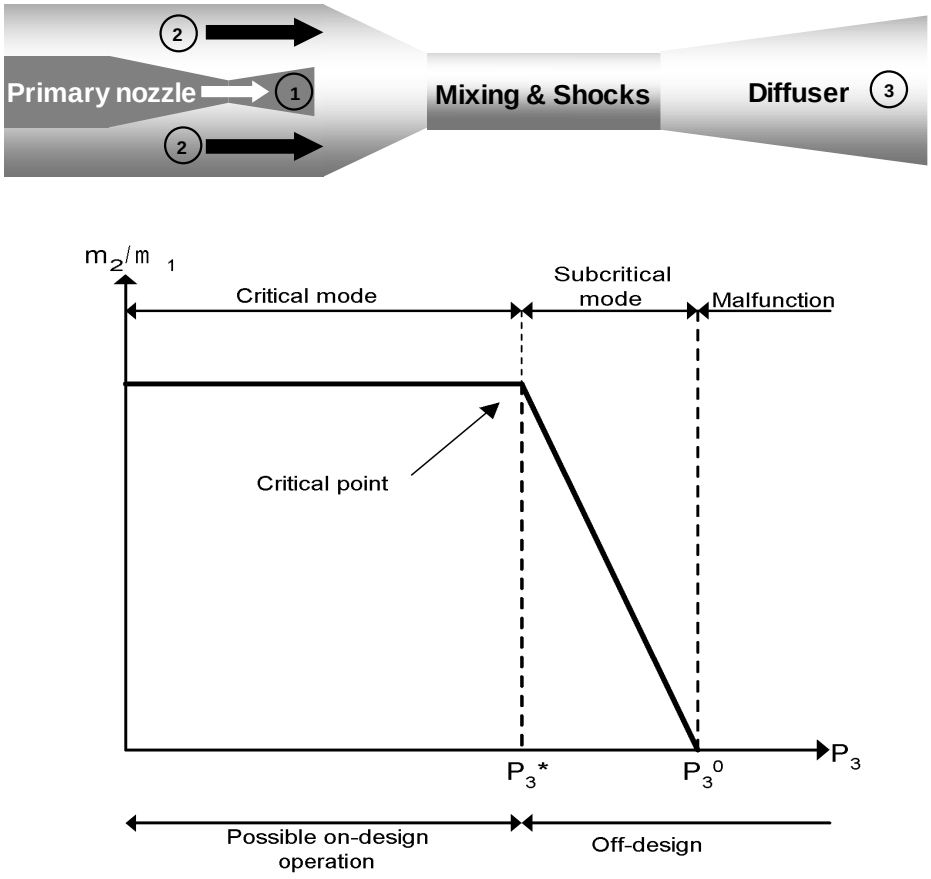

Figure 1: Ejector operation

At the nozzle exit, the flow is supersonic with low temperature and pressure. This induces the flow of a low energy stream (2) from the evaporator, through a secondary nozzle at the exit

of which sonic conditions are reached (design point). The main characteristic of the performance curve shown in Figure 1 is that the entrainment ratio m2/m1 remains constant up to a threshold (design point) before dropping rapidly (off design operation zone). Energy exchange between streams occurs in the mixing chamber but high mixing losses, friction, shock formation etc., are also expected because of the streams very different conditions. The flow leaving the mixing chamber becomes subsonic as a result of all the losses and shocks. It then enters a diffuser where it is further compressed (3).

3 PREVIOUS RESEARCH ON EJECTORS

Current needs for efficient and environmentally sound heating, air conditioning and refrigeration systems have revived research interests in order to improve ejector performance and competitiveness. Experimental and theoretical work has been extensively performed on ejector operation for some decades and it is currently continuing but despite the apparent simplicity of the ejector geometry, there is still no comprehensive theory capable of completely describing its working mechanisms and ejector modeling remains a problem not yet completely resolved. Available literature, some going back to very early years, contributes however to a better understanding of ejector design and operation.

3.1 One-dimensional approach

Earlier theoretical and experimental work using gases and vapours was based on the one-dimensional theory developed by Keenan and his collaborators. Two design methods emerged out of these efforts, due to Keenan & Newman (1946) and Keenan et al. (1950), who proposed 1-D models with constant area and with constant pressure mixing respectively, but ignoring heat and friction losses. They first introduced the constant-area-mixing principle (1946) and performed their mathematical development by assuming that the working fluid behaved like an ideal gas. This approach considers a constant cross-sectional area for the entire mixing chamber (Figure 2).

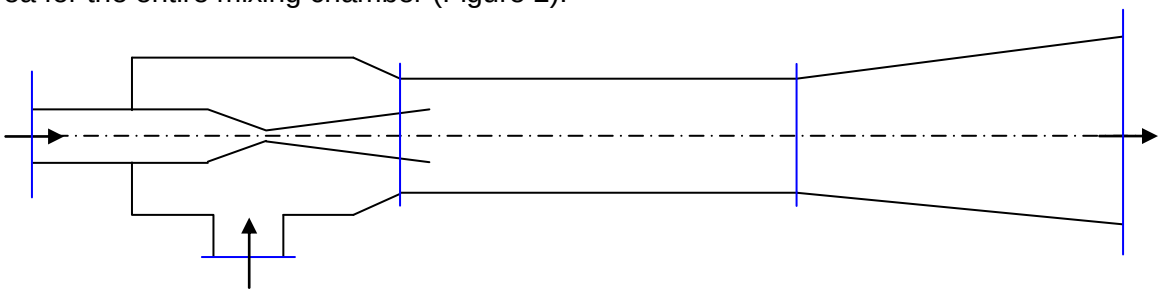

Figure 2: Constant area ejector

The concept of constant pressure design was subsequently introduced (1950). This principle is the most frequently used nowadays for its better performance and more favourable comparison against experimental data. The geometry of a constant pressure design includes a variable cross section zone immediately before the constant cross section part, with the nozzle exit located within this zone (Figure 3).

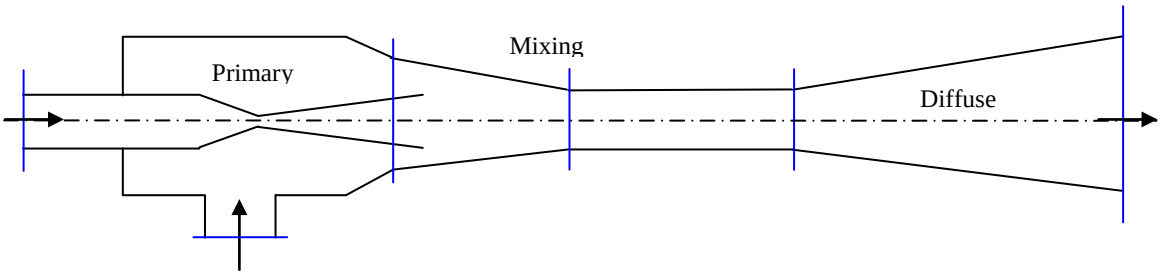

Figure 3: Constant pressure ejector

In 1977, Munday and Bagster proposed a semi-empirical approach in an attempt to explain the constant capacity characteristics of ejectors represented in Figure 1. This approach introduces a new concept by assuming that two discrete streams, the primary and secondary flows, maintain their identity up to a certain distance down the mixing chamber. Accordingly, the primary stream fans out into the mixing chamber without mixing with the entrained flow, forms with the internal walls of the chamber a converging channel that acts as a nozzle for the secondary stream and eventually creates a low pressure region in the mixing section. The secondary fluid accelerates to sonic velocity without mixing with the primary stream. The location of the point where critical conditions occur is the effective throat of the secondary nozzle beyond which stream mixing at constant pressure begins. Downstream of the mixing section, a normal shock is induced, causing a sudden increase of pressure and a simultaneous decrease of the flow Mach number. According to this concept, it is assumed that the shock wave occurs at the end of the constant area section. In the mixing process, the flow transits from supersonic to subsonic. The diffuser compresses the flow further as it is brought to a stagnation state.

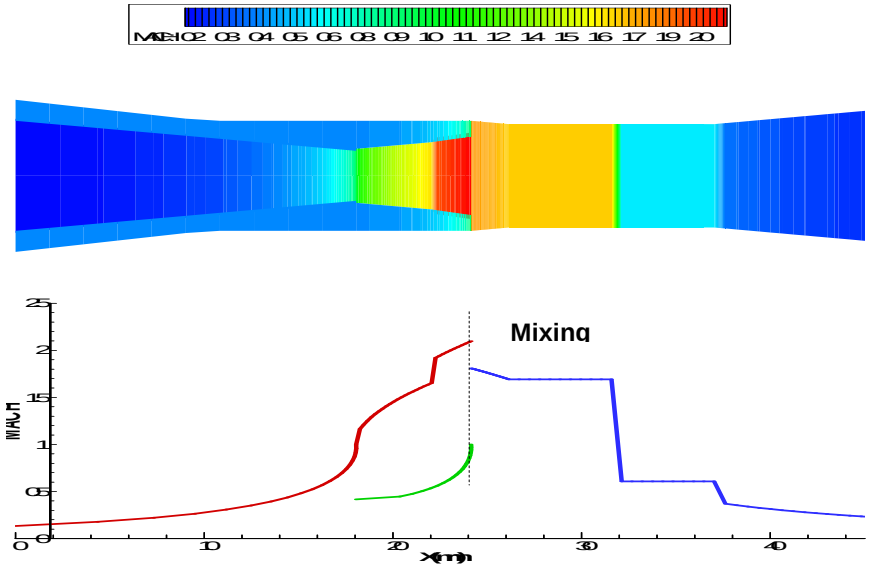

Figure 4: Mach distribution in the ejector (1-D)

Subsequent work was essentially based on these theories and, recognising the effects of parameters such as internal geometry, mixing-shocks interactions and refrigerant effects, researchers have progressively lifted many of the restrictive assumptions made in the previous theories. Huang et al. (1999), for example, used Munday and Bagster's approach with R141b and accounted for frictional and mixing losses by means of empirical coefficients which were later confirmed experimentally. Aidoun and Ouzzane (2004), inspired by the Munday and Bagster approach, took into account the change in refrigerant properties within

the flow with axial position in order to more accurately represent the operation of an ejector and estimate the ejector characteristic parameters locally (Figure 4). An extensive and more detailed account of these developments over the last few decades can be found in Ablwaifa (2006).

3.2 CFD approach

The amount of theoretical and experimental work devoted to providing simple analysis and design tools has been and continues to be very useful in promoting the general understanding of ejectors. There is however a serious limitation to its capability in correctly reproducing the flow physics locally along the ejector. It is the understanding of local interactions between shock waves and boundary layers, and their influence on mixing and recompression rates, that will allow minimizing internal losses based on optimized design in terms of geometry, refrigerants and operating conditions. Such an objective can be achieved at a reasonable cost through the use of CFD. Studies with some fluids commonly used in refrigeration or having such a potential were performed, (Chen et al. 1994; Desevaux et al. 1994; Riffat et al. 1996; Wang and Chen 1996; Riffat and Everitt 1999; Riffat and Omer 2001), being a representative sample. However, some very fundamental problems were yet to be overcome, especially the modeling of shock-mixing layer interaction or ejector operation at different conditions. Indeed, some of them did not consider compressibility, turbulence, nor did they track shocks. Desevaux et al. did obtain some local pressure measurements which compared reasonably well with simulations using the Fluent CFD package. These data were also used by Bartosiewicz et al. (2005, 2006) to validate their modeling of ejectors for refrigeration where the influence of turbulence, shock reflections and shock-mixing layer interaction were assessed. The work of Ablwaifa (2006), cited previously, included CFD analysis and validation data in terms of global performance parameters.

3.3 Ejector cycles and applications

Ejector driven heat pump systems have a large potential for using energy sources at low temperature. The simplest configuration of an ejector heat pump cycle is represented in Figure 5. The utilization of working fluids more volatile than water makes it possible to extend the range of applications, which are currently unexploited. For example in the industrial sector where low grade thermal energy is wasted, ejectors offer a potential to use it for cooling or refrigeration, increasing process efficiencies. They are also considered in combination with distributed generation systems to manage excess heat for cooling or refrigeration in tri-generation systems. Combinations of ejectors with other cycles to form hybrid systems (solar collectors, absorption or mechanical compression) provide a considerable potential for cycle optimization and performance enhancement. As a result, ejector-compressor, ejector-absorption and ejector-solar collector cycles continue to receive increased attention in view of their positive impact on performance in exchange for relatively minor modifications to the overall system.

3.3.1 Compressor-assisted ejector

The work of Sokolov & Hershal (1990, 1991), Sun and Eames (1995), Dorantes et al. (1996), Sun (1997) and those of Huang et al. (1998) are worth mentioning. Sokolov and his collaborators demonstrated that performance comparable to those of absorption systems could be attained with booster assisted ejector systems running on low grade heat. Depending on the particular operating conditions and cycle configurations, COP improvements reported ranged from 5 % to 40% over conventional cycles.

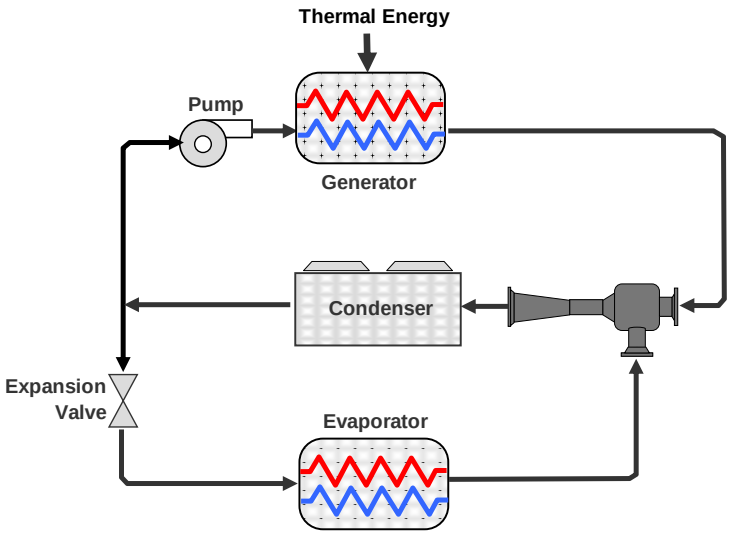

Figure 5: Schematic drawing of the simplest configuration of a supersonic ejector cycle

Ejector – Expander

Ejectors may be used inside vapour compression cycles for heating, cooling or refrigeration applications, to reduce the compressor work. In this configuration (Figure 6), the ejector plays the role of the low temperature stage of a two-stage compression cycle to some extent. It is introduced instead of the expansion valve. Its role is to reduce the compression ratio and increase the cycle COP from 10 to 15%. The ejector is driven by the high temperature liquid refrigerant coming out of the condenser.

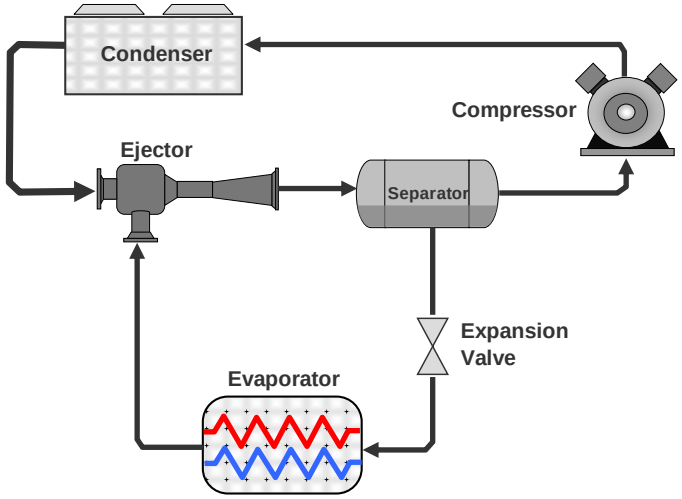

Figure 6: Schematic drawing of a compressor-assisted ejector cycle

Ejector for pressure lift increase

Another interesting application is the utilization of the ejector at the compressor outlet for reducing compression ratio and work. As shown in Figures 7 (external energy input) and 8 (without external energy input), the discharge pressure is reduced further to the addition of an ejector that provides a compression stage. The ejector plays the role of the high stage of a two-stage compression cycle. With this system, COP cycle improvements have been evaluated at 30 to 40%.

The configuration presented in Figure 7 requires additional thermal energy to drive the ejector and increasing the size of the condenser as, in this case, it must reject the heat of the generator and of the vapour compression cycle.

In the configuration presented in Figure 8, also known as Condensing ejector, the ejector is driven by the condensate but prior to being sent to the ejector its pressure is raised by a pump so that the ejector can draw vapour refrigerant from the compressor. The challenge is to have the refrigerant condensed in the ejector. The condenser is replaced by a heat exchanger (fluid cooler).

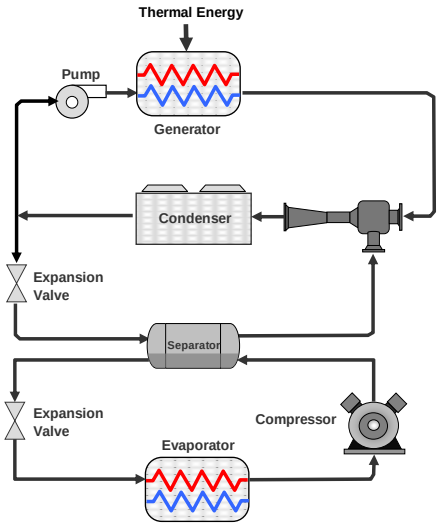

Figure 7: Ejector for pressure lift increase

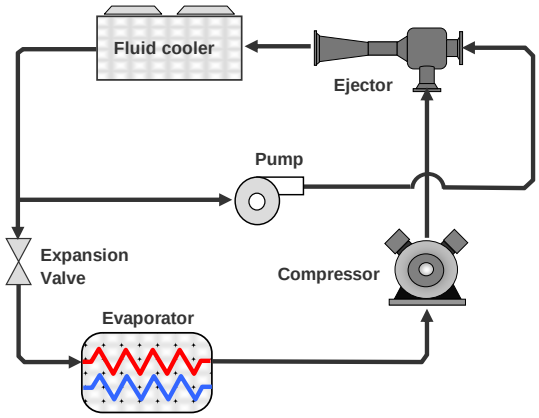

Figure 8: Condensing ejector

In the two cases above, Ejector-expander and condensing ejector, the ejector works in two-phase mode (two-phase flow).

3.3.2 Other applications

Ejector-enhanced absorption

The application of ejectors in absorption cycles is another area for which substantial improvement in COP is expected by enhancing evaporation, absorption and concentration processes and by carefully selecting the refrigerant. Several studies were conducted on absorption cycles integrating the use of ejectors. The works of Chung et al (1984), Chen (1988), Sun et al. (1996) and Aphornratana et al. (1998) are well documented.

Solar activated ejectors

Fluid temperatures provided by thermal solar collectors are appropriate to be exploited to drive ejectors for cooling, refrigeration or heat pumping. Considerable analytical and experimental effort was invested by many researchers to investigate the implementation of solar energy to drive ejector based cycles (Sokolov 1993, Huang 1998, Alexis and Karaiyannis 2005).

Compressor superheat activated ejector

In many instances superheat at the compressor discharge is considerable. Huang et al. (2001) analyzed the effect of its recovery to activate an ejector in order to subcool the refrigerant condensate. Refrigerant subcooling is a common practice in refrigeration installations, in order to increase performance. As a result, refrigeration performance increases between 9% and 24% in terms of COP.

4 RESEARCH HIGHLIGHTS AT CanmetENERGY

Ejector research performed at CanmetENERGY includes numerical modeling and experimental investigations.

4.1 Modeling and simulation

One-dimensional and detailed computational fluid dynamics (CFD) models were developed. Validation was performed, using data from the literature, collaborative exchanges and results from an experimental test bench that was designed and built for this purpose. Results from CFD models provide detailed images of parameter distributions throughout the ejector, allowing users to “see” inside the walls and to identify problem areas such as zones with recirculation and flow separation. Figure 9, based on the simulations of Scott et al. (2008), shows some generic results from one-dimensional CFD models. The single curve showing the variation of the entrainment ratio with ejector exit pressure may be generated by a one-dimensional model. The same curve may be generated by a CFD model, however the results of the CFD model also permit “snapshots” of the flow inside the ejector to be taken, these snapshots showing the variation of the velocity profile inside the ejector at the given operating conditions.

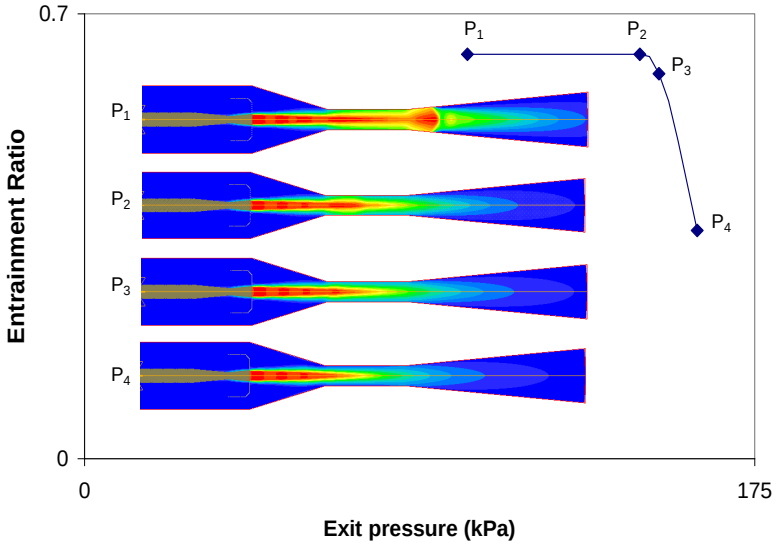

Figure 9: Typical CFD and 1-D ejector simulation results

4.2 Experimental Research

A well instrumented experimental test bench was designed and assembled at CanmetENERGY. While the primary purpose of the set-up is to generate data for the validation of the numerical models, it also provides information on start-up and shut-down procedures, performances, as well as general operation. Only a brief description of the test bench is given here; details can be found in Scott et al. (2009).The configuration of the simplest one-phase ejector cycle is shown in Figure 5. The working fluid is R245fa, an HFC that has been shown to have appropriate properties for ejector operation. Ejector capacities up to 9 kW can be tested on this installation. Typical experimental results showing the variation of the entrainment ratio with condenser pressure is shown in Figure 10, with fixed generator and evaporator conditions. The constant entrainment ratio that exists at pressures below the critical condenser pressure is clearly shown, as is the rapid decrease in entrainment ratio above this critical pressure. These and other such results from the test bench were used to validate the numerical models.

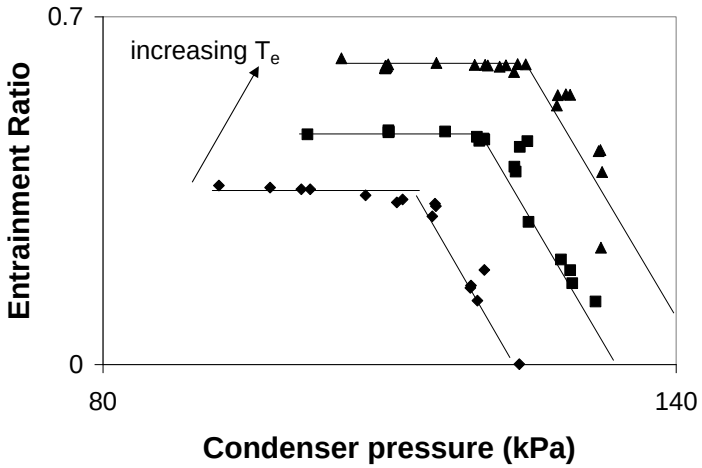

Figure 10: Variation of the entrainment ratio with condenser pressure.

Further R&D activities in ejectors are on-going, particularly on two-phase flow ejectors, using modeling-simulation and experimental work, evaluation of solar assisted ejector cycles for cooling applications, and experimentation of a 30 kW prototype for cooling applications using waste heat.

5 CONCLUSION

Ejectors are a unique technology involving simple components but of which the operation, based on the mixing of two fluid streams in sub- super- sonic conditions, is quite complex. This technology is currently unexploited due to the lack of fundamental knowledge on its operation, while it presents interesting opportunities for thermal energy upgrading for heating, cooling or refrigeration applications, and for heat pump cycle improvements in hybrid systems. Other advantages of the technology are the simplicity of the components (nozzles) and their low costs, its compactness, particularly compared to absorption, and its reliability as no moving parts are involved. The most promising applications are waste heat valorization in the industry and combinations with thermal solar energy for buildings.

Ejectors must not be considered as a competitive technology to vapour compression systems, due to their low coefficients of performance and small temperature lifts of the basic cycles. However, the technology must be seriously examined for thermal energy valorization, for heat pump cycle improvements and particularly in hybrid cycles. The benefits are the significant COP increases, the possibility to reduce compressor work, or increase pressure or temperature lift and power, with low cost and reliable additional components.

The development of fundamental knowledge on the mechanisms involved in ejectors in one- or two- phase flow, as well as knowledge on system performance and control as stand alone or hybrid systems are required to better evaluate and design the most judicious applications of ejectors. Investigation of refrigerants and their mixtures is also a promising avenue to expand their range of applications.

6 REFERENCES

ASHRAE 1969. Steam-jet refrigeration equipment, Chapter 13, ASHRAE Guide and Data Book.

Ablwaifa A. 2006. “A Theoretical and Experimental Investigation of Jet-Pump Refrigeration’’, PhD thesis, Nottingham University, England, UK.

Aidoun Z., M. Ouzzane 2004. ‘’The effect of operating conditions on the performance of a supersonic ejector for refrigeration’’, *Int. Journal of Refrigeration,* Vol. 27, pp. 974-984.

Alexis G., E. Karayiannis 2005. ‘’A solar ejector cooling system using refrigerant R134a in the Athens area’’, *Renewable Energy*, Vol. 30, pp. 1457–1469.

Aphnonratana S., I.W. Eames 1998. ‘’Experimental investigation of a combined ejector-absorption refrigerator’’, *Int. J. of Energy Research*, Vol. 22, pp. 195-207.

Bartosiewicz Y., Z. Aidoun, P. Desevaux, Y. Mercadier 2005. ‘’Numerical and experimental investigations on supersonic ejectors’’, *Int. J. Ht. & Fl. Flow*, Vol. 26, pp. 56–70.

Bartosiewicz Y., Z. Aidoun, Y. Mercadier 2006. ‘’Numerical assessment of ejector operation for refrigeration applications based on CFD’’. *Appl. Th. Eng.*, Vol. 26, pp. 604–612.

Chen F., C. Liu, J. Yang 1994. ‘’Supersonic flow in the second-throat ejector-diffuser system’’, *Journal of Spacecraft and Rockets,* Vol. 31, pp. 123–129.

Chen L.T. 1988. ‘’A new ejector-absorber cycle to improve COP of an absorption system’’, *Appl. Energy,* Vol. 30, pp. 1-37.

Chung H., M.H. Huor, M. Prevost, R. Bugarel 1984. ‘’Domestic heating application of an absorption heat pump. Direct fired heat pumps’’, *Proc. Int. Conf. Univ. of Bristol,* pp. 19-21.

Desevaux P., J.P. Prenel, P. Jacquet 1994. ‘’Static Pressure Measurement along the Centerline of an Induced Flow Ejector’’, *Experiments in Fluids*, Vol. 16, pp. 289-291.

Dorantes R., C.A. Estrada, I. Pilatowski 1996. ‘’Mathematical simulation of a solar ejector-compression refrigeration system’’, *ATE,* Vol.16, (8/9), pp. 669-675.

Huang B., J.M. Chang, V.A. Petrenko, K.B. Zhuk 1998. ‘’A solar ejector cooling system using refrigerant R141b’’, *Solar Energy,* Vol. 64, Nos 4-6, pp. 223-226.

Huang B., J.M. Chang, C.P. Wang, V.A. Petrenko 1999. ‘’A 1-D Analysis, of Ejector Performance’’, *Int. J. of Refrigeration,* Vol. 22, pp. 354-364.

Huang B., V.A. Petrenko, J.M. Chang, C.P. Lin, S.S. Hu 2001. ‘’A combined-cycle refrigeration system using ejector-cooling cycle as the bottom cycle’’, *Int. J. of Refrigeration,* Vol. 24, pp. 391-399.

Keenan J. H., E.P. Newman 1946. ‘’A simple air ejector”, *J. Appl. Mech., Trans. ASME*, Vol. 64, pp. A75-A81.

Keenan J. H., E.P. Newman, F. Lustwerk 1950. ‘’An Investigation of Ejector Design by Analysis and Experiment’’, *J. Applied Mechanics, Trans. ASME*, 72, pp. 299-309.

Munday J.T., D.F. Bagster 1977. ‘’A New Ejector Theory Applied to Steam Jet Refrigeration’’, *Ind. Eng. Chem. Process Res Dev*., Vol. 16(4), pp. 442-449.

Ouzzane M., Z. Aidoun 2003. ‘’Model development and numerical procedure for detailed ejector analysis and design’’, *Applied Thermal Engineering,* Vol. 23, pp. 2337-2351.

Riffat S.B., G. Gan, S. Smith 1996. ''Computational fluid dynamics applied to ejector heat pumps'', *Applied Thermal Engineering,* Vol. 16, pp. 291-297.

Riffat S.B., P. Everitt 1999. ''Experimental and cfd modelling of an ejector system for vehicle air conditioning'', *Journal of the Institute of Energy,* Vol. 72, pp. 41-47.

Riffat S.B., S.A. Omer 2001. ''CFD modelling and experimental investigation of an ejector refrigeration system using methanol as the working fluid'', *Int. J. of Engng. Research,* Vol. 25, pp. 115-128.

Scott, D.A., Z. Aidoun, M. Ouzzane 2009. "An experimental investigation of an ejector operating with R245fa", *Proc. Int. Seminar on ejector/jet-pump technology and applications, Sept. 7-9*, Louvain-la-Neuve, Belgium, Paper No. 21.

Scott D.A., Z. Aidoun, O. Bellache, M. Ouzzane 2008. "CFD simulations of a supersonic ejector for use in refrigeration applications", *Proc. 12th Int. Refr. and Air Cond. Conf. at Purdue, July 14-17*, India.

Sokolov M., D. Hershgal 1990. ''Enhanced ejector refrigeration cycles powered by low grade heat. Part 1: Systems characterization'', *Int. J. of Ref.,* Vol. 13, pp. 351-356.

Sokolov M., D. Hershgal 1990. ''Enhanced ejector refrigeration cycles powered by low grade heat. Part 2: Design procedures'', *Int. J. of Refrigeration,* Vol. 13, pp. 357-363.

Sokolov M., D. Hershgal 1991. ''Enhanced ejector refrigeration cycles powered by low grade heat. Part 3: Experimental results'', *Int. J. of Refrigeration,* Vol. 14, pp. 24-31.

Sokolov M., D. Hershgal 1993a. ''Optimal coupling and feasibility of solar powered year-round ejector air conditioner'', *Solar Energy,* Vol. 50, pp. 507-516.

Sokolov M., D. Hershgal 1993b. ''Solar powered compression enhanced ejector air conditioner'', *Solar Energy,* Vol. 51, pp. 183-194.

Sun D.W., I.W. Eames 1995. ''Recent Development in the Design Theories and Applications of Ejector - a Review'', *Journal of the Institute of Energy,* Vol. 68, pp. 65-79.

Sun D., I. Eames, S. Aphornratana 1996. ''Evaluation of a novel combined ejector-absorption refrigeration cycle. 1. computer simulation'', *Int. J. of Ref.,* Vol. 19 (3), pp. 172-180.

Sun D. 1997. ''Solar powered combined ejector-vapour compression cycle for air conditioning and refrigeration'', *Energy Convers. Mgmt.,* Vol. 38, No 5, pp. 479-491.

Wang J., F. Chen 1996. ''On the start condition of a second throat ejector diffuser'', *Aeronautical Journal*, pp. 321–326.

OPERATIONAL EXPERIENCES OF A TDHP SYSTEM FOR SOLAR COOLING AND HEATING OF A CANTEEN

Matthias Schicktanz, Florian Mehling, Fraunhofer-Institute for Solar Energy Systems ISE, Department Thermal Systems and Buildings, Heidenhofstr. 2, D-79110 Freiburg, Germany, Florian.mehling@ise.fraunhofer.de

Abstract: Solar cooling systems offer the possibility to use primarily the renewable energy source solar heat for space cooling. Moreover, a solar cooling system can also be used to provide heat for space heating, in the case of working in heat pump mode. Besides theoretical investigations practical experience is required to evaluate the performance of solar cooling in the field. This document presents the main results from a solar cooling installation for canteen cooling, which is in operation since 2007. The data evaluation shows a seasonal electrical performance factor of 26.1 for space heating and 6.5 for space cooling. A seasonal thermal performance factor for cooling of 0.4 has been determined.

Key Words: adsorption chiller, solar cooling, operational experience, seasonal performance figures

1 INTRODUCTION

This report is about a thermally driven heat pump (TDHP) system operating in cooling as well as in heating mode. It is installed at the canteen of Fraunhofer ISE in Freiburg, Germany. This system is in operation since 2007. The main purpose is to provide air-conditioning for the kitchen of the canteen. If capacity is available the system supports the building main system with heat for the lobby. Depending on the inlet air temperature the operation between cooling and heating can switch during a day. For example, heat for space heating can be provided in the morning and afternoon while at noon the system switches to chill the kitchen.

The solar collector field of 22 m² aperture area is installed at the roof of the building and a hot water buffer storage of 2 m³ is installed in the basement. From the hot water buffer storage heat is taken to power the thermally driven heat pump system. Heat from the heating network of the ISE institute can be used as backup. Three bore holes are a part of the system. In cooling operation these holes reject waste heat to the ground while in heating operation heat is taken from the ground.

2 GENERAL DESCRIPTION OF THE SYSTEM

The ACS08 from the manufacturer Sortech AG is an adsorption type thermally driven heat pump. The rated chilling capacity in cooling operation at 15°C is about 8 kW, while the heating capacity in heating operation at 30°C is approx. 20 kW.

The 2 m² hot water storage with a stratified charger is only heated by the flat panel collector field. An external heat exchanger between the storage and collector field is used to separate the brine from the storage.

While the system is operating in cooling mode the rejected heat is pumped to three terrestrial probes, which are acting as a heat sink. Each of those heat probes is installed vertically into

the ground as an 80 m long double-U-pipe. When the system is operating in heat pump mode the natural ground heat of approx. 13°C will be utilized as thermal output to preheat the air condition system of the foyer by an air-to-water heat exchanger.

An institute internal CHP-system is maintaining a heating network at 75°C. As backup the high temperature driving circuit can switch from the solar storage to this heat network, which is separated from the TDHP system via heat exchanger. No additional backup cooling or heating system is installed for the canteen kitchen.

3 HYDRONIC CONNECTION AND CONTROL STRATEGIES

3.1 Heating operation

During the heating season the use of heat from the buildings heating network dominates the driving heat supply for the TDHP. However, on sunny winter days sometimes the collectors provide heat for several hours at a temperature level which is sufficient to power the TDHP. The heat pump mode will be enabled in a time frame from 6:45 and 19:00 o'clock. To start the adsorption heat pump, the inlet temperature in the main air duct has to be between 14.5°C and 17.5°C (3 K hysteresis) due to the freeze protection of the chiller.

Figure 1 shows the hydronic connection of the system in heating operation. The cooling water loop is connected to the air handling unit to heat up fresh air for the foyer. Natural ground heat is taken via the bore hole. Heat from the solar collector or from the heating network as backup is used as hot water driving source.

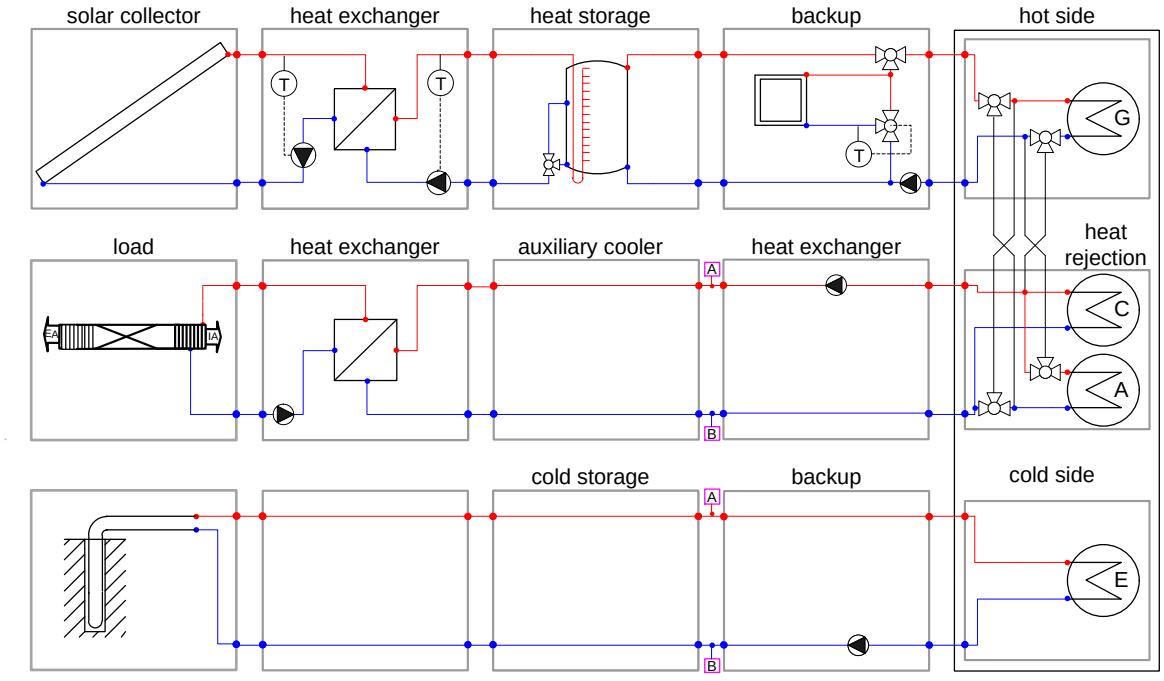

Figure 1: Hydronic representation of the system in heating operation

3.2 Cooling operation

During the summer the cooling process will be enabled in the time between 6:45 and 16:00 o'clock. The adsorption chiller is operating, when the inlet air temperature at the air-to-water heat exchanger exceeds 20°C (2 K hysteresis) and the air temperature in the kitchen is above 23°C (2 K hysteresis) at the same time.

The solar heat is used whenever the mean temperature in the upper part of the storage is above 65°C with a 5 K hysteresis for turning of solar heat supply. Figure 2 shows the hydronic representation of the system in cooling operation.

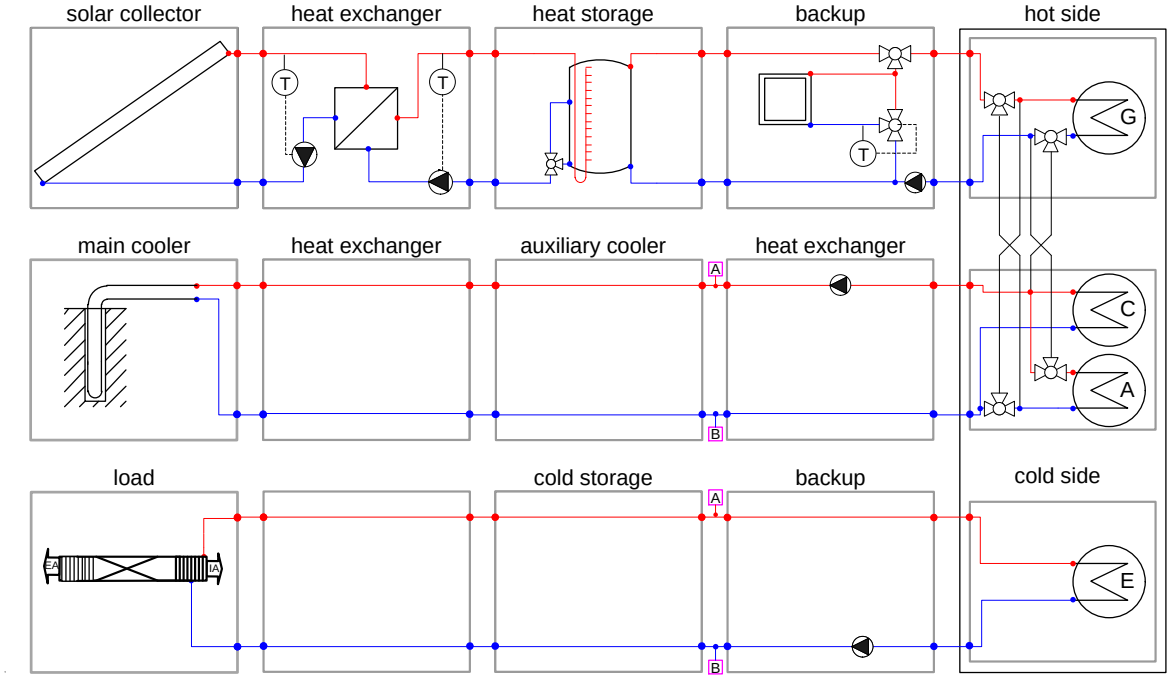

Figure 2: Hydronic representation of the system in cooling operation

The volume flows in the three circuits are kept constant and correspond to the nominal flows required by the chiller. Energy efficient pumps have been installed and the flow rate is set via the controller of the pumps.

In spring and autumn it may happen that the air temperature falls below 14.5°C in the mornings and thus the heating mode is activated, but later during the day temperatures in the canteen kitchen rise above the threshold for cooling operation. In these cases the system is operated in the heating mode first and later in the cooling mode.

4 MONITORING DATA AND PERFORMANCE EVALUATION

The system is under monitoring since 2007. Here, the data evaluation of the year 2009 is presented. Since the system could switch the operation mode on a daily basis the data are not presented in heating and cooling operation rather than in summer and winter period. However, intervals with heating and cooling operation are limited to several days per year in the transitional period between summer and winter.

4.1 Monitoring equipment

The monitoring system consists of internally integrating heat meters with paired Pt100 type temperature sensors. The integrator has a sampling rate of 1 s and calculates cumulated energy amounts, mean temperatures and powers. This internal sampling rate assures a correct collection of energy data for the highly dynamic temperature patterns characteristic of adsorption systems. The integrator and further temperature sensors are read out by a computer with a sampling rate of 15 s. The monitoring software further reduces these values to cumulated energies and mean temperatures which are stored within an interval of 5 minutes in the raw data measurement file. The storage interval can be set by the system

operator and thus allows a flexible data management. The post processing of the raw data further reduces the values to hourly accumulated and mean values – depending on the quantity considered. For the hourly mean temperature values also a standard deviation is calculated in order to judge the stability of the temperature within the evaluated hour.

4.2 Cooling Operation

In cooling operation the system shows a seasonal thermal performance factor of 0.40. Thus, per unit of consumed heat 0.40 units of cold were produced. However, this seasonal value includes all disadvantageous operation states. As shown in Núñez (2008) the seasonal thermal performance factor has a value of 0.57 when neglecting the disadvantageous states. With a more sophisticated operation strategy the seasonal performance factor can be increased.

The seasonal electrical performance factor of the system is 6.5. This means that per unit of electricity consumed 6.5 units of cold were produced. The system still has potential to increase this parameter.

The following reasons are responsible for disadvantageous operation states:

- The temperature of the institutes heating network drops down from time to time. These fluctuations are not caused by TDHP system. The lower or fluctuating driving temperatures lead to a reduced seasonal performance factor of the TDHP.
- The performance calculation takes into account all starts and stops. Many such operation times occur which favour disadvantageous operation states. The short operation periods could partly be avoided by implementing a controller with forecasting strategy and the usage of chilled water buffer storage. Partly, the short operation times cannot be avoided if they belong to user behaviour.
- The design of the hydronic system was sized for a smaller cooling capacity chiller in the first place. However, the TDHP was replaced by a later system with higher capacity. While the installed hydraulic system couldn't been modified for the higher nominal flow rates of these later generations, the pumping capacity had to be increased to meet the higher flow rates. This fact led to a higher electricity consumption and thus to a lower seasonal electrical performance factor of the system.

4.3 Heating Operation

The seasonal thermal performance factor for heating operation is 1.24 and the seasonal electrical performance factor is 26.1. As shown in Núñez (2008) the seasonal thermal performance factor of the system in heating mode is 1.43 when neglecting disadvantageous states. The reduction of efficiency from 1.43 to 1.24 is caused by the same reasons as described above.

5 SUMMARY

The seasonal performance figures of a solar cooling system were presented. In cooling operation the seasonal electrical performance factor is 6.5 and the seasonal thermal energy efficiency ratio is 0.4, though can be increased to 0.57. In heating operation the seasonal electrical performance factor is 26.1 and the seasonal coefficient of performance is 1.24. It was already proven that the last factor can be increased when avoiding disadvantageous states.

The results show that a reliable operation of the solar cooling system is ensured. However, the heating network of the ISE institute used as backup shows irregular behaviours which

affects the performance of the system. This raises the question how necessary operation conditions can be assured in applications with different needs to the supply system.

Moreover, frequent start/stops may be avoided with a better control strategy and will result in a better performance. It becomes clear, that a high potential lies in controller development. Future research should address this issue.

6 REFERENCE

Núñez, T., B. Nienborg, Y. Tiedtke 2008. “Heating and Cooling with a Small Scale Solar Driven Adsorption Chiller Combined with a Borehole System”, *Proc. 1st Int. Congress on Heating, Cooling and Buildings (EUROSUN 2008), 7th to 10th October*, Lisbon, Portugal.

RECENT DEVELOPMENTS IN ADSORPTION MATERIALS AND HEAT EXCHANGERS FOR THERMALLY DRIVEN HEAT PUMPS

Matthias Schicktanz, Kai Thomas Witte, Gerrit Füldner, Stefan K. Henninger, Fraunhofer-Institute for Solar Energy Systems ISE, Heidenhofstr. 2, D-79110 Freiburg, Germany
Andrea Frazzica, Angelo Freni, Institute for Advanced Energy Technologies, Salita Santa Lucia Sopra Contesse 5, 98126 Messina, Italy, Matthias.Schicktanz@ise.fraunhofer.de

Abstract:
Adsorption chillers and heat pumps are a promising technology for the supply of heating and cooling, especially in the small scale range. Therefore, adsorption materials with a high load capacity and heat exchangers with effective heat and mass transfer ratios are required. To compare the characteristics of adsorption-refrigerant working pairs from different manufacturers a common measurement method is required. This paper gives a literature survey about the state of the art in adsorption material developments and proposes a common measurement procedure for adsorbents. Moreover the latest activities in heat exchanger developments for adsorption heat exchangers and evaporators are represented.

Key Words: adsorption, heat exchangers, measurement procedure, evaporation, boiling

1 INTRODUCTION

In this paper an overview is given about ongoing research on thermally driven heat pump (TDHP) machines, especially adsorption TDHPs. In the first part the focus is on the adsorption material. Much research is performed in developing new materials and characterizing their physical properties. Yet, there is no common method or standard to measure and describe the adsorbent characteristics. Therefore, in the first section a proposal for a common measurement procedure is described.

The next question arises when adjusting the adsorbent to the heat exchanger. Different methods like coating and loose grain are available each with specific pros and cons. The target is to increase the heat and mass transfer for adsorption and desorption processes and at the same time increasing the adsorbent per heat exchanger capacity ratio.

When aiming for cheap and compact TDHPs a point is reached when the evaporator is the limiting component. In the last section improvements are shown to increase the heat transfer characteristics of the evaporator. The focus is to increase the heat transfer coefficients between the primary and secondary site of the evaporator and thus enhance the overall heat transfer mechanism between chilled water and refrigerant.

2 CHARACTERISATION OF ADSORPTION MATERIALS

For further improvement of adsorption type TDHPs it is of importance to identify useful working pairs, to measure their physical properties and to proof the stability. Many working groups in different research institutes are working in this field, focusing on different material classes and manufacturing processes.

Publications about the developments of new materials can be found e.g. at (Wang, Metcalf et al. 2012) and (Grekova, Gordeeva et al. 2012). Carbon materials in combination with methanol as refrigerant can be found e.g. at (Gordeeva, Freni et al. 2012) or at (Gordeeva, Freni et al. 2012; Henninger, Schicktanz et al. 2012; Schicktanz, Hügenell et al. 2012). The possibilities of metal-organic frameworks for water adsorption are described e.g. in (Henninger, Habib et al. 2009; Henninger, Jeremias et al. 2011; Henninger, Jeremias et al. 2012). Another material class are salt embedded frameworks such as described in (Sapienza, Glaznev et al. 2011). Further publications about adsorption materials are e.g.(Srivastava and Eames 1998; Aristov, Restuccia et al. 2002; Janchen, Ackermann et al. 2002; Critoph and Zhong 2005; Henninger, Schmidt et al. 2010).

To describe the performance of adsorption-refrigerant working pairs several physical properties need to be known, such as

- the ability of adsorption (equilibrium conditions)
- density
- thermal conductivity

It turns out that some of the working pairs although showing promising characteristics may lose stability with time. This is due to different mechanisms during the manufacturing process and the operation conditions. The materials therefore need to prove their stability against

- mechanical stress
- thermal stress under adsorption and desorption conditions (hydrothermal stability)

The hydrothermal stability of some materials are investigated e.g. in (Henninger, Munz et al. 2011) and (Freni, Frazzica et al. 2011) and (Freni, Frazzica et al. 2013).

In order to compare the measurement results and to find the working pair best fitting to a certain application it is of importance to have a common methodology for measurements. Such methodologies are described e.g. in (Henninger, Freni et al. 2011) with further improvements as described in (Henninger, Freni et al. 2012). Within the next section a procedure is proposed.

2.1 General overview

Three possibilities exist to measure the ability of adsorption materials each with their individual pros and cons. The most frequent measurement method used is thermogravimetry (TGA) and differential thermogravimetric (DTG). The detection of hysteresis and the determination of the loading at ambient conditions are challenging.

For open systems another possibility in to use a well-defined humidified carrier gas (e.g. Setaram WetSys) which flows around the sample. To prevent condensation, the transfer line and the measurement cell have to be temperature controlled in an accurate way.

The third possibility is to measure at closed working fluid atmosphere. As shown in (Henninger, Schmidt et al. 2010) measurements with open and closed systems are comparable if using the same reference conditions.

In order to define a common measurement procedure several influencing factors have to be taken into account. An overview is given in Figure 1.

Beside differences in the described measurement method also differences in the measurement processes exist. Some processes are performed at isobaric some processes are performed isothermal. Isothermal measurements in principle allow the determination of the heat of adsorption, by calculation for at least two isotherms or direct measurement within

a simultaneous TG/DSC. In addition, especially with regard to the Dubinin transformation, the temperature independency can be verified.

Figure 1: Influencing factors for thermal analysis of the adsorption characteristics

Isobaric measurement can in principle be performed in a broader temperature range therefore covering a larger range of the adsorption potential $A = RT \ln p/p_0$. Furthermore as the real cycle (ideally) consists of two isobaric phases of desorption and adsorption at condenser and evaporator pressure, the isothermally measured data is not directly adoptable to the operating device.

2.2 Proposed procedure

All of the described aspects need to be regarded when it comes to the definition of a universal valid measurement procedure. As a result of the consideration a common method for determination of water adsorption characteristics with focus on adsorption heat pumps and chillers has been developed (Henninger, Freni et al. 2011). The procedure consists of a pre-treatment of the sample under continuous evacuation (vacuum level: $1e^{-4}$ kPa). The optimal sample pre-treatment temperature should be selected according to the following classification.

- Strongly hydrophilic zeolites (4A, 13X): pre-treatment T=300°C.
- Hydrophilic aluminosilicates (NaY): pre-treatment T=200°C
- Hydrophobic aluminosilicates (silicalites, ZSM5): T=150°C
- Aluminophospates (AlPO, SAPO): T=150°C
- Others (silica gels, activated carbons): T=150°C

The sample is heated starting from ambient conditions with a heating rate of 1 K/min followed by an isothermal drying step for another 8 hours. In the following step, isobar measurement at a water vapour pressure of 1.2 and 5.6 kPa takes place.

The selection of the two pressure levels is motivated with respect to the possible applications in TDHP systems. The pressure level of 1.2 kPa corresponds to an evaporation temperature of 10°C, which marks a useful temperature level for cooling applications. The second pressure level of 5.6 kPa corresponds to 35°C which either marks the temperature where heat can be rejected (cooling application) or can be used for low temperature heating (heat pumping application). Figure 2 shows the pressure and temperature profile for the measurement procedure. For each pressure level the sample temperature is varied in 5 or 10 K steps between 150°C and 40°C (for 5.6 kPa) or 20°C (for 1.2 kPa) respectively. In addition at least one adsorption and desorption measurements should be performed in order to detect possible hysteresis effects.

For other refrigerants different pressure steps need to be performed but with properties similar to the described procedure.

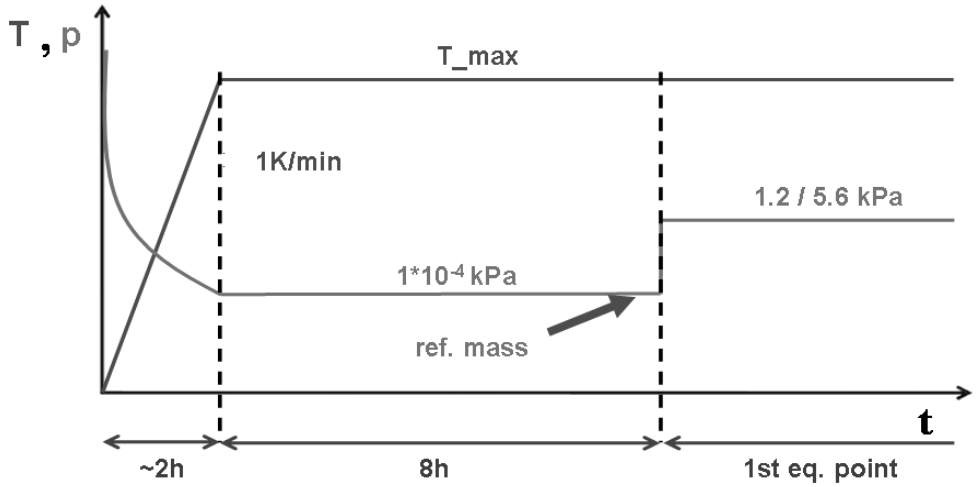

Figure 2: Proposed measurement procedure, including sample pre-treatment and the first isobaric step

The proposed procedure is still under discussion and not yet a standard. This requires further measurements.

3 ADSORPTION HEAT EXCHANGERS

Intensification of the heat transfer quality in adsorbers is a key-factor for development of dynamically efficient adsorption refrigeration and heat pump systems. Several concepts are proposed in literature to contact the adsorbent with the heat exchanger. These concepts can be essentially classified in granular (loose grains) configuration, mechanically consolidated layers and coated heat exchangers HEXs (see Figure 3).

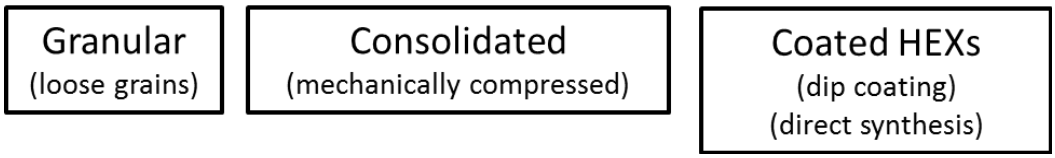

Figure 3: Different adsorber concepts

Consolidation of the adsorbent material is usually achieved by mechanically compressing the adsorbent powder into a mould. Addition of highly conductive compounds (e.g. expanded graphite) is often adopted to further enhance the thermal conductivity of the adsorbent layer (Wang, Metcalf et al. 2012), (Critoph and Metcalf 2011), (Wang, Metcalf et al. 2012), (Kummer, Füldner et al. 2012).

The compacted layer may be highly dense (low gas permeability) and rather thick (large pressure drops), so that this solution appears especially suitable for activated carbon/ammonia systems, where the high ammonia pressure allows to avoid limitations in the process rate (Wang, Tamainot-Telto et al. 2011).

Differently, the concept of coating the heat exchanger surface with a thin layer of active material appears appropriate for low-pressure zeolite (or silica gel)/water systems. In this case, heat transfer rate is increased by improving the thermal contact between active material and heat exchanger, rather than the thermal conductivity of the adsorbent layer itself. Proper selection of the coating density and thickness can prevent high mass transfer resistances (Dawoud 2010), (Dawoud, Höfle et al. 2010).

Many coating methods have been reported in literature, including in-situ zeolite crystallization (Bonaccorsi, Freni et al. 2006; Bauer, Herrmann et al. 2009; Schnabel, Tatlier et al. 2010), (Freni, Bonaccorsi et al. 2006), (Freni, Bonaccorsi et al. 2009; Jeremias, Henninger et al. 2012), adhesive coating (Dawoud, Vedder et al. 2007), (Bonaccorsi, Bruzzaniti et al. 2012) and dip coating process (Freni, Russo et al. 2007; Okamoto 2010; Kummer, Füldner et al. 2012). Direct accretion of zeolite crystals of the metal surface is a very interesting concept, as the resulting thermal contact is expected to be nearly perfect. However, in order to reach an acceptable zeolite layer thickness (> 0.1 mm), multiple depositions are necessary.

Hydrothermal synthesis of zeolite can be a quite complex and expensive process, especially for the SAPO family, which requires a long treatment in autoclave under high pressure and temperature. Moreover, one has to consider possible problems of different thermal expansion between the zeolite layer and the metal substrate due to the high temperature reached during the treatment (up to 550°C for SAPOs).

The dip-coating method represents an alternate way to deposit a thin layer of adsorbent on the heat exchanger surface. According to the techniques reported in literature, the metal substrate is immersed into a liquid solution made of active powder and an organic (e.g. resins) or inorganic substance (Aluminium hydroxide clays, etc.), acting as a binder. A final thermal treatment is applied to remove the excess solvent, so obtaining a compact adsorbent layer. Advantage of this method is the possibility to easily vary the coating thickness in the range 0.1 – 1 mm by, for example, controlling the viscosity of the liquid solution and the dipping velocity. Experimental studies on full-scale coated adsorbers returned encouraging results, especially in terms of adsorption cycle time reduced down to a few minutes (Dawoud 2012), that can be translated to an elevated specific power.

However, the presence of binder reduces the overall sorption ability of the resulting coating and - in case of organic compounds - production of volatile substances is possible during operation of the adsorber, so altering the system pressure.

The most simple (and cheap) adsorber concept consists of the embedding of adsorbent grains between the fins of the heat exchanger. It is self-evident that the adsorbent granules present intrinsically poor heat transfer properties. However, recent experimental data demonstrated that a granular adsorber can provide acceptable performance when small-size grains (< 0.5 mm) and extended surfaces heat exchangers (> 1000 m^2/m^3) are employed (Grisel, Smeding et al. 2010; Sapienza, Santamaria et al. 2011).

Figure 4 illustrates the performance enhancement of the adsorber heat exchanger in several development steps as presented in (Schossig, Witte et al. 2011). The left-hand photo shows an automotive cooling unit used to create a packed bed adsorber where the sorbent is prevented from falling out at the bottom by a wire mesh, and a brush helps to fill in the sorbent very closely. Although the volume specific density (sorbent per volume) is very high in this case, the thermal connection between the sorbent and the heat exchanger fin is fairly poor, hindering the released heat (arising by adsorption of the water molecules on the adsorber) to flow from the granules to the heat transfer fluid. The reason is that there exists at most two point contacts per sphere only between the sorbent (sphere) and the heat exchanger fin (the fin gap is greater than sphere's diameter) and the remaining surface area of the sphere has to face a higher thermal resistance (air gap) while transporting the released heat to the fins. To overcome this, for example a binder based dip coating of the lamella heat exchanger can be applied as next step (middle). Here, a uniform connection is realised all over the heat exchanger and only small air gaps (if any) exist between sorbent and fin. Finally, a direct crystallisation connection, as can be seen in the right hand photograph (150 times enlarged), can be done on top of a metallic short fibre structure (sinter-fused structure), giving an enormous increase of surface area (3-D) (see e.g. (Füldner, Schnabel et al. 2011)). This combination provides both good thermal conductivity in

the metal and an excellent sorption-material-to-metal-mass ratio (Schossig, Witte et al. 2011). Numerical values for the increase of surface area are available in (Füldner, Schnabel et al. 2011) for example.

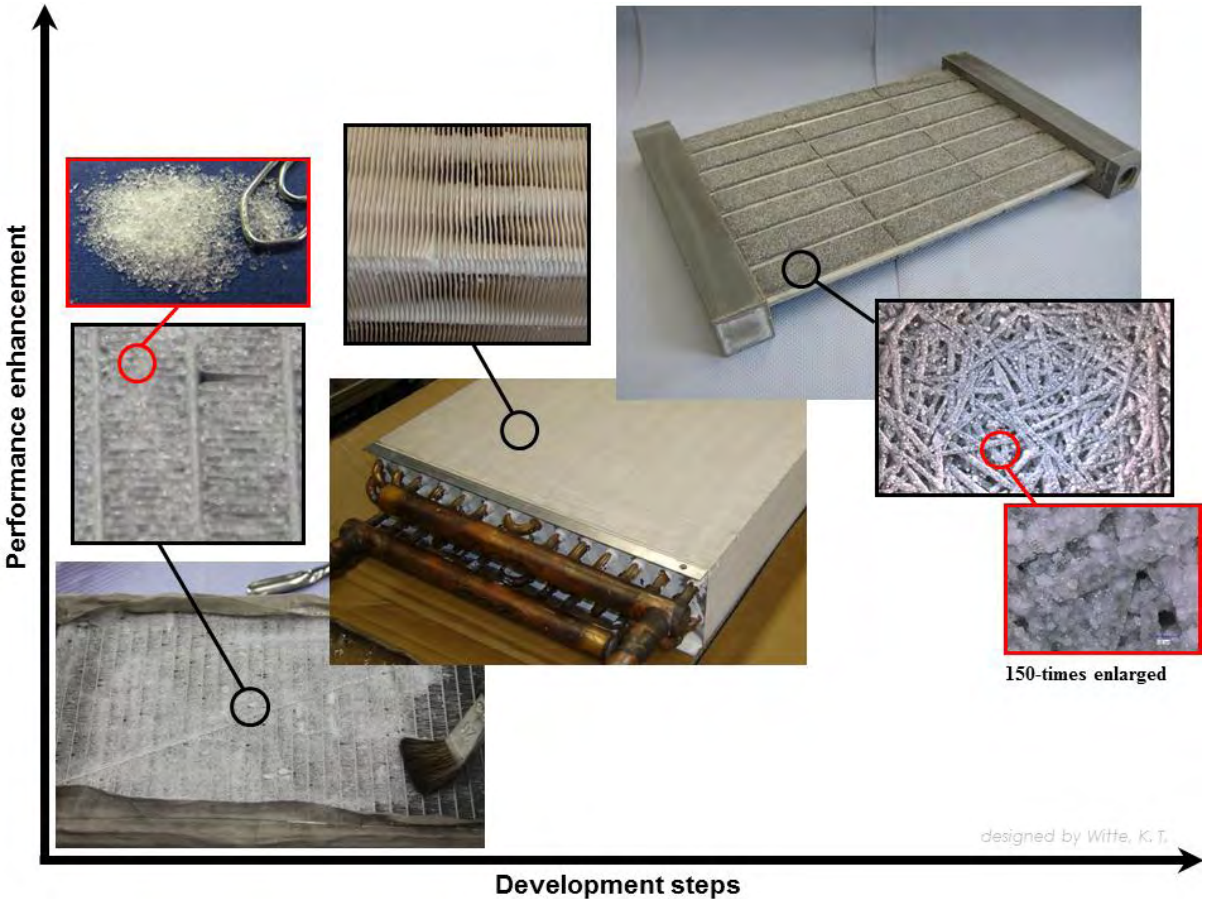

Figure 4: Different evolution steps of the performance enhancement in adsorber development: Packed-bed heat exchanger (left), binder based dip-coated lamella heat exchanger (middle) and direct crystallisation connection of the sorbent (right) on 3D-metal structure heat exchanger. Source (Schossig, Witte et al. 2011)

To evaluate the performance of the coating on the adsorption heat exchanger adequate measurements are required. Such measurement methods are described in (Freni, Santamaria et al. 2012), (Frazzica, Füldner et al. 2012), (Sapienza, Glaznev et al. 2011) and (Sapienza, Santamaria et al. 2011). A comparison between different evaluation and measurement procedures is performed in (Wittstadt, Sapienza et al. 2011).

Since sufficient methods for measurements are available, the design of adsorption heat exchangers can be optimized. An optimization is performed in (Füldner, Laurenz et al. 2012).

4 EVAPORATORS

The evaporator is the heat exchanger that connects the chilled water circuit to the refrigerant. Three major principles exist in the design of the evaporator heat exchangers: falling film, pool boiling and dry expansion evaporators. In falling film evaporators drops flow around the tubes of the heat exchanger tubes and evaporate. In pool boiling the heat exchanger tube bundle is embedded in a pool of refrigerant. In dry expansion evaporators the refrigerant flows in a two phase state through a tube which is heated from the outside. For water as refrigerant only

pool boiling and falling film evaporation is applied since dry expansion evaporation is subjected to higher pressure drops.

Figure 5 shows a tube bundle immersed into a pool as well as a corresponding cross sectional view for pool boiling and falling films. Left hand describes the pool boiling case at a low filling level – typically the tubes are entirely immersed - where the refrigerant (blue) is supplied from the bottom. In contrast the falling film concept is explained via the illustration on the right hand.

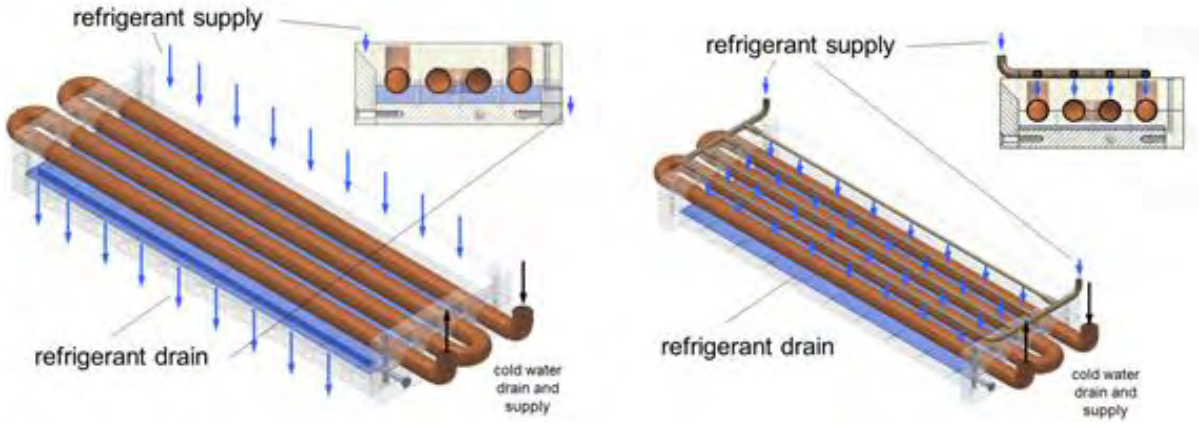

Figure 5: Comparison of pool boiling at a low filling level (left) versus falling film evaporation (right) as investigated in the SORCOOL project at Fraunhofer ISE (see e.g. (Schnabel, Witte et al. 2011)

Improving the heat transfer characteristics of evaporator heat exchangers mainly focuses on two aspects: increasing the heat transfer coefficient between the chilled water circuit and the heat exchanger tubes and increasing the heat transfer coefficient between the heat exchanger and the refrigerant.

For the heat transfer between chilled water and tube wall two options are well known:

- increasing the volume flow inside the tube
- Inserting turbulent flow generators.

Both methods increase the pressure drop within the tubes. Therefore an optimum has to be found between additional electricity consumption and compact design.

Observing the resistances outside the tube several options are available:

- reaching the boiling regime of nucleate boiling
- Lower the thickness of the water layer in the region of convective boiling.

Figure 6 left side shows a high performance 3D-metal structure, manufactured by Fraunhofer IFAM, where the initiation of nucleate boiling has been observed at wall superheats of already 8 K at a pressure of 10 mbar. Tube wetting is reached through capillary surface structuring where water moves upwards automatically. The cut-out on the right side shows high performance evaporation tubes able to make use of this capillary-assisted-evaporation. Additionally, these pictures show turbulent flow generators realised through internal fins (top) and a tube deformation (bottom). Both combinations result in a high tube performance. Thus, performance enhancements of up to factor 14 could have been observed in comparison to a plain reference tube. More information about the evaporator developments for TDHPs can be found in (Schnabel and Weigand 2007), (Schnabel, Scherr et al. 2008), (Witte, Schnabel et al. 2009), (Schnabel, Witte et al. 2010), (Schnabel, Witte et al. 2011), (Witte, Dammel et al. 2011). Measurements of plate evaporators can be found in (Clausse, Leprieur et al. 2011).

More information about the evaporator developments for TDHPs can be found in (Witte, Schnabel et al. 2009), (Schnabel, Witte et al. 2011), (Witte, Schnabel et al. 2011) and (Witte, Dammel et al. 2011). Measurements of plate evaporators can be found in (Clausse, Leprieur et al. 2011).

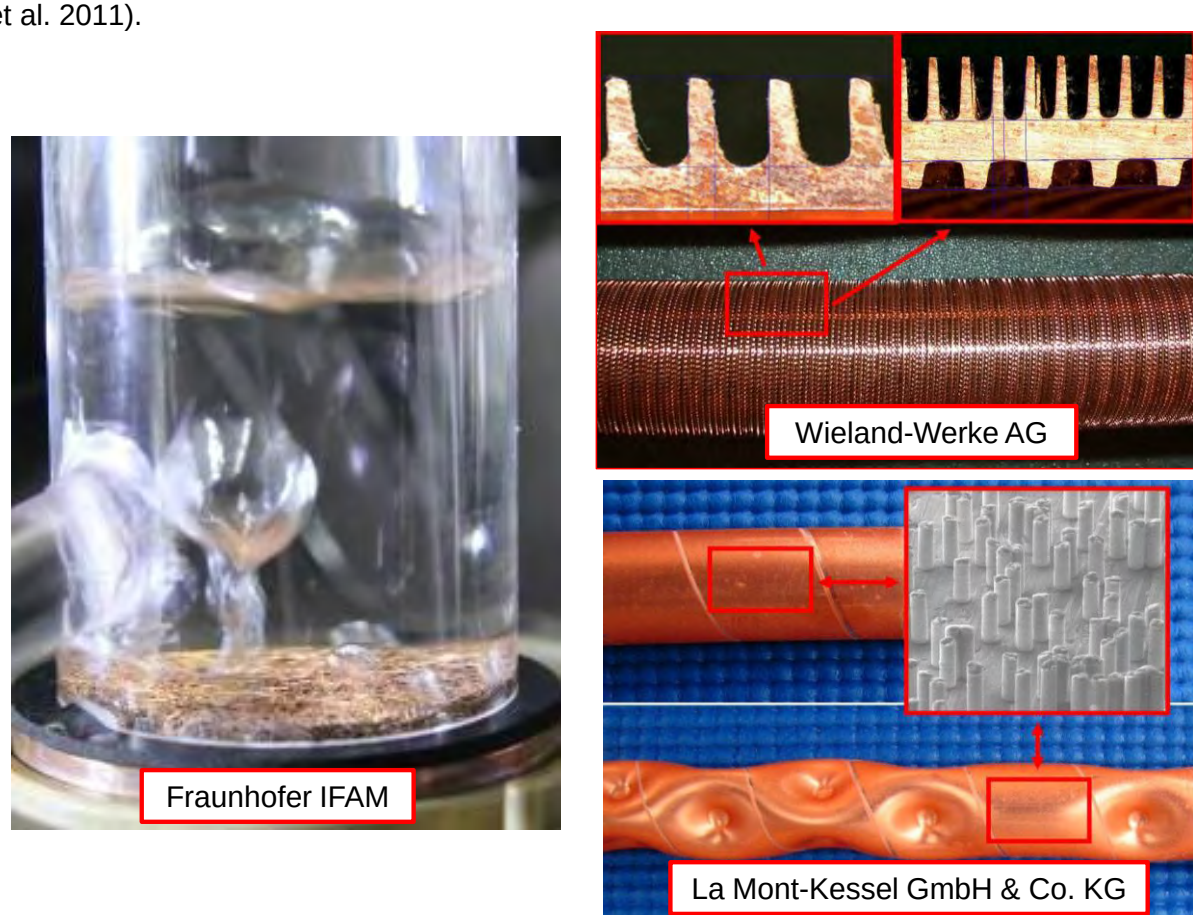

Figure 6: Left: 3D-metal structure manufactured by Fraunhofer Institute for Manufacturing Technology and Advanced Materials (IFAM); top right: high performance evaporation tubes from the manufacturer Wieland-Werke AG; bottom right: So-called Industrial Power Tubes ip tube® from the manufacturer La Mont-Kessel GmbH & Co. KG with a surface treatment by MiCryon Technik GmbH

5 SUMMARY

Current developments on the different components and characterization of adsorption type thermally driven heat pumps were reviewed.
With regard to the basic working pair characteristics, a common measurement procedure for adsorption-refrigerant working pairs is proposed. In addition the activities of different research groups regarding adsorption characteristics, adsorption heat exchanger and evaporator development are summarized.

The proposed procedure for adsorbent characterization covers all measurement aspects, ranging from the pre-treatment and measurement up to the analysis by different thermodynamic models. The method offers the potential to be developed to an international specification or standard.

The current developments on sorption materials, coatings of these materials on supports and new heat exchanger concepts lead to a new generation of adsorbent heat exchangers. However, further improvements are possible regarding the heat capacity and heat and mass

transfer. Due to the cyclic process, a reduction of the heat capacity of the adsorption heat exchanger is beneficial. Increasing the heat and mass transfer ratio, also leads to more efficient TDHPs, as the cycling time can be reduced. However, an optimized sorbent-mass-to-metal-mass ratio has to be chosen regarding the application boundary conditions.
Like in the case for the adsorption material a common measurement procedure for the adsorption heat exchanger is required and under current development.

The improvement of the heat transfer of the evaporator heat exchanger is another important part in order to enhance the overall machine output. Several new developments including different surface structured heat exchangers were reported. The next development step will be the transfer of these new surface structures to a feasible technical scale production. Though, heat exchangers with higher heat transfer coefficients are in direct competition with simply larger heat exchangers. However, the new highly porous surface structures may show a beneficial reduction on the needed metal masses combined with a compact design for a given evaporation power output.

6 REFERENCES

Aristov, Y. I., G. Restuccia, et al. (2002). A family of new working materials for solid sorption air conditioning systems. *Applied Thermal Engineering* 22(2): 191-204.

Bauer, J., R. Herrmann, et al. (2009). Zeolite/aluminum composite adsorbents for application in adsorption refrigeration. *Int. Journal of Energy Research* 33(13): 1233-1249.

Bonaccorsi, L., P. Bruzzaniti, et al. (2012). SYNTHESIS OF SAPO-34 ON GRAPHITE FOAMS FOR ADSORBER HEAT EXCHANGERS. *Proc. Heat Powered Cycles,* ECN, Alkmaar, The Netherlands.

Bonaccorsi, L., A. Freni, et al. (2006). Zeolite coated copper foams for heat pumping applications. *Microporous and Mesoporous Materials* 91(1-3): 7-14.

Clausse, M., J. Leprieur, et al. (2011). EXPERIMENTAL TEST OF PLATE EVAPORATOR FOR SORPTION REFRIGERATION SYSTEMS. *Proc. Int. Sorption Heat Pump Conf.,* Padua, Italy.

Critoph, R. E. and S. J. Metcalf (2011). PROGRESS IN THE DEVELOPMENT OF A CARBON-AMMONIA ADSORPTION GAS-FIRED DOMESTIC HEAT PUMP. *Proc. Int. Sorption Heat Pump Conf.*, Padua, Italy.

Critoph, R. E. and Y. Zhong (2005). Review of trends in solid sorption refrigeration and heat pumping technology. *Proc. of the Institution of Mechanical Engineers, Part E-Journal of Process Mechanical Engineering* 219(E3): 285-300.

Dawoud, B. (2010). WATER VAPOR ADSORPTION KINETICS ON SMALL AND FULL SCALE ZEOLITE COATED ADSORBERS; A COMPARISON. *Proc. Int. Symposium on Innovative Materials for Processes in Energy Systems*, Nov. 29 - Dec. 1, Singapore.

Dawoud, B. (2012). Water vapor adsorption kinetics on small and full scale zeolite coated adsorbers; A comparison. *Applied Thermal Engineering*.

Dawoud, B., P. Höfle, et al. (2010). EXPERIMENTAL INVESTIGATION OF THE EFFECT OF ZEOLITE COATING THICKNESS ON THE PERFORMANCE OF A NOVEL ZEOLITE-WATER ADSORPTION HEAT PUMP MODULE. *Proc. Int. Conference for Enhanced Building Operations*, October 26-28, Texas, USA.

Dawoud, B., U. Vedder, et al. (2007). Non-isothermal adsorption kinetics of water vapour into a consolidated zeolite layer. *Int. Journal of Heat and Mass Transfer* 50(11-12): 2190-2199.

Frazzica, A., G. Füldner, et al. (2012). ADSORPTION KINETICS MEASUREMENTS OF ADSORBENT COATINGS FOR THE USE IN ADSORPTION CHILLERS AND HEAT PUMPS. *Proc. Heat Powered Cycles,* ECN, Alkmaar, The Netherlands.

Freni, A., L. Bonaccorsi, et al. (2009). Zeolite synthesised on copper foam for adsorption chillers: A mathematical model. *Microporous and Mesoporous Materials* 120(3): 402-409.

Freni, A., L. Bonaccorsi, et al. (2006). AN INNOVATIVE ADSORBER: ZEOLITE SYNTHESISED ON COPPER FOAM FOR ADSORPTION AIR CONDITIONING. *Proc. Int. Conference on Heat Powered Cycles*,11-14 September 2006; Newcastle upon Tyne, UK.

Freni, A., A. Frazzica, et al. (2011). Adsorbent coatings for heat pumping applications: Verification of hydrothermal and mechanical stabilities. *Applied Thermal Engineering*.

Freni, A., A. Frazzica, et al. (2013). Adsorbent coatings for heat pumping applications: Verification of hydrothermal and mechanical stabilities. *Applied Thermal Engineering* 50(2): 1658-1663.

Freni, A., F. Russo, et al. (2007). An advanced solid sorption chiller using SWS-1Ll. *Applied Thermal Engineering* 27(13): 2200-2204.

Freni, A., S. Santamaria, et al. (2012). EXPERIMENTAL TESTING OF A COATED ADSORBER. *Proc. Heat Powered Cycles,* ECN, Alkmaar, The Netherlands.

Füldner, G., E. Laurenz, et al. (2012). SIMULATION OF ADSORPTION CYCLES IN ADSORPTION HEAT PUMPS: DETAILED HEAT AND MASS TRANSFER COMPARED TO LUMPED PARAMETER MODELLING. *Proc. Heat Powered Cycles*, ECN, Alkmaar, The Netherlands.

Füldner, G., L. Schnabel, et al. (2011). Numerical layer optimization of aluminum fibre/sapo-34 composites for the application in adsorptive heat exchangers. *Proc. International Sorption Heat Pump Conference*. Padua, Italy.

Gordeeva, L. G., A. Freni, et al. (2012). A NEW FAMILY OF METHANOL SORBENTS FOR ADSORPTIVE AIR CONDITIONING DRIVEN BY LOW TEMPERATURE HEAT. *Proc. Heat Powered Cycles,* ECN, Alkmaar, The Netherlands.

Grekova, A. D., L. G. Gordeeva, et al. (2012). NANOTAILORING COMPOSITES “BARIUM HALIDE/VERMICULITE” FOR ICE MAKING AND AIR CONDITIONING ADSORPTION CYCLES. *Proc. Heat Powered Cycles*, ECN, Alkmaar, The Netherlands.

Grisel, R. J. H., S. F. Smeding, et al. (2010). Waste heat driven silica gel/water adsorption cooling in trigeneration. *Applied Thermal Engineering* 30(8-9): 1039-1046.

Henninger, S. K., A. Freni, et al. (2011). Unified water adsorption measurement procedure for sorption materials. *Proc. Int. Sorption Heat Pump Conference*, April 6-8, Padua, Italy.

Henninger, S. K., A. Freni, et al. (2012). REVISION OF A COMMON MEASUREMENT PROCEDURE FOR ADSORPTION EQUILIBRIUM CHARACTERISATION. *Proc. Heat Powered Cycles,* ECN, Alkmaar, The Netherlands.

Henninger, S. K., H. A. Habib, et al. (2009). "MOFs as adsorbents for low temperature heating and cooling applications." *J. of the American Chemical Society* 131(8): 2776-2777.

Henninger, S. K., F. Jeremias, et al. (2011). The potential of PCPs/MOFs for the use in Adsorption heat pump processes. *Proc. Int. Sorption Heat Pump Conference*. Padua, Italy.

Henninger, S. K., F. Jeremias, et al. (2012). MOFs for Use in Adsorption Heat Pump Processes. *European Journal of Inorganic Chemistry* 2012(16): 2625-2634.

Henninger, S. K., G. Munz, et al. (2011). Cycle stability of sorption materials and composites for the use in heat pumps and cooling machines. *Renewable Energy.*

Henninger, S. K., M. Schicktanz, et al. (2012). Evaluation of methanol adsorption on activated carbons for thermally driven chillers part I: Thermophysical characterisation. *Int. J. of Refrigeration-Revue Internationale Du Froid* 35(3): 543-553.

Henninger, S. K., F. P. Schmidt, et al. (2010). Water adsorption characteristics of novel materials for heat transformation appli cations. *Applied Thermal Engineering* 30: 1692-1702.

Henninger, S. K., F. P. Schmidt, et al. (2010). Water adsorption characteristics of novel materials for heat transformation applications. *Applied Thermal Eng.* 30(13): 1692-1702.

Janchen, J., D. Ackermann, et al. (2002). Adsorption properties of aluminophosphate molecular sieves - Potential applications for low temperature heat utilisation. *Proc. of the International Sorption Heat Pump Conference*: 635-638.

Jeremias, F., S. K. Henninger, et al. (2012). High performance metal-organic-framework coatings obtained via thermal gradient synthesis. *Chem Commun (Camb)* 48(78): 9708-9710.

Kummer, H., G. Füldner, et al. (2012). INNOVATIVE WATER VAPOR PERMEABLE COATINGS SUITABLE FOR THE USE IN ADSORPTION CHILLERS AND HEAT PUMPS. *Proc. Heat Powered Cycles,* ECN, Alkmaar, The Netherlands.

Kummer, H., G. Füldner, et al. (2012). Innovative water vapor permeable coatings suitable for the use in adsorption chillers and heat pumps. *Proc. Heat Powered Cycles,* ECN, Alkmaar, The Netherlands.

Okamoto, K., Teduka, M., Nakano, T., Kubokawa, S., Kakiuchi, H. (2010). The development of AQSOA water vapor adsorbent and AQSOA coated heat exchanger. *Proc. of Innovative Materials for Processes in Energy Systems IMPRES 2010*, Singapore.

Sapienza, A., I. S. Glaznev, et al. (2011). Adsorption chilling driven by low temperature heat: New adsorbent and cycle optimization. *Applied Thermal Engineering*.

Sapienza, A., S. Santamaria, et al. (2011). Influence of the management strategy and operating conditions on the performance of an adsorption chiller. *Energy* 36: 5532-5538.

Schicktanz, M., P. Hügenell, et al. (2012). Evaluation of methanol/activated carbons for thermally driven chillers, part II: The energy balance model. *Int. J. of Refrigeration* 35(3): 554-561.

Schnabel, L., C. Scherr, et al. (2008). Water as Refrigerant - experimental evaluation of boiling characteristics at low temperatures and pressures. *Proc. Int. Sorption Heat Pump Conf.,* Seoul, Korea.

Schnabel, L., M. Tatlier, et al. (2010). Adsorption kinetics of zeolite coatings directly crystallized on metal supports for heat pump applications (adsorption kinetics of zeolite coatings). *Applied Thermal Engineering* 30(11-12): 1409-1416.

Schnabel, L. and A. Weigand (2007). Water as refrigerant - Comparison of different evaporation structures. *Proc. Int. Conf. on Solar Air Conditioning*, Tarragona, Spain.

Schnabel, L., K. T. Witte, et al. (2010). Vergleich von Verdampferstrukturen für das Kältemittel Wasser. *Proc. Deutsche Kälte-Klima-Tagung*. Magdeburg.

Schnabel, L., K. T. Witte, et al. (2011). Evaluation of different evaporator concepts for thermally driven sorption heat pumps and chillers. *Proc. International Sorption Heat Pump Conference (ISHPC11),* Padua, Italy.

Schnabel, L., K. T. Witte, et al. (2011). EVALUATION OF DIFFERENT EVAPORATOR CONCEPTS FOR THERMALLY DRIVEN SORPTION HEAT PUMPS AND CHILLERS. *Proc. Int. Sorption Heat Pump Conference*, April 6-8, Padua, Italy.

Schossig, P., K. T. Witte, et al. (2011). Annex 34 - Thermally Driven Heat Pumps for Heating and Cooling - Aims and State of the Art. *Proc. 10th IEA Heat Pump Conference*, May 16 - 19, online.

Srivastava, N. C. and I. W. Eames (1998). A review of adsorbents and adsorbates in solid-vapour adsorption heat pump systems. *Applied Thermal Engineering* 18(9-10): 707-714.

Wang, L. W., S. J. Metcalf, et al. (2012). Development of thermal conductive consolidated activated carbon for adsorption refrigeration. *CARBON* 50(3): 977-986.

Wang, L. W., Z. Tamainot-Telto, et al. (2011). Study of thermal conductivity, permeability, and adsorption performance of consolidated composite activated carbon adsorbent for refrigeration. *Renewable Energy* 36(8): 2062-2066.

Witte, K. T., F. Dammel, et al. (2011). Heat Loss Evaluation of an Experimental Set-up for predicting the Initial Stage of the Boiling Curve for Water at Low Pressure. *Proc. COMSOL Conference 2011*, Stuttgart.

Witte, K. T., F. Dammel, et al. (2011). Heat Loss Evaluation of an Experimental Set-up for Predicting the Initial Stage of the Boiling Curve for Water at low Pressure. *Proc. COMSOL Conference 2011,* Stuttgart.

Witte, K. T., L. Schnabel, et al. (2009). Verdampferentwicklung für den Einsatz in thermisch betriebenen Kältemaschinen. *Proc. Deutsche Kälte-Klima-Tagung,* Berlin.

Witte, K. T., L. Schnabel, et al. (2009). Verdampferentwicklung für den Einsatz in thermisch betriebenen Kältemaschinen. *Proc. Deutsche Kälte-Klima-Tagung*, Berlin.

Witte, K. T., L. Schnabel, et al. (2011). Evaluation of different evaporator concepts for thermally driven sorption heat pumps and chillers. *Proc. Int. Sorption Heat Pump Conf.,* Padua, Italy.

Wittstadt, U., A. Sapienza, et al. (2011). ADSORPTION HEAT EXCHANGERSA COMPARISON OF TWO EXPERIMENTAL METHODS FOR THEIR CHARACTERIZATION. *Proc. Int. Sorption Heat Pump Conf.*, Padua, Italy.

IONIC LIQUIDS AS NEW ABSORBENTS FOR ABSORPTION CHILLERS AND HEAT PUMPS

Annett Kühn, Technische Universität Berlin, Institute of Energy Engineering, Marchstr. 18, KT2, D-10587 Berlin, Germany, annett.kuehn@tu-berlin.de
Matthias Seiler, Evonik Industries AG, BU Advanced Intermediates, Innovation, Rodenbacher Chaussee 4, D-63457 Hanau, Germany, matthias.seiler@evonik.com
Michael Radspieler, Bavarian Center for Applied Energy Research (ZAE Bayern), Walther-Meissner-Str. 6, D-85748 Garching, Germany, radspieler@muc.zae-bayern.de
Oleksandr Kotenko, Harald Moser, René Rieberer, Graz University of Technology, Institute of Thermal Eng., Inffeldgasse 25 B, A-8010 Graz, Austria, rene.rieberer@tugraz.at

Abstract: In this paper, ionic liquids are proposed as new absorbents for absorption chillers and heat pumps. The theoretical and experimental based research of Technische Universität Berlin, Bavarian Center for Applied Energy Research (ZAE Bayern) and Graz University of Technology is presented and test and simulation results are discussed. The results show the suitability and promising potential of ionic liquids as absorbents but the research organizations agree in the need of further effort in R&D.

Key Words: ionic liquids, absorption chiller, absorption heat pump

1 INTRODUCTION

Up to the 1980s many different working pairs for absorption chillers have been proposed. Later, only few research groups investigated new absorption working pairs. This is because the prevalent working pairs water/LiBr and ammonia/water meet the existing requirements of common applications quite well. Water/LiBr is used for air-conditioning and NH_3/water mainly for refrigeration.

Nowadays, applications with further requirements have been discussed as there are high medium temperature level (solar cooling in hot climate, heat pump use in retrofit applications) and high driving temperature level (high efficient triple-effect chillers, heat transformers for industrial applications). This required a reanimation of research activities regarding new working pairs to overcome the drawbacks of the prevalent working pairs. LiBr solution runs the risk of crystallization at high temperature lift and the corrosion problem becomes grave at high driving temperatures. The drawback of ammonia/water systems is the remarkably increasing pressure with higher medium temperature level. This is problematic on the one hand regarding construction issues and on the other regarding pump energy consumption.

In the last few years, ionic liquids (ILs) - organic salts composed entirely of ions which remain liquid at or close to ambient temperature - have been discussed as absorbents capable to replace LiBr solution as they do not have the crystallization risk and they are potentially less corrosive.

2 RESEARCH AT TU BERLIN

In 2008, the Technische Universität (TU) Berlin and the company Evonik Industries AG started a public funded project (German Federal Ministry of Economics and Technology by grant no. 0327472A and B) to evaluate the potential of ionic liquids as new absorbents for absorption chillers (Kühn et al. 2009, Seiler et al. 2010, Schneider et al. 2011). In the course of the project Evonik produced several customized ionic liquids which have been tested in a small scale absorption chiller prototype with glass shell at the TU Berlin (see Figure 1).

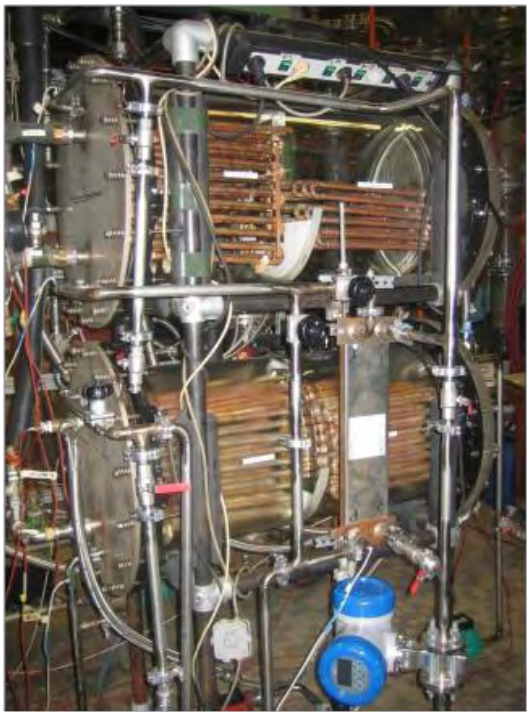

Figure 1: Photograph of the test rig at TU Berlin

The best tested ILs showed the same efficiency (COP) as the water/LiBr system and a cooling capacity (Q_E) representing 80% of the cooling capacity of a water/LiBr system without additives (65% of a water/LiBr system with 2-ethyl-1-hexanol additive, see Figure 2). The tests presented in Figure 2 have been carried out with 75°C driving temperature, 27°C cooling water temperature and 18°C chilled water inlet temperature. Due to the higher viscosity of the ILs a more powerful solution pump has been installed after testing IL3 in order to achieve a solution flow rate (V_Sd) of 100 l/h or more for ILs, too. The test of IL7 has been carried out after the installation of a new condenser (C) and a new generator (G) heat exchanger with slightly other dimensions. Therefore, this test results must be compared to the appropriate LiBr test results (previous column). The analysis of different influencing parameters indicated that the reduced cooling capacity results from a mass transfer inhibition probably due the higher average solution concentration during operation.

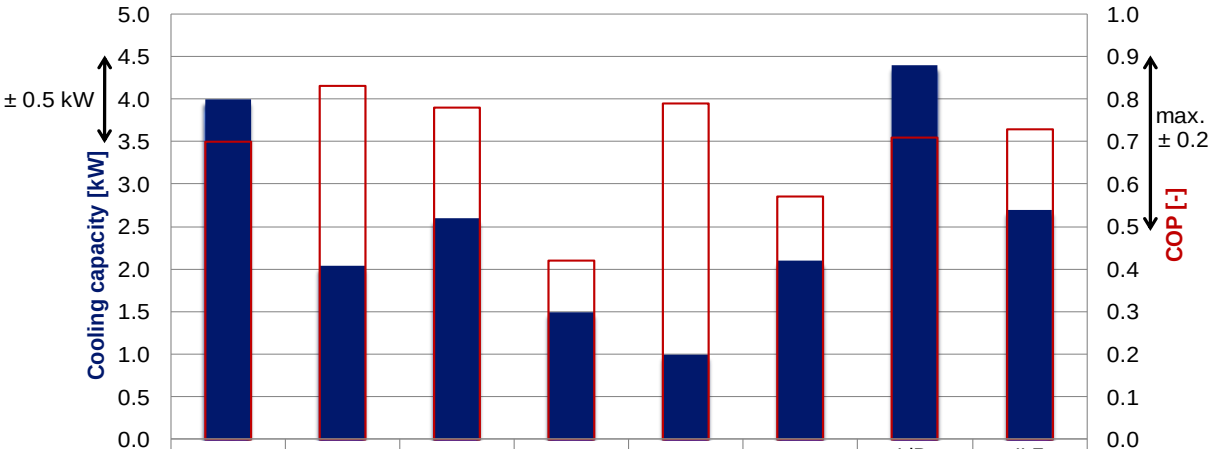

	LiBr	IL2	IL3	IL4	IL5	IL6	LiBr (new C/G)	IL7 (new C/G)
Q_E [kW]	4.0	2.0	2.6	1.5	1.0	2.1	4.4	2.7
COP [-]	0.70	0.83	0.78	0.42	0.79	0.57	0.71	0.73
V_Sd [l/h]	100	70	65	100	100	100	100	100
m_Sd [g/s]	40	18	17	30	33	31	44	32

Figure 2: Test results of water/LiBr and water/IL working pairs (Kühn et al. 2012)

Nevertheless, the potential of ionic liquids as absorbents for absorption chillers and heat pumps has been shown. It has been experimentally demonstrated that the tested ionic liquids allow a depression of the water partial pressure in the same order of magnitude as LiBr solution, but in most cases at higher salt concentrations. It has also been demonstrated that they do not crystallize at temperatures above 20°C and that a stable operation over a wide range of driving, heat sink and heat source temperatures is possible. The use of ionic liquids in absorption chillers and heat pumps appears to be possible under conditions at which LiBr solution runs the risk of crystallization. Heat sink temperatures up to 60°C have been tested without crystallization of the IL. Additionally, potential advantages by using adiabate absorption have been studied. First experiments using a spray dispersion test rig have been carried out.

3 RESEARCH AT ZAE BAYERN

To investigate the suitability of ionic liquids - especially 1-ethyl-3-methylimidazolium ethyl sulfate – as sorbent at the Bavarian Center for Applied Energy Research (ZAE Bayern) an experimental absorption chiller was built. Due to the expected properties of ionic liquids, particularly high viscosity and surface tension, generator and absorber of the system were built as spray chambers with external plate heat exchangers (see Figure 3). This optimizes the heat and mass transfer, since both processes are separated and the wetting of a tube bundle heat exchanger is not further required.

The measurements show the general feasibility. Thermally driven chillers can run and supply chilling capacity with an ionic liquid as sorbent. While operated with EMIM $EtSO_4$ the experimental plant reached a lower specific capacity per volume compared to commercial systems based on H_2O/LiBr and using tube bundle heat exchangers (LT2, LT10, LT52, suninverse), see Figure 4 (Radspieler and Schweigler 2011).

Figure 3: Photograph of the test rig at ZAE Bayern

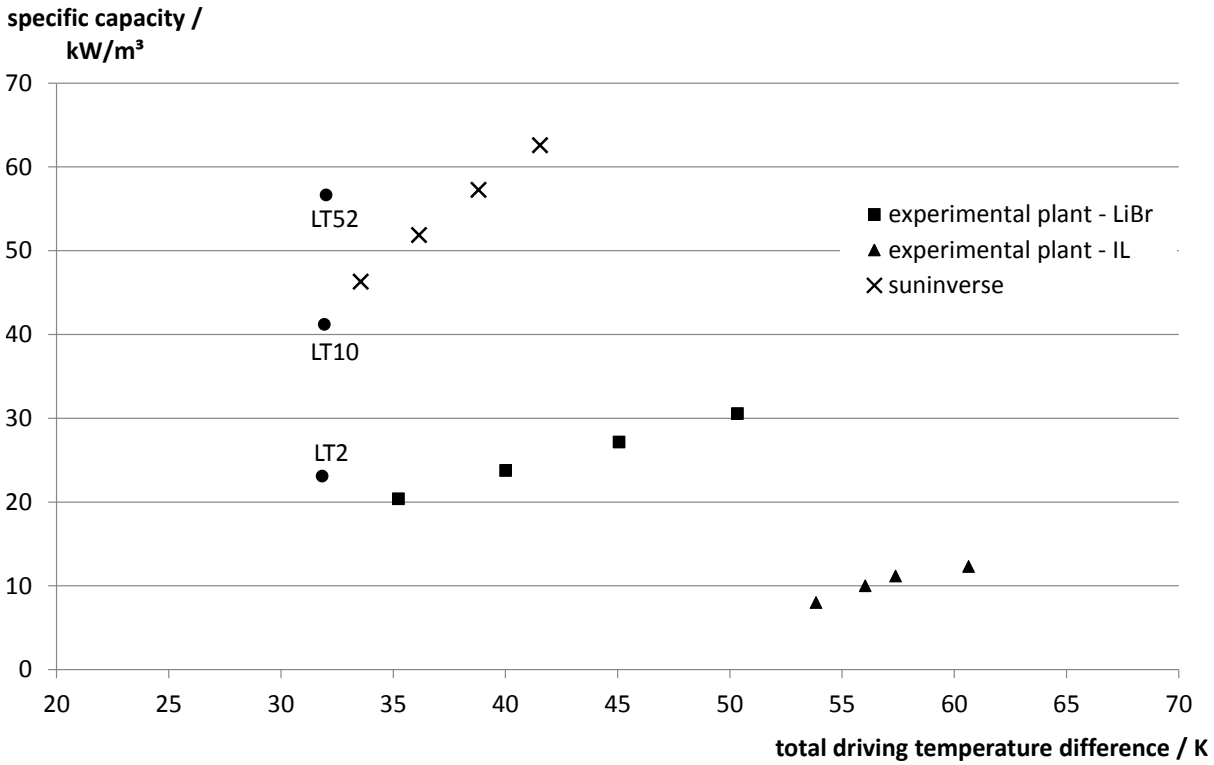

Figure 4: Comparison of capacity (IL and LiBr)

Figure 4 shows the capacities of the test rig operated with LiBr and IL compared to commercial chillers (suninverse and three different chiller of Thermax ltd.) During the experiments a reaction between the refrigerant (water) and the ionic liquid was observed. Due to the decreased capacity and the lack of chemical stability further efforts are needed to find a suitable combination of working fluid and applied process.

4 RESEARCH AT TU GRAZ

A single-stage absorption heat pump (AHP) process with working mixtures of ammonia as the refrigerant and ionic liquids as the absorbent were investigated at TU Graz by means of thermodynamic simulations using the software program ASPEN Plus (Kotenko et al. 2011). From the literature the following binary mixtures of NH_3/IL were found: NH_3/[bmim][BF_4], NH_3/[bmim][PF_6], NH_3/[emim][$EtSO_4$] and NH_3/[emim][TF_2N] (Yokozeki und Shiflett 2007a;b). Thermodynamic simulations of the investigated NH_3/IL AHP-processes at TU Graz have shown that their efficiencies at certain boundary conditions are higher than those of a conventional NH_3/H_2O AHP. However, the COP of the investigated NH_3/IL AHP-processes decreases more in comparison with a conventional NH_3/H_2O AHP when the temperature lift increases. The reason for that is a low difference between the NH_3 mass concentration in the rich and poor solution and therefore a high solution flow rate.

The “best” simulation results have been obtained for the AHP-process using the working mixture NH_3/[bmim][PF_6] (see Figure 5). It is more efficient than a conventional NH_3/H_2O AHP at absorber / evaporator outlet temperatures t_{ABS_OUT} / t_{EVA_OUT} of 25/5°C and 35/5°C if the generator outlet temperature t_{GEN_OUT} is higher than ca. 75°C and ca. 115°C respectively.

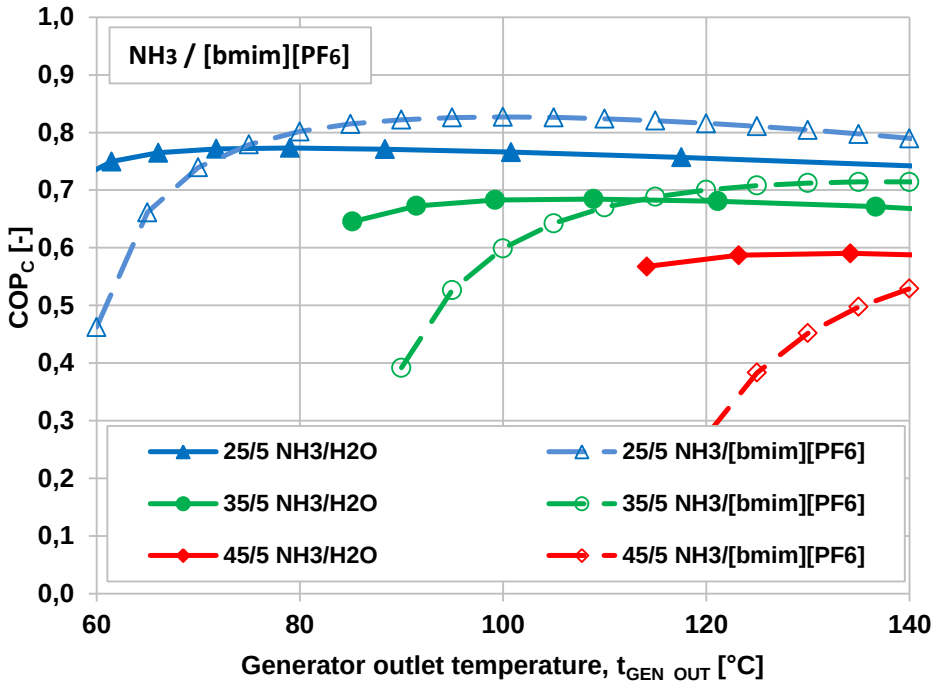

Figure 5: Simulation results of the COP for t_{ABS_OUT}/t_{EVA_OUT}=25/5°C, 35/5°C and 45/5°C of NH_3/[bmim][PF_6] AHP-processes without rectification column in comparison to a conventional NH_3/H_2O AHP-process with rectification column depending on t_{GEN_OUT}

In general, it was concluded that the following are consequences caused by ILs instead of H_2O with NH_3 as refrigerant:

- the rectification column is not necessary;
- the ratio of the required solution pump power demand to the generator heating capacity increases significantly;
- the required capacity of the solution heat exchanger increases as well and has stronger influence on the process COP.

As the next step in the research of NH_3/IL AHP-processes experimental investigations are necessary.

5 SUMMARY

At TU Berlin seven ionic liquids tailor-made by Evonik Industries AG have been tested as absorbents for water in a small scale absorption chiller. At ZAE Bayern tests with water and 1-ethyl-3-methylimidazolium ethyl sulfate have been carried out using a test rig with adiabatic absorption and desorption. At TU Graz simulations have been performed using ammonia as refrigerant and ionic liquids as absorbents. The results show the suitability and promising potential of ionic liquids as absorbents for absorption cooling machines and heat pumps. The possibility to tailor the properties according to the requirements described is intriguing. More tests are required, but a competitive IL-based working pair seems to be possible in the near future.

6 NOMENCLATURE

[bmim][BF_4]	1-butyl-3-methylimidazolium tetrafluoroborate
[bmim][PF_6]	1-butyl-3-methylimidazolium hexafluorophosphate
[emim][$EtSO_4$]	1-ethyl-3-methylimidazolium ethylsulfate
[emim][TF_2N]	1-ethyl-3-methylimidazolium bis(trifluoromethylsulfonyl)imide

7 REFERENCES

Kotenko O., H. Moser, R. Rieberer 2011. “Thermodynamic analysis of ammonia/ionic liquid absorption heat pumping processes”, *Proc. of the Int. Sorption Heat Pump Conf., April 6-8,* Padua, Italy.

Kühn A., O. Buchin, M. Seiler, P. Schwab, F. Ziegler 2009. *“*Ionic liquids - a promising solution for solar absorption chillers?”, *Proc. of the 3rd Int. Conf. Solar Air Conditioning, October 30-November 2*, Palermo, Italy*.*

Kühn A., F. Ziegler, O. Zehnacker, M. Seiler 2012. Verbundprojekt: Verwendung von ionischen Flüssigkeiten in Absorptionskälteanlagen: Schlussbericht; BMWI-Forschungsvorhaben 0327472A/B*.*

Radspieler M., C. Schweigler 2011. “Experimental investigation of ionic liquid EMIM EtSO4 as solvent in a single-effect cycle with adiabatic absorption and desorption”, *Proc. of the Int. Sorption Heat Pump Conf.*, *April 6-8,* Padua, Italy.

Schneider M.-C., R. Schneider, O. Zehnacker, O. Buchin, F. Cudok, A. Kühn, T. Meyer, F. Ziegler, M. Seiler 2011*.* “Ionic Liquids: New high-performance working fluids for absorption chillers and heat pumps”, *Proc. of the Int. Sorption Heat Pump Conf., April 6-8,* Padua, Italy.

Seiler M., M.-C. Schneider, A. Kühn, F. Ziegler 2010. “New high-performance working pairs for absorption chillers and heat pumps”, *Proc. of the 2nd Int. Conf. Innovative Materials for Processes in Energy Systems (IMPRES), November 29-December 1,* Singapore*.*

Yokozeki A., M.B. Shiflett 2007a. “Ammonia solubilities in room-temperature ionic liquids”, *Ind. Eng. Chem. Res.* Vol. 46 (5), pp. 1605-1610.

Yokozeki A., M.B. Shiflett 2007b. “Vapor–liquid equilibria of ammonia + ionic liquid mixtures”, *Appl. Energy*, Vol. 84, pp. 1258-1273.

THE FORMATION OF NON-CONDENSABLE GASES IN AMMONIA/ WATER ABSORPTION HEAT PUMPS MADE OF STAINLESS STEEL - LITERATURE REVIEW AND EXPERIMENTAL INVESTIGATION

H. Moser, G. Zotter, O. Kotenko, R. Rieberer, Graz University of Technology, Institute of Thermal Engineering, Inffeldgasse 25 B, A-8010 Graz, Austria, rene.rieberer@tugraz.at

This paper was published in the proceedings of the 4th IIR International Conference on Ammonia Refrigeration Technology, Ohrid, April 14-16, 2011 (www.iifiir.org)

Abstract: Highly efficient ammonia/water absorption heat pumping (AHP) processes (e.g. the GAX-process) require a high desorption temperature level of e.g. 200°C and above. At these conditions the formation of non-condensable gases can take place, which can be dedicated to two chemical processes: corrosion of steel and thermal decomposition of ammonia.

Within a research project the possible use of stainless steel components at high temperature level has been investigated. Tests with an absorption/desorption test rig operating at temperatures up to 290°C as well as corrosion tests using autoclaves at temperatures up to 220°C have been performed. The produced non-condensable gas has been analysed using gas-phase chromatography in order to identify the responsible chemical process.

The results show a large initial corrosion rate which decreases with time. This may be explained by a passivation process of the steel surface. At all tests the carbon steel (ST37) autoclaves has shown significant lower corrosion rates compared to the stainless steel components. Regarding the thermal decomposition no dissociation products has been detected up to a temperature level of 290°C.

Key Words: absorption heat pump, non-condensable gases, corrosion, ammonia decomposition

1 INTRODUCTION

In recent years absorption heat pumps (AHP) for both cooling and heating applications attract increasing research interest, in particular in the small-capacity range. In order to increase the efficiency of natural gas driven ammonia/water absorption heat pumps advanced processes using high driving temperatures like multiple stage or the generator-absorber-heat-exchanger (GAX) process has been developed. One barrier which has been detected in particular at high temperature applications is the formation of non-condensable gases which influences the thermodynamic process negatively.

In general two main chemical mechanisms may cause the formation of non-condensable gases in ammonia/water absorption systems: corrosion of iron (Eq. 1) and the thermal dissociation of ammonia (Eq. 2). The products of these reactions are: solid magnetite and gaseous hydrogen in case of corrosion as well as gaseous nitrogen and hydrogen in the case of dissociation. In principle by analysing the composition of the non-condensable phase, the responsible chemical process can be determined. However, it shall be mentioned, that beside thermal decomposition the presence of nitrogen can also be caused by other chemical processes. McKelvy and Isaacs (1920) have described that if air is in the system

the oxygen is used up for corrosion and mainly nitrogen and hydrogen can be detected in the gas samples. Furthermore it has been shown (Mansfeld and Sun 2003) that when sodium chromate ($NaCrO_2$) is used as corrosion inhibitor it can react with ammonia at high temperatures to form nitrogen and NaOH according to Eq. 3.

$$3Fe + 4H_2O \rightarrow Fe_3O_4 + 4H_2 \quad (1)$$

$$2NH_3 \rightarrow N_2 + 3H_2 \quad (2)$$

$$NH_3 + H_2O + Na_2CrO_4 \rightarrow 1/2N_2 + 2NaOH + Cr(OH)_3 \quad (3)$$

1.1 Corrosion of Steel

According to (1 even small corrosion rates lead to the formation of a considerable hydrogen amount, e.g. if a 0.01 mm thick layer of a 1 m² iron surface corrode uniformly to magnetite approx. 42 liter of gaseous hydrogen (at 1 bar and 20°C) are generated.

One problem of the investigation of corrosion phenomena regarding ammonia/water solution is that usually there are many variables like ammonia concentrations, temperature level, existing impurities, possible pre-treatment of the surface etc., which can greatly influence the corrosion rate. This is particular of interest, because even a very low corrosion rate must be avoided due to the formation of a considerable amount of non-condensable gases.

Typically, the material of choice for NH_3/H_2O absorption heat pumps is carbon steel. In order to prevent corrosion in these systems usually corrosion inhibitors like sodium chromate (Na_2CrO_4) and/or sodium dichromate ($Na_2Cr_2O_7$) are used (McKelvy and Isaacs 1920). However, these chemical compounds are highly toxic and carcinogenic and the use within EU member states has been widely banned by 2002/95/EG (RoHS - Restriction of Hazardous Substances). Currently some exceptions to this regulation exist. One is the use of “hexavalent chromium as anti-corrosion of the carbon steel cooling system in absorption refrigerators”. However, it can be expected that this exception will expire in the near future (Gensch et al. 2009). In order to overcome the drawbacks of the conventional inhibitors using chromates alternative inhibiting substances and pre-treatment procedures for the system carbon steel and NH_3/H_2O have been suggested by several authors.

Agrawal and Hindin (1994) and Hindin (1995) from “Gas Research Institute” (GRI) have proposed to use silicon compounds which are soluble and stable in the ammonia and water solution (e.g. approx. 0.2 wt% of sodium silicate) as inhibitor. However, further investigations at GRI have shown that sodium silicate-inhibited directly gas fired chillers either have generated excessive amounts of non-condensable gas or they have developed excessive generator temperatures due to low solubility of the silicate in various regions of the chillers.

Downey (1996) from “Carrier Corp.” has proposed different silicates, molybdates or borates together with a hydroxide for ammonia/water systems. However, this is only mentioned in the patent but has not been claimed and no experimental results have been found.

Phillips and Whitlow (1998) have proposed strong bases such as sodium hydroxide, potassium hydroxide, caesium hydroxide or lithium hydroxide, preferably in combination with a buffer (like alkali-borate, -silicate, -molybdate or -acetate) to be used as corrosion inhibitors for aqueous ammonia systems. The presented test results show low hydrogen formation for the carbon steel test apparatus of less than 0.003 ml/day (at atmospheric pressure).

Erickson (2001) has proposed a process consisting of pre-treatment (pre-oxidizing) of the surface, the use of de-oxygenated and de-carbonated water as well as the use of inhibitors

such as alkali metal base preferably with addition of one of alkali metal chromate, germanium dioxide, alkali molybdate or alkali thungstate.

Guerra (2002) from the company “Robur S.p.A” has suggested another inhibitor based on a strong base. The mixture consists of zinc borate, potassium hydroxide and potassium nitrate. From tests with commercial Robur chillers stable production rates of non-condensable gases of ca. 0.1 to 0.2 ml/hour are expected (after an initial operation period of ca. 100 days).

Hannon et al. (2000) and Mansfeld and Sun (2003) have proposed a dual protection method of pre-treating the carbon steel surface with a cerium oxide/hydroxide layer to prevent both corrosion of the metal and ammonia dissociation, and adding rare earth metal salts (preferably cerium nitrate) to the solution to act as a corrosion inhibitor. The presented experimental results show comparable to or better results than that of chromate inhibited systems even at high temperature levels between 205 and 245°C.

Even if there are several alternative inhibitors found in literature - to the knowledge of the authors - up to now only chromate based inhibitors are used in commercially available carbon steel ammonia/water heat pumps. At the first glance in the literature stainless steel is often treated as absolutely corrosion-resistant to ammonia/water and therefore it is recommended in many chemical stability brochures. In the above mentioned literature the main reason for using carbon steel instead of stainless steel is the lower material cost and better machinability (Agrawal und Hindin 1994, Phillips and Whithlow 1998).

At the second glance contradictory statements for stainless steel and ammonia/water can also be found in literature. Mansfeld and Sun (2003) state that corrosion problems can also be found where stainless steel and chrome-plated steel are used. At the Oak Ridge National Laboratory corrosion investigations with autoclaves have shown, that for ammonia/water (5% NH_3) at 180°C the corrosion rate was less than 0.002 mm/year for 304 stainless steel (Griess et al. 1985). The DECHEMA Corrosion Handbook (Behrens 1998, Kreysa and Schütze 2007) states that aqueous, diluted and concentrated ammonium hydroxide solutions attack austenitic CrNi- and CrNiMo-steels only slightly less than 0.05 mm/year at room temperature. At the boiling point (and/or at 100°C), however, the material losses increase to 0.5 mm/year. Above 100°C significant uniform surface corrosion can be expected. If the ammonia hydroxide solution contains additional substances, e.g. carbon dioxide or chloride, these steels often fail after a short period of use.

Generally it can be concluded from the literature review, that for carbon steel corrosion inhibitors are needed. Alternatives to chromate inhibitors are currently under development. The use of stainless steel for high temperature ammonia/water heat pumps is questionable at present and no information regarding corrosion inhibitors for this system have been found.

1.2 Dissociation of Ammonia

As discussed above the second chemical mechanism beside corrosion of steel which can be responsible for the formation of non-condensable gases is dissociation of ammonia according to Eq. 2.

Regarding this phenomenon only a few contrary literature sources have been found for the prevailing thermodynamic conditions in AHP. Broesby-Olsen (1996) discusses catalytically augmented dissociation of ammonia with nickel as catalyst at temperatures as low as 110-120°C. Seidel (1996) investigated the dissociation of NH_3/H_2O solutions in a stainless steel autoclave at temperatures above 200°C. He concluded that the formation of the non-condensable gases by means of the dissociation and corrosion is almost equal and should not be an obstacle for the construction of a triple-effect-machine. Guerra (2002) discusses

the splitting of ammonia molecules when in certain situations, which can be brief and transient, extremely high temperatures exceeding 300-350°C are attained in the circuit. Generally from the literature review no clear information acc. the thermal dissociation of ammonia/water at different temperature levels has been found.

2 EXPERIMENTAL SETUP

Initially the aim of the project discussed in this paper was to investigate thermal decomposition of ammonia under typical conditions occurring in high temperature AHP made of stainless steel and to determine the temperature limits for trouble-free operation. Therefore a test rig comprising of a thermosiphon cycle has been constructed. The first test results turned out, that the initial assumption, that for stainless steel components corrosion plays a minor role compared to dissociation, was wrong and thus autoclaves for corrosion tests have been constructed.

2.1 Thermosiphon Test Rig

In order to investigate thermal dissociation of ammonia a test rig has been designed and constructed in such a way that preferably realistic conditions for an AHP can be simulated. For the test rig common stainless steel components (1.4301, 1.4404 and 1.4571) has been used, in order to heat ammonia/water solution up to 300°C and withstand pressures up to 120 bar.

In Figure 1 a schematic drawing of the test rig is shown. The generator - which consists of a co-axial tube-in-tube heat exchanger - is heated by a secondary water loop, which itself is electrically heated. Both circuits, the secondary water loop and the ammonia water solution are circulated by means of a thermosiphon, where the electrically heated water circuit and the generator work as a bubble pump. This approach allows to easily control and measure the temperature level of the driving heat for the generator and at the same time avoids local over-heating (which likely occurs in an electrically heated generator). The partly evaporated ammonia/water solution rises up and flows into an air-cooled condenser/absorber section. This includes a vessel where test probes can be inserted. The vapour-phase coming from the generator is then absorbed by the solution and is fed back to the generator, completing the working cycle. At the top of the condenser there is a connector through which the gas sample for the analysis can be extracted.

For the experiments the electrical heater has been controlled with respect to a certain temperature level of the heating water. In the test rig the ammonia/water solution circulates and the absorption and desorption process takes place under similar conditions as in a typical AHP. After a certain operation period a gas sample was withdrawn and analyzed.

2.2 Autoclaves

Because the first tests with the thermosiphon test rig turned out that considerable corrosion take place a second test facility consisting of an oven and 16 gas tight vessels (autoclave) have been build up (Figure 2). Four different kinds of steel (ST37, 1.4307, 1.4404 and 1.4571) each for four vessels has been used. All 16 vessels were equipped with a ball valve on one side and the 12 stainless steels vessels had different welding treatment: no acid cleaning and no forming gas; only forming gas (N_2); only acid cleaning (with Antox 71 E Plus, Chemetal); acid cleaning and forming gas (N_2). The vessels made of carbon steel (ST37) were thought as a reference, and they were not treated by acid cleaning nor forming gas during welding.

As it is shown in Figure 2 only the vessels are situated inside the oven, the ball valves are outside. All of the 16 vessels have been pressure and leak tested, evacuated and filled with ammonia/water solution. Then they were put into an oven, heated up and remained in this condition for several days. In order to detect the possible occurrence of small leaks during operation the mass of autoclaves have been exactly measured with a balance before and after the test period. Furthermore the valves are turned to bottom, in order to establish a liquid barrier between gas phase and valves.

It should be mentioned, that the results obtained in autoclaves often do not match observations done on real life absorption heat pumps, as discussed by Guerra (2002). However, the results from autoclave testing can serve as an approximate evaluation of the corrosion of different materials, welding treatment and possible inhibitors.

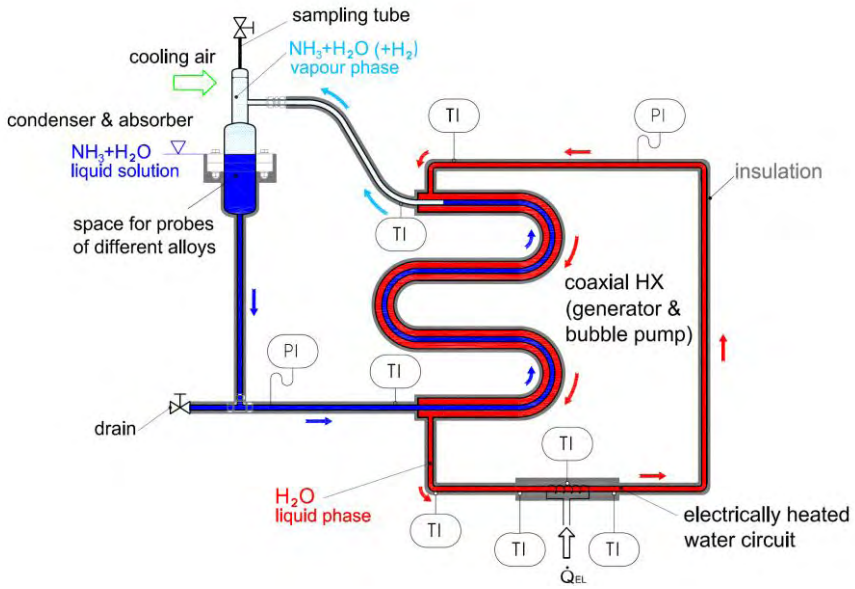

Figure 1: Schematic drawing of the thermosiphon cycle test rig with indicated instrumentation

Figure 2: Photo of the autoclaves in the oven

2.3 Sampling and Measurement Procedure

In order to determine corrosion and thermal decomposition the quantification of the products N_2 and H_2 is necessary. Therefore a gas chromatography setup (GC) has been used and calibrated for the molecules of NH_3, H_2, N_2 and O_2.

As shown in Figure 3 two syringes have been used for gas sampling, one syringe is empty and the second one is filled with approx. 20 ml of water. Before gas sampling the oven (or test rig) is heated up to a certain temperature level in order to achieve a pressure level slightly above atmospheric pressure and all tubes are purged with pure ammonia. By operating the valves the initially empty syringe is filled automatically with sampling gas and serves as a gas volume meter. By pushing down the plunger of the first syringe the gas is passed through a non-return valve to the second syringe where the ammonia is absorbed in the water and the plunger is lifted only due to the non-condensable components. This procedure has been repeated until the plunger of the second syringe was not moving anymore when sample gas was introduced. This means that all non-condensable gases have been withdrawn from the autoclave or thermosiphon test rig respectively. The gas phase of the second syringe has then been analysed using gas-chromatography to determine the components and assign it to the responsible chemical process, i.e. corrosion or thermal decomposition.

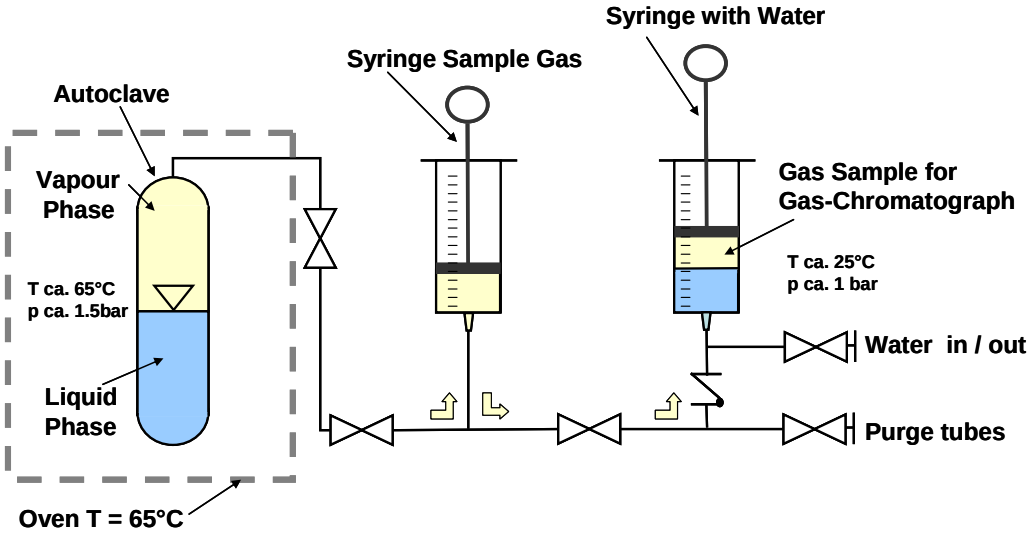

Figure 3: Schematic drawing of the experimental setup for gas sampling

Note: The amount of water in the second syringe has been limited to 20 ml in order to accomplish both, absorb a major amount of ammonia and limit the possible effect of dissolving a part of the non-condensable components of the sample gas in the water.

3 RESULTS AND DISCUSSION

The analysis of all samples from the autoclaves and the thermosiphon test rig showed only very moderate amounts of nitrogen and oxygen. Since the percentage of nitrogen to oxygen in the samples was similar to the air composition, it has been concluded, that a small amount of air was within the sample and that the whole amount of hydrogen can be attributed to corrosion. This means, that no thermal decomposition not even at temperatures up to 290°C has been detected.

Because corrosion of the inner surface is the assumed origin of non-condensable gases the hydrogen production rate has been related to the inner surface area of the thermosiphon test rig (0.18 m²) and the autoclaves (ca. 0.038 m²), in order to obtain comparable results for the corrosion rate. The volume has been measured at room temperature and ambient pressure.

Figure 4 shows the hydrogen production rates of the four different autoclave materials ST37, 1.4307, 1.4404 and 1.4571 (mean value of four autoclaves with different welding precautions) over the operation period. The temperatures and ammonia concentration (x in $kg_{NH3}/kg_{solution}$) of the solution filled into the autoclaves are given in the upper section of Figure 4. The stainless steel autoclaves show similar hydrogen production rates to each other, but compared to the ST37 autoclaves these rates are much higher. E.g. within the initial operation period of 20 days in the 1.4307 autoclaves ca. 145 $ml_{H2}/(m^2\ day)$ and in the ST37 autoclaves ca. 28 $ml_{H2}/(m^2\ day)$ have been generated. Furthermore a sharp decrease of the hydrogen production rate with increasing operation period can be seen, which might be explained with the initial formation of a protective layer (passivation) within the autoclaves.

Figure 5 shows the evaluation of the same set of experimental data. Here the hydrogen production rates are shown for the different welding treatment methods (mean values of three stainless steel autoclave materials). It is clearly visible that those autoclaves which underwent acid cleaning produce substantially more hydrogen then those which were not acid cleaned, at the initial period of testing. After approx. 50 days the difference in the hydrogen production rate is negligible, no matter if there was any welding treatment or not.

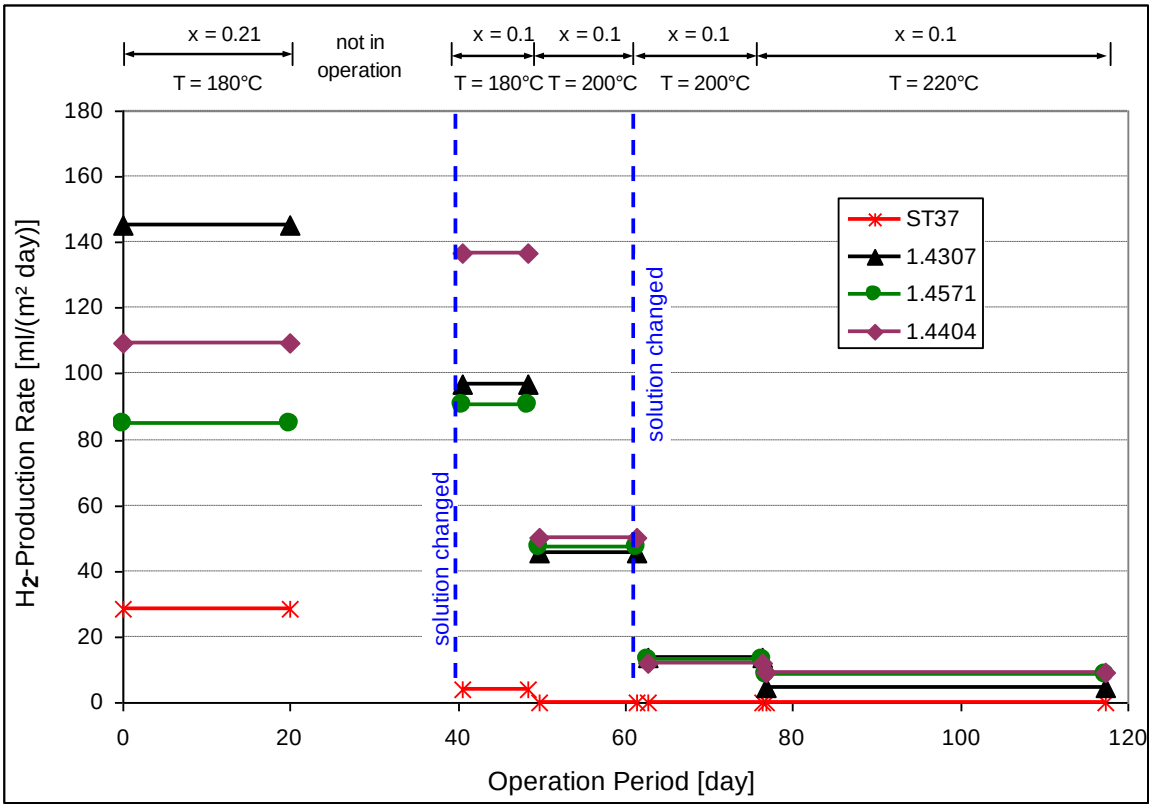

Figure 4: Mean value of the hydrogen production rates for different autoclave material (ST37, 1.4307, 1.4404 and 1.4571)

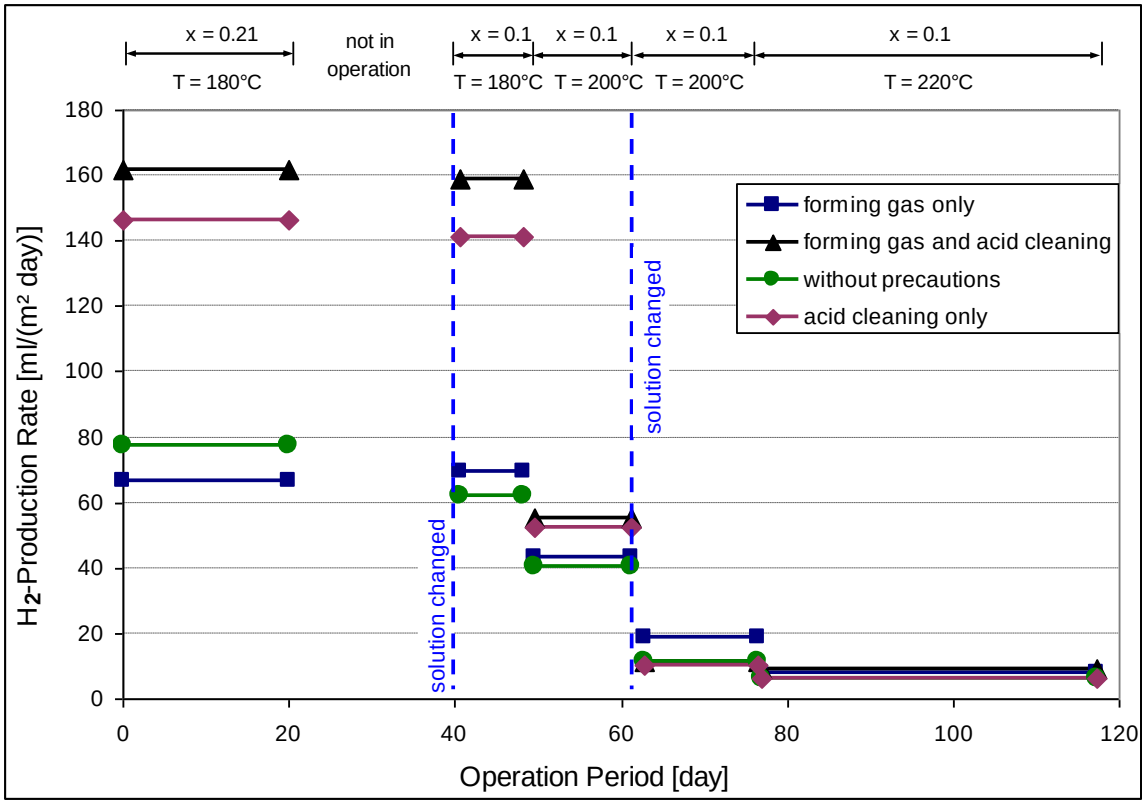

Figure 5: Mean values of the hydrogen production rates for different welding treatment methods

Note: In order to recheck the experimental setup in two ST37 vessels a certain amount of hydrogen has been added to the ammonia/water solution. After one week of operation at 200°C and 25 bar the amount of hydrogen have been measured and the results complied with the previously inserted amount in a range of +/- 9%. Thus it has been concluded that the experimental setup is appropriate for the quantitative evaluation of the hydrogen production rates.

Figure 6 shows the results obtained with the thermosiphon test rig. The initial ammonia concentration of the solution was ca. 20%. Due to the sampling process the ammonia concentration has been decreased to approx. 7% within the total operation period. The first test which was carried out at 180°C for about 7 weeks could not be evaluated with enough precision due to gas sampling problems and therefore this measurement value is missing in Figure 6. After this operation period test runs at 120, 150 and 180°C have been done. Those at lower temperatures show lower hydrogen production rates than at 180°C. This indicates that in the initial phase of operation (ca. 70 days) the temperature (between 120 and 180°C) influences the corrosion rates. After further 38 days operation at ca. 70°C two tests at 180°C have been conducted. The results show much lower hydrogen production rates compared to previous results at 180°C. Compared to the results observed with the autoclaves a similar decrease of the hydrogen production rate with time has been observed at 180°C. After further 53 days of operation at ca. 90°C the temperature level has been increased to 200, 250, 270 and 290°C. For these temperature levels a moderate increased hydrogen production rate has been observed.

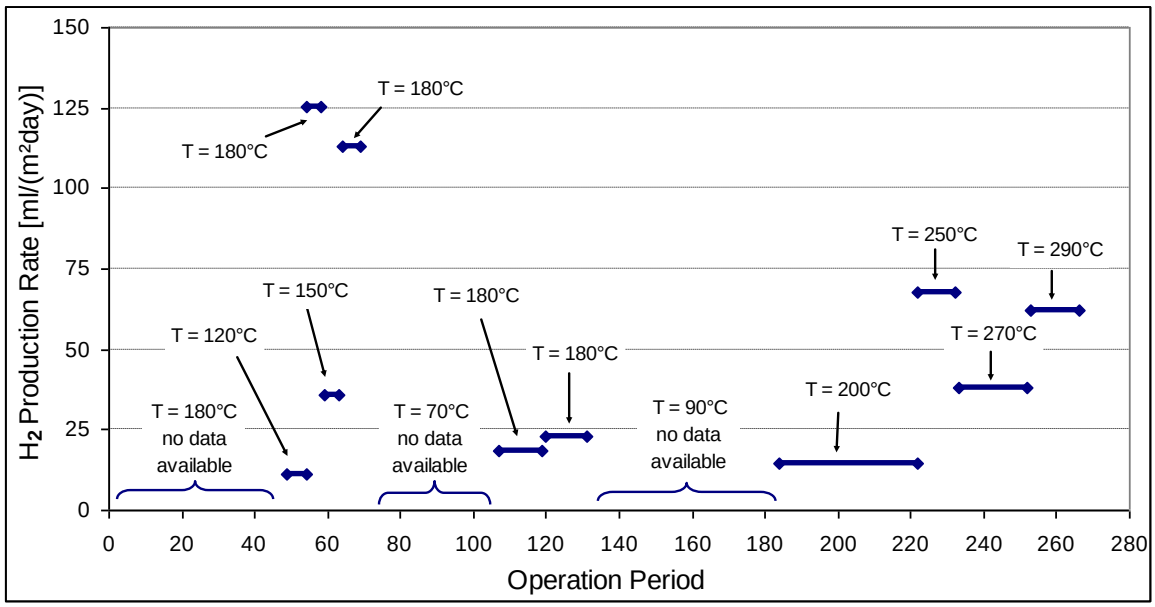

Figure 6: Hydrogen production rates measured at the thermosiphon test rig

4 CONCLUSION

The formation of non-condensable gases in AHP has a negative effect to the process or even may lead to system malfunction. From a literature review two possible reasons have been evaluated, corrosion and thermal dissociation. However, the gathered information is not totally consistent and information regarding the system stainless steel and ammonia/water is very limited. Within this work two test facilities, a stainless steel thermosiphon cycle and 16 autoclaves (12 made of stainless steel and 4 carbon steel) have been investigated with ammonia/water at different temperatures.

Following main findings can be summarized:

- No thermal decomposition of ammonia has been detected up to temperatures of 290°C.
- Mild carbon steel (ST37) has shown significantly lower hydrogen production rates compared to stainless steel.
- A large initial hydrogen production rate which decreases with time has been observed.

From the results obtained up to now it can be concluded that in contradiction to the expectations carbon steel might be the material of choice instead of stainless steel for ammonia/water absorption heat pumps. If and how corrosion can be reduced for stainless steel components by means of pre-treatment or inhibitors has not been investigated up to now. In order to investigate this phenomenon in detail further tests are planned.

5 ACKNOWLEDGEMENTS

This work has been carried out within the “IEA HPP Annex 34” and the project “InnoGEN”. Annex 34 is financially supported within the framework of the “IEA Forschungskooperation” on behalf of the “Austrian Federal Ministry for Transport, Innovation and Technology”. The project “InnoGEN” is financially supported by the “Klima und Energiefonds” within the research program “NEUE ENERGIEN 2020”. The authors wish also to thank our “InnoGEN” project partners, the “Austrian Institute of Technology” and “Heliotherm Wärmepumpentechnik Ges.m.b.H.” for there support and contributions.

6 REFERENCES

Agrawal A.K., B. Hindin 1994. “Corrosion Inhibition of Ammonia-Water Absorption Chillers”, United States Patent US 5,342,578, Aug. 30, 1994.

Behrens D. 1988. “DECHEMA - Corrosion Handbook Vol. 2, Aliphatic Aldehydes, Ammonia and Ammonium Hydroxide, Sodium Hydroxide, Soil (Underground Corrosion)”, VCH Verlagsgesellschaft, Weinheim, Germany, p. 340.

Broesby-Oelsen F. 1996. “Chemical reactions in ammonia, carbon dioxide and hydrocarbon systems”, *Proc. IIF-IIR Conference*, Aarhus, Denmark.

Downey S.J. 1996. “Absorption Refrigeration System Working Fluid with Molybdate, Borate, Silicate Inhibitor Blend”, US Patent No.: 5 547 600, Assignee: Carrier Corporation.

Erickson D.C. 2001. “Aqueous Ammonia Corrosion Inhibitor”, US Patent No.: 6 203 718 B1.

Gensch C., S. Zangl, R. Groß, A.K. Weber, O. Deubzer 2009: “Adaptation to Scientific and Technical Progress under Directive 2002/95/EC”, Final Report, Öko-Institut e. V., Frauenhofer Institut IZM (Download: http://ec.europa.eu/environment/waste/weee/pdf/ final_reportl_rohs1_en. pdf; 3.8.2010, 10:57)

Griess J.C., J.H. DeVan, H. Perez Blanco 1985: “Corrosion of Materials in Absorption Heating and Refrigeration Fluids”, Oak Ridge National Laboratory, ORNL / TM-9646.

Guerra M. 2002: “Corrosion inhibitor for ammonia/water absorption systems”, European Patent No.: 1,304,398 A2, Assignee: Robur S.p.A.

Hannon C.L., J. Gerstmann, F.B. Mansfeld, Z.N. Sun 2000. “Development of Improved Corrosion Inhibitors for Ammonia-Water Absorption Heat Pumps”, *AES-Vol. 40 Proc. of ASME Advanced Energy Systems Division-2000*.

Hindin B. 1995. “Evaluation of Alternative Corrosion Inhibitors for Gas-Fired Ammonia/Water Refrigeration Machines”, Final Report Gas Research Institute (GRI-95/0075).

Kreysa G., M. Schütze 2007. “DECHEMA - Corrosion Handbook Vol. 9, Potassium Hydroxide, Ammonium and Ammonium Hydroxide”, Wiley-VCH Verlag GmbH.

Mansfeld F.B., Z.N. Sun 2003. “Corrosion protection of steel in ammonia/water heat pumps”, United States Patent US 6,632,294 B2, Oct. 14, 2003.

McKelvy E.C., A. Isaacs 1920. “Causes and Prevention of the Formation of Non-Condensable Gases in Ammonia Absorption Refrigeration Machines”, Technologic Paper of the Bureau of Standards.

Phillips B.A., E.P. Whithlow 1998. “Corrosion inhibitor for aqueous ammonia absorption system”, United States Patent US 5,811,026, Sep. 22, 1998.

Seidel S. 1996. “Thermische Stabilität von Ammoniak-Wasser bei hohen Temperaturen in Edelstahlbehältern“, Diplomarbeit an der Technischen Universität München, Institut E19.

Global heating and cooling demand is expected to grow rapidly in the coming decades. The use of thermally driven heat pumps and cooling machines enables a reduction in the associated fossil fuel consumption and CO_2 emission. This book provides information on both the fundamentals and the recent developments in this environmentally friendly technology for planners, scientists, students and anyone interested in thermally driven heat pumps for heating and cooling.

Universitätsverlag der TU Berlin

ISBN (online) 978-3-7983-2596-8